

**THE NEUREGULIN GROWTH FACTORS AND THEIR RECEPTOR
ERBB4 IN THE DEVELOPING BRAIN: DELINEATION OF
NEUREGULIN-3 EXPRESSION AND NEURITOGENESIS**

Afrida Rahman

Submitted to the faculty of the University Graduate School

in partial fulfillment of the requirements

for the degree

Doctor of Philosophy

in the Department of Psychological & Brain Sciences

and Program in Neuroscience,

Indiana University

June 2019

Accepted by the Graduate Faculty, Indiana University, in partial fulfillment of the requirements
for the degree of Doctor of Philosophy.

Doctoral Committee

Anne L. Prieto, Ph.D.

Andrea Hohmann, Ph.D.

Cary Lai, Ph.D.

Kenneth Mackie, M.D.

April 17, 2019

Dedicated to my parents, Nasima and Asirur Rahman,
Who left everything in Bangladesh to come to America for a better life.
Your courage has taught me to always be fearless. Thank you.

Acknowledgements

I would first and foremost like to express my heartfelt gratitude to Dr. Anne Prieto for giving me the opportunity to work in her laboratory and for offering her continuous mentorship. Her patience in teaching and constructive assessments of my science helped shape my critical thinking skills, my aptitude to do research, and my ability to teach. Her constant support and push also gave me the motivation and confidence to continue and finish my Ph.D.

I would also like to thank my committee members who have dedicated their time to serve on my committee: Dr. Cary Lai, for essentially being another mentor to me and always providing me with Oreos and chocolate; Dr. Andrea Hohmann, for all her great experimental suggestions and for always supporting my immunofluorescence artwork; and Dr. Ken Mackie, for giving me countless troubleshooting advice and introducing me to calcium phosphate transfection.

Furthermore, I would like to thank the Department of Psychological and Brain Sciences (PBS) and Program in Neuroscience (PNS) for years of financial support, travel grants, and opportunities to further my teaching aspirations. I would also like to thank the administrative, business, and technical support staff in PBS and PNS, especially Patricia Crouch, JeanneMarie Heeb, Amy Holtzworth-Monroe, Misti Bennett, LeAnna Faubion, Misty Theodore, Susanne Kindred, and Faye Caylor, for their willingness to help me whenever they could. Additionally, I would like to express gratitude to the Office of the Provost and Center of Excellence for Women in Technology (CEWiT) for their travel support and opportunities they have presented to me and other women in science.

I am also fortunate to have made several close friends and a solid support group during my graduate career including, Erika Perez, Dr. Richard Slivicki, Dr. Justin Bollinger, Lawrence Carey IV, and Nathan Berbesque. The countless shenanigans that we've been a part of are some of my favorite memories and their friendships have meant absolutely everything to me. I

would also like to thank past and current members of my lab, especially Natalie Wallace, Sarah Huber, Jeff Yu, Grace Shariat Panahi, Sarah Hocesvar, and Ashwin Biju for always being entertaining lab mates and providing me with a great deal of assistance with my experiments. A special “thank you” to Meredith Krodel for not only being an amazing role model and teacher, but for also becoming my friend in the process.

Lastly, I would like to thank several people that I love, especially Mom, Dad, Aftab, and Micah. Each one of you has played such a crucial role in my life through loving me, taking care of me, overprotecting me, and supporting me. You have all gotten me through some of my roughest days and have also been there to celebrate all the good ones. I will always be grateful that I have you in my life and know that I support each one of you in everything you do.

**THE NEUREGULIN GROWTH FACTORS AND THEIR RECEPTOR ERBB4 IN THE
DEVELOPING BRAIN: DELINEATION OF NEUREGULIN-3 EXPRESSION AND
NEURITOGENESIS**

The developing brain is a highly dynamic structure, making it repeatedly vulnerable to possible developmental abnormalities that can endure into adulthood. The neuregulin (Nrg) family of growth factors (Nrg1-4) and their receptor, ErbB4, have been linked to mental illnesses considered to emerge as a result of abnormal neural development, such as schizophrenia, bipolar disorder, and depression. In the normal central nervous system (CNS), Nrg-ErbB ligand-receptor pairs regulate several cellular functions integral to neural development, including the enhancement of neurite extension and roles in polarity-driven events such as neuronal migration and the establishment of radial glial morphology. Due to the roles of Nrg-ErbB pairs in the healthy and malignant brain, the aims of this thesis were to address fundamental gaps in knowledge and to expand on the roles of the Nrgs and ErbB4 in neural development. Towards these goals, we **1)** characterized the spatiotemporal localization of Nrg3, an understudied Nrg, in the rat brain, **2)** defined and characterized the effects of Nrgs1-3 and ErbB4 in neurite outgrowth of GABAergic interneurons, and **3)** studied the potential role of Nrg-ErbB4 signaling in neuronal polarization through its interaction with the Par polarity complex. The results from this thesis revealed that the Nrgs and ErbB4 play important roles in the development of the CNS, specifically in the differentiation of GABAergic interneurons. Nrg3 was found to be the most widely expressed Nrg in CNS neurons, including GABAergic interneurons, and likely plays non-overlapping functional roles with the other Nrgs. Our studies also revealed that Nrgs1-3 do play redundant roles in neurite development of early GABAergic interneurons by increasing the number of neurites and dramatically enhancing neurite length, including axonal elongation. These effects were driven by the activation of ErbB4. Lastly, using biochemical and

immunocytochemical techniques, we uncovered a novel Nrg-dependent association of ErbB4 with members of the Par polarity complex (Par6, Par3, aPKC, and Cdc42), a group of proteins important for radial glial morphology, neuronal migration, and axonal specification. Collectively, the findings of this thesis highlight biological processes of the Nrgs and ErbB4 in the developing CNS, including roles in neuronal differentiation. In addition, these findings may contribute to the development of promising therapies addressing ErbB4-driven psychiatric disorders, such as depression, bipolar disorder, and schizophrenia.

Anne L. Prieto, Ph.D.

Andrea Hohmann, Ph.D.

Cary Lai, Ph.D.

Kenneth Mackie, M.D.

Table of Contents

Table of Contents	viii
List of Figures and Tables	xv
List of Abbreviations	xix
Chapter 1: Introduction	1
1.1 Neural Development.....	1
1.1.1 Cortical Interneuron Subtypes	3
1.1.2 Stages of Neuronal Development in Culture	4
1.1.3 Neurite Outgrowth and Axon Formation	7
1.1.4 Neuronal Polarity and the Par Polarity Complex	12
1.2 The Neuregulin (Nrg) Family of Growth Factors.....	20
1.2.1 Discovery and Isolation of the Nrgs	21
1.2.2 Molecular Structures of Nrg1-3 and Their Isoforms	22
1.2.2.1 Molecular Architecture and Alternative Splicing	22
1.2.2.2 Proteolytic Cleavage.....	23
1.2.2.3 Glycosylation	24
1.3 The ErbB Receptor Tyrosine Kinase Family	26
1.3.1 ErbB4 Alternative Spliced Variants	27
1.4 Functions of Nrg-ErbB Signaling Outside of the CNS	32
1.4.1 Heart Development	32

1.4.2	Breast Development.....	33
1.4.3	Schwann Cell Development and Myelination	36
1.5	Functions of Nrg-ErbB Signaling in the CNS	39
1.5.1	Synaptic Formation	39
1.5.2	Neurotransmission and Neuroplasticity	42
1.5.3	Neuronal Migration.....	46
1.5.4	Neuronal Differentiation and Neurite Outgrowth	50
1.5.5	Oligodendrocyte Development and Myelination	53
1.6	Nrg-ErbB4 Signaling in CNS Mental Illnesses.....	55
1.6.1	Schizophrenia.....	55
1.6.2	Other Mental Illnesses	60
Chapter 2: Materials and Methods		63
2.1	Materials	63
2.1.1	Reagents	63
2.1.2	cDNA Constructs	64
2.1.3	Antibodies	65
2.1.4	Animals	68
2.2	Methods.....	68
2.2.1	GST-Nrg Fusion Proteins and Nrg cDNA Constructs	68
2.2.2	Generation of Anti-Nrg and Purification of Anti-Nrg3 Antibodies	69
2.2.3	ErbB4 cDNA Cloning and Mutagenesis	69

2.2.4	DNA Sequencing and Verification of ErbB4 cDNA Mutants	71
2.2.5	Preparation and Maintenance of Cell Cultures	72
2.2.6	Cell Transfection	73
2.2.7	Nrg Activation	73
2.2.8	Immunoprecipitations and Western Blotting	75
2.2.9	Deglycosylation	78
2.2.10	Immunocytochemistry	79
2.2.11	Immunohistochemistry	80
2.2.12	<i>In Situ</i> Hybridization	82
2.2.13	Neurite Outgrowth Measurements	83
2.2.14	Statistical Analyses	85
 Chapter 3: Developmental Expression of Nrg3 in the Rat Central Nervous System.....		86
3.1	Introduction.....	86
3.2	Results.....	89
3.2.1	Characterization of Anti-Nrg3 Antibodies	89
3.2.1.1	Antibody Specificity	89
3.2.1.2	Developmental Expression of Nrg3 in Whole Brain Lysates and Cortical Cultures.....	90
3.2.1.3	Enzymatic Deglycosylation of Nrg3.....	91
3.2.2	Compartmentalization of Nrg3 by Immunocytochemistry.....	94
3.2.2.1	Nrg3 Expression in N2a/Nrg3 Cells	94

3.2.2.2	Anti-Nrg3 Antibodies do not Cross-React with Nrg1 and Nrg2 in Transfected N2a Cells	94
3.2.2.3	Nrg3 is Enriched in the Golgi Apparatus	100
3.2.3	Expression of Nrg3 in Primary Cortical Neurons and Glia <i>in vitro</i>	103
3.2.3.1	Nrg3 is Abundantly Expressed in Cortical Neurons	103
3.2.3.2	Nrg3 is Expressed at Low to Background Levels in Glia	106
3.2.4	Overall Expression of Nrg3 mRNA in the Rat CNS	109
3.2.5	Developmental Localization of Nrg3 in the Cortex	114
3.2.6	Developmental Localization of Nrg3 in the Cerebellum	117
3.2.7	Developmental Localization of Nrg3 in the Hippocampus	120
3.2.8	Comparison of the Localization of Nrg1 Type III, Nrg2, and Nrg3 mRNAs in P7 Rat Brain	122
3.3	Discussion	126

Chapter 4: The Nrgs and ErbB4 Developmentally Regulate Neurite Outgrowth of Cortical GABAergic Interneurons	134
4.1 Introduction	134
4.2 Results	138
4.2.1 Characterization of Primary Cortical Cultures and GST-Nrg Activation	138
4.2.2 GST-Nrg1-3 Factors Enhance Neurite Outgrowth in ErbB4/GABA Positive Interneurons Following 2 Days of Treatment	142

4.2.3 GST-Nrg1-3 Factors Enhance Neurite Outgrowth in ErbB4/GABA Positive Interneurons Following 5 Days of Treatment.....	147
4.2.4 GST-Nrg Treatment Enhances the Growth of the Axon of Cortical Interneurons Following 5 Days of Treatment	154
4.2.5 Axonal Expression of ErbB4 is Transient	158
4.2.6 Nrg-Induced Neurite Outgrowth is Limited to ErbB4-Expressing GABAergic Interneurons	161
4.2.7 Overexpression of ErbB4 Enhances Neurite Outgrowth in GABAergic Interneurons	169
4.3 Discussion	177

Chapter 5: Activation-Dependent Association of ErbB4 with Members of the Par Polarity Complex.....	184
5.1 Introduction.....	184
5.2 Results.....	189
5.2.1 Characterization of ErbB4 and Par Complex cDNA Plasmid Constructs, Antibodies, and GST-Nrg Fusion Proteins.....	189
5.2.2 ErbB4 Associates with Par6 and Par3 in a Nrg and Time Dependent Manner.....	198
5.2.3 ErbB4 Associates with aPKC ζ in a Nrg and Time Dependent Manner in aPKC ζ Overexpressing Cells	207
5.2.4 ErbB4 Does Not Directly Associate with Cdc42 but Can Indirectly Associate Through Par6.....	215

5.2.5 ErbB4 Associates with Members of the Par Polarity Complex in Primary Cortical Cultures	221
5.2.6 Nrg-Dependent ErbB4 and Par6 Co-Localization in Primary Cortical Neurons	231
5.2.7 Developmental Expression and Association of ErbB4 and Members of the Par Complex in Cortical Tissue	236
5.2.8 ErbB4- Δ 204 Mutant Can Interact with Par6 and Par3 in N2a Cells.....	240
5.3 Discussion	246
Chapter 6: Discussion and Future Directions	254
6.1 Summary and Significance	254
6.2 Does the Nrg-ErbB4 Signaling Network Play a Role in Neuronal Polarity and/or Neuronal Morphology?	255
6.3 Nrg-ErbB4 Signaling in Neurite Outgrowth: What are some Potential Downstream Signaling Pathways?	258
6.4 Nrg-ErbB4 Signaling in Axonal Elongation: What are Some Potential Downstream Signaling Pathways?	261
6.5 Could Nrg-ErbB4 Pairs Along with the Par Polarity Complex be a Part of the Positive Feedback Loop Regulating Axon Formation?	263
6.6 Potential Roles for Nrg Signaling in the Golgi Apparatus.....	267
6.7 Potential Roles for Nrg3 in the Developing CNS and Schizophrenia.....	268
6.7.1 The Developing Cortical Plate and the Cerebral Cortex	269
6.7.2 The Developing Hippocampus.....	273

References..... 275

CURRICULUM VITAE

List of Figures and Tables

Chapter 1: Introduction	1
Figure 1.1: Radial and Tangential Migration of Neurons in the Developing Cerebral Cortex	2
Figure 1.2: Stages of Neuronal Development	6
Figure 1.3: The Growth Cone and Motility During Neurite Outgrowth and Axon Formation	8
Figure 1.4: The Positive/Negative Feedback Loop Model of Axon Specification	11
Figure 1.5: The Par Polarity Complex in Axon Specification	17
Figure 1.6: Nrg1-4 Domain Organization and Structure	25
Figure 1.7: Simplified Schematic of ErbB4 Structure and Alternatively Spliced Variants ..	31
Chapter 3: Developmental Expression of Nrg3 in the Rat Central Nervous System	86
Figure 3.1: Characterization of Specific Nrg3 Antibodies	92
Figure 3.2: Compartmentalization of Nrg3 by Immunocytochemistry	97
Figure 3.3: Nrg3 is Enriched in the Golgi Apparatus	101
Figure 3.4: Expression of Nrg3 in Neurons	104
Figure 3.5: Expression of Nrg3 in Glia	107
Figure 3.6: Overall Distribution of Nrg3 mRNA by <i>in situ</i> hybridization	112
Figure 3.7: Nrg3 Expression in the Cortex	115
Figure 3.8: Developmental Expression of Nrg3 in the Cerebellum	119

Figure 3.9: Nrg3 Expression in the Hippocampal Formation.....	121
Figure 3.10: Comparison of Nrg1 Type III, Nrg2, and Nrg3 mRNA Distribution	124
Chapter 4: The Nrgs and ErbB4 Developmentally Regulate Neurite Outgrowth of Cortical GABAergic Interneurons.....	134
Figure 4.1: Characterization of Primary Cortical Cultures and GST-Nrg Activation	140
Figure 4.2: GST-Nrg1-3 Factors Enhance Neurite Outgrowth in ErbB4/GABA Positive Interneurons Following 2 Days of Treatment.....	145
Figure 4.3: GST-Nrg1-3 Factors Enhance Neurite Outgrowth in ErbB4/GABA Positive Interneurons Following 5 Days of Treatment.....	151
Figure 4.4: GST-Nrg Treatment Enhances the Growth of the Axon of Cortical Interneurons Following 5 Days of Treatment	156
Figure 4.5: Axonal Expression of ErbB4 is Transient.....	159
Figure 4.6: GST-Nrg1-3 Factors do not Enhance Neurite Outgrowth of ErbB4(-)/ β -tubulin(+) Cortical Neurons Following 2 Days of Treatment	163
Figure 4.7: GST-Nrg1-3 Factors do not Enhance Neurite Outgrowth of ErbB4(-)/ β -tubulin(+) Cortical Neurons Following 5 Days of Treatment	165
Figure 4.8: GST-Nrg1-3 Factors do not Enhance Neurite Outgrowth of ErbB4(-)/GABA(+) Cortical Neurons Following 5 Days of Treatment	167
Figure 4.9: Overexpression of ErbB4 Enhances Neurite Outgrowth in GABAergic Interneurons.....	173
Table 4.1: Neurite Outgrowth Measures Following GST or GST-Nrg Treatment for 2 or 5 Days.....	153

Table 4.2: Neurite Outgrowth Measures in ErbB4 Overexpressing Neurons Following GST or GST-Nrg Treatment for 5 Days.....	176
--	-----

Chapter 5: Activation Dependent Association of ErbB4 with Members of the Par Polarity Complex..... 184

Figure 5.1: Characterization of ErbB4 and Par Complex cDNA Plasmid Constructs, Antibodies, and GST-Nrg Fusion Proteins.....	193
Figure 5.2: ErbB4 Associates with Par6 and Par3 in a Nrg and Time Dependent Manner in N2a/ErbB4/myc-Par6 Cells	201
Figure 5.3: ErbB4 Associates with aPKCζ in a Nrg and Time Dependent Manner	209
Figure 5.4: ErbB4 Does Not Directly Associate with Cdc42, But Can Indirectly Associate Through Par6.....	217
Figure 5.5: Developmental Expression of ErbB4 and Members of the Par Polarity Complex in Primary Cortical Cultures.....	223
Figure 5.6: ErbB4 and Members of the Par Polarity Complex Associate in Primary Cortical Cultures in a Nrg-Dependent Manner	238
Figure 5.7: ErbB4 and Par6 Co-Localize in Primary Cortical Cultures	233
Figure 5.8: Developmental Expression and Association of ErbB4 and Members of the Par Complex in Cortical Tissue.....	238
Figure 5.9: Characterization of C-terminal ErbB4 Mutant Constructs	243
Figure 5.10: ErbB4-Δ204 Does Not Bind to PSD-95 but Can Bind to Par6.....	245
Figure 5.11: Proposed Interaction of ErbB4 with the Par Polarity Complex	253

Chapter 6: Discussion and Future Directions 254

Figure 6.1: Schematic of Theoretical Positive Feedback Loop Regulating Axon

Specification 266

List of Abbreviations

5HT3aR, serotonin receptor 5HT3a

7^o, facial nucleus

α -MHC, chain α -myosin heavy chain

A, adult

AA, anterior amygdaloid area

AIS, axon initial segment

Ala, alanine

AMPA, α -amino-3-hydroxy-5-methyl-4-isoxazolepropionic acid receptor

ank-G, ankyrin-G

AON, anterior olfactory nucleus

aPKC, atypical protein kinase C

Aq, aqueduct

Arc, arcuate hypothalamic nucleus

ARIA, acetylcholine receptor inducing activity

BACE, β -site amyloid precursor protein cleaving enzyme 1

BD, bipolar disorder

BLA, basolateral amygdala

BMA, basomedial amygdaloid nucleus

Br, brain

BSA, bovine serum albumin

C, control

CA1-CA3, fields of the hippocampus

Calb, calbindin

Cb, cerebellum

cc, corpus callosum

CD, cytoplasmic domain

Cdc42, Cell division control protein 42

CerN, cerebellar nuclei

Cg, cingulate cortex

ChP, choroid plexus

CNPase, 2',3'-cyclic-nucleotide 3'-phosphodiesterase

CNS, central nervous system

Cons, conservative

CP, cortical plate

CPu, caudate/putamen, striatum

CRD, cysteine-rich domain

CRIB, Cdc42/Rac-interactive binding

Cx, cortex

CxP, cortical plate

CYT, cytoplasmic

D4R, D4 dopamine receptor

DAPI, 4'-6-diamidino-2-phenylindole

DEn, dorsal endopiriform nucleus

det, detergent

DG, dentate gyrus

DIV, days *in vitro*

Dlg1, Drosophila disc large tumor suppressor

DLPFC, dorsolateral prefrontal cortex

DMEM, Dulbecco Modified Eagle's Minimal Essential Medium

DN, dominant-negative

DRG, dorsal root ganglion

E, embryonic day

EDTA, ethylenediaminetetraacetic acid

EGF, epidermal growth factor

EGFP, enhanced green fluorescent protein

EGFR, epidermal growth factor receptor

EGL, external granule cell layer

Endo-H, Endoglycosidase

EPSC, excitatory postsynaptic potential

ERK, extracellular signal-regulated kinase-1

FCS, fetal calf serum

fMaSC, fetal mammary stem cell

Fr, frontal cortex

Gab, Grb-2-associated-binding protein

GABA, γ -Aminobutyric acid

GAD, glutamic acid decarboxylase

GAPDH, glyceraldehyde-3-phosphate dehydrogenase

GDP, guanosine diphosphate

GEF, guanine nucleotide exchange factor

GFAP, glial fibrillary acidic protein

GFP, green fluorescent protein

GGF, glial growth factor

GL, granule cell layer

GI, glomerular cell layer

gly, glycosylation

GM-130, Golgi matrix protein 130

Grb2, growth factor receptor-bound protein 2
GST, glutathione-S-transferase
GTP, guanosine-5'-triphosphate
HER, human epidermal growth factor receptor
Hi, hippocampus
HRG, heregulin
HRP, horse radish peroxidase
ic, internal capsule
IC, inferior colliculi
ICD, intracellular domain
Ig, immunoglobulin
IGL, internal granule cell layer
IGr, internal granule layer of the olfactory bulb
IP, immunoprecipitation
IPSC, inhibitory postsynaptic potentials
IZ, intermediate zone
JM, juxtamembrane
Kr, kringle
LGE, lateral ganglionic eminence
LH, lateral hypothalamic area
LP, lateral posterior nuclei of the thalamus
LPC, lysophosphatidyl-choline
LSN, lateral septal nucleus
LTP, long-term potentiation
lv, cortical layer V
LV, lateral ventricle

MAP2, microtubule-associated protein 2
MAPK, mitogen-activated protein kinase
MBP, myelin basic protein
mcp, middle cerebellar peduncle
MD, medial-dorsal thalamic nuclei
MDD, major depressive disorder
MGE, medial ganglionic eminence
Mhb, medial habenula
Mi, mitral cell layer of the olfactory bulb
ML, molecular layer
mPFC, medial prefrontal cortex
MS, medial septal nucleus
MT, microtubule
mTor, mammalian target of rapamycin
MZ, marginal zone
N, N-terminal domain
N1-3, neuregulin1-3
N2a, Neuro2a
NDF, neu-differentiation factor
NMDAR, N-methyl-D-aspartate receptor
Nrg/NRG, neuregulin
NSC, neural stem cell
OCT, Tissue-Tek Optimum cutting temperature
O-gly, O-glycosidase
OPC, oligodendrocyte precursor cell
Orb, orbital cortex

P, postnatal day

p, phospho-

Pa, paraventricular nucleus of the thalamus

PAGE, polyacrylamide gel electrophoresis

Par, partitioning-defective

PBS, phosphate-buffered saline

PC, Purkinje cell

PCL, Purkinje cell layer

PCR, polymerase chain reaction

PDZb, PSD-95, Dlg1, zo-1 binding domain

PFC, prefrontal cortex

PI3K, phosphatidyl inositol 3-kinase

PIP₃, phosphatidylinositol (3,4,5)-trisphosphate

Pir, piriform cortex

PKC, Protein kinase C

PLCo, posterolateral cortical amygdaloid nucleus

PLL, poly-L lysine

Pn, pontine nuclei

PNGase F, N-glycosidase F

PNS, peripheral nervous system

PPI, prepulse inhibition

PSD-95, postsynaptic density protein 95

PTB, phosphotyrosine binding domain

PV, parvalbumin

PVDF, polyvinylidene difluoride

Rac1, Ras-related C3 botulinum toxin substrate 1

RIP, regulated intramembrane proteolysis

RMS, rostral migratory stream

Rt, reticular nucleus of the thalamus

RTK, receptor tyrosine kinase

SC, superior colliculi

SCI, spinal cord injury

SDS, sodium dodecyl sulfate

SH2, src homology 2 domain

Shc, src homology 2 domain containing transforming protein

SMDF, sensory and motor neuron-derived factor

SN, substantia nigra

SNP, single nucleotide polymorphism

SP, subplate

SST, somatostatin

SVZ, subventricular zone

SZ, schizophrenia

TAB2, TAK1 binding protein 2

TACE, tumor necrosis factor- α converting enzyme

TAK1, transforming growth factor beta-activated kinase 1

TBST, tris-buffered saline-tween

TCA, thalamocortical axon

Th, thalamus

TKD, tyrosine kinase domain

TM, transmembrane domain

Tris, -*tris*(hydroxymethyl)aminomethane

TT, tenia tecta

Tyr, tyrosine

U/UNT, untransfected

V, vector

VCA, ventral cochlear nucleus

VIP, vasoactive intestinal peptide

VL, ventrolateral nuclei of the thalamus

VMH, ventromedial hypothalamic nucleus

VP, ventral thalamic nuclei

VPL, ventral posterolateral nucleus of the thalamus

VPM, ventral posteromedial thalamus

VZ, ventricular zone

wm, white matter

WT, wild-type

zo-1, zonula occludens-1

Chapter 1: Introduction

1.1 Neural Development

The mammalian central nervous system (CNS) is a highly intricate and connected network of billions of neurons (Pakkenberg & Gundersen, 1997). As a result, the organization of a healthy and intact CNS is contingent upon the coordination of several cellular events during neural development. These events include **1)** the proliferation of neural stem (NSC) and/or progenitor cells, **2)** the differentiation of neurons and glia, **3)** the migration of neurons to their final destinations, **4)** the formation of distinct axons and dendrites, and **5)** the establishment of functional synapses (Nicolas & Hassan, 2014; Stiles & Jernigan, 2010). In the developing cortex (Fig. 1.1), most excitatory glutamatergic neurons are generated in the ventricular (VZ) and subventricular zones (SVZ) and radially migrate to their final destinations. In contrast, inhibitory GABAergic interneurons are born in the ganglionic eminences and tangentially migrate to their final positions (Fig. 1.1) (Corbin, Nery, & Fishell, 2001; Franco & Müller, 2013; H Troy Ghashghaei, Lai, & Anton, 2007; Luhmann, Fukuda, & Kilb, 2015; Marín & Rubenstein, 2003; Métin, Baudoin, Rakić, & Parnavelas, 2006; Nadarajah & Parnavelas, 2002). After migration, both excitatory and inhibitory neurons undergo the remaining steps of neural development described above, including axon/dendrite specification and elaboration, target selection, and synaptogenesis in order to establish a functional neural circuitry. The disturbance of one or more of these processes can often lead to neurodevelopmental disorders, resulting in abnormal brain morphology and function (Rubenstein, 2011). Therefore, it is crucial that we understand the biological processes that underlie neural development and can alter its normal course in the diseased state.

Fig. 1.1

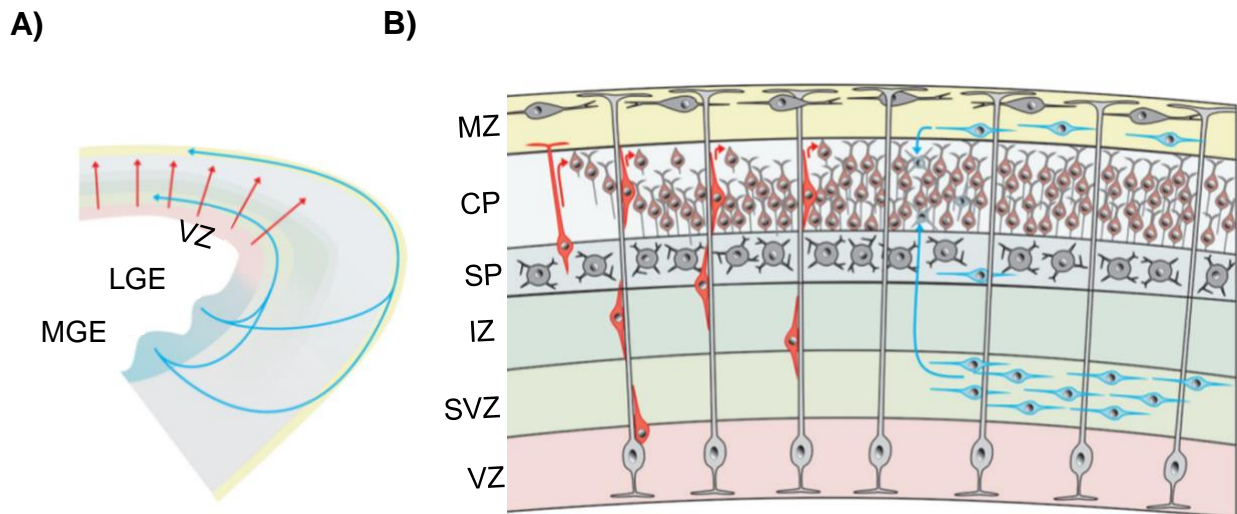


Figure 1.1: Radial and Tangential Migration of Neurons in the Developing Cerebral Cortex.

A) Schematic diagram of the radial migration of glutamatergic neurons (red arrows) born in the ventricular zone (VZ) to the cerebral cortex and the tangential migration of GABAergic interneurons (blue arrows) born in the medial (MGE) and lateral ganglionic eminences (LGE) to the cerebral cortex.

B) Glutamatergic neurons (different shades of red) migrate from the VZ by somal translocation or along radial glial fibers (light gray cells) to the marginal zone (MZ) and align on top of the previous layer of neurons of the cortical plate (CP). GABAergic neurons (different shades of blue) migrate in a tangential manner in the deep pathway within the subventricular (SVZ) and intermediate (IZ) zones or the superficial pathway in the MZ. Other GABAergic neurons travel within the subplate (SP).

This image was taken from (Luhmann et al., 2015) and was made available via license: CC BY

4.0

1.1.1 Cortical Interneuron Subtypes

Interneurons play a vital role in the proper wiring and circuitry of the developing CNS, as well as in their functionality. Cortical GABAergic interneurons encompass a highly heterogeneous group of cells that can mainly be divided into three large classes based on the expression of the calcium-binding protein parvalbumin (PV), the neuropeptide somatostatin (SST), or the ionotropic serotonin receptor 5HT3a (5HT3aR) [reviewed in (Kelsom & Lu, 2013; Rudy, Fishell, Lee, & Hjerling-Leffler, 2011)]. It is important to note that the heterogeneity of cortical interneurons leaves a minor subset of cells that do not fall in one of these three categories. The experiments in Chapter 4 of this thesis focus primarily on the morphometric analyses of PV (+) interneurons.

The PV (+) group of interneurons are born primarily in the ventral MGE and make up about 40% of the GABAergic cortical interneuron population (Ansen-Wilson & Lipinski, 2017; Rudy et al., 2011). PV (+) interneurons mainly consist of fast-spiking basket and chandelier cells (Kawaguchi & Kubota, 1997; Petilla Interneuron Nomenclature Group et al., 2008). These subtypes of interneurons differ in their morphology and axonal targeting. Basket cells, the most abundant and widespread subtype of GABAergic interneurons in the cortex, form synapses at the soma and proximal dendrites of their target neurons, while chandelier cells target the axonal initial segment (AIS) of pyramidal neurons (Kawaguchi & Kubota, 1997; Petilla Interneuron Nomenclature Group et al., 2008).

The SST (+) group of interneurons are born in the dorsal MGE and are the second largest interneuron group, making up about 30% of the total GABAergic cortical interneuron population (Ansen-Wilson & Lipinski, 2017; Kelsom & Lu, 2013; Rudy et al., 2011). The majority of SST (+) interneurons are Martinotti cells, which are most abundant in layer V of the cortex (Kawaguchi & Kubota, 1997; Uematsu et al., 2008; Yun Wang et al., 2004). These cells have

the ability to project their axons to layer I and establish synapses on the distal dendrites of pyramidal neurons (Kawaguchi & Kubota, 1997). The firing pattern of Martinotti cells is unique as they can display both “regular” and “burst” firing patterns (Kelsom & Lu, 2013; Rudy et al., 2011).

The 5HT3aR (+) group of interneurons are born in the caudal ganglionic eminence and account for about 30% of the total GABAergic cortical interneurons (Ansen-Wilson & Lipinski, 2017; S. Lee, Hjerling-Leffler, Zagha, Fishell, & Rudy, 2010; Rudy et al., 2011). 5HT3aR (+) interneurons can be further broken down into two subgroups: those that express vasoactive intestinal peptide (VIP (+)) and those that do not (VIP (-)) (Kawaguchi & Kubota, 1997; Q. Xu, Cobos, De La Cruz, Rubenstein, & Anderson, 2004; X. Xu, Roby, & Callaway, 2010). The fast-adapting VIP (+) interneurons generally form synapses on proximal dendrites; whereas the late spiking accommodating VIP (-) interneurons tend to target other GABAergic interneurons to provoke long-lasting inhibitory responses onto pyramidal neurons (Kelsom & Lu, 2013).

It is important to note that even though PV (+), SST (+), and 5HT3aR (+) interneurons can account for nearly 100% of the GABAergic interneurons in the cortex (Rudy et al., 2011), the high level of heterogeneity within the subtypes adds to the complexity of studying the development of cortical interneurons.

1.1.2 Stages of Neuronal Development in Culture

The current understanding of neuronal development, including neurite outgrowth, the establishment of neurite identity, and the regulation of neuronal polarity is largely based on research done in excitatory neurons and has extensively used *in vitro* model systems due to their advantages. Neuronal differentiation has been well-studied in the PC12 and neuroblastoma cell lines and also in primary hippocampal and cortical neuronal cultures (R. Hu et al., 2018; Kiryushko, Berezin, & Bock, 2004). First reported by Dotti, Sullivan, & Banker

(1988), several distinct stages (Fig. 1.2) were identified in the development of pyramidal hippocampal neurons when grown *in vitro* and used to identify distinct stages of neuronal development. Shortly after plating dissociated cells from E18 hippocampi, cells appear as round spheres containing several thin filopodia (**Stage 1**). Within 12-24 hours after plating, cells become multipolar displaying neurites (**Stage 2**). After 24-48 hours, one of these neurites shows an enlarged growth cone and begins to extend rapidly becoming the axon (**Stage 3**). About 3-4 days after plating, the remaining neurites differentiate into dendrites (**Stage 4**). At later stages the dendrites continue to mature and form dendritic spines and synapses (**Stage 5**) (Dotti, Sullivan, & Banker, 1988) (Fig. 1.2). These stages of *in vitro* neuronal development have been compared to and also match the stages of development observed for the more heterogeneous group of cortical neurons (Sakakibara & Hatanaka, 2015). However, it is important to note that the stages of GABAergic interneuronal differentiation may not follow this exact timeline *in vitro*, as it has previously been reported that cultured inhibitory cortical neurons exhibit delayed axon formation that may surpass 3 days *in vitro* (DIV) (Hayashi, Kawai-Hirai, Harada, & Takata, 2003). Taking this into consideration, the developmental stages first outlined by Dotti et al can still be used as landmarks to study the effects of various molecules, biological events, or other intrinsic and extrinsic factors on the progression of interneuronal development and differentiation in culture.

The use of such *in vitro* systems to follow the stages of neuronal development has the advantage of allowing the identification of cell autonomous mechanisms that may drive neuronal differentiation, such as those presented in this thesis. Furthermore, these systems also possess reproducible conditions and allow accessible manipulations of the levels of molecules driving differentiation through the introduction of plasmids and RNAs.

Fig. 1.2

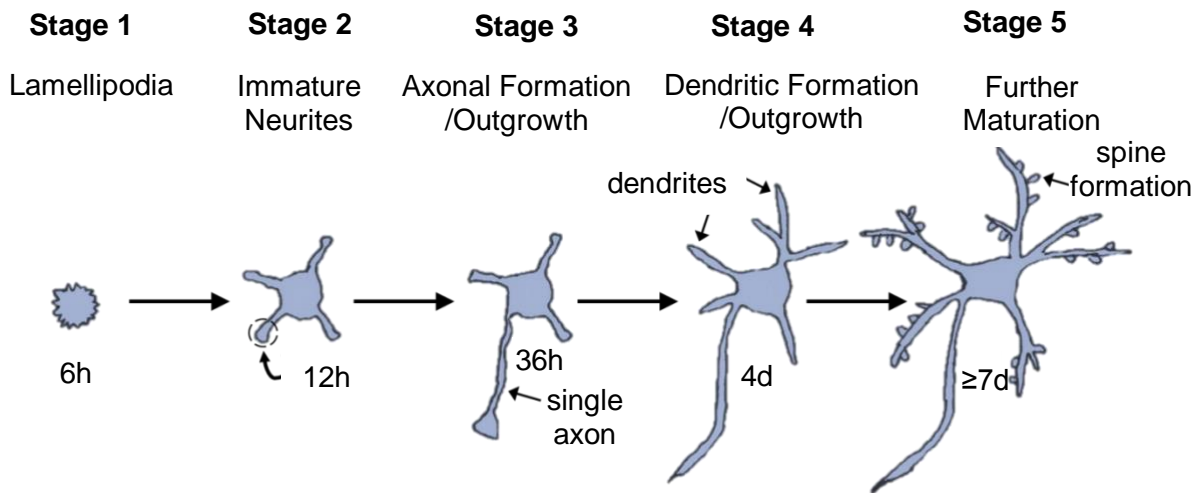


Figure 1.2: Stages of Neuronal Development *in vitro*.

Shown here is a simplified schematic, first reported by Dotti, Sullivan, and Banker in 1988, illustrating five stages of neuronal development that can be distinguished in cultured pyramidal hippocampal neurons. This figure was modified from (Govek, Newey, & Van Aelst, 2005) and was made available via license: CC BY 4.0.

1.1.3 Neurite Outgrowth and Axon Formation

Neurons have a particularly unique and characteristic morphology, consisting of a cell body from which several processes (neurites) can extend. Eventually, these neurites become structurally and functionally distinct, giving rise to generally one axon and multiple dendrites. The initiation and progression of neurite outgrowth and extension is one of several biological aspects that underlie proper neuronal differentiation (Khodosevich & Monyer, 2010).

There are four main steps that regulate neurite extension: an increase in the amount of plasma membrane, the localization and activation of various signaling molecules such as phosphatidylinositol 3-kinase (PI3K) and the Rho GTPases, an increase in actin dynamics, and the enhancement of microtubule formation (Fig. 1.4) (Arimura & Kaibuchi, 2007). During Stage 1 (Fig. 1.2) of neuronal development, the circumferential lamellipodium collapses in discrete regions and extends in others, giving rise to the newly formed dynamic neurites (Dehmelt, Smart, Ozer, & Halpain, 2003; Flynn, 2013; Flynn et al., 2012). One of the defining features of growing neurites and the developing axon are their highly dynamic growth cones (Fig. 1.3A), located within the distal tip of the processes. First described by Santiago Ramón y Cajal (1890), the growth cone has the ability to sense the environment and respond to extracellular cues to regulate neurite elongation and axonal pathfinding (Berzati & Hall, 2010; Lowery & Van Vactor, 2009). The main components that make up the growth cone are microtubules (MTs) and F-actin filaments, which are compartmentalized within specific domains of the growth cone (Fig. 1.3A for detailed description). The structure of the growth cone rapidly changes (Fig. 1.3B) in response to extracellular cues and is dependent on the polymerization and depolymerization of F-actin filaments. This gives rise to the three morphological changes observed in the growth cone during neurite and axonal growth: protrusion, engorgement, and consolidation (Fig. 1.3B for a detailed description) (Dent, Gupton, & Gertler, 2011; Lowery & Van Vactor, 2009).

Fig. 1.3

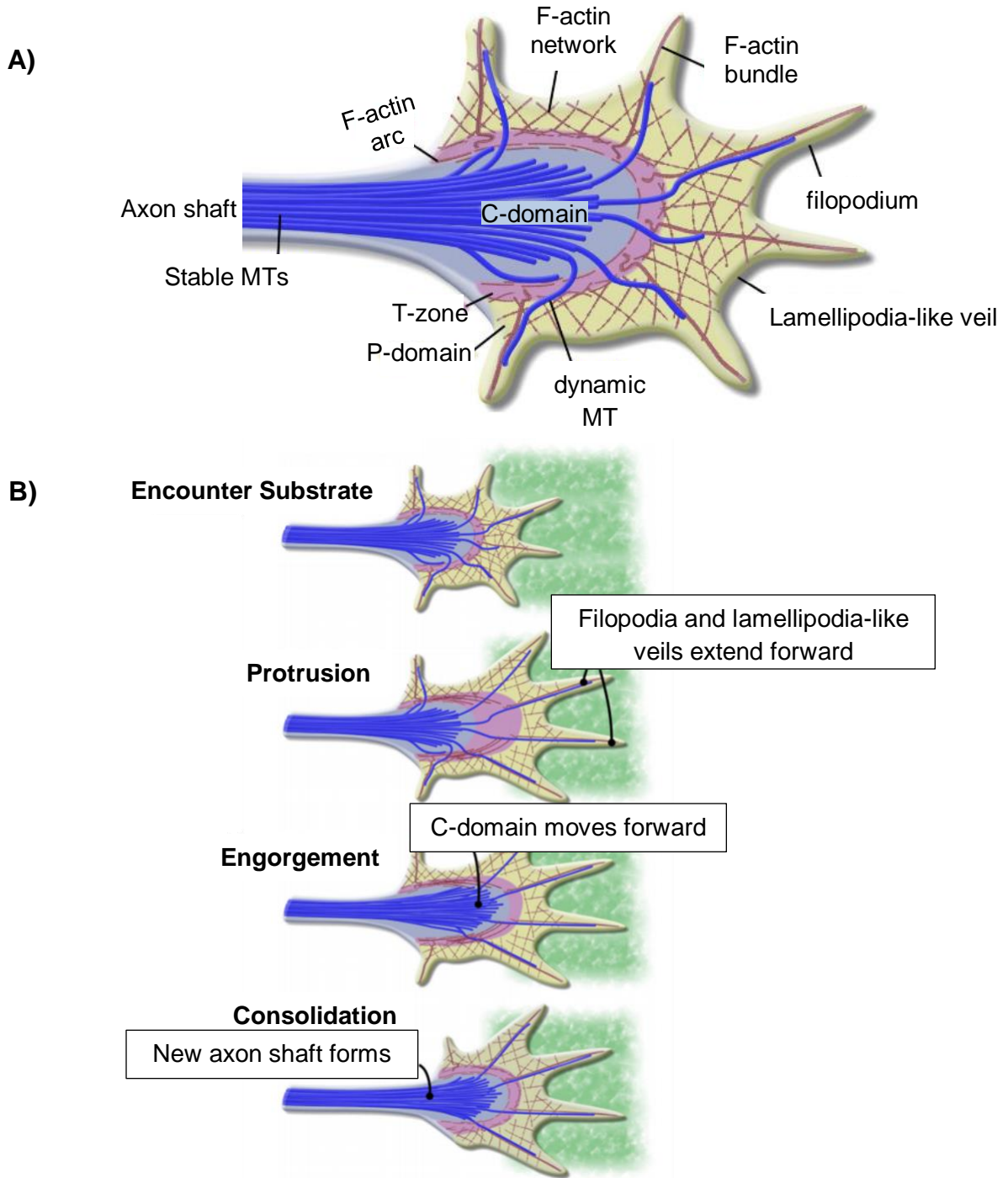


Fig. 1.3: The Growth Cone and Motility During Neurite Outgrowth and Axon Formation.

A) The structure of the growth cone. The leading edge of the growth cone consists of finger-like filopodia that are separated by sheets of membrane (lamellipodia-like veils). Three main domains can be identified in the growth cone based on distribution of cytoskeletal elements: the peripheral (P)-domain containing F-actin bundles, the central (C)-domain composed of stable and bundled MTs along with numerous organelles and vesicles, and the transition (T)-zone consisting of a thin interface between the P- and C-domains, containing anti-parallel bundles of F-actin and myosin known as actin arcs.

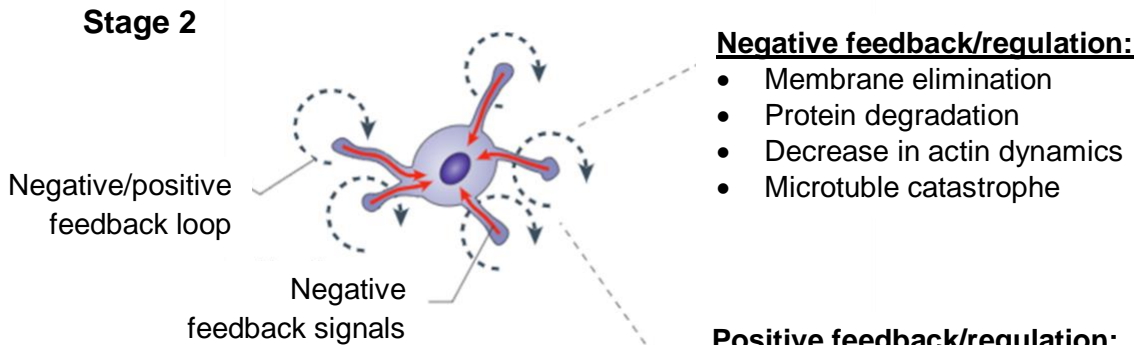
B) Growth cone motility. Filopodia first respond to guidance cues and stabilize (**panel 1**). During protrusion (**panel 2**), the F-actin further stabilizes and actin polymerization continues, resulting in the forward extension of filopodia and lamellipodia-like veils of the peripheral (P)-domain. Engorgement (**panel 3**) occurs after actin arcs clear and reorient towards the site of new growth. This is followed by C-domain MTs invading this region, bringing membranous vesicles and organelles. Finally, consolidation (**panel 4**) of the recently advanced C-domain occurs as the majority of F-actin depolymerize at the neck of the growth cone, allowing the membrane to compact around the MT bundle and form the new segment of axon shaft.

These figures were modified and used with permission from (Lowery & Van Vactor, 2009).

Prior to axonal and dendritic specification (Stage 2) (Fig. 1.2), neurites continue to undergo changes in cytoskeletal architecture resulting in neurite extension and retraction of all processes to maintain their overall neurite length. Although the exact mechanisms regulating this phenomenon are unknown, it is thought to involve positive and negative feedback loops mediated by signaling factors (Fig. 1.4) (Andersen & Bi, 2000; Arimura & Kaibuchi, 2007; Hapak, Ghosh, & Rothlin, 2018; Naoki, Nakamuta, Kaibuchi, & Ishii, 2011; Samuels, Hentschel, & Fine, 1996; Toriyama, Sakumura, Shimada, Ishii, & Inagaki, 2010). Immediately after neurite extension (described above), the neurite retracts counteracting the positive regulators of extension. This is followed by microtubule catastrophe, a decrease in actin dynamics, and a decrease in the amount of plasma membrane mediated by endocytosis and by blocking plasma membrane vesicle fusion (Fig. 1.4). Eventually, a positive cue initiated by extracellular signals, activation of receptors or adhesion molecules, and/or the recruitment of signaling molecules leads to a constitutive positive feedback loop, resulting in one of the neurites to elongate rapidly and become the axon. Simultaneously, strong negative feedback signals are generated in the axon, preventing other neurites from undergoing axon specification (Fig. 1.3) (Andersen & Bi, 2000; Arimura & Kaibuchi, 2007). This process gives rise to the polarized neuron. Although the exact mechanisms that regulate the positive feed loop are unknown, it has been suggested that the Par polarity complex is central in regulating the positive feedback loop that culminates in neuronal polarization (Arimura & Kaibuchi, 2007).

Fig. 1.4

A)



B)

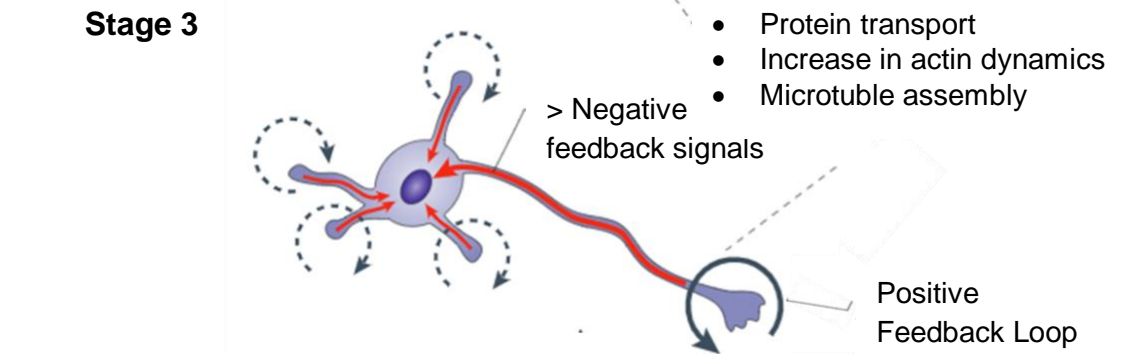


Fig. 1.4: The Positive/Negative Feedback Loop Model of Axon Specification.

This is a schematic of a tentative model for axon specification. **A)** At stage 2, all neurites extend and retract to maintain overall length via a positive/negative feedback loop. **B)** When the balance between the positive and negative signals is disrupted, one neurite rapidly elongates and becomes the axon. The axon further antagonizes the ability of axon specification of the other neurites via enhanced negative feedback signals (red arrows). This figure was modified and used with permission from (Arimura & Kaibuchi, 2007).

1.1.4 Neuronal Polarity and the Par Polarity Complex

Neurons are one of the most highly polarized cells in the body as they generally display a distinct morphology consisting of one long axon and several shorter dendrites that are molecularly, structurally, and functionally unique. It is important to note that this stereotypical morphology may not apply to a large number of neurons, as cortical neurons possess tremendous morphological variations. For example, Chapter 4 of this thesis contains an in-depth analysis of neurite outgrowth of cortical GABAergic interneurons, mainly PV (+) cells. Cortical PV (+) basket cells consist of three subtypes with highly diverse morphologies: small, large, and nest type (Yun Wang, Gupta, Toledo-Rodriguez, Wu, & Markram, 2002). Small basket cells extend short axons that innervate within the cell's dendritic range. In comparison, large basket cells have the ability to innervate through several cortical layers due to a long axon. Nest type cells are an intermediate, containing axons that can span a single cortical layer. A key player in the establishment of neuronal polarity and these morphological variations, including axonal growth, is a group of proteins known as the Par polarity complex [reviewed in (Arimura & Kaibuchi, 2007)], which are further studied in Chapter 5 of this thesis.

The active Par complex consists of a series of interacting proteins, including the partitioning-defective 3 (Par3), Par6, atypical protein kinase C (aPKC), and GTP-bound cell division cycle 42 (Cdc42) or Ras-related C3 botulinum toxin substrate 1 (Rac1) (Fig. 1.5A). The Par complex is responsible for multiple polarity-dependent events including asymmetric cell division, tight junction formation, directional migration, axon specification/growth, and the maintenance of the radial glial scaffold (Arimura & Kaibuchi, 2005; Bultje et al., 2009; Cappello et al., 2006; L. Chen et al., 2006; Chou, Li, & Wang, 2018; Costa, Wen, Lepier, Schroeder, & Götz, 2008; Dow & Humbert, 2007; Ghosh et al., 2008; Goldstein & Macara, 2007; Hapak, Rothlin, & Ghosh, 2018; Izumi et al., 1998; Knoblich, 2001; Takashi Nishimura et al., 2005; Solecki, Govek, & Hatten, 2006; Atsushi Suzuki & Ohno, 2006; Yokota et al., 2010). In a normal

cell, aPKC and Par6 can exist in a complex mediated through a high affinity binding interaction between their N-terminal PB1 (Phox and Bem1) domains (Hirano et al., 2005; A Suzuki et al., 2001). Par3 (via either its PDZ1 or PDZ3 domains) can associate with the Par6/aPKC complex and directly interact with the PDZ-binding motif in Par6 (Joberty, Petersen, Gao, & Macara, 2000; J. Li et al., 2010; Lin et al., 2000; Renschler et al., 2018). In addition, Par6 contains a CRIB (Cdc42/Rac-interactive binding) motif that is N-terminal to its PDZ domain and can interact with a small GTPase such as Cdc42 or Rac1. Association of Par6-aPKC with GTP-bound Cdc42 or Rac1 induces a conformational change of Par6 which leads to recruitment of Par3 and the phosphorylation of aPKC by Par3. This results in the active Par complex (Fig. 1.5A) (Henrique & Schweisguth, 2003; Krahn, Klopfenstein, Fischer, & Wodarz, 2010; Morais-de-Sá, Mirouse, & St Johnston, 2010; Nagai-Tamai, Mizuno, Hirose, Suzuki, & Ohno, 2002; Soriano et al., 2016). The active complex can then regulate changes in cytoskeletal architecture that are responsible for the establishment of cell polarity, morphology, and directed migration.

During the transition from Stage 2 to Stage 3 (Fig. 1.2) of hippocampal neuronal development, members of the Par complex shift from being compartmentalized to all neurites to being enriched in the distal tip of the future axon (Fig. 1.5B), where it regulates actin dynamics responsible for axon formation and growth (Takashi Nishimura et al., 2004; S.-H. Shi, Jan, & Jan, 2003). The suppression or ectopic expression of Par3 or Par6 in cultured hippocampal neurons inhibits neurons from undergoing axon specification (Takashi Nishimura et al., 2005; S.-H. Shi et al., 2003). In particular, the ectopic expression of Par3 results in multiple axon-like neurites which fail to differentiate into axons (S.-H. Shi et al., 2003). The transport of the Par complex to the distal end of the axon is regulated by the direct interaction of Par3 with the motor protein kinesin-2/KIF3A. The Par3-kinesin-2/KIF3A interaction results in Par3 performing as a cargo adaptor between the Par complex and kinesin-2/KIF3A, allowing for the transport of the entire complex to the distal axon (Funahashi et al., 2013; Takashi Nishimura et al., 2004). In

addition to the increased concentration of members of the Par complex, the axonal growth cone also shows an accumulation of ERK (Funahashi et al., 2013). A previous study demonstrated that ERK can phosphorylate Par3 at serine 1116, resulting in the disassociation of Par3 from kinesin-2/KIF3A but no disruption of the Par complex, suggesting that phosphorylation of Par3 may be necessary for the Par complex unloading from kinesin-2/KIF3A. These findings correspond with immunostaining in developing hippocampal neurons showing high levels of phosphorylated Par3 at the tip of the growing axon and the inability of axon formation in neurons expressing a phosphomimetic mutant of Par3 at serine 1116 (Funahashi et al., 2013). Disruption of the microtubule regulatory activity of Par3, via knockdown of endogenous Par3 and introduction of mutant Par3, results in impaired axon specification in hippocampal neurons (S. Chen et al., 2013).

Additionally, Par3 can play the role of a microtubule associated protein (MAP) in hippocampal neurons by binding to, bundling, and stabilizing microtubules (S. Chen et al., 2013). This role for Par3 in microtubule organization is dependent on Par3 conformation. In the closed conformation, the N-terminal and the C-terminal portions of Par3 interact, which suppresses the ability of Par3 to regulate microtubule organization. In the open conformation, Par3 accumulation results in intermolecular oligomerization allowing for the N-terminal portion of Par3 to directly bind to, bundle, and stabilize microtubules.

The kinase function of the Par complex is carried out by aPKC, allowing the complex to recruit other downstream molecules important for neuronal polarization. This kinase, in addition to being phosphorylated by Par3, can phosphorylate components of Par3 and Par6 as well as other polarity proteins [reviewed in (Hapak, Rothlin, et al., 2018)]. In vertebrates, there are two well classified aPKCs: aPKC ζ and aPKC λ/ι (λ in mouse, ι in humans) (Hirai & Chida, 2003). Further diversification of the aPKC isoforms in vertebrates arises from a constitutively active and truncated form lacking the N-terminus of aPKC ζ , known as PKM ζ (Hernandez et al., 2003). The

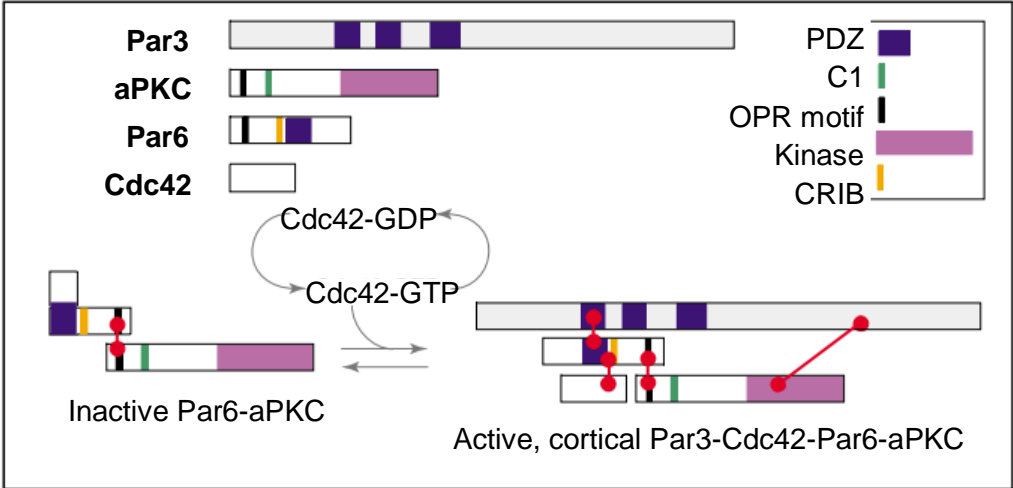
majority of reports demonstrating aPKC's role in neuronal polarity are attributed to the aPKC ζ variant (Hapak, Rothlin, et al., 2018). However, whether full length aPKC ζ is expressed in hippocampal neurons during axon formation is controversial and previous reports have suggested that the lack of isoform specific reagents have made it difficult to distinguish between the two full length aPKC ζ and aPKC λ variants (Hapak, Rothlin, et al., 2018; Parker et al., 2013). Nonetheless, there is strong evidence supporting a role for aPKC in the establishment of neuronal polarity, including roles in axon specification. Specifically, aPKC ζ was shown to regulate neuronal polarity of cultured hippocampal neurons, as the reduction of aPKC ζ activity, using a pharmacological approach, resulted in the inhibition of axon specification (S.-H. Shi et al., 2003). However, this pharmacological inhibitor, which was reported as a myristoylated pseudosubstrate peptide inhibitor selective for PKC ζ , has been challenged for its specificity to aPKC ζ (Hapak, Rothlin, et al., 2018). Furthermore, the overexpression in hippocampal neurons of the amino terminal domain of aPKC ζ (aPKC ζ -N), the domain which binds to Par6 and is absent in PKM ζ , resulted in neurites which failed to develop into axons (X. Zhang et al., 2007). A previous study showed distinct spatial localization of aPKC λ and PKM ζ in cultured hippocampal neurons and competing interactions of aPKC λ and PKM ζ with Par3 (Parker et al., 2013). Specifically, this study demonstrated that in Stage 3 neurons, aPKC λ and Par3 are expressed in the presumptive axon whereas PKM ζ and Par3 are expressed in the non-axon-forming neurites (Fig. 1.5B). Furthermore, they observed that PKM ζ competes with aPKC λ for Par3 association resulting in the dissociation of Par3-aPKC λ . In addition, the overexpression of PKM ζ inhibited axon specification; whereas, the silencing of PKM ζ or overexpression of aPKC λ resulted in supernumerary axons. The findings of this study suggest that aPKC λ -Par3 favors axon specification whereas PKM ζ -Par3 inhibits axon formation (Parker et al., 2013).

Other key players in regulating neuronal polarity are the Rho family of small GTPases, such as Rac1, RhoA, and Cdc42 (Hall, Paterson, Adamson, & Ridley, 1993). Rho GTPases

cycle between inactive GDP-bound and active GTP-bound states, allowing them to act as molecular switches for downstream molecules, which ultimately regulate changes in neuronal morphology through cytoskeletal reorganization (Hall et al., 1993). Cdc42 plays crucial roles in axon formation, including extension of growth cone filopodia (Arimura & Kaibuchi, 2007; Schwamborn & Püschel, 2004; Witte & Bradke, 2008). The conditional knockout of Cdc42 in the mouse cortex and hippocampus results in neurons with sprouted neurites but the inability to form axons, disrupted cytoskeletal organization, enlarged growth cones, and the inhibition of actin dynamics in filopodia (Garvalov et al., 2007). In comparison, expression of a constitutively active Cdc42 mutant induces the extension of multiple axon-like neurites in hippocampal neurons, but still shows impaired axon specification, suggesting an importance for the cycling of Cdc42 between its GDP-bound and GTP-bound states (Schwamborn & Püschel, 2004). The regulation of neuronal polarity via Cdc42 requires Cdc42 activity upstream of the Par3-Par6-aPKC complex (Schwamborn & Püschel, 2004). Phosphatidylinositol (3,4,5)-trisphosphate (PIP₃), a product of phosphoinositide 3-kinase (PI3K), activates Cdc42 and results in Cdc42 interaction with Par6 and then subsequently with the remaining Par complex members (Joberty et al., 2000; Johansson, Driessens, & Aspenström, 2000; Lin et al., 2000; Qiu, Abo, & Martin, 2000). Par3 can then directly interact with the Rac-specific guanine nucleotide exchange factors (GEFs) Tiam1/STEF, thus mediating Rac1 activation (Hamelers et al., 2005; Takashi Nishimura et al., 2005). Since Cdc42 is activated by a product of PI3K and GTP-Rac1 can activate PI3K, it has been suggested that a positive feedback loop involving PI3K, Cdc42, the Par complex, and Rac1 may be critical for actin filament remodeling regulating proper neuronal polarity (Arimura & Kaibuchi, 2007; Namba et al., 2015). It has previously been shown that the dominant-negative Par3 or the knockdown of Par3 inhibits Cdc42-regulated activation of Rac1 in the N1E-115 neuroblastoma cell line, suggesting an intimate role for Par3-Par6 with Cdc42 in regulating neuronal polarity through the activation of Rac1 (Takashi Nishimura et al., 2005).

Fig. 1.5

A)



B)

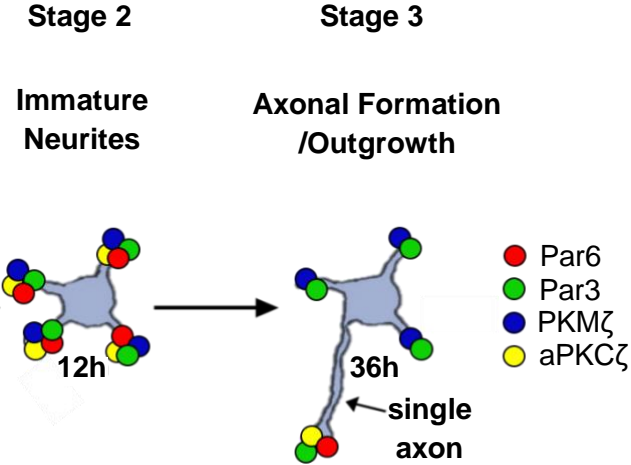


Fig. 1.5: The Par Polarity Complex in Axon Specification.

A) Shown here is a schematic of the domain organization and protein-protein interactions of the members of the Par polarity complex. Association of GTP-bound Cdc42 to the inactive Par6-aPKC complex induces a conformational change of Par6. Recruitment of Par3 can then initiate the phosphorylation of aPKC, resulting in the active Par complex. Direct associations between the Par complex members are designated with a red line. This image was used with permission from (Henrique & Schweisguth, 2003).

B) Localization of the members of the Par complex prior to and during axon specification. At Stage 2, Par6, Par3, aPKC, and PKM ζ are expressed in all neurites. During axon specification, at Stage 3, Par6, Par3, and aPKC are enriched at the tip of the axon; whereas, PKM ζ is enriched in the future dendrites and co-localizes with Par3.

Other than playing roles in axon/dendrite specification and axonal formation, the Par polarity complex has also been shown to be an important regulator of the radial glial scaffold. During the development of the brain, transient populations of highly polarized cells known as radial glia form a scaffold that is essential for guiding neurons from the germinal layers to their final destination. In radial glial progenitors, the Par complex is found to localize at the apical adherens junctions and this assembly is important for regulating asymmetric cell division, extension of radial glial fibers, and the branching of radial glial endfeet (Bultje et al., 2009; Cappello et al., 2006; L. Chen et al., 2006; Costa et al., 2008; Ghosh et al., 2008; Yokota et al., 2010). The asymmetric enrichment of the Par complex at the apical membrane of radial glial progenitors is important for undergoing self-renewal divisions (Singh & Solecki, 2015; Tabata, Yoshinaga, & Nakajima, 2012). As cortical development proceeds, there is a decrease in the amount of Par complex proteins at the apical surface, resulting in greater neurogenic divisions. The loss-of-function of Par3 in rodent models leads to premature cell cycle exit; whereas, the overexpression of Par3 or Par6 increases the number of self-renewing progenitor cells (Costa et al., 2008).

In addition to its role in polarity, the Par complex has also been observed to play a role in neuronal maturation of hippocampal pyramidal neurons through the formation and maintenance of dendritic spines (H. Zhang & Macara, 2006, 2008). Dendritic spines are small protrusions that receive the majority of excitatory synaptic inputs and are formed during later stages of neuronal development. Par3-TIAM1 interaction and localization to dendritic spines has previously been observed to regulate spine formation in hippocampal neurons (H. Zhang & Macara, 2006). This effect is independent of Par6-Par3 association. This same study showed that the silencing of Par3 resulted in the downregulation of spine formation and instead gave rise to multiple filopodia- and lamellipodia-like protrusions along the dendrites (H. Zhang & Macara, 2006). The Par6-aPKC complex has also been shown to play a role in dendritic spine morphogenesis,

independent of Par3 (H. Zhang & Macara, 2008). The knockdown of Par6 resulted in a lack of dendritic spine formation; whereas, the overexpression of Par6 increased spine density. These two studies suggest that Par6 may be playing a role the biogenesis and maintenance of dendritic spines; whereas, Par3 may be playing a role in their maturation (H. Zhang & Macara, 2006, 2008). The morphological changes that are observed during dendritic spine growth are regulated by actin dynamics (Martino et al., 2013). Therefore, unsurprisingly, the actin-regulating small G-proteins of the Rho-family play essential roles in spine formation and morphogenesis (Martino et al., 2013; Mi, Si, Kapadia, Li, & Muma, 2017). The activation of both Rac1 and Cdc42 has previously been shown to promote spine formation, growth, and stabilization of hippocampal pyramidal neurons (Martino et al., 2013). Overall, these aforementioned studies show that the members of the Par polarity complex play pertinent roles in dendritic spine morphogenesis.

To better understand the molecular mechanisms regulating the Par complex and its roles in neuronal polarity or other biological processes in the CNS, it is essential to identify both upstream and downstream molecules that can associate with the complex and ultimately alter actin dynamics. Previous studies have shown that activation of the receptor tyrosine kinases (RTKs) EGFR/ErbB1 and ErbB2 can phosphorylate Par3 or associate with Par6-aPKC respectively, resulting in alterations in epithelial polarity (Aranda et al., 2006; Yiguo Wang et al., 2006). In Chapter 5 of this thesis, we explore the association of ErbB4, another ErbB family member, with members of the Par complex. ErbB4-Par complex association was regulated by the activation of ErbB4 by its ligands, the neuregulin (Nrg) family of growth factors.

1.2 The Neuregulin (Nrg) Family of Growth Factors

The neuregulin (Nrg) growth factors (Fig. 1.6) are a family of four (Nrg1-4) structurally related signaling molecules that play important roles in the developing and mature nervous

system. In addition, the Nrgs have also been identified as key players in the development and maintenance of other organs such as the heart, breast, lungs, intestines, kidneys, gonads, and stomach (Douglas L Falls, 2003; Mei & Xiong, 2008). They are encoded by four genes (*nrg1-4*) of which three (*nrg1-3*) are expressed in the CNS and will be the subject of study in this thesis (Birchmeier & Bennett, 2016; Carraway et al., 1997; M. S. Chen et al., 1994; D L Falls, Rosen, Corfas, Lane, & Fischbach, 1993; Douglas L Falls, 2003; Holmes et al., 1992; Xihui Liu et al., 2011; Marines Longart, Liu, Karavanova, & Buonanno, 2004; Marchionni et al., 1993; Meyer et al., 1997; Rahman, Weber, Labin, Lai, & Prieto, 2018; D. Wen et al., 1992; D. Zhang et al., 1997).

1.2.1 Discovery and Isolation of the Nrgs

Nrg1 was the first of the Nrgs to be discovered and was done so by four independent groups in the early 1990s. These groups identified different biological functions of Nrg1 resulting in a diverse nomenclature distinguishing several multiple spliced variants of Nrg1 which are encoded by the same gene. Two groups first identified neu-differentiation factor (NDF) / heregulin after they observed a ligand that activated the ErbB2 (HER2) receptor (Holmes et al., 1992; Peles et al., 1992; D. Wen et al., 1992). Another group documented acetylcholine receptor inducing activity (ARIA) after the ligand was observed to enhance the surface expression of nicotinic acetylcholine receptors in cultured myotubes (Jessell, Siegel, & Fischbach, 1979). Finally, glial growth factor (GGF) was identified by another group after it induced proliferation and survival of Schwann cells (Goodearl et al., 1993; G. E. Lemke & Brockes, 1984; Marchionni et al., 1993). A few years subsequent to the discovery of Nrg1, the remaining three Nrgs (Nrg2/Don-1/NTAK, Nrg3, and Nrg4) were identified due to their sequence similarities to Nrg1 (Busfield et al., 1997; Carraway et al., 1997; Chang, Riese, Gilbert, Stern, & McMahan, 1997; Harari et al., 1999; Higashiyama et al., 1997; D. Zhang et al., 1997).

1.2.2 Molecular Structures of Nrg1-3 and Their Isoforms

1.2.2.1 Molecular Architecture and Alternative Splicing

The unprocessed Nrgs are membrane-bound proteins consisting of an extracellular domain, a transmembrane domain(s), and a cytoplasmic tail. They all contain an epidermal growth factor (EGF)-like domain in their extracellular region, which is required to activate members of the ErbB receptor tyrosine kinase (RTK) family. Although they share these structural features, the Nrgs (1, 2, and 3) differ in their domain organization and function (Fig. 1.6). Our current understanding of the biological functions of the Nrgs is complicated by not only the large number of isoforms that arise as a result of alternative splicing, but also by the diversity of posttranslational processing events such as proteolytic cleavage and glycosylation.

Among the Nrgs, Nrg1 has been the most extensively characterized and it exhibits the highest level of structural complexity (Fig. 1.6). The *Nrg1* gene gives rise to >30 isoforms of Nrg1, displaying a diversity of structural domains. These have been grouped into six types (I-VI) based on the presence or absence of several domains including an immunoglobulin (Ig)-like domain (found in Nrg1 Types I, II, IV, and V), a kringle domain (found in Nrg1 Type II), or a hydrophobic cysteine-rich domain (CRD; found in Nrg1 Type III) (Douglas L Falls, 2003; G. E. Lemke & Brockes, 1984; Xihui Liu et al., 2011; Steinthorsdottir et al., 2004). The extracellular domain of Nrg2 resembles the Ig-like domain containing isoforms of Nrg1, a domain absent from Nrg3 isoforms (Fig. 1.6). Little is known about the alternative splicing of Nrg3 in the rodent, in contrast to its detailed characterization in human (Carteron, Ferrer-Montiel, & Cabedo, 2006; Kao et al., 2010; Paterson et al., 2017; Zeledon et al., 2015). The *Nrg3* human transcripts have been categorized into four major types (I-IV) and have been shown to be dynamically regulated throughout prefrontal cortical development (Paterson et al., 2017).

Downstream of the variable portion of the N-terminal region, the Nrgs all contain an EGF-like domain which is sufficient to bind and activate the ErbB receptors (Fig. 1.6). Further structural diversity occurs through the alternative splicing at the carboxy-terminus of the EGF-like domain leading to α and β variants. These variants have shown distinct affinities for the ErbB3 and ErbB4 receptors, with preferential binding of the β variants to ErbB2/4 heterodimers (J. T. Jones, Akita, & Sliwkowski, 1999). In the brain, in parallel with higher affinities for ErbB3 and ErbB4, expression of the Nrg- β variants are more prevalent (Burgess, Ross, Qian, Brankow, & Hu, 1995; Kerber, Streif, Schwaiger, Kreutzberg, & Hager, 2003; D. Wen et al., 1994).

1.2.2.2 Proteolytic Cleavage

Most of the Nrg1 isoforms (type I, II, and IV) are single-pass transmembrane proteins with their EGF-like domain and N-terminal region located within the extracellular domain (Douglas L Falls, 2003). Nrg1 Type III is unique since it contains a CRD with an internal hydrophobic sequence, giving rise to a Nrg1 isoform containing two membrane-spanning regions with the N-terminus located in the cytosol (Fig. 1.6) (Schroering & Carey, 1998; J. Y. Wang, Miller, & Falls, 2001). Membrane bound Nrg1 can undergo proteolytic cleavage at the juxtamembrane region by α - and β -secretases (Fig. 1.6), including tumor necrosis factor- α converting enzyme (TACE) (Loeb, Susanto, & Fischbach, 1998), β -site amyloid precursor protein cleaving enzyme 1 (BACE1) (X. Hu et al., 2006; Willem, 2016), and meltrin β /ADAM19 (Yokozeki et al., 2007). For the single-pass transmembrane proteins, this results in the shedding of the Nrg1 ectodomain (including the EGF-like domain) into the extracellular space. This processed form of Nrg1 can then engage in ErbB receptor activation (Douglas L Falls, 2003). Catalytic cleavage of Nrg1 Type III leads to an EGF-like domain containing ectodomain, which can undergo ErbB receptor activation, but remains tethered to the cell membrane (J. Y. Wang et al., 2001). The cytoplasmic tail of Nrg1 Type III can be further cleaved by γ -secretase to release

the intracellular domain (ICD), which can then translocate to the nucleus to modulate transcription and gene expression (Bao et al., 2004; Bao, Wolpowitz, Role, & Talmage, 2003). Nrg2, similar to Nrg1 Type I, II, and IV, is also a single-pass transmembrane protein which has been observed to undergo proteolytic processing (Fig. 1.6) (Marines Longart et al., 2004).

Nrg3 resembles Nrg1 Type III in its topological organization, as it also contains two transmembrane domains (TM_N and TM_C) with its N-terminus located in the cytoplasm. Recent work using Nrg3-transfected neurons has shown that BACE1 proteolytically cleaves Nrg3 at a site between the second transmembrane domain (TM_C) and the EGF-like domain (Vullhorst, Ahmad, Karavanova, Keating, & Buonanno, 2017). Similar to Nrg1 Type III, this yields a transmembrane form of Nrg3 that remains tethered to the membrane via its TM_N domain (Fig. 1.6), giving rise to a structure that permits the EGF-like domain to engage ErbB receptors.

1.2.2.3 Glycosylation

Another potential post-translational modification that the Nrgs can undergo is the addition of carbohydrate moieties, referred to as protein glycosylation. All of the Nrgs produce gene products that are capable of post-translational modification by glycosylation within their extracellular domains. The Ig-containing isoforms of Nrg1 have the ability to undergo both N-linked and O-linked glycosylation in the region between the Ig and EGF-like domains (Burgess et al., 1995). In comparison, Nrg2 contains a potential site in the EGF-like domain for the addition of only N-linked sugars (Higashiyama et al., 1997). Nrg3 contains multiple potential glycosylation sites for O-linked sugars but does not contain sites for N-linked glycosylation (D. Zhang et al., 1997).

Fig. 1.6

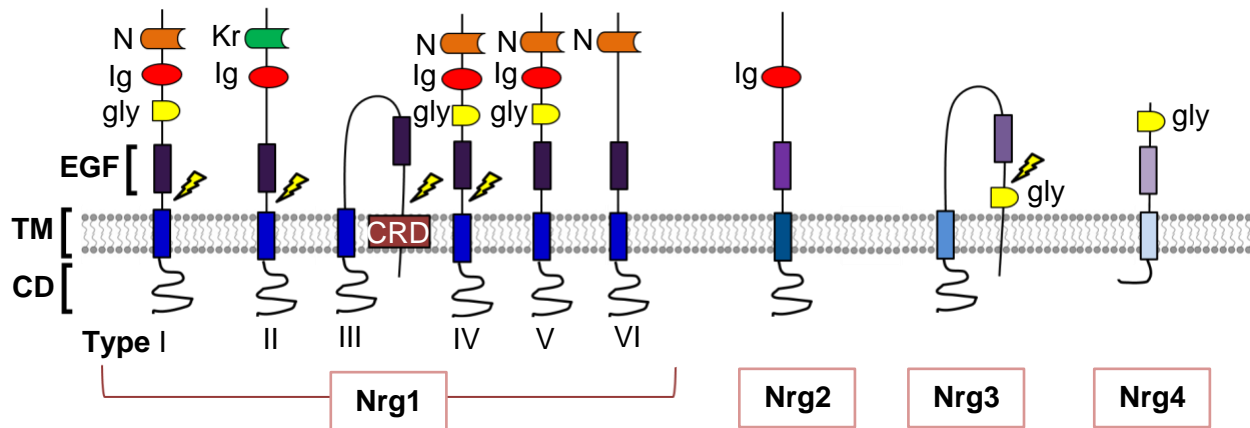


Figure 1.6: Nrg1-4 Domain Organization and Structure.

Shown here is a schematic of Nrg1 spliced variants, Nrg2, Nrg3, and Nrg4. All Nrgs, although they differ in their extracellular domains, contain an EGF-like domain required to bind to the ErbB receptors. Abbreviations: ARIA, acetylcholine receptor inducing activity; CRD, cysteine rich domain; CD, cytoplasmic domain; EGF, epidermal growth factor-like domain; GGF, glial growth factor; gly, glycosylation sites; HRG, heregulin; Ig, immunoglobulin-like domain; Kr, kringle domain; N, N-terminal domain (type specific); NDF, NEU differentiation factor; SMDF, sensory and motor neuron-derived factor; TM, transmembrane region; lightning bolt, proteolytic cleavage

1.3 The ErbB Receptor Tyrosine Kinase Family

The Nrg ligands signal through the binding and activation of members of the ErbB receptor tyrosine kinases (RTKs; Fig. 1.7A) (Mei & Nave, 2014). The ErbB family consists of four members, including epidermal growth factor receptor (EGFR/ErbB1), ErbB2, ErbB3, and ErbB4. The ErbBs were all cloned within the span of a decade from 1984-1993 (Bargmann, Hung, & Weinberg, 1986; Coussens et al., 1985; Kraus, Issing, Miki, Popescu, & Aaronson, 1989; Plowman et al., 1993; Ullrich et al., 1984; Yamamoto et al., 1986), and have been identified as important regulators of cellular responses fundamental for the development and maintenance of several tissues and organs [reviewed in (Paul & Hristova, 2018; Wieduwilt & Moasser, 2008)]

The ErbB receptors have also been well-studied in the context of their roles during tumorigenesis [reviewed in (Appert-Collin, Hubert, Crémel, & Bennisroune, 2015; Arteaga & Engelman, 2014; Roskoski, 2004; Z. Wang, 2017)]. Similar to other RTKs, the ErbB receptors all consist of an extracellular ligand binding-domain, a single transmembrane region, and an intracellular portion containing a tyrosine kinase domain and a cytoplasmic tail. Ligand binding of an ErbB receptor can initiate receptor homo- or heterodimerization, resulting in the activation of the kinase. This leads to the phosphorylation of specific tyrosine residues along the cytoplasmic tail (Fig. 1.7A). Phosphorylation of tyrosine residues creates docking sites for downstream signaling molecules which can trigger diverse intracellular signaling pathways, such as the MAPK and PI3K/AKT/mTor pathways (Mei & Nave, 2014). Activation of these downstream signaling pathways can then regulate numerous biological functions such as cellular differentiation, growth, migration, survival, and/or apoptosis (Grant, Qiao, & Dent, 2002; Mei & Nave, 2014). Functional diversification amongst the ErbBs arises from both the ability of various ligands and different receptor combinations to initiate unique receptor phosphorylation patterns, resulting in distinctive downstream signaling and cellular functions (Alroy & Yarden, 1997). It has previously been shown that Nrg1 can activate ErbB1/ErbB4 heterodimers

(Olayioye et al., 1998). ErbB2 has no known ligands that can activate it as a homodimer (“orphan receptor”), but it can participate and initiate signaling as part of a heterodimer with another ErbB family member (Fig. 1.7A) (Tzahar et al., 1996). ErbB3 can directly bind to Nrg1 and Nrg2 and also has unique receptor properties, as it has previously been reported to be kinase inactive or kinase “dead” (Guy, Platko, Cantley, Cerione, & Carraway, 1994). Other reports have indicated that ErbB3 has an active tyrosine kinase domain but shows low levels of activity (F. Shi, Telesco, Liu, Radhakrishnan, & Lemmon, 2010; Steinkamp et al., 2014). Of the ErbBs, ErbB4 is the only family member that can bind to and be activated by all four Nrgs and has been observed to function as both a homo- or heterodimer upon Nrg1, Nrg2 and Nrg3 activation (Fig. 1.7A) (Mei & Nave, 2014; Mei & Xiong, 2008).

1.3.1 ErbB4 Alternative Spliced Variants

The full length human cDNA clone of ErbB4 was first reported in 1993 and was observed to have structural similarities with the other members of the EGFR/ErbB family (Plowman et al., 1993). ErbB4 consists of an extracellular N-terminal region, a transmembrane domain, and a cytoplasmic C-terminal region. Similar to the other ErbBs, the extracellular portion of ErbB4 consists of a signal sequence, which is cleaved, and a ligand binding domain. The ligand binding domain can also be further divided into four subdomains (I-IV), which include two cysteine rich domains (II and IV) and two flanking domains (I and III). ErbB4 also contains 11 potential N-linked glycosylation sites within its extracellular domain. The cytoplasmic domain of ErbB4 consists of a juxtamembrane region, a tyrosine kinase domain, and a carboxy-terminal tail containing autophosphorylation sites (Fig. 1.7B) (Plowman et al., 1993).

Alternative splicing of *erbB4* can generate functionally distinct isoforms (Fig.1.7B). The differences between the isoforms are within the juxtamembrane (JM) domain (JM-a, JM-b, JM-c, and JM-d) or the C-terminal cytoplasmic (CYT) tail (CYT-1 and CYT-2) of the receptors (K

Elenius et al., 1999; Klaus Elenius et al., 1997; Gilbertson et al., 2001). These isoforms vary in their sequences, how they are processed, and their signaling potential [reviewed in (Junttila, Sundvall, Määttä, & Elenius, 2000) and discussed below].

The JM region of ErbB4 has been recognized to have four variants: JM-a, JM-b, JM-c, and JM-d (Klaus Elenius et al., 1997; Gilbertson et al., 2001). These isoforms of ErbB4 vary in their susceptibility to proteolytic cleavage (Fig. 1.7, B and C). The JM-a isoform contains a 23 amino acid sequence, with a cleavage site recognized by the tumor necrosis factor- α converting enzyme (TACE) and γ -secretase (Klaus Elenius et al., 1997; Rio, Buxbaum, Peschon, & Corfas, 2000). This type of cleavage is also known as ligand-activated regulated intramembrane proteolysis (RIP) (Fig. 1.7C) (Lal & Caplan, 2011; H.-J. Lee et al., 2002; Ni, Murphy, Golde, & Carpenter, 2001; Rio et al., 2000). ErbB4 JM-a RIP involves two distinct proteolytic cleavage events by TACE and γ -secretase, resulting in the release of the extracellular and intracellular domains of the receptor, respectively (H.-J. Lee et al., 2002; Ni et al., 2001; Rio et al., 2000). The cleaved intracellular domain can then traffic to the nucleus where it can operate as a transcriptional co-activator or co-repressor (Veikkolainen et al., 2011). A study by Sardi et al (2006) demonstrated that the cleaved intracellular domain of ErbB4 can form a ternary complex with TAK1 binding protein 2 (TAB2) and the transcriptional co-repressor N-CoR, resulting in their translocation to the nucleus and the repression of gene transcription involved in astrocyte differentiation (Sardi, Murtie, Koirala, Patten, & Corfas, 2006). In contrast to the JM-a isoform, the JM-b isoform contains a 13 amino acid sequence which does not contain any proteolytic cleavage sites (Klaus Elenius et al., 1997). The difference between JM-a and JM-b isoforms have not been observed to affect the affinity of ligand binding or tyrosine kinase activity (Klaus Elenius et al., 1997). The rare isoforms JM-c and JM-d either lack or contain both JM sequences, respectively (Gilbertson et al., 2001). The expression patterns of the JM isoforms of ErbB4 have been observed to be tissue specific. Epithelial tissues, such as the mammary gland,

have been reported to exclusively express the cleavable JM-a isoform (Veikkolainen et al., 2011); whereas, the JM-b isoform is found predominately in the heart, lung, and skeletal muscles (Klaus Elenius et al., 1997; Veikkolainen et al., 2011). Neural tissues, such as the cortex, hippocampus, and cerebellum express both JM-a and JM-b isoforms, but in general predominantly express the JM-b isoform (Klaus Elenius et al., 1997; Erben, He, Laeremans, Park, & Buonanno, 2018; Veikkolainen et al., 2011). JM-c and JM-d isoforms are rare and have been reported in medulloblastoma and fetal cerebellum; however, they have not been reported in normal adult tissues (Gilbertson et al., 2001).

In addition to the diversity in the JM region, ErbB4 isoforms can also differ in a region within the cytoplasmic tail of the receptor, resulting in the CYT-1 and CYT-2 variants (Fig. 1.7, B and C). The CYT-1 isoform contains a 16 amino acid sequence that is absent in the CYT-2 isoform (Fig. 1.7B) (K Elenius et al., 1999). This extra portion in the CYT-1 variant includes the consensus motif “Y-X-X-M”, which is a consensus binding site for the regulatory p85 subunit of PI3K (Cohen, Green, Foy, & Fell, 1996; K Elenius et al., 1999; Songyang et al., 1993). It has been verified that CYT-1 containing ErbB4 variants, but not CYT-2, are capable of directly recruiting the p85 subunit of PI3K, which leads to the activation of the PI3K pathway (Fig. 1.7C) (K Elenius et al., 1999). In contrast, the CYT-2 isoform is incapable of directly activating PI3K (Cohen et al., 1996; K Elenius et al., 1999). Other differences between the CYT isoforms have been observed in regards to endocytosis. CYT-1 isoforms can be efficiently endocytosed, whereas CYT-2 isoforms are endocytosis-deficient (Sundvall et al., 2008). This is due to the CYT-1 specific PPXY motif, which contains a site for a WW domain-containing E3 ubiquitin ligase, resulting in the localization of CYT1 isoforms into intracellular vesicles (Sundvall et al., 2008). Similar to the JM isoforms, the CYT isoforms also have been observed to be tissue specific. The CYT-1 isoform is predominately seen in the heart and breast whereas neural

tissues and kidney predominately express the CYT-2 isoform (K Elenius et al., 1999; Erben et al., 2018).

Fig. 1.7

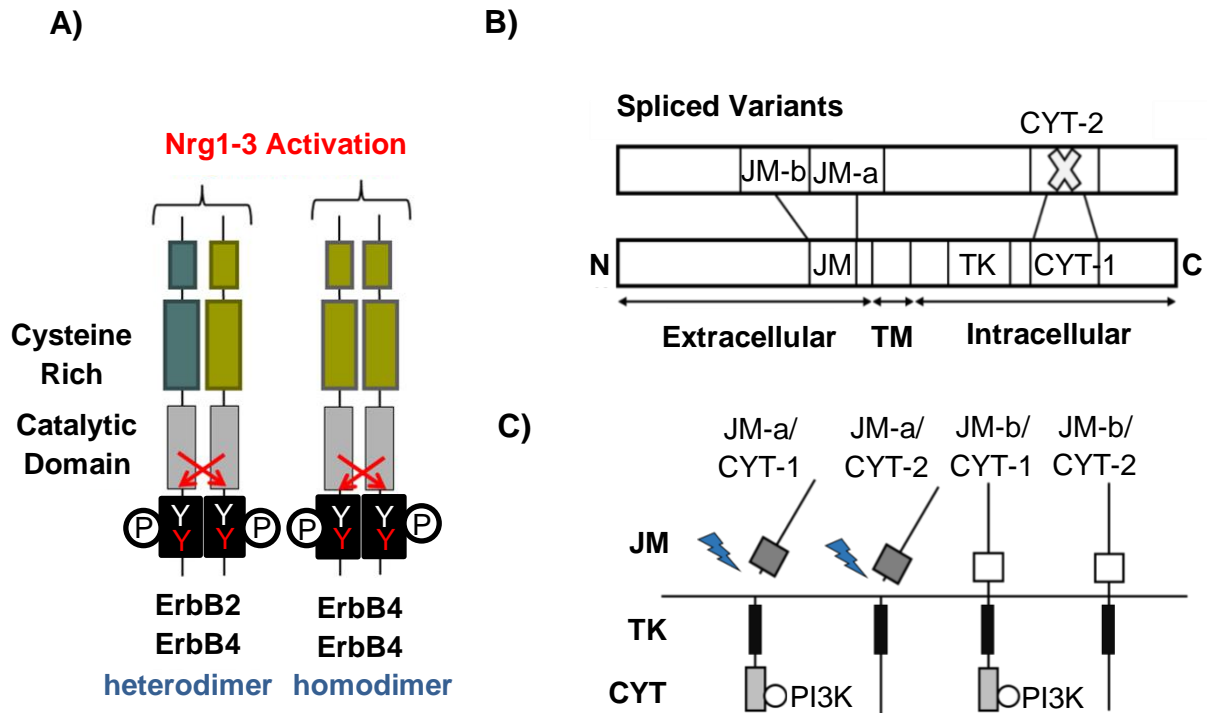


Fig. 1.7: Simplified Schematic of ErbB4 Structure and Alternatively Spliced Variants.

A) Nrg activation of ErbB homo- and heterodimers. Upon Nrg binding, ErbB receptors dimerize, inducing their kinase activity. This, in turn, results in the phosphorylation of tyrosine (red Y) residues, which act as docking sites for SH2 and PTB domain containing signaling molecules.

B and C) Alternative splicing gives rise to the four isoforms of ErbB4 found in the CNS. These isoforms differ in the extracellular juxtamembrane (JM) region, giving rise to the cleavable JM-a (23 amino acids) or membrane-bound JM-b (12 amino acids) variants. They also differ in their cytoplasmic region, giving rise to the CYT-1 (16 amino acids) or CYT-2 (absence of the CYT-1 region) variants. The CYT-1 region allows the ErbB4 receptor to activate the PI3K pathway, absent in the CYT-2 variants. Other abbreviations: TM, transmembrane domain; TK, tyrosine kinase domain. This figure was adapted with permission from (Law, Kleinman, Weinberger, & Weickert, 2007) and (Junttila et al., 2000).

1.4 Functions of Nrg-ErbB Signaling Outside of the CNS

1.4.1 Heart Development

Nrg1, ErbB2, and ErbB4 signaling play critical roles in heart development. In the embryonic heart, Nrg1 is expressed in the endothelial lining of the heart known as the endocardium; whereas ErbB2 and ErbB4 are expressed directly opposite to the endocardium in myocardial cells of developing cardiac muscle (Gassmann et al., 1995; K. F. Lee et al., 1995; Meyer & Birchmeier, 1995). In mice, between embryonic day 9 (E9) and E10.5, a significant transformation occurs. Cardiac myocytes proliferate and form trabeculae that are essential for later embryonic blood circulation [reviewed in (G. Lemke, 1996)]. Mice carrying homozygous mutations for ErbB2, ErbB4, Nrg1 (Nrg1^{-/-}), all Ig-Nrg1 isoforms (Ig-Nrg1^{-/-}), or the Nrg1 cytoplasmic tail die from heart defects associated with a failure of ventricular trabeculation at E10.5 (Erickson et al., 1997; Gassmann et al., 1995; Kramer et al., 1996; K. F. Lee et al., 1995; X Liu et al., 1998; Meyer & Birchmeier, 1995). It is important to note that ErbB3 is not expressed in the endocardium or the myocardium, but in the mesenchymal cells of the endothelial cushion (Meyer & Birchmeier, 1995), suggesting that the development of the trabeculae is dependent on ErbB2 and ErbB4 signaling. That is not to say that ErbB3^{-/-} mice do not show heart defects, as most of them die by E13.5 and exhibit cardiac cushion abnormalities leading to a reflux of blood through malfunctioning valves (Erickson et al., 1997). Nrg2 is expressed in the endothelial lining of the embryonic heart but, although there are changes in other phenotypes, Nrg2 knockouts have no apparent heart defects and survive embryogenesis (Britto et al., 2004; Carraway et al., 1997). Nrg3 is not detected in the heart, but is enriched in neural tissues instead, and Nrg3 knockout mice have not been reported to have any heart defects (Hayes et al., 2016; D. Zhang et al., 1997).

ErbB2 and ErbB4 knockout mice can survive embryogenesis via a “heart rescue” where the receptors are only expressed in cardiac cells. To rescue the ErbB2 null mutants, rat ErbB2 cDNA can be expressed under the control of a cardiac-specific α -myosin heavy chain (α -MHC) promoter (Morris et al., 1999) or under the control of the myocardium-specific *Nkx2.5* gene (ErbB2^{-/-} HER2^{heart}) (Woldeyesus et al., 1999). To rescue the ErbB4 null mutants, human ErbB4 cDNA can be expressed under the control of the α -MHC promoter (ErbB4^{-/-} HER4^{heart}) (Tidcombe et al., 2003). At E10.5, the “heart rescue” mice show ventricular trabeculation that is comparable to wild-type controls (Morris et al., 1999; Tidcombe et al., 2003; Woldeyesus et al., 1999). Although, the ErbB2^{-/-} HER2^{heart} mice survive embryogenesis, they are stillborn due to the loss of innervation within the diaphragm muscle (Morris et al., 1999; Woldeyesus et al., 1999). The ErbB4^{-/-} HER4^{heart} mice, on the other hand, survive until adulthood and are fertile (Tidcombe et al., 2003).

1.4.2 Breast Development

Nrg-ErbB signaling is crucial for the development of the mammary gland. Although the role of Nrg3 in the CNS is not well characterized, Nrg3 has been well-studied in the context of mammary development. Nrg3 is critical for the formation of mammary placode three, a cluster of primitive epithelial cells whose interactions direct the formation of the rest of the mammary gland [reviewed in (Cowan et al., 2003)]. Placode three is the first of the five placodes to form during embryonic mammary development in mice and occurs around E11.5 [reviewed in (Hens & Wysolmerski, 2005)]. Around the time of placode development, Nrg3 and ErbB4 are expressed in the presumptive mammary region around the future placode site (B. Howard, Panchal, McCarthy, & Ashworth, 2005). The co-expression of Nrg3 and ErbB4 at this site directly precedes the morphological appearance of mammary placodes (B. Howard et al., 2005), suggesting that Nrg3-ErbB4 signaling may regulate placode formation.

It has previously been shown that the downregulation of Nrg3, by a spontaneous hypomorphic allele of *nrg3* (*Nrg3^{ska}*) in mice, resulted in the unsuccessful formation of placode three, such that placode three was either hypoplastic or completely absent (B. A. Howard & Gusterson, 2000; B. Howard et al., 2005). Transgenic mice ectopically expressing full length *nrg3*, under the control of the periderm-expressing human K14 promoter, displayed abnormal mammary development (Panchal, Wansbury, Parry, Ashworth, & Howard, 2007). In particular, *nrg3* transgenic female mice showed supernumerary nipples and multiple mammary glands along and adjacent the mammary line when observed at postnatal day (P)12 (Panchal et al., 2007). Another study showed that the implantation of recombinant Nrg3 soaked agarose beads, along the mammary line of mouse embryonic explants, resulted in ectopic placode formation adjacent to the beads and the upregulation of the epithelial mammary bud marker *Lef1* (B. Howard et al., 2005). This effect was not observed when using agarose beads soaked with Nrg1 (B. Howard et al., 2005). Since Nrg3 soaked beads resulted in adjacent placode formation and in sites where endogenous placodes would not usually form, it is likely that Nrg3-ErbB signaling affects the migration of these cells during early mammary morphogenesis. It is important to note that since all the Nrgs and ErbBs are expressed in the developing mammary epithelium from E11-E13.5 (Wansbury et al., 2008), the entire Nrg-ErbB signaling network has the potential to play roles in mammosgenesis. In fact *ErbB4^{-/-} HER4^{heart}* mutant embryos exhibit minor defects in the mammary placode formation compared to *Nrg3^{ska}* embryos (Kogata, Zvelebil, & Howard, 2013; Tidcombe et al., 2003), suggesting that ErbB4 may predominantly be signaling through heterodimers, giving the ErbBs a redundant role during this early stage of mammary development.

Nrg1-ErbB signaling may play a role in fetal mammary stem cell (fMaSC) function, which are abundant during late fetal mammosgenesis (Spike et al., 2012). It was previously shown that the recombinant Nrg1-EGF domain enhanced the formation of large fMaSC-derived

mammospheres, while fMaSc cultures treated with the ErbB inhibitors Lapatinib and Neratinib inhibited fMaSc-derived sphere growth (Spike et al., 2012). These data suggest that Nrg1-ErbB signaling may be important for the regulation of mammary progenitor cells.

Other than the specification and formation of the basic mammary epithelium, the development of the mammary gland mainly occurs postnatally [reviewed in (Muraoka-Cook, Feng, Strunk, & Earp, 2008)]. ErbB2 plays a particularly interesting role in the mammary gland as it is amplified in up to 30% of human breast cancers (Slamon et al., 1987; M. Tan & Yu, 2013). ErbB2^{-/-} mammary buds transplanted into wild-type mammary fat pads resulted in a reduction in ductal outgrowth into the mammary fat pad due to defects in terminal end buds and increased lateral branching (Jackson-Fisher et al., 2004). Since there were no changes in cell proliferation or apoptosis, it is possible that lateral branching is preferred in the absence of ErbB2; whereas, the forward penetrations of the terminal end buds requires ErbB2 signaling. Lobuloalveolar development, on the other hand, was not affected in glands that developed from ErbB2^{-/-} mammary buds (Jackson-Fisher et al., 2004). These data suggest that ErbB2 signaling regulates the migration of mammary buds and may explain the metastatic nature of ErbB2 (+) breast cancers.

ErbB4 expression and activity has previously been observed to be the highest in mammary tissue during late pregnancy and early lactation (Schroeder & Lee, 1998). A previous study by Jones et al (1999) showed that mice lacking the intracellular domain of ErbB4 (ErbB4 Δ IC) showed condensed and undifferentiated lobuloalveoli at P12, suggesting a role for ErbB4 in the differentiation of the mammary epithelium (F. E. Jones, Welte, Fu, & Stern, 1999). These findings were later confirmed by two other groups using mouse models also lacking ErbB4 expression in the mammary gland (Long et al., 2003; Tidcombe et al., 2003). Furthermore, these ErbB4-deficient mouse models showed a deficiency in the transcription factor Stat5 and a downregulation of Stat5-regulated milk proteins β -casein and whey acidic

protein (F. E. Jones et al., 1999; Long et al., 2003; Tidcombe et al., 2003). In addition, previous studies have shown that Stat5 interacts with the intracellular domain of ErbB4 and mammary glands from *Stat5* null mice share strikingly similar phenotypes to ErbB4-deficient models. These data suggest that the intracellular domain of ErbB4 may regulate the translocation of Stat5 to the nucleus to regulate the expression of milk proteins.

In addition, it has been shown that the effects of ErbB4 in mammary development are dependent on whether ErbB4 is of the CYT-1 or CYT-2 variant. Ectopic expression of the intracellular domain of ErbB4 CYT-2 (ErbB4-ICD^{CYT2}) in mammary ductal epithelium resulted in enhanced ductal growth and epithelial hyperplasia (Muraoka-Cook et al., 2009). In contrast, the ectopic expression of the intracellular domain of ErbB4 CYT-1 (ErbB4-ICD^{CYT1}) resulted in a decrease in ductal growth and enhanced epithelial differentiation. Additionally, these mice showed Stat5 activation and consequently milk production (Muraoka-Cook et al., 2009). Taken together, previous findings have revealed that the Nrg-ErbB signaling is critical for embryonic and postnatal development of the mammary gland.

1.4.3 Schwann Cell Development and Myelination

In the PNS, Nrg1, ErbB2, and ErbB3 regulate Schwann cell development and myelination. It has previously been reported *in vitro* that Nrg1 Type I and Nrg 1 Type II can play a role in Schwann cell development (Dong et al., 1995; G. E. Lemke & Brockes, 1984). In particular, purified Nrg1 Type I was shown to enhance proliferation of cultured rat Schwann cells (G. E. Lemke & Brockes, 1984) and recombinant soluble Nrg1 Type II was observed to enhance proliferation, survival, and maturation of rat Schwann cell precursors (Dong et al., 1995). Although these isoforms of Nrg1 can play a role in Schwann cell development *in vitro*, the critical Schwann cell growth factor *in vivo* is axonal Nrg1 Type III [reviewed in (Mei & Nave, 2014)]. Mice lacking Nrg1 Type III (Nrg1 Type III^{-/-}) showed a striking reduction in the number of

Schwann cells, as well as a downregulation in the number of dorsal root ganglion (DRG) neurons and motor neurons, suggesting a function for the absent Schwann cells in the survival of their associated DRG and motor neurons (Wolpowitz et al., 2000). In addition, ErbB3 homozygous mutant mouse embryos (ErbB3^{-/-}) showed a lack of Schwann cell precursors and Schwann cells associated with sensory and motor neurons (Riethmacher et al., 1997). Furthermore, similar to the Nrg1 Type III^{-/-} mice, ErbB3^{-/-} mice also exhibited a severe loss of sensory DRGs and spinal motor neurons (Riethmacher et al., 1997; Wolpowitz et al., 2000). In parallel, ErbB2^{-/-} HER2^{heart} mutant mice displayed a complete lack of Schwann cells associated with peripheral nerves. In addition, these mice exhibited motor and sensory axons that were severely defasciculated and that projected abnormally (Morris et al., 1999). In the Nrg1 Type III, ErbB3, and ErbB2 mutants described, the mice either died prior to reaching full term or shortly after birth (Morris et al., 1999; Riethmacher et al., 1997; Wolpowitz et al., 2000). ErbB4, unlike ErbB2 and ErbB3, does not seem to play a role in the development of Schwann cells (Tidcombe et al., 2003). These studies show that Nrg1, ErbB2, and ErbB3 play a crucial role in Schwann cell development and consequently the survival and projection of the associated DRG and motor neurons.

The analyses of ErbB2 and ErbB3 mutant mice, at stages when myelination occurs, provided important evidence that the Nrg-ErbB signaling network also played a role in regulating myelin. A previous study deleted ErbB2 expression prior to myelination, using Cre-recombinase under the control of the *Krox20* gene (Garratt, Voiculescu, Topilko, Charnay, & Birchmeier, 2000). These postnatal mice displayed abnormally thin myelin sheaths, fewer myelin wraps, and aberrancies in the establishment of the Schwann cell precursor pool (Garratt et al., 2000). Furthermore, ErbB3 deletion in Schwann cells, using Cre-recombinase under the control of the *CNP* gene, resulted in postnatal mice with an even more severe deficit in myelination than that

observed for ErbB2 (Brinkmann et al., 2008). These data suggest that ErbB3 may partially compensate for the role of ErbB2 in peripheral myelination.

Axonal Nrg1 Type III can also play a role in regulating the amount of myelin that is generated in the PNS. A study by Michailov et al (2004) showed that heterozygotes with loss of gene dosage of *Nrg1* Type III (*Nrg1*^{+/-}) exhibited hypomyelination and consequently reduced nerve conduction velocity of peripheral nerves. However, heterozygotes with comparable loss of gene dosage of *erbb2* (*ErbB2*^{+/-}) did not result in a deficiency of myelin (Michailov et al., 2004). Moreover, this same study demonstrated that transgenic mice overexpressing Nrg1 Type III in neurons induced hypermyelination of axons in peripheral nerves. This effect was not observed when overexpressing Nrg1 Type I in neurons (Michailov et al., 2004). These data suggest that Nrg1 Type III is the responsible isoform for peripheral nerve myelination and the amount of axonal Nrg1 Type III may provide cues to myelinating Schwann cells regarding axon size (Michailov et al., 2004).

Schwann cells have the ability to individually myelinate large axons or ensheath a group of multiple thinner axons into “Remak bundles.” Taveggia et al (2005) previously showed that the amount of axonal Nrg1 Type III may provide information about axon size to the associated Schwann cells. In co-cultures of Schwann cells and sympathetic ganglion neurons from *Nrg1* Type III^{-/-} mice, the lentiviral-mediated overexpression of Nrg1 Type III in neurons resulted in hypermyelination by Schwann cells and an increase in the myelination of individual axons compared to wild-type. In comparison, nerve fibers of mice haplosufficient for Nrg1 Type III (*Nrg1* Type III^{+/-}) resulted in a greater proportion of axons with thinner myelin sheaths and an enhanced number of axons that were unmyelinated and fasciculated together in “Remak bundles.” In *Nrg1* Type III null mutants, Schwann cells failed to ensheath axons and even large axons remained unmyelinated (Taveggia et al., 2005). These data show that the amount of Nrg1 Type III can intimately regulate peripheral nerve myelination.

1.5 Functions of Nrg-ErbB4 Signaling in the CNS

1.5.1 Synaptic Formation

The work of several groups has revealed Nrg-ErbB signaling to play a significant role in synaptic formation in the CNS. Nrg-ErbB signaling has been demonstrated to mediate the formation and maturation of excitatory synapses on GABAergic interneurons. A previous study (Ting et al., 2011) demonstrated that treatment with Nrg1 enhanced the formation of excitatory synapses on cultured cortical GABAergic interneurons (5 DIV and 12 DIV), as quantified by the number of PSD-95 (+) excitatory synapses on proximal dendrites. Nrg1 treatment also enhanced the size of PSD-95 puncta, which is thought to be correlated with the maturation of excitatory synapses (El-Husseini, Schnell, Chetkovich, Nicoll, & Brecht, 2000; Keith & El-Husseini, 2008). It is important to note that this effect was dependent on developmental age of the culture, as Nrg1 treatment at 19 DIV increased the size of PSD-95 puncta but had no effect on number (Ting et al., 2011). Treatment at 13 DIV with ecto-ErbB4, which can bind and block the effects of endogenous Nrgs, resulted in a reduction in the number and size of excitatory synapses, suggesting a role for endogenous Nrg1 in synapse formation (Ting et al., 2011). A study by Abe et al (2011) demonstrated that the subcutaneous administration of Nrg1 to mouse pups resulted in an increase in excitatory inputs on parvalbumin (PV)-positive interneurons, as quantified by measuring miniature excitatory postsynaptic potential (mEPSC) frequency. Cortical GABAergic interneurons from these Nrg-treated mice also showed increased intensity in the immunoreactivity of GluA1 (+) puncta along the dendrites, confirming a role for Nrg1-ErbB signaling in excitatory synapse formation (Abe, Namba, Kato, Iwakura, & Nawa, 2011). In addition, a study by Krivosheya et al (2008) demonstrated that the postsynaptic overexpression of ErbB4 in hippocampal neurons increased the size, but not the number, of excitatory presynaptic inputs, as measured by staining for the excitatory synapse markers synaptophysin and vGlut1. In contrast, the shRNA knockdown of ErbB4 in GABAergic hippocampal

interneurons decreased the size of excitatory synapses (Krivosheya et al., 2008). The genetic deletion of ErbB4 from PV (+) interneurons resulted in reductions in the frequency of mEPSCs as well as in the density of vGlut1 (+) terminals, further suggesting a role for Nrg-ErbB4 signaling in excitatory synapse formation (Del Pino et al., 2013; Fazzari et al., 2010; Ting et al., 2011). It is important to note, however, that *erbb4* was only observed to play a role in the maturation but not in initial formation of excitatory synapses on PV (+) interneurons of the medial prefrontal cortex (mPFC) (J.-M. Yang et al., 2013).

In addition to Nrg1 playing a role in the formation of excitatory synapses on interneurons, it has recently been shown that Nrg3 can regulate the formation of excitatory synapses on hippocampal neurons. A study by Müller et al (2018) demonstrated that presynaptic Nrg3 acted on postsynaptic ErbB4 to increase the number of excitatory synapses on ErbB4 (+) interneurons. This effect by Nrg3 required postsynaptic ErbB4 but not ErbB4 kinase activity. In addition, cultured hippocampal neurons from Nrg3 mutant mice (*Nrg3^{-/-}*) showed a reduction in the number of vGlut1/2 (+) excitatory synapses on ErbB4/PV (+) interneurons, further suggesting a role for Nrg3 in excitatory synaptogenesis (Müller et al., 2018).

In addition to their role in the formation and maturation of excitatory synapses on interneurons, Nrg-ErbB4 signaling has been found to play a role in the formation and maturation of GABAergic inhibitory synapses onto pyramidal neurons. Using a tetracycline-inducible (*Tet-On*) expression system to deplete Nrg2, it was previously shown that the extracellular domain of Nrg2 was important for GABAergic synaptogenesis on newborn dentate gyrus granule neurons, as measured by GABAergic postsynaptic currents in organotypic slice cultures (K.-H. Lee et al., 2015). Additionally, it has previously been observed that the ablation of *erbb4* in chandelier cells resulted in this subtype of PV (+) interneuron to make fewer synapses on the axon initial segment (AIS) of pyramidal neurons in the hippocampus and prefrontal cortex (Del Pino et al., 2013; Fazzari et al., 2010). Furthermore, the overexpression of Nrg1 Type III in pyramidal

neurons increased the number of inhibitory synapses onto the AIS of pyramidal neurons (Fazzari et al., 2010). These effects were not observed for basket cells, suggesting functional differences of ErbB4 signaling in different subtypes of PV (+) interneurons (Del Pino et al., 2013).

The role of Nrg-ErbB4 signaling on synapse formation between pyramidal neurons or between interneurons is less understood. Treatment of cultured cortical cells with Nrg1 showed no changes in the size or number of PSD-95 (+) puncta in CaMKII (+) pyramidal neurons (Ting et al., 2011). These findings were additionally confirmed by other studies since there were no observed changes in mEPSCs in pyramidal neurons after Nrg1 treatment. In contrast, using a *Tet-On* expression system to deplete Nrg2, it was previously shown that the intracellular domain of Nrg2 was critical for glutamatergic synapse formation on granule cells of the dentate gyrus, as measured by EPSCs in organotypic slice cultures. This effect was independent of ErbB4 (K.-H. Lee et al., 2015).

Furthermore, Nrg1 treatment of cultured cortical neurons showed no changes in the number or size of puncta in GABAergic interneurons expressing gephyrin, a marker for inhibitory synapses (Ting et al., 2011). In addition, it has been shown that the formation and maturation of inhibitory synapses on basket cells of the mPFC may be independent of ErbB4 signaling, as there were no observed changes in inhibitory postsynaptic potentials (IPSCs) in ErbB4 mutants (J.-M. Yang et al., 2013). In contrast, a previous study (Krivosheya et al., 2008) reported that the overexpression of ErbB4 in hippocampal interneurons showed increased intensity in immunoreactivity, but not increased density, of the inhibitory synapse markers vGAT or synaptophysin in GABAergic interneurons. The opposite effect was observed in GABAergic interneurons where ErbB4 was knocked down (Krivosheya et al., 2008). These findings suggest a possible role for Nrg-ErbB4 signaling in the maturation but not formation of inhibitory synapses on interneurons. Furthermore, low levels of Nrg3 staining were previously reported in inhibitory

synapses in GABAergic interneurons (Müller et al., 2018); however, the effects of Nrg3 signaling on inhibitory synaptogenesis remain unexplored. Further studies are required to delineate the role of Nrg-ErbB4 signaling in synapse formation between interneurons.

1.5.2 Neurotransmission and Neuroplasticity

In the postnatal brain, Nrg-ErbB signaling has been shown to regulate neurotransmission and neuroplasticity. In the mature CNS, ErbB4 is expressed mainly in GABAergic interneurons, with preferential expression in a subset of PV (+) interneurons (Fazzari et al., 2010; Krivosheya et al., 2008; Neddens et al., 2011; Vullhorst et al., 2009; Woo et al., 2007). ErbB4 has previously been reported to localize to glutamatergic synapses on interneurons, the axon terminals of PV (+) basket and chandelier cells, and the somatodendritic compartment adjacent to glutamatergic postsynaptic sites in basket cells (Fazzari et al., 2010; Ting et al., 2011; Vullhorst et al., 2009; Woo et al., 2007).

ErbB4 signaling has been observed to promote GABA release in both the hippocampus and the cortex, which can be further accentuated with the treatment of Nrg1 (Y.-J. Chen et al., 2010; Woo et al., 2007). In support for these observations, it has previously been shown that the treatment of hippocampal slices with Nrg1 resulted in a suppression of long-term potentiation (LTP) at Schaffer collateral-CA1 synapses (Y. Z. Huang et al., 2000; Ma et al., 2003). Treatment with a pharmacological inhibitor against the ErbB tyrosine kinase or the deletion of the *erbb4* gene had opposite effects of Nrg1 treatment and resulted in a reduction of GABAergic transmission, an increase in glutamatergic transmission, and enhanced LTP (Y.-J. Chen et al., 2010; O.-B. Kwon, Longart, Vullhorst, Hoffman, & Buonanno, 2005; Pitcher, Beggs, Woo, Mei, & Salter, 2008; Shamir et al., 2012; L. Wen et al., 2010; Woo et al., 2007). In PV-Cre; ErbB4^{-/-} mutant mice, in which ErbB4 was specifically knocked out in PV (+) interneurons, Nrg1 treatment was unable to suppress LTP in CA1 pyramidal cells (Y.-J. Chen et al., 2010; Shamir

et al., 2012). These data suggest that Nrg1-induced suppression of LTP requires the signaling of ErbB4 in PV (+) interneurons.

Further evidence that Nrg-ErbB signaling plays a role in synaptic transmission was observed in mouse models of epilepsy. It was previously shown that both endogenous and exogenous Nrg1 increased the excitability of cortical fast-spiking PV interneurons and decreased the excitability of pyramidal neurons (K.-X. Li et al., 2012). This effect was found to be mediated in an ErbB4-dependent manner by the phosphorylation of the voltage-gated potassium channel, Kv1.1, resulting in reduced epileptogenesis (K.-X. Li et al., 2012; G.-H. Tan et al., 2011). In addition, PV-Cre; ErbB4^{-/-} mutant mice were more susceptible to seizures, and did not show Nrg1-mediated inhibition of epileptogenesis. They also showed decreases in Kv1.1 tyrosine phosphorylation, suggesting hyperexcitability of pyramidal neurons in these mutant mice (K.-X. Li et al., 2012; G.-H. Tan et al., 2011). Interestingly, these excitatory effects in interneurons were not observed in dissociated ErbB4 (+) hippocampal cells (Janssen, Leiva-Salcedo, & Buonanno, 2012) or in granule neurons (Yao, Sun, Zhao, Wang, & Mei, 2013). In addition, Janssen et al (2012) previously reported that Nrg1 treatment decreased voltage-gated sodium currents in hippocampal interneurons and reduced their excitability (Janssen et al., 2012).

There are several models as to how Nrg1-ErbB4 signaling may regulate neurotransmission and neuroplasticity [reviewed in (Mei & Nave, 2014)]. First, it is possible that Nrg1 activation of ErbB4 at axon terminals results in GABA release causing the inhibition of firing by pyramidal neurons and LTP suppression. In support of this model are studies showing that the effects of Nrg1 treatment in reducing LTP are blocked by GABA_A receptor antagonists (Y.-J. Chen et al., 2010; Woo et al., 2007). A study by Woo et al (2007) showed that, in cortical slices, Nrg1 treatment increased GABA release and that this effect was dependent on ErbB4 activation at axon terminals of GABAergic neurons. The use of a GABA_A receptor antagonist

abolished the effects of Nrg-induced GABA release but the effects of Nrg1 remained unchanged with treatment of antagonists against metabotropic glutamate receptors, cholinergic receptors, serotonin receptors, adrenergic receptors, dopamine receptors, or a combination of the antagonists (Woo et al., 2007). In addition, a study by Mitchell et al (2013) showed that treatment of dissociated hippocampal cultures with Nrg2 promoted the clustering and association of ErbB4 with α 1-containing GABA_A receptors in interneurons. This resulted in the internalization of the GABA_A receptors, via clathrin-dependent endocytosis which required PKC activity. Nrg2-induced GABA_A receptor internalization was correlated with a decrease in synaptic GABAR currents on hippocampal inhibitory neurons (Mitchell et al., 2013), suggesting an increase in GABAergic transmission.

The second model suggests that Nrg1-ErbB4 signaling functions by affecting glutamatergic synapses through its regulation of N-methyl-D-aspartate receptors (NMDARs) and α -amino-3-hydroxy-5-methyl-4-isoxazolepropionic acid receptors (AMPA receptors). In a study by Gu et al (2005), Nrg1 treatment of cultured prefrontal cortex (PFC) pyramidal neurons and PFC slices reduced NMDAR-mediated currents and EPSCs. This effect was blocked by an ErbB receptor tyrosine kinase inhibitor as well as inhibitors of the PLC/IP₃R/Ca²⁺ and Ras/MEK/ERK signaling pathways (Gu, Jiang, Fu, Ip, & Yan, 2005). A study by Pitcher et al (2011) demonstrated that Nrg1-ErbB4 signaling suppressed NMDAR currents, by presumably, preventing Src-mediated enhancement of NMDAR function (Pitcher et al., 2011). These results were particularly interesting as previous reports have shown that ErbB activation actually enhances the activity of Src or Src-like kinases (H. Kim et al., 2005; Olayioye, Beuvink, Horsch, Daly, & Hynes, 1999). In addition, Nrg2 signaling has also been shown to regulate the expression of NMDARs in cortical interneurons. A study by Vullhorst et al (2015) showed that ErbB4 and Nrg2 were co-expressed in cortical interneurons and activation of NMDARs resulted in the shedding of the Nrg2 extracellular domain in these cells. As a result, Nrg2-ErbB4

activation stimulated ErbB4 receptor association with GluN2B-containing NMDARs, leading to their internalization, and consequently a reduction in NMDA currents in ErbB4 (+) interneurons (Vullhorst et al., 2015).

The third model suggests a role for Nrg1-ErbB signaling in the regulation of dopamine and D4 dopamine receptors (D4Rs) in LTP. A study by Kwon et al (2008) showed that Nrg1 treatment stimulated the release of dopamine and activation of D4Rs, resulting in a reduction in LTP in the hippocampus. Treatment of acute hippocampal slices with D4R antagonists or slices obtained from D4R null mice failed to depotentiate LTP upon exposure to Nrg1, suggesting a role for Nrg1-ErbB signaling in dopamine release (O. B. Kwon et al., 2008). Future studies are required to determine which neuron subtypes expressing D4Rs are affected by Nrg1-regulated dopamine release. In one study, Andersson et al (2012) reported that D4Rs and ErbB4 were co-expressed in a subset of PV (+) interneurons in the CA3 region of the hippocampus (Andersson et al., 2012). Since it has previously been shown that dopamine can promote the release of GABA (Harsing & Zigmond, 1997), it is possible that the D4Rs located in ErbB4/PV (+) cells may be promoting GABA release in these cells.

In addition to the roles of Nrg1 and Nrg2 in synaptic transmission, Nrg3 has recently been identified to mediate glutamatergic transmission independent of ErbB4 activation (Müller et al., 2018; Y.-N. Wang et al., 2018). Using a *Nrg3*-floxed mouse (*Nrg3^{fl/fl}*) crossed with *hGFAP::Cre* mice, Wang et al (2018) generated mice lacking Nrg3 expression in the brain (*GFAP-Nrg3^{fl/fl}*). *GFAP-Nrg3^{fl/fl}* mutant mice showed an increase in glutamatergic transmission as measured by an enhancement in sEPSC frequency. Knocking out Nrg3 specifically in pyramidal neurons (*Nex-Nrg3^{fl/fl}*) had similar effects to *GFAP-Nrg3^{fl/fl}* mutant mice, suggesting that these effects on glutamatergic transmission were regulated by Nrg3-expressing pyramidal neurons. Enhancing Nrg3 resulted in the suppression of glutamate release and the inhibition of the assembly of the SNARE-complex, a group of proteins critical for vesicle fusion, at presynaptic

terminals (Y.-N. Wang et al., 2018). These findings support a role for Nrg3 in the regulation of glutamatergic transmission in a cell-autonomous manner in pyramidal cells.

1.5.3 Neuronal Migration

In the developing cortex, Nrg-ErbB signaling has been suggested to play a role in the tangential migration of GABAergic interneurons from the ganglionic eminences to their final destinations (Bartolini et al., 2017; Fisahn, Neddens, Yan, & Buonanno, 2009; Flames et al., 2004; Fornasari et al., 2016; H. Li, Chou, Hamasaki, Perez-Garcia, & O'Leary, 2012; Perez-Garcia, 2015). In support of the role of Nrg-ErbB signaling in GABAergic neuron migration is the early expression of ErbB4 detected in progenitors of the medial ganglionic eminence (MGE), as well as the sustained expression of ErbB4 in interneurons tangentially migrating from the MGE to the dorsal telencephalon (Yau, Wang, Lai, & Liu, 2003). Nrg1 is also expressed in the trajectory that migrating interneurons follow to the cortex and has been suggested to act as a long and short-range chemoattractant for MGE-derived neurons expressing ErbB4 (Flames et al., 2004; Fornasari et al., 2016). In addition, the ectopic expression of Nrg1 Type I in slice cultures can divert the normal route of migration of ErbB4 (+) migrating interneurons in the MGE towards Nrg1-expressing cell aggregates (Flames et al., 2004). More recently, it has been reported that Nrg3 expressed by developing pyramidal neurons can act as a short-range chemoattractant and guide ErbB4-expressing interneurons into the developing cortical plate (Bartolini et al., 2017). An overexpression of Nrg3 in developing pyramidal cells in the VZ of the pallium resulted in an invasion of interneurons within the cortical plate (Bartolini et al., 2017). Furthermore, the deletion of *nrg3* from developing pyramidal neurons or the conditional knockout or disruption of the *erbb4* gene upset the laminar distribution of cortical interneurons and interneuron migration to the cortex and hippocampus (Bartolini et al., 2017; Fisahn et al., 2009; Flames et al., 2004; H. Li et al., 2012; Perez-Garcia, 2015). In contrast to the studies just described, a previous study by Li et al (2012) suggested that Nrg1 and Nrg3 could be acting as

chemorepellents for migrating ErbB4 expressing MGE interneurons. This study reported that Nrg1 Type I, Nrg1 Type III, and Nrg3 expression showed minimal overlap with ErbB4 (+) interneurons migrating from the MGE to the cortex. They further demonstrated that MGE-derived migrating ErbB4 (+) interneurons avoided domains that expressed Nrg1 and Nrg3, suggesting that these Nrgs create barriers that define migratory pathways that funnel the developing GABAergic interneurons to their final destinations in the cortex (H. Li et al., 2012). Although there are discrepancies in how the Nrgs affect the migration of developing ErbB4 interneurons, there is mounting evidence suggesting that Nrg-ErbB4 signaling is a key player in proper interneuron migration.

Nrg1-ErbB4 signaling has also been suggested to play a role in the migration of MGE-derived striatal interneurons (Villar-Cerviño et al., 2015). It has previously been shown that both Nrg1 Type III and ErbB4 are expressed in the developing striatum during the time of cortical and striatal interneuron migration (Flames et al., 2004; Villar-Cerviño et al., 2015), suggesting a role for Nrg1-ErbB4 signaling in the migration of striatal interneurons to their final destinations. Using conditional ErbB4 knockout mice (*ErbB4*^{-/-}; *HER*^{heart}), Villar-Cerviño et al (2015) observed that a lack of ErbB4 in MGE-derived migrating interneurons resulted in a reduction in neurons reaching the striatum; however, this phenotype was not a result of impaired motility but impaired migratory direction (Villar-Cerviño et al., 2015). These findings suggest that Nrg1 may be playing chemoattractive roles in the developing striatum and regulating the proper migration of MGE-derived striatal interneurons to their final destination. Since this study did not address the direct association of Nrg1-ErbB4 signaling on the migration of developing striatal interneurons, it is possible that the chemoattractive properties might be attributed to other ErbB4 ligands as well.

Furthermore, it has previously been shown that Nrg1-ErbB4 signaling can regulate thalamocortical axon (TCA) navigation from the dorsal thalamus to the cerebral cortex (López-

Bendito et al., 2006), which transmit sensory and motor inputs. A study by López-Bendito et al (2006) demonstrated that the proper guidance of TCAs depended on the early tangential migration of “corridor cells”, a neuronal population derived from the ventral telencephalon. The migration of these cells resulted in a permissive corridor that was required for TCA pathfinding. Through loss-of-function experiments, it was revealed that Nrg1 Type III in “corridor cells”, secreted Ig-containing Nrg1 from the pallium, and ErbB4 in the dorsal thalamus were required for the proper navigation of TCAs through this corridor, but not for the migration of “corridor cells”(López-Bendito et al., 2006). These findings suggest that Nrg1 may serve as a guidance cue for TCAs and that Nrg1 and ErbB4 are required for the normal axonal pathfinding of thalamocortical neurons.

Nrg1 and the ErbBs have also been shown to play a role in the migration of neurons along radial glial fibers. Using cortical imprint assays, containing intact radial glia and migrating neurons, Anton et al (1997) demonstrated that the migrating neurons expressed high levels of GGF/Nrg1 Type II and ErbB2, while the radial glia expressed lower levels of ErbB4. This pattern of expression suggested a role for Nrg-ErbB signaling in radial migration of cortical neurons. The addition of recombinant GGF/Nrg1 Type II to cortical imprints enhanced neuronal migration along the radial glial fibers (Anton, Marchionni, Lee, & Rakic, 1997). Consistent with these findings, another study by Rio et al (1997) demonstrated a role for Nrg1-ErbB4 signaling in the migration of cerebellar granule neurons along the radial fibers of Bergmann glia (Rio, Rieff, Qi, Khurana, & Corfas, 1997). As shown in this study, the cerebellum is unique in that the majority of granule cells migrate postnatally, with peak migration at P6 in the rat cerebellum. Granule neurons express Nrg1 from an early pre-migratory (P0) stage, until they have finalized their migration into the internal granule layer (P19). This study also reported that ErbB4, but not ErbB2 or ErbB3 were detected in Bergmann glia, suggesting that Nrg1-ErbB4 signaling may play a role in granule cell migration along Bergmann glia fibers, in analogy to the migration of

neuroblasts along radial glia fibers in the developing cortex. Using time-lapse microscopy of pure cultures of cerebellar granule cells and astroglia expressing dominant-negative ErbB4 (DN-erbB4), it was demonstrated that expression of DN-erbB4 led to a dramatic reduction in granule neuron migration along glial fibers. It is important to note that blocking ErbB4 signaling did not completely immobilize these granule neurons, but reduced the speed of their migration (Rio et al., 1997).

In addition to their roles in neuronal migration along radial glial cells, Nrg1, ErbB2, and ErbB4 have also been shown to be important regulators in the morphology of the highly polarized radial glial cells, including their establishment, maintenance, elongation, and differentiation into astrocytes (Anton et al., 1997; Louhivuori et al., 2018; Rio et al., 1997; Schmid et al., 2003). The generation of radial glial cells is severely impaired in Nrg1 deficient mice but the addition of exogenous Nrg1 can rescue this deficiency (Schmid et al., 2003). In addition, the downregulation of ErbB2 promotes the transformation of radial glial into astrocytes (Schmid et al., 2003). A recent study by Louhivuori et al (2018) showed that exogenous Nrg1 treatment of cortical neurospheres promoted the growth of radial glial fibers. When ErbB4 was blocked in these neurospheres, radial glial process extension was inhibited and could not be rescued by Nrg1 treatment (Louhivuori et al., 2018).

Nrg-ErbB4 signaling can also effect the migration of newly born cells in the adult rodent brain (Anton et al., 2004; H T Ghashghaei et al., 2006). Neurogenesis can occur in two areas of the rodent brain: the SVZ of the lateral ventricle and the dentate gyrus of the hippocampus. In the adult rodent brain, newly generated neuroblasts of the SVZ migrate tangentially to the olfactory bulb, generating the rostral migratory stream (RMS) [reviewed in (Alvarez-Buylla & Garcia-Verdugo, 2002; Gage, 2002; Kaneko, Sawada, & Sawamoto, 2017)]. In the SVZ and RMS, ErbB4 is highly expressed in progenitors which ultimately differentiate into interneurons of the olfactory bulb (Anton et al., 2004). In addition, Nrg1, Nrg2, and Nrg3 are expressed adjacent

to the RMS. Conditional null mice that lacked ErbB4 under the nestin or hGFAP promoters, showed deficits in the morphology, migration, and placement of newly generated interneurons. These ErbB4 mutant mice showed a reduction in the number of interneurons in the glomerular layer of the olfactory bulb, suggesting that Nrg-ErbB4 signaling plays a role in the correct migration and placement of newly generated olfactory neurons in the adult rodent brain (Anton et al., 2004).

1.5.4 Neuronal Differentiation and Neurite Outgrowth

A number of studies have implicated Nrg1 and ErbB4 signaling in neuronal differentiation, including a pronounced role in neurite outgrowth (Anton et al., 1997; Audisio et al., 2012; Bermingham-McDonogh, McCabe, & Reh, 1996; M E Cahill et al., 2012; Y. Chen, Hancock, Role, & Talmage, 2010; Gamett & Cerione, 1994; Gamett et al., 1995; Kimberly M Gerecke, Wyss, & Carroll, 2004; Krivosheya et al., 2008; Mòdol-Caballero, Santos, Navarro, & Herrando-Grabulosa, 2017; Nakano, Kanekiyo, Nakagawa, Asahi, & Ide, 2016; Pinkas-Kramarski et al., 1997; Rieff et al., 1999; Rio et al., 1997; Schmid et al., 2003; Vaskovsky, Lupowitz, Erlich, & Pinkas-Kramarski, 2000; Villegas et al., 2000; L. Zhang et al., 2004; Q. Zhang, Yu, & Huang, 2016; Zheng & Feng, 2006). Nrg1 signaling has been reported to mediate neurite outgrowth and extension in several neuronal populations, including neurons of the rodent retina, hippocampus, cerebral cortex, thalamus, midbrain, spinal cord, cerebellum and the PC12 cell line (Anton et al., 1997; Audisio et al., 2012; Bermingham-McDonogh et al., 1996; M E Cahill et al., 2012; Y. Chen et al., 2010; Gamett & Cerione, 1994; Gamett et al., 1995; García et al., 2013; Kimberly M Gerecke et al., 2004; Krivosheya et al., 2008; Mòdol-Caballero et al., 2017; Rieff et al., 1999; Tal-Or et al., 2006; Vaskovsky et al., 2000; Villegas et al., 2000; R. Xu et al., 2013; L. Zhang et al., 2004; Q. Zhang et al., 2017, 2016). Using a processing-defective mutant of Nrg1 Type III (V321L), a previous study demonstrated that the proteolytic processing of the intracellular domain of Nrg1 Type III is required for Nrg1-induced dendritic

outgrowth of cultured cortical neurons. In contrast, the expression of V321L did not affect axon length compared to wild-type controls, even though Nrg1 Type III knockout mice did show a reduction in the length of the axon. These findings suggest that the extracellular and intracellular domains of Nrg1 Type III have unique effects on axonal extension and dendritic outgrowth, respectively (Y. Chen et al., 2010). The roles of Nrg2 in neurite outgrowth are less understood, but it was previously reported that Nrg2 secreted from astrocytes promoted neurite outgrowth and survival of cultured hippocampal neurons (Nakano et al., 2016). There are currently no reports on the effects of Nrg3 on neurite outgrowth in any neuronal population; however, this gap in literature is addressed in Chapter 4.

One of the main setbacks of studies analyzing the roles of the Nrgs and ErbB4 in neurite outgrowth is the lack of neuron subtype identification within the cultures, making it difficult to conclude whether excitatory, inhibitory, or all types of neurons are being affected by Nrg-ErbB4 signaling. Since ErbB4 is expressed primarily in GABAergic interneurons, it is likely that Nrg-ErbB4 signaling is affecting the differentiation of this subtype of neurons. In agreement, a few studies have shown that Nrg1-ErbB4 signaling promotes neurite outgrowth in ErbB4-expressing GABAergic interneurons in both cortical and hippocampal cultures (M E Cahill et al., 2012; Fazzari et al., 2010; Krivosheya et al., 2008). Nrg1-ErbB4 signaling has been shown to promote dendritic outgrowth in mature cortical interneurons through the activation of the src-family tyrosine kinase member, *fyn*, and the phosphorylation of kalirin-7, a dendritic Rac1-GEF (M E Cahill et al., 2012). Furthermore, cortical cultures from conditional ErbB2/ErbB4 knockout mice have shown that interneurons exhibit reduced dendritic length compared to cultures from wild-type controls (M E Cahill et al., 2012).

Consistent with these observations of ErbB-dependent dendritic outgrowth of GABAergic interneurons, a previous study demonstrated that Nrg1 treatment of hippocampal interneurons increased the number of primary neurites in ErbB4-expressing interneurons (Krivosheya et al.,

2008). Overexpressing ErbB4 resulted in an increase in the number of primary neurites; however, these cells displayed a loss of mature and elongated dendrites. The effects of Nrg1-ErbB4 signaling were further observed to be mediated by the receptor's tyrosine kinase domain and the PI3K signaling pathway (Krivosheya et al., 2008).

Previous reports have shown that Nrg1 treatment does not enhance the dendritic remodeling of pyramidal or ErbB4 (-) cells (M E Cahill et al., 2012; Krivosheya et al., 2008) and ErbB2/ErbB4 conditional knockout mice showed no abnormalities in dendritic length in pyramidal neurons (M E Cahill et al., 2012), suggesting that Nrg1-induced neurite outgrowth is limited to ErbB4 (+) interneurons.

Other than limited reports of the roles of the Nrgs (especially Nrg2 and Nrg3) in neurite outgrowth of ErbB4/GABA interneurons, a majority of studies conduct neurite outgrowth analyses in cultures in more mature and polarized neurons (8 DIV or older). Our experiments in Chapter 4 of this thesis have addressed these gaps in the literature and, for the first time, compare the effects of Nrg1, Nrg2, and Nrg3 treatment on neurite outgrowth of cultured ErbB4/GABA (+) cortical neurons at early stages of development (2-5 DIV).

In addition to their roles in neurite outgrowth, Nrg-ErbB signaling has also been observed to play roles in later stages of neuronal differentiation, including dendritic spine morphogenesis (Barros et al., 2009; Michael E Cahill et al., 2013; Y.-J. J. Chen et al., 2008; B. Li, Woo, Mei, & Malinow, 2007; Yin, Chen, et al., 2013). Conditional deletions of ErbB2/4 and Nrg1 Type III from the CNS or ErbB4 deletion from PV (+) interneurons resulted in a reduction of spine density in pyramidal neurons of the hippocampus and prefrontal cortex (Barros et al., 2009; Y.-J. J. Chen et al., 2008; Yin, Sun, et al., 2013). The overexpression of ErbB4 or treatment with exogenous Nrg1 increased dendritic spine size and density (Barros et al., 2009;

Michael E Cahill et al., 2013; B. Li et al., 2007), suggesting a role for Nrg-ErbB4 signaling in dendritic spine formation and maintenance.

1.5.5 Oligodendrocyte Development and Myelination

In both the CNS and PNS, Nrg1-ErbB signaling has been observed to affect myelination, albeit in a considerably different manner. Unlike Schwann cells which express predominately ErbB2 and ErbB3, oligodendrocytes express ErbB2 and ErbB4 (Vartanian, Goodearl, Viehöver, & Fischbach, 1997). Earlier studies showed that Nrg1 treatment enhanced the proliferation and survival of cultured oligodendrocyte precursor cells (OPCs) (Canoll et al., 1996; Fernandez et al., 2000; Flores et al., 2000; Park, Solomon, & Vartanian, 2001; Vartanian, Fischbach, & Miller, 1999) and that this effect was mediated by the activation of the PI3K/AKT pathway (Flores et al., 2000). Spinal cord explants from E9.5 *nrg1* null mice failed to develop oligodendrocytes, compared to their wild-type and heterozygous littermates (Vartanian et al., 1999). The addition of recombinant Nrg1 to spinal cord explants from *nrg1* null mice rescued oligodendrocyte development. Furthermore, this same study showed that the addition of the Nrg inhibitor, IgB4, in wild-type spinal cord explants showed an inhibition of oligodendrocyte development that was parallel to the observations in explants from *nrg1* null mice (Vartanian et al., 1999). The chronic treatment of Nrg1 in cultured OPCs, derived from neonatal rat cortex, showed that Nrg1 enhanced proliferation of OPCs but these cells failed to differentiate into oligodendrocytes (Canoll et al., 1996). In addition, chronic treatment of Nrg1 in differentiated cultures resulted in a loss of the oligodendrocyte specific proteins, O1 and myelin basic protein (MBP) (Canoll et al., 1996). Another study reported that the transgenic overexpression of Nrg1 Type I and Nrg1 Type III resulted in hypermyelination in the spinal cord and corpus callosum (Brinkmann et al., 2008), further suggesting a role for Nrg1 signaling in oligodendrocyte development and CNS myelination. Although the roles of Nrg2 and Nrg3 in CNS myelination have not been directly explored, a previous genetic study (Shimojima et al., 2011) identified two patients with a

submicroscopic deletion of 5q31.3 which contains the *nrg2* gene. These patients showed several pathological abnormalities including developmental clinical features, such as epileptic/non-epileptic encephalopathy corresponding with delayed myelination, showing a possible link between Nrg2 and CNS myelination (Shimojima et al., 2011).

A more recent study by Kataria et al (2018) reported the effects of Nrg1 signaling in the remyelination of axons in a rodent model of lysolecithin lysophosphatidyl-choline (LPC)-induced focal demyelination. This study showed that the intraspinal injection of Nrg1, near the LPC-induced focal demyelination, promoted oligodendrocyte proliferation and development, as well as enhanced remyelination of damaged axons by both Schwann and oligodendrocyte cell populations (Kataria et al., 2018). These findings were consistent with spinal cord injury (SCI) models which have previously been shown to have reduced Nrg1 expression in the spinal cord (Gauthier, Kosciuczyk, Tapley, & Karimi-Abdolrezaee, 2013). The intrathecal administration of recombinant Nrg1 into rats with SCI resulted in an increase in the proliferation and survival of oligodendrocytes, as well as axonal preservation, in an ErbB2/4-dependent manner (Gauthier et al., 2013).

In contrast to reports supporting Nrg signaling as a player in oligodendrocyte development and CNS myelination, experiments in *nrg1* and *erbb3/erbb4* conditional null mutants have suggested that the development of oligodendrocytes and CNS myelination may be independent of Nrg1-ErbB signaling (Brinkmann et al., 2008). In a study by Brinkmann et al (2008), several Nrg1 conditional knockout lines were generated to study the effects of Nrg1 signaling on CNS myelination at different stages of neural development, including Cre driver lines deleting *nrg1* in cortical pyramidal neurons, in cortical projection neurons, in multipotent populations of progenitor cells in the embryonic forebrain, or in the entire CNS. Unexpectedly, all the conditional null mutants showed myelination and oligodendrocyte morphology which was comparable to normal wild-type controls. In addition, double mutants lacking oligodendroglial

ErbB3 and ErbB4 showed normal differentiation of oligodendrocytes and CNS myelination (Brinkmann et al., 2008).

Although conditional null mutations of *nrg1* and *erbb3/erbb4* showed normal myelination of the CNS (Brinkmann et al., 2008), other downregulation studies have produced conflicting results. A study by Taveggia et al (2008) showed that mice that were haploinsufficient for Nrg 1 Type III showed hypomyelination in the CNS, including reduced expression of myelin-specific proteins and lipids as well as thinner myelin sheaths (Taveggia et al., 2008). Furthermore, another study showed that blocking ErbB4 signaling in oligodendrocytes, via expression of dominant-negative ErbB4 under the control of the 2',3'-cyclic nucleotide 3'-phosphodiesterase (CNP) promoter, resulted in deficiencies in oligodendrocyte differentiation and morphology. The lack of oligodendrocyte development ultimately affected the myelin thickness and the conduction velocity of axons in these mutant mice (Roy et al., 2007). It is unclear why conditional null mutations of *nrg1* and *erbb3/erbb4* show no abnormalities in CNS myelination, considering several of the aforementioned studies have reported a role for Nrg-ErbB signaling in oligodendrocyte development. One possibility for these contrasting findings may be due to compensation of Nrg1-ErbB signaling by the other Nrgs and ErbBs or via compensatory or redundant signaling of another receptor family. However, addressing the contribution and further clarification of Nrgs and ErbBs to CNS myelination and the biology of the oligodendrocyte fate will require additional studies.

1.6 Nrg-ErbB4 Signaling in CNS Mental Illnesses

1.6.1 Schizophrenia

Mutations in the *nrgs* and *erbb4* genes have been strongly associated with a number of mental illnesses. Stefansson et al (2002) originally identified *NRG1* as a candidate risk gene for SZ through a genome wide scan of families affected by SZ in Iceland, showing that the disorder

maps to chromosome 8p12-p21, a region encoding *NRG1*. Several SZ-associated single nucleotide polymorphisms (SNPs) were identified, mainly within the intronic regions of *NRG1* gene (Stefansson et al., 2002). Since then, a number of studies have supported the genetic association between *NRG1* and SZ and have identified many other SZ-associated SNPs within the *NRG1* gene in diverse groups of people (Hashimoto et al., 2004; He et al., 2016; Kukshal et al., 2013; Naqvi, Huma, Waseem, Zaidi, & Abidi, 2018; Stefansson et al., 2003; J. X. Tang et al., 2004; Z. Wen et al., 2016; Williams et al., 2003; J.-M. Yang et al., 2018; S.-A. Yang, 2012; Yoosefee et al., 2016). These findings have also revealed that the disease related SNPs are mainly found within intronic or noncoding regions. *NRG3* has also been recognized as a risk gene for SZ. Genome-wide linkage scans in Ashkenazi Jewish families and Han Chinese families identified chromosome 10q22.3 as a SZ susceptibility locus (Fallin et al., 2003; Faraone et al., 2006). Through fine mapping of chromosome 10q22.3 in the Ashkenazi Jewish population, it was later identified that several SNPs were located within intron 1 of the *NRG3* gene (P.-L. Chen et al., 2009). Three of these SNPs were associated with the delusional phenotype of SZ patients (P.-L. Chen et al., 2009). A majority of studies have confirmed the genetic association between *NRG3* and SZ (Kao et al., 2010; Morar et al., 2011; Y.-C. Wang et al., 2008; Zeledón et al., 2015); however, there have also been reports that have not found such associations (Pasaje et al., 2011; R. Zhang et al., 2013). The association between *NRG2* and SZ is less understood. Several studies have associated the region encompassing the *NRG2* gene with disease risk (C. M. Lewis et al., 2003; Schwab et al., 1997; Sklar et al., 2004; Straub, MacLean, O'Neill, Walsh, & Kendler, 1997) and one study identified a single SNP in *NRG2* that showed an association with SZ (Benzel et al., 2007). In addition, the NRG receptor, *ERBB4* has also been recognized as a SZ susceptibility gene. Norton et al (2006) conducted a mutation screening of *ERBB4* in Caucasians born in the United Kingdom and Ireland and revealed 15 SNPs within the gene associated with SZ (Norton et al., 2006). Shortly after that study was published, two other groups confirmed several SNPs within *ERBB4* that were associated with

disease presentation (Norton et al., 2006; Silberberg, Darvasi, Pinkas-Kramarski, & Navon, 2006).

Since a majority of disease-associated SNPs within the *NRG* genes are intronic, it is possible that they regulate gene expression, as opposed to effect the protein sequence. A study by Hashimoto et al (2004) showed that *Nrg1* Type I mRNA was significantly increased in the dorsolateral prefrontal cortex (DLPFC) of patients with SZ (Hashimoto et al., 2004). This finding was also observed when analyzing human postmortem hippocampi (Law et al., 2006). An increase in the expression of *Nrg1* Type II, III, and IV mRNA have also been reported in the postmortem PFC or hippocampi of patients with SZ (Law et al., 2006; Parlapani et al., 2010; Weickert, Tiwari, Schofield, Mowry, & Fullerton, 2012). In contrast, several studies have reported lower expression of *NRG1* α and Type I in the brain or Ig-*NRG1* in serum in SZ patients (Bertram et al., 2007; Parlapani et al., 2010; Shibuya et al., 2010). A recent study, using an enzymatic assay, reported elevated levels of *NRG1* protein that had been cleaved by *BACE1* in plasma from patients with SZ compared to healthy controls (Z. Zhang et al., 2019). The analyses of *NRG3* mRNA in postmortem brain studies have revealed that *NRG3* Types I and IV were significantly increased in the DLPFC of patients with SZ compared to healthy controls (Kao et al., 2010; Paterson et al., 2017). Postmortem brain studies analyzing the expression of *ErbB4* in SZ patients have revealed increases in *ErbB4* which are isoform-specific. Several studies have reported that *ErbB4* JM-a isoforms were elevated in the PFC of patients with SZ (Chung et al., 2016; Joshi, Fullerton, & Weickert, 2014; Law et al., 2007; Silberberg et al., 2006). Within those same studies, two of them also observed an increase in the levels of *CYT-1* isoforms (Law et al., 2007; Silberberg et al., 2006); whereas, two other studies reported unaltered levels of this variant (Chung et al., 2016; Joshi et al., 2014).

In addition, the *Nrgs* and *ErbB4* have also been associated with several behavioral phenotypes observed in SZ patients. To investigate the roles of *Nrg1* in SZ, *Nrg1* heterozygous

mice were generated with deletions or targeted mutations of Nrg1 (Ehrlichman et al., 2009; Gerlai, Pisacane, & Erickson, 2000), the EGF-like domain (Liesl Duffy, Cappas, Scimone, Schofield, & Karl, 2008), the TM domain (Boucher et al., 2007; Karl, Duffy, Scimone, Harvey, & Schofield, 2007; C M P O'Tuathaigh et al., 2007; Colm M P O'Tuathaigh et al., 2008; Stefansson et al., 2002), the Ig-like domain (Rimer, Barrett, Maldonado, Vock, & Gonzalez-Lima, 2005), or of Nrg1 Type III (Y.-J. J. Chen et al., 2008). These Nrg1 mutant mice displayed phenotypes that displayed behaviors and physiological features also observed in SZ patients, such as hyperactivity (Y.-J. J. Chen et al., 2008; Liesl Duffy et al., 2008; Gerlai et al., 2000; Karl et al., 2007; C M P O'Tuathaigh et al., 2007; Colm M P O'Tuathaigh et al., 2008; Rimer et al., 2005; Stefansson et al., 2002), impaired prepulse inhibition (PPI) (Y.-J. J. Chen et al., 2008; Rimer et al., 2005; Stefansson et al., 2002), compromised latent inhibition (Rimer et al., 2005), deficits in social interaction (Ehrlichman et al., 2009; C M P O'Tuathaigh et al., 2007; Colm M P O'Tuathaigh et al., 2008), and reduction in contextual fear conditioning (L Duffy, Cappas, Lai, Boucher, & Karl, 2010; Ehrlichman et al., 2009). In addition, mice overexpressing Nrg1 Type I (Deakin et al., 2009, 2012; Yin, Chen, et al., 2013), Nrg1 Type III (Olaya, Heusner, Matsumoto, Sinclair, et al., 2018) and Nrg1 Type IV (Papaleo et al., 2016) showed reduced PPI, changes in motor activity, as well as impairments in cognition, fear associated memory, and social preference. A recent study showed that female mice overexpressing Nrg1 Type III in the forebrain did not show any effects in several behavioral phenotypes associated with SZ, including motor functions, baseline locomotion, sociability, social recognition memory, fear conditioning, and PPI (Olaya, Heusner, Matsumoto, Shannon Weickert, & Karl, 2018). These findings suggest that the behavioral effects observed for the overexpression of Nrg1 Type III might be gender specific.

The association between Nrg2 and SZ has not been well characterized and, to date, there is currently only one published behavioral study that has analyzed the phenotypes

associated with psychiatric disorders in *Nrg2* knockout mice. Mice deficient for *Nrg2* exhibit several behavioral phenotypes also observed in SZ patients, including hyperactivity, deficits in PPI, and impairments in sociability (L. Yan et al., 2018). Behavioral studies analyzing the association between *Nrg3* and SZ-like behaviors are also limited. A study by Loos et al (2014) measured impulsivity in mice using the 5-choice serial reaction time task. This study revealed that mice overexpressing *Nrg3* in the mPFC displayed increased impulsivity; whereas, mice with a constitutive *Nrg3* loss-of-function mutation showed a reduction in impulsivity (Loos et al., 2014). Another study peripherally injected the EGF-like domain of *Nrg3* in neonatal mice and ran behavioral tests during adulthood. The developmental overexposure of *Nrg3* resulted in these mice showing anxiogenic-like phenotypes and social deficits in adulthood (Paterson & Law, 2014). In comparison, the developmental overexposure of *Nrg1* resulted in mice showing deficits in sensorimotor gating as measured by PPI. These findings suggest distinct roles for the developmental exposure of *Nrg1* and *Nrg3* in behavioral phenotypes (Paterson & Law, 2014).

Behavioral studies in *ErbB4* mutant mice that were heterozygous for *ErbB4* have also reported associations between *ErbB4* and SZ (Shamir et al., 2012; Stefansson et al., 2002). Mice lacking *ErbB4* in mPFC chandelier cells (J.-M. Yang et al., 2018), in all chandelier and basket cells (Del Pino et al., 2013), in PV (+) interneurons (Y. H. Chen et al., 2017; Shamir et al., 2012), from medium spiny neurons of the nucleus accumbens (Geng et al., 2017), or lacking *ErbB2* and *ErbB4* expression in the CNS (Barros et al., 2009) showed several behavioral phenotypes present in patients with SZ, including hyperactivity (Del Pino et al., 2013; Geng et al., 2017; Shamir et al., 2012; Stefansson et al., 2002; J.-M. Yang et al., 2013), reduced PPI (Barros et al., 2009; Geng et al., 2017; Shamir et al., 2012; J.-M. Yang et al., 2018), social deficits (Barros et al., 2009; Del Pino et al., 2013; Geng et al., 2017; J.-M. Yang et al., 2018), reduced anxiety-like behaviors (Barros et al., 2009; Shamir et al., 2012), and impaired fear conditioning (Y. H. Chen et al., 2017; Shamir et al., 2012).

1.6.2 Other Mental Illnesses

The NRGs and ErbB4 have been associated with several other mental disorders, including those showing comorbidity with SZ, suggesting that the NRG-ErbB signaling network may be the underlying player in the presentation of these comorbid illnesses. *NRG1*, *NRG3*, and *ErbB4* have all been associated with substance abuse (Han et al., 2012; Loukola et al., 2014; Turner et al., 2014; Vaht et al., 2017), the most common disorder to co-occur with SZ (Buckley, Miller, Lehrer, & Castle, 2009). The majority of these studies have associated the NRG-ErbB4 signaling network with an increased risk for nicotine dependence (Gupta et al., 2017; Loukola et al., 2014; Turner et al., 2014). A previous behavioral study by Turner et al (2014) demonstrated that WT mice chronically treated with nicotine showed an increase in Nrg3 levels in hippocampal tissue during early withdrawal. This surge in Nrg3 also correlated with increased anxiety. *NRG1* has also been associated with cannabis dependence in African Americans (Han et al., 2012). A very recent study showed preliminary data reporting that blood samples from Caucasian patients with SZ who abuse cannabis, showed higher levels of *NRG1* in comparison to patients who did not abuse cannabis (Aukst Margetic, Peitl, Vukasović, & Karlović, 2019). These findings suggest that *NRG1*-ErbB signaling may be playing a role in the comorbidity of SZ and substance abuse.

In addition to substance abuse and SZ, *NRG1*, *NRG3*, and *ErbB4* have been linked to an increased risk with major depressive disorder (MDD) (Bertram et al., 2007; Paterson et al., 2017; Z. Wen et al., 2016) and bipolar disorder (BD) (Cao et al., 2014; Georgieva et al., 2008; Goes et al., 2009; Meier et al., 2013; Paterson et al., 2017; Prata et al., 2009; Walker et al., 2010; Z. Wen et al., 2016). A study by Bertram et al (2007) found that *NRG1 α* was significantly reduced in the white matter of the PFC of patients with SZ but not in patients with affective disorder (BP and MDD); however, in PFC gray matter, *NRG1 α* levels were reduced in both patients with SZ and MDD (Bertram et al., 2007). These data suggest that *NRG1* may be a risk

gene for these disorders, but their expression levels in different brain regions or cell types might not be the same. Another variation between the roles of the NRGs in the etiology of SZ, MDD, or BP might be within alternative spliced variants. As described in **Molecular Architecture and Alternative Splicing**, there have been four variants (Type I-IV) of NRG3 that have been identified in humans (Paterson et al., 2017). The same study showed that NRG3 Type I was increased in BP and MDD, NRG3 Type II was increased in BP, and NRG3 Type III was increased in MDD, suggesting possible specificity of NRG3 variants to particular mental illnesses (Paterson et al., 2017).

The NRGs and ErbB4 have been associated with several other mental disorders as well, including autism (Abbasy et al., 2018; Balciuniene et al., 2007; Esnafoglu, 2018; Yoo et al., 2015), developmental and intellectual delays (Hoffmann et al., 2010; Kasnauskiene et al., 2013; Shimojima et al., 2011), and Alzheimer's disease (Go et al., 2005; Q. Jiang et al., 2016; K.-S. Wang et al., 2014; Woo, Lee, Yu, Song, & Baik, 2010). Due to the diverse functions of the Nrg-ErbB4 signaling network in the developing and mature CNS, it is anticipated that their dysregulation would play such a prevalent role in mental illness.

1.6 Aim of Thesis

The Nrgs and their receptor ErbB4 play important roles in the developing and mature CNS. Mutations in the Nrg-ErbB4 signaling pathway are intimately associated with several mental illnesses, including SZ, BD, and MDD. The aims of this thesis were driven by the limited knowledge about Nrg3 in the CNS and the fundamental gaps in understanding of the roles that the Nrgs play in neuronal differentiation of GABAergic interneurons, specifically in neurite outgrowth and cortical neuronal polarity. Towards these goals we **1)** characterized the spatiotemporal localization of Nrg3 mRNA and protein in the developing rat CNS (Chapter 3), **2)** analyzed the roles of GST-Nrg treatment and ErbB4 activation in neurite outgrowth of cortical

ErbB4/GABA (+) interneurons (Chapter 4), and **3**) explored novel protein-protein interactions between ErbB4 and members of the Par polarity complex, a group of proteins essential for axon formation and growth (Chapter 5). The findings of this thesis pave potential avenues for studying the molecular mechanisms underlying Nrg-ErbB4 signaling in neuronal differentiation of the normal and diseased CNS.

Chapter 2: Materials and Methods

2.1 MATERIALS:

2.1.1 Reagents:

The reagents were obtained from the following sources - from Sigma-Aldrich (St. Louis, MO): Phosphatase Inhibitor Cocktail 2 (#P5726), Phosphatase Inhibitor Cocktail 3 (#P0044), Poly-L-lysine hydrobromide (PLL, #P2636), 4'-6-diamidino-2-phenylindole (DAPI, #508741). The following items were purchased from Life Technologies (Grand Island, NY): Penicillin-Streptomycin (#15140-122), Penicillin-Streptomycin-Glutamine (#10378-016), Glutamine (#25030-081), L-Glutamic Acid (#A37840SA), Neurobasal Medium (#21103-049), B27 Supplement (#A35828-01), Opti-MEM I Reduced Serum Media (#31985-070), Dulbecco's Modified Eagle Medium (DMEM, #12800-017), Hoechst 33342 (#H3570), Lipofectamine Reagent (#18324-020), Plus Transfection Reagent (#11514-015), Novex 8% Tris-glycine gels (#EC60152), Novex 4-20% Tris-glycine gels (#EC60285), SlowFade Antifade Kit (#S2828). The following items were purchased from Thermo Fisher Scientific Inc (Rockford, IL): SuperSignal West Pico Chemiluminescent Substrate (#34078), SuperSignal West Femto Chemiluminescent Substrate (#34096), Frosted Microscope Slides 3 x 1 in. (#12-552-5), Gold Seal™ Cover Slips (#3317), Cover Glasses (#12-545-82), Bovine serum albumin (BSA, #BP9703). The following items were purchased from New England Biolabs (NEB, Beverly, MA): T4 DNA ligase (#M0202), BspEI (#R0540), NotI (#R0189), PflMI (#R0509), Color Prestained Protein Standard, Broad Range (11-245 kDa; #P7712), N-glycosidase (PNGase F; #P0704), Endoglycosidase H (Endo H; #P0702), O glycosidase (O-gly; #P0733), O-gly and Neuraminidase (NA) bundle (#E0540). Other reagents were obtained from: G418 (#GN04) from Omega Scientific (Tarzana, CA); Fetal Calf Serum (FCS, #S11150) and Goat Serum (GS, #S13150H) from Atlanta Biologicals (Flowery Branch, CA); pGEM-T Easy Vectors (#A1360) from Promega (Madison, WI);

Immobilion-P PVDF transfer membrane (#IPVH00010) from Millipore (Billerica, MA); Tissue-Tek optimum cutting temperature (O.C.T) medium (#25608-930) from Sakura Finetek (AJ Alphen aan den Rijn, The Netherlands); Autoradiography film (#EBA45) from MIDSCI (St. Louis, MO); Complete-Ultra Protease Inhibitor Cocktail Tablets (#0653830400) from Roche (Mannheim, Germany).

2.1.2 cDNA Constructs:

Full length human Partitioning-defective protein 3b (pK-myc-Par3b) cDNA (clone #19388), full length rat Protein kinase C ζ (pCMV5-FLAG.PKC ζ) cDNA (clone #10799), full length human Partitioning-defective protein 6C (pK-myc-Par6C) cDNA (clone #15474), full length human Cell division cycle 42 (pRK5-myc-Cdc42-T17N) cDNA (clone #12973), and full length rat Post synaptic density protein 95 (pcDNA5/FRT/TO-FLAG.PSD-95) cDNA (clone #15463) were purchased from Addgene (Cambridge, MA).

Full length wild-type ErbB4 cloned into p-EGFP-N1 vector (isoform JM-b CYT-2; p-N1-ErbB4) was a gift from Dr. Cary Lai. The coding sequence for EGFP was removed digesting with NheI and NotI. ErbB4 was introduced into the digested vector in multiple pieces, resulting in a BglII site at the 5' end and a Sall site at the 3' end. The 3' NotI site of the EGFP-N1 vector remained after the insertion of ErbB4; however, the 5' NheI site was eliminated. The ErbB4 sequence was altered to add and remove restriction endonuclease sites without a disturbance in the sequence that would affect amino acid coding. Nucleotide changes were compared to the original *mus musculus* ErbB4 JM-b CYT-2 sequence (NCBI RefSeq XM_006495694.3; (O'Leary et al., 2016)). Two BglII restriction sites were deleted with c.1593 C>T and c.3456 A>G mutations. SmaI, TspMI, XmaI, Cfr9I single restriction sites were introduced with c.1716 G>C and c.1719 A>G mutations. Eco104I, BstSNI, and SnaBI single restriction sites were added with c.1992 T>C and c.1995 C>A mutations. One XbaI site was generated by introducing a c.2469

C>T mutation. Deletion of a HindIII site was generated by a c.3468 T>A mutation. The c.3504 T>G and c.3507 A>C mutations generated single cut sites for Bsp120I, PspOMI, BseSI, BaeGI, BstSLI, and ApaI. Single restriction sites for Bsh1285I, BsiEI, MclI, PvuI, BstMCI, BpvUI, Ple19I, and Mvrl were introduced with c.3672 delG with c.3676 insG mutations.

ErbB4 deletion and mutant constructs were further generated using the p-N1-ErbB4 construct as described in detail in the section “**ErbB4 cDNA Cloning and Mutagenesis.**” The pcDNA-CAG-mCherry construct was a gift from Drs. Ken Mackie and Hui-Chen Lu.

Glutathione-S-transferase (GST)-Nrg1, GST-Nrg2, and GST-Nrg3 cDNA constructs were generated in the pGEX-6P-2 vector (GE Healthcare Bio-Sciences Pittsburgh, PA). These constructs encode GST-Nrg fusion proteins encoding the corresponding epidermal-growth factor (EGF)-like domain and flanking regions in the Nrgs, as described in (H T Ghashghaei et al., 2006) (for Nrg1 and Nrg2) and in further detail below (for Nrg3) (Rahman et al., 2018).

2.1.3 Antibodies:

Commercial antibodies were obtained from the following sources: rabbit polyclonal anti- γ -Aminobutyric acid (GABA) raised using GABA-BSA as the immunogen (#A2052), mouse monoclonal purified anti-glial fibrillary acidic protein (GFAP) raised against recombinant human GFAP (#672402), mouse monoclonal anti-microtubule-associated protein 2 (MAP2) raised against mammalian MAP2 (#801801), and mouse monoclonal anti-myelin 2',3'-cyclic-nucleotide 3'-phosphodiesterase (CNPase) raised against human myelin CNPase (#836404) all from BioLegend (San Diego, CA); mouse monoclonal anti-calbindin D-28k produced by hybridization of mouse myeloma cells with spleen cells from mice raised against chicken calbindin D-28k (#300), mouse monoclonal anti-parvalbumin produced by hybridization of mouse myeloma cells with spleen cells from mice raised against parvalbumin purified from carp muscles (#235) both from Swant (Marly, Switzerland); mouse monoclonal anti-O4 clone 81 produced using

homogenate of white matter of corpus callosum from bovine brain (#MAB345), rabbit polyclonal Par-3 against residues 457-744 of mouse Par-3 (#07-330), and mouse monoclonal anti-glyceraldehyde-3-phosphate dehydrogenase (GAPDH) against GAPDH from rabbit muscle (#MAB374) all from EMD Millipore (Burlington, MA); mouse monoclonal anti-Golgi matrix protein of 130 kDa (GM130) raised against amino acids 869-982 corresponding to rat GM130 (#610822) from BD Biosciences (San Jose, CA); rabbit polyclonal anti-phospho-PKC ζ / λ against a synthetic phosphopeptide corresponding to residues surrounding Thr410 of human PKC ζ (#9378), rabbit polyclonal anti-PKC ζ against a synthetic peptide corresponding to human PKC ζ (#9372), rabbit polyclonal anti-Cdc42 against a synthetic peptide corresponding to residues surrounding Lys135 of human Cdc42 (#2462), rabbit polyclonal anti-phospho-Rac1/cdc42 against a synthetic phosphopeptide corresponding to residues surrounding Ser71 of human Rac1/cdc42 (#2461), rabbit polyclonal anti-postsynaptic density protein 95 (PSD95) against residues surrounding Gln53 of human PSD95 (#3450), rabbit polyclonal anti-myc-tag raised against residues 410-419 of human c-Myc (#2278), mouse monoclonal anti- β -actin raised against a synthetic peptide corresponding to amino-terminal residues of human β -actin (#3700), rabbit polyclonal anti- β -tubulin raised against a synthetic peptide corresponding to the sequence of human β -tubulin (#2146) all from Cell Signaling Technology (Danvers, MA); mouse monoclonal anti-myc-tag raised against amino acid residues EQKLISEEDL of the human c-Myc protein (#1A5A2) from Proteintech (Rosemont, IL); rabbit polyclonal anti-FLAG against the peptide sequence DYKDDDDK (#F7425) from Millipore Sigma (Burlington, MA); mouse monoclonal anti-phospho-tyrosine (pTyr) PY99 raised against pTyr (#sc-7020), anti-pTyr PY20 raised against pTyr (#sc-508), rabbit polyclonal anti-PARD6A raised against amino acids 257-346 at the C-terminus of human PARD6A (#sc-25525), mouse monoclonal anti-PARD6A raised against amino acids 257-346 of human PARD6A (#sc-74479) all from Santa Cruz Biotechnology (Santa Cruz, CA); mouse monoclonal anti-Ankyrin-G against a fusion protein of ~1,000 amino acids of Ankyrin-G (#75-146), mouse monoclonal anti-parvalbumin against fusion protein amino

acids 1-110 (full length) of parvalbumin (#75-479) both from UC Davis/NIH NeuroMab Facility (Davis, CA); rabbit polyclonal anti-Ankyrin-G against recombinant protein corresponding to amino acids 1784-1961 from mouse Ankyrin-G (#386 003) from SYnaptic SYstems (Göttingen, Germany); mouse monoclonal anti-ErbB4 against the extracellular fragment of recombinant human c-erbB-4/HER-4 oncoprotein (#MA5-12888), rabbit polyclonal Alexa Fluor 594 goat-anti-mouse raised against gamma immunoglobulin heavy and light chains (#A-11005), polyclonal Alexa Fluor 488 goat-anti-rabbit raised against gamma immunoglobulin heavy and light chains (#A-11008) from Thermo Fisher Scientific (Waltham, MA); polyclonal horse radish peroxidase (HRP) conjugated goat-anti-rabbit IgG raised against immunoglobulin heavy and light chains (#111-035-045), polyclonal HRP conjugated goat anti-mouse IgG raised against immunoglobulin heavy and light chains (#115-035-062) from Jackson ImmunoResearch Labs (West Grove, PA). The anti-GAD-6 monoclonal antibody specific against rat GAD-65 (#GAD65) from the Developmental Studies Hybridoma Bank (DSHB) was developed by David Gottlieb (Washington University School of Medicine St. Louis, MO). It was obtained from the DSHB developed under the auspices of the Eunice Kennedy Shriver National Institute of Child Health and Human Development (NICHD) and maintained by The University of Iowa, Department of Biological Sciences.

Polyclonal rabbit antibodies recognizing human ErbB4 (#615) residues between 1038-1105 (excluding residues 1047-1063) (García-Rivello et al., 2005; Plowman et al., 1993), human ErbB4 (#616) residues 1185-1238 (Plowman et al., 1993; Zhu, Lai, Thomas, & Burden, 1995), human ErbB (#618) residues 1108-1136 (Plowman et al., 1993; Zhu et al., 1995) were gifts from Dr. Cary Lai.

Polyclonal rabbit antibodies recognizing the EGF-like domain and flanking regions of Nrg1 (#4116), Nrg2 (#4122), and Nrg3 (#6144) were produced and affinity purified as previously

described in (A L Prieto, Weber, & Lai, 2000; Rahman et al., 2018) and discussed in further detail below.

2.1.4 Animals:

Sprague Dawley rats (Envigo, Indianapolis, IN) were used to obtain tissues for *in situ* hybridization, immunohistochemistry, immunocytochemistry, and Western blotting experiments. Rat embryos of day 17 or 18 were used to prepare primary cortical cultures, as described below. Both embryonic (E) and postnatal (P) rats were utilized for Western blotting, immunohistochemistry, and *in situ* hybridization experiments. Depending on the experiment, pregnant and postnatal rats were euthanized by CO₂ inhalation. Embryos were removed via caesarian section to prepare primary cortical cultures. For immunohistochemistry and *in situ* hybridization, postnatal rats were first anesthetized prior to perfusion (as described in detail below). For all experiments in which animals were involved, including immunizations, we followed guidelines established by the NIH Guide for the Care and Use of Laboratory Animals and a protocol approved by The Scripps Research Institute Institutional Animal Care and Use Committee and also approved by the Indiana University Institutional Animal Care and Use Committee.

2.2 METHODS:

2.2.1 GST-Nrg Fusion Proteins and Nrg cDNA Constructs:

Glutathione-S-transferase (GST) fusion protein encoding the EGF-like domain and flanking regions of Nrg1, Nrg2, and Nrg3 were generated and used for antibody production and purification. Information regarding the production of Nrg1 and Nrg2 fusion proteins was previously published in (H T Ghashghaei et al., 2006). Nrg3 fusion proteins were generated using polymerase chain reaction (PCR) to amplify a region corresponding to the Nrg3 EGF-like

domain cassette region between base pairs 1132-1368 in accession number NM_001190187.1 corresponding to murine Nrg3 reference sequence (variant 2) (Rahman et al., 2018). This amplified sequence corresponds to amino acids:

SEHFKPCRDKDLAYCLNDGECFVIETLTGSHKHCRCKEGYQGVRCDQFLPKTDSILSDPTDHL
GIEFMESEDVYQR.

The PCR products were subcloned into the pGEX-6P-2 vector (GE Healthcare Bio-Sciences Pittsburgh, PA, #28954650). After nucleotide sequence verification, the recombinant constructs or the unmodified vectors were transformed into the Origami strain of *E. coli* (EMD Millipore, Burlington, MA, #71408) and used for fusion protein production and purification (GST-Nrg3 and GST) as previously described in detail in (H T Ghashghaei et al., 2006).

2.2.2 Generation of Anti-Nrg and Purification of Anti-Nrg3 Antibodies:

The anti-Nrg1 (#4116), Nrg2 (#4122), and Nrg3 (#6144) antisera were raised in rabbits by the subcutaneous injection of GST-Nrg fusion proteins, in complete Freund's adjuvant, followed by booster injections in incomplete Freund's every 3 weeks closely following the protocol described in Prieto et al (A L Prieto et al., 2000). Anti-Nrg1-3 antibodies were affinity purified by passing the #4116, #4122, and #6144 sera through GST, GST-Nrg1, GST-Nrg2, GST-Nrg3 -Sephacryl 4B columns prepared by covalently coupling the proteins to CN-Br Sepharose (GE Healthcare Bio-Sciences, Marlborough, MA, # 17043001) following the purification protocol described in detail in Prieto et al (A L Prieto et al., 2000). The immunoreactivities of the antibodies were tested by immunocytochemistry and Western blot analyses, as described below.

2.2.3 ErbB4 cDNA Cloning and Mutagenesis:

The original full length ErbB4 (isoform JM-b CYT-2) construct was a gift from Dr. Cary Lai and was generated by cloning a Nhe and NotI fragment from mouse ErbB4 transcript variant X3 (accession #XM_006495694) into the pEGFP-N1 vector (Clontech, Mountain View, CA, #6085-1). The coding sequence for EGFP was removed and the full length wild type ErbB4 sequence was added with modified restriction sites (described in the section **cdNA Constructs**), without changing the ErbB4 amino acid coding sequence. This construct will be referred to as p-N1-ErbB4.

ErbB4 PDZ domain deletions and mutant constructs were first generated by PCR. The ErbB4- Δ 4PDZb, ErbB4- Δ 6PDZb, ErbB4-AlaPDZb, and ErbB4-ConsPDZb mutants were generated by amplifying a segment in the intracellular region of ErbB4 using primers containing BspEI and NotI restriction sites. For all mutants, the following forward primer was used – CAAGCATTAGATAATCCGGAGTATCACAGTGCT.

The following reverse primers were used for each mutant –

ErbB4- Δ 4PDZb (deletion of last four amino acids):

tagagtcgcgccgctgcgacTCACCGGTGTCTGTAGGGCGGAGGGGGCAGCAT

ErbB4- Δ 6PDZb (deletion of last six amino acids):

tagagtcgggcccgcgctgcgacTCATCTGTAGGGCGGAGGGGGCAGCATAGTGCC

ErbB4-AlaPDZb (mutation of last four amino acids to Ala):

tagagtcgcgccgctgcgacTCACGACGACGACGACCGGTGTCTGTAGGGCGGAGGGGGCAGCA

ErbB4-ConsPDZb (mutation of last four amino acids to Gln, Ser, Ile, Ile):

tagagtcgcgccgctgcgacTCACAGAGTATCATCCCGGTGTCTGTAGGGCGGAGGGGGCAGCAT

The ErbB4- Δ 103 and ErbB4- Δ 204 mutants were generated by amplifying a segment of the intracellular region of ErbB4 using primers containing AgeI and NotI restriction sites. For the two mutants, the following forward primer was used – TATTACCATACCATTAAGTGGACTCTTC.

The following reverse primers were used for each mutant –

ErbB4-Δ103 (*deletion of the last 103 amino acids*):

tagagtcgcgccgctcgacTCACTCATTACGTATTCATCCTCCGCCTT

ErbB4-Δ204 (*deletion of the last 204 amino acids*):

tagagtcgcgccgctcgacTCAGTCATCAAACATCTCAGCCGTTGCACCCTG

The amplified ErbB4 segments were then ligated into pGEM-T Easy Vectors (Promega, Madison, WI, #A1360). For ErbB4-Δ4PDZb, ErbB4-Δ6PDZb, ErbB4-AlaPDZb, and ErbB4-ConsPDZb mutants, both pGEM-T vectors with the mutated ErbB4 inserts and the p-N1-ErbB4 recipient vector were digested with BspEI and NotI restriction enzymes. For the ErbB4-Δ103 and ErbB4-Δ204 mutants, both pGEM-T vectors with the mutated ErbB4 inserts and p-N1-ErbB4 recipient vector were digested with Pf1MI and NotI restriction enzymes. Digests were run on an agarose gel and vector and insert DNAs were extracted, followed by ligation of the recipient vector with the mutated ErbB4 insert using T4 DNA ligase (NEB, #M0202). Upon completion of the cloning steps we had the following plasmids encoding ErbB4 mutants: ErbB4 lacking the last four amino acids (p-N1-ErbB4-Δ4PDZb); ErbB4 lacking the last six amino acids (p-N1-ErbB4-Δ6PDZb); ErbB4 in which the last four amino acids were substituted by alanines (p-N1-ErbB4-AlaPDZb); ErbB4 in which the last four amino acids were replaced by glutamine, serine, isoleucine, isoleucine (conservative substitutions, p-N1-ErbB4-ConsPDZb); a truncated ErbB4 lacking the last 103 amino acids (p-N1-ErbB4-Δ103); and a second truncated ErbB4 construct lacking the last 204 amino acids (p-N1-ErbB4-Δ204).

2.2.4 DNA Sequencing and Verification of ErbB4 cDNA Mutants:

The ability of the ErbB4 mutant constructs to encode for functional ErbB4 was verified at several levels. The DNA sequences of the mutants were determined by sequencing performed

at the Molecular Cloning Laboratories (MCLAB, San Francisco, CA). Samples were prepared according to the protocol obtained from MCLAB.

Several aspects of the ErbB4 mutant constructs were monitored through transfection of N2a cells. Expression of the ErbB4 polypeptide, its compartmentalization, its ability to traffic to the plasma membrane, and its ability to be activated at the cell surface by ligand activation were verified through immunocytochemistry and/or immunoprecipitations (IPs) and Western blotting techniques, as described below.

2.2.5 Preparation and Maintenance of Cell Cultures:

Neuro2a Cells: The Neuro2a (N2a) neuroblastoma cell line was obtained from American Tissue Culture Collection (ATCC, Manassas, VA, #CCL-131). The N2a cell line stably expressing ErbB4 (N2a/ErbB4) was a gift from Dr. Cary Lai and was generated through the isolation of clonal N2a cells permanently transfected with p-N1-ErbB4 encoding isoform JM-b, CYT-2 and a neomycin resistance gene under neomycin exposure.

N2a cells were grown in Dulbecco Modified Eagle's Minimal Essential Medium (DMEM, Thermo Fisher Scientific, #12800-017), containing 10% FCS (Atlanta Biologicals, #S11150), L-glutamine (2 mM), penicillin (100 U/ml), and streptomycin (100 µg/ml) (from Thermo Fisher Scientific, #10378-016). N2a/ErbB4 cells were grown in the aforementioned media with the addition of G418 (300 µg/ml, Omega Scientific, #GN04).

Primary cortical cultures: Primary cortical cultures were derived from E17-E18 rat embryos. Cultures were prepared and maintained as previously described in detail in Prieto et al (A L Prieto, O'Dell, Varnum, & Lai, 2007). Once plated, the cells were grown in media containing Neurobasal (#21103-049), B27 (#A35828-01), penicillin (100 U/mL)/streptomycin (100 µg/ml, #15140-122), 0.5 mM L-glutamine (#25030-081), and 0.025 mM L-glutamate (#A37840SA) (all

from Thermo Fisher Scientific). Half of the media was replaced every 4 days with media without glutamate. The cells were cultured for 2-24 days prior to lysing, fixation, or transfection, depending on the experiment.

2.2.6 Cell Transfection:

Lipofectamine transfection reagent: N2a cells were plated in 6 well tissue culture dishes at a density of 5×10^5 cells/well or in 24 well tissue culture dishes at a density of 5×10^4 cells/well. After 24 hrs post-plating, cells were transfected with 0.25-2 μ g of one or two plasmids encoding Nrg1, Nrg2, Nrg3, mCherry, ErbB4, myc-Par6, myc-Par3, myc-cdc42, FLAG-aPKC ζ , FLAG-PSD-95, or ErbB4 mutants (described above). Both single transfections and co-transfections with two plasmids were carried out using Lipofectamine Plus following manufacturer instructions (Thermo Fisher Scientific, #18324-020 and #11514-015). The N2a cells were grown for 48 hrs post transfection prior to preparation of detergent extracts or fixation for immunocytochemistry, as described in the sections **Immunoprecipitations and Western Blotting** and **Immunocytochemistry**.

Calcium phosphate transfection: For transfection of primary neurons, cortical cultures derived from E17-18 rat embryos were plated at 25,000 cells/well or 75,000 cells/well (depending on the experiment) and grown for 2 or 5 days *in vitro* (DIV) prior to transfection. Cultures were singly transfected with plasmids encoding EGFP-N1 vector control (2 μ g), co-transfected with plasmids encoding mCherry and ErbB4 (1.65-2 μ g each), or co-transfected with plasmids encoding myc-Par6 and ErbB4 (2 μ g each). The transfections were completed using the calcium phosphate method previously described in detail in Jiang et al 2006 (M. Jiang & Chen, 2006). Cultures were maintained until 5-8 DIV (depending on the experiment) prior to fixation for immunocytochemistry, as described in the sections **Immunocytochemistry**.

2.2.7 Nrg Activation:

For Nrg activation experiments in N2a cells, untransfected, transiently transfected, and permanently transfected N2a/ErbB4 cells cultured in 6-well plates were serum starved for 24 hours in 3 mLs/well of 0.5% FCS/DMEM. This media was then replaced with 1 mL/well of 0% FCS/DMEM four hours prior to activation. For Nrg activation experiments in neuronal cultures, the media was reduced from 3 mL/well to 1 mL/well 45 min prior to activation. To activate both N2a cells and cortical neuronal cultures plated in 6-well plates, 500 ng/mL of GST, GST-Nrg1, GST-Nrg2, or GST-Nrg3 fusion proteins were added for 0, 5, 15, 20, 30, 60 min, 6 hrs, 12 hrs, or 24 hrs at 37°C, depending on the experiment.

Nrg activation was stopped by washing the cells three times with cold PBS (137 mM NaCl, 2.7 mM KCl, 8.45 mM Na₂HPO₄, and 1.46 mM KH₂PO₄, pH 7.30) on ice prior to harvesting. For activation experiments in which the lysates were not analyzed for changes in protein phosphorylation, the cells were harvested with lysis buffer consisting of: 50 mM *tris*(hydroxymethyl)aminomethane –HCl (Tris-HCl), pH 7.5; 150 mM sodium chloride (NaCl); 1 mM Ethylenediaminetetraacetic acid (EDTA), pH 8.0; 50 mM sodium fluoride (NaF); 0.5 mM sodium orthovanadate (Na₃VO₄); 5 mM sodium pyrophosphate (Na₄P₂O₇); 0.1% sodium dodecyl sulfate (SDS); 1% Triton X-100; and 0.5% Nonidet P-40 (NP-40) supplemented with protease inhibitor cocktail (Roche, #0653830400). For activation experiments where protein phosphorylation was monitored, cells were harvested with lysis buffer (as described above) supplemented with phosphatase inhibitor cocktails II and III (Sigma Aldrich, #P5726 and #P0044). After harvesting, lysates were vortexed and incubated on ice for one hour prior to centrifugation at 15,000 rpm for 15 min at 4°C. Lysate supernatants were then normalized for protein concentration using the DC Protein Assay following manufacturer's instructions (Bio-Rad Laboratories, Inc., #5000111). Cell lysates were then used for IPs or Western blotting, as described in the section **Immunoprecipitations and Western Blotting**.

For experiments analyzing neurite outgrowth in cortical cultures, 500 ng/mL of GST, GST-Nrg1, GST-Nrg2, or GST-Nrg3 were added upon plating 25,000 cells/well in a 24-well tissue culture plates fitted with a glass coverslip coated in 250 µg/ml PLL. For experiments analyzing neurite outgrowth in transfected cortical cultures, 500 ng/mL of factors were added to the cultures post-transfection at 2 DIV. Depending on the neurite outgrowth experiment, cells were cultured for 2 or 5 days with constant exposure to the GST or Nrg factors (once they were introduced). For cultures grown for 5 DIV, half the media was removed and fresh media without glutamate was added at 4 DIV. In addition to the media change, 500 ng/mL of fresh GST or Nrg factors were also added at 4 DIV. Nrg activation was stopped by washing cells once with cold PBS prior to fixation with 4% paraformaldehyde/4% sucrose in PBS. Cells were immuno-stained prior to imaging and neurite outgrowth analyses, as described in detail in the sections **Immunocytochemistry** and **Neurite Outgrowth Measurements**.

Time course of ErbB4 and Par6 expression: To determine whether ErbB4 and Par co-localize in cortical neurons in a time dependent manner, ErbB4 and Par6 were double-transfected into cortical cultures, and after 8 DIV activated with 500 ng/mL of GST or GST-Nrg1 for 0 min, 20 min, 1 hr, 6 hrs, 12 hrs, or 24 hrs. Nrg activation was stopped by washing the cells once with cold PBS prior to fixation with 4% paraformaldehyde/4% sucrose in PBS. The cells were then immuno-stained and analyzed for ErbB4 and Par6 co-localization, as described in detail in the section **Immunocytochemistry**.

2.2.8 Immunoprecipitations and Western Blotting:

N2a cells and cortical cultures: For IP of ErbB4, Par6, myc-Par6, myc-Par3, and myc-Cdc42, detergent cell extracts were normalized for protein levels and were incubated overnight at 4°C with 30 µl of a 1:1 dilution of Protein G agarose (Thermo Scientific, #20399) in lysis buffer (described in **Nrg Activation**) and 0.2 µg of anti-ErbB4 (Thermo Fisher Scientific, #MA5-

12888), 0.2 µg of anti-Par6 (Santa Cruz, #sc-74479), or 0.8 µg of anti-myc for Par6, Par3, or Cdc42 IPs (Proteintech, #1A5A2). For the IP of Cdc42, aPKCζ, and FLAG-PSD-95, normalized detergent cell extracts were incubated overnight at 4°C with 30 µl of a 1:1 dilution of Protein A sepharose CL-4B beads (GE Healthcare, #17-0780-01) in lysis buffer and 1:400 dilution of anti-aPKCζ (Cell Signaling, #2058), 1:400 dilution of anti-Cdc42 (Cell Signaling, #2462), or 0.8 µg anti-FLAG for the PSD-95 IP (Millipore Sigma, #F7425). Following an overnight incubation, the samples were washed four times in cold lysis buffer, and the supernatant removed. After the last wash, the samples were resuspended in 40 µl of 2X Laemmli sample buffer (0.5 M Tris-HCl, pH 6.8; 20% glycerol; 0.5% bromophenol blue, 4% SDS, 10% β-mercaptoethanol) and heated for 5 min at 98°C. After centrifugation, the samples were subjected to SDS-PAGE using 8% or 4-20% gradient Tris-glycine gels (Thermo Fisher Scientific, #EC60152 and #EC60285 respectively) for protein separation.

For Western blotting, 5X Laemmli sample buffer (0.5 M Tris HCl, pH 6.8; 50% glycerol; 0.5% bromophenyl blue, 10% SDS, 25% β-mercaptoethanol) was added to normalized cell lysates to dilute the samples to 1X sample buffer. The samples were then heated for 3 min at 98°C. After centrifugation the proteins were separated by SDS-PAGE using 8% or 4-20% gradient Tris-glycine gels.

Brain tissue: Whole brain extracts or cortical tissue extracts were prepared from E18, P0, P3, P5, P7, P11, P14, P20, P25, P28, and adult Sprague Dawley rats. These tissues were used as positive controls and also to determine the developmental time course of expression for several proteins. Samples were homogenized using a Polytron™ in one of the following lysis buffers: 50 mM Tris HCl (pH 7.5), 150 mM NaCl, 500 mM EDTA, 0.5 mM Na-orthovanadate, 50 mM NaF, 5 mM Na₄P₂O₇, 0.5% NP-40, 1% Triton X-100, 0.1% SDS, and protease inhibitor tablet (Roche, #0653830400) for experiments in Chapter 3 or 25 mM Tris-HCl (pH 7.5), 150 mM NaCl, 1 mM EDTA, 1% NP-40, and protease inhibitor tablet for experiments in Chapter 5. Brain

tissue lysates were then used for IPs and Western blotting using the same protocol described above for cell lysates.

For both tissue and cell extracts, samples were subjected to protein separation by SDS-PAGE followed by transfer onto Immobilon P PVDF membranes (Millipore, #IPVH00010). Membranes were then incubated for 30 mins at room temperature with blocking buffer. To detect non-phosphorylated proteins the blocking buffer consisted of 3% milk (Carnation) in 1X TBST (50mM Tris, pH 7.5; 150 mM NaCl; 0.1% Tween-20). To detect phosphorylated proteins the blocking buffer consisted of 1% BSA (Fisher Scientific, #BP9703), 50mM NaF, 0.5 mM Na₃VO₄, and 5mM sodium pyrophosphate in 1X TBST.

Following blocking, the membranes were incubated overnight at 4°C in the presence of primary antibodies. The following antibodies were used for the Western blot analyses: affinity purified anti-Nrg1 and affinity-purified anti-Nrg3 at 0.27 µg/mL; affinity purified anti-Nrg2 at 0.28 µg/mL; anti-Nrg3 serum #6144 at 1:2,000 dilution; anti-ErbB4 serum #616 at 1:5,000 dilution; anti-GAPDH (Millipore, #MAB374) and anti-β-actin (Cell Signaling Technology, #3700) at a 1:10,000 dilution; a 1:1 mixture of anti-pTyr PY99 (#sc-7020) and PY20 (#sc-508) from Santa Cruz Biotechnology at a 1:3,500 dilution; anti-Par6 (#sc-25525) from Santa Cruz Biotechnology at a 1:2,000 dilution; anti-Par3 (#07-330) from EMD Millipore at a 1:2,000 dilution; anti-myc-tag (#2278), anti-PKCζ (#9372), anti-p-PKCζ/λ (#9378), anti-Cdc42 (#2462), anti-p-Cdc42 (#2461), and anti-PSD-95 (#3450) all from Cell Signaling at a 1,2000 dilution. For experiments including pre-absorption, serum #6144 (1:2,000) and affinity purified anti-NRG3 (0.27ug/ml) were resuspended in 10 mLs of blocking buffer in the presence or absence of 1.46 µg GST-Nrg3 and incubated overnight at 4°C. Following pre-absorption the membranes were incubated further overnight with the absorbed or control antibodies.

After the overnight incubation with the primary antibodies, the membranes were washed 5 times for 5 min with TBST, blocked for 15 min as described above, and then incubated for 60 min with either horse-radish peroxidase (HRP) conjugated goat anti-rabbit IgG (#31460) or goat anti-mouse IgG (#31432) both from Thermo Scientific (1:15,000). The blots were washed 5 times for 5 min with TBST and processed for chemiluminescence using Super Signal West Pico or Femto Chemiluminescent Substrate ECL system (#34078 and #34096 respectively from Thermo Fisher Scientific) according to instructions provided by the manufacturers.

Western blot quantification: For some experiments in Chapter 5, densitometry band measurements were obtained from X-ray films using Image J software. The densitometry ratios between Par3 and ErbB4/myc (Par6) bands and the Par3, aPKC ζ , paPKC ζ , Par6, Cdc42, and pCdc42/ErbB4 bands were used to calculate relative levels of association. The values are represented as fold increases from the baseline level (considered 1), determined in the absence of Nrg activation (GST control) or 0 min time point depending on the experiment. Densitometry data were analyzed statistically using one-way ANOVAs with Tukey post hoc analyses as described in the section **Statistical Analyses** (n = 2-3 per data set).

2.2.9 Deglycosylation:

For the Nrg3 deglycosylation experiments, detergent extracts using the lysis buffer described for experiments in Chapter 3 (see above) lacking SDS were prepared from P25 rat cortices. The tissue lysates were homogenized using a Polytron™ homogenizer (Kinematica, Lucerne, Switzerland, #PT10-35) and then incubated on ice for 60 min. The extracts were spun for 15 min at 15,000 rpm. The pellet was discarded and supernatant was used for the deglycosylation experiment. Tissue extract supernatants were subjected to protein determination as previously described. Tissue lysates corresponding to 30 μ g of protein were treated overnight at 37°C with 500 units of N-glycosidase F (PNGase F), Endoglycosidase H (Endo H), O

glycosidase, or O glycosidase/Neuraminidase mixture using the conditions and reagents provided by the manufacturers (NEB). The reactions were stopped by the addition of 2X Laemmli sample buffer, denatured for 3 min at 98°C, and analyzed by SDS-PAGE as described in **Immunoprecipitations and Western Blotting**.

2.2.10 Immunocytochemistry:

Primary cortical neurons from E17-E18 Sprague Dawley rats were seeded at 25,000-80,000 cells/well and untransfected or transfected N2a cells were seeded at 50,000 cells/well onto 12 mm glass coverslips (Thermo Fisher Scientific, #12-545-83) coated with 250 µg/mL of poly-L lysine (PLL) (EMD Millipore, # P2636). The cells were fixed with cold 4% paraformaldehyde/4% sucrose in PBS for 20 min, followed by 5 washes of 5 min each with cold PBS. The cells were incubated for 30 min with blocking buffer consisting of 5% goat serum (Atlanta Biologicals, #S13150H) and 5% FCS in PBS with or without 0.01% Triton X-100.

Following the blocking step, the cells were incubated overnight at 4°C with the following primary antibodies: anti-Nrg3 serum #6144 at a 1:250 dilution; affinity purified anti-Nrg3 at 2.14 µg/mL; anti-GFAP (BioLegend, #672402), anti-GM130 (BD Biosciences, #610822), anti-ErbB4 (Thermo Fisher, #MA5-12888), anti-Par6 (Santa Cruz Biotechnology, #sc-25525) all at 1:500 dilution; anti-O4 (Millipore, #MAB345), anti-MAP2 (BioLegend, #801801), anti-GABA (BioLegend, #A2052), and anti-β-tubulin (Cell Signaling, #2146), anti-Ankyrin-G (NeuroMab, #75-146; SYnaptic SYstems, #386003) all at 1:1,000 dilution; anti-parvalbumin (NeuroMab, #75479) at 1:5,000 dilution; and anti-GAD-65 (SDHB, #GAD65) at 1:25,000 dilution.

The cells were then washed 5 times for 5 min in PBS, and further blocked for 30 min. The cells were incubated with Alexa Fluor 488-labeled goat-anti-rabbit (Thermo Fisher Scientific, #A-11008) antibodies and/or Alexa Fluor 594-labeled goat-anti-mouse (Thermo Fisher Scientific, #A-11005) antibodies (1:300 dilution in blocking buffer) for 90 min at room

temperature in the dark. The cells were then washed 2 times for 5 min in PBS. To visualize the cell nuclei the cells were further incubated for 10 minutes in PBS/10 µg/mL 4'-6-diamidino-2-phenylindole (DAPI, EMD Millipore, #508741) or Hoechst 33342 in PBS/1 µg/mL (Thermo Fisher Scientific, #H3570). The cells were further washed 3 times for 5 min with PBS, and then mounted onto glass slides (Thermo Fisher Scientific, #12-552-5) using SlowFade Antifade (Thermo Fisher Scientific, #S2828). The cells were photographed under epifluorescence, with immunofluorescence considered to be at background level when the intensity of the signal (very low) matched that observed when only secondary antibodies were used. A subset of images were acquired using a Nikon TE2000 inverted microscope and BD CARVIL White light confocal imaging system equipped with a Cascade 16 bit CCD camera. The images were generated using the Universal Imaging Corporation Metamorph 6.1 software package. Other images were acquired using a Nikon NiE upright microscope and Lemuncor SpectraX light source for fluorescence imaging equipped with a Hamamatsu Orca-Flash 2.8 sCMOS high resolution camera. The images were generated using the Nikon Elements software. The images were not modified other than relative adjustments of brightness, contrast and magnification.

2.2.11 Immunohistochemistry:

For immunohistochemistry reported in Chapter 3, coronal and sagittal sections were prepared from E17, P3, P7, and P20 Sprague Dawley rats. The brains from E17-E19 rat embryos were dissected after removal from the pregnant females, and fixed in 4% paraformaldehyde in PBS. Postnatal rats were first anesthetized with urethane and then transcardially perfused for 2-5 min with 0.1M PB (pH 7.2) followed by 4% paraformaldehyde in PB for 20 min. After dissection, the tissues were further fixed in 4% paraformaldehyde for 4 hrs and equilibrated successively in 15% and 30% sucrose in dH₂O for cryoprotection. In preparation for sectioning, tissues were frozen in dry ice and embedded in Tissue-Tek O.C.T medium (Sakura, #25608-930). Cryostat sections of 15 µm were collected onto chrom-alum

coated slides. Prior to staining, the fixed sections were hydrated in PBS for 10 min and incubated for 30 min at room temperature with blocking buffer (as described in the section **Immunocytochemistry**) containing either 0.01% Triton X-100 or 0.1% saponin.

Following the blocking step, the cells were incubated overnight at 4°C with the following primary antibodies: anti-Nrg3 6144 serum at a 1:250 dilution; anti-GFAP (BioLegend, #672402) and anti-GM130 (BD Biosciences, #610822) both at 1:500 dilution; anti-MAP2 (BioLegend, #801801), anti-parvalbumin (Swant, #235), and anti-calbindin (Swant, #300) all at 1:1,000 dilution; anti-CNPase (BioLegend, #836404) at 1:5,000 dilution.

The procedures followed for the immunohistochemistry and its visualization closely followed the protocol described in the section **Immunocytochemistry**. Slides were mounted with 50 x 22 mm cover glass (Thermo Fisher Scientific, #3317) using SlowFade Antifade. A subset of images were collected using a Nikon TE2000 inverted microscope (as described above). Confocal images were collected using a Leica SP5 Scanning Confocal with a DMI 6000 CS inverted microscope platform and controlled by Leica LAS software. All images were not modified other than adjustments of brightness, contrast, and magnification.

Two-step procedure. For staining done in P4 coronal sections of rat cortices, a two-step method for immunofluorescence was implemented to retain the surface staining generally lost through incubation with blocking buffers containing detergents. The procedure for the two-step method was modified from (Vernay & Cosson, 2013). After hydration of the tissue sections in PBS, as described above, the slides were incubated in blocking buffer without any detergent for 30 min at room temperature. The anti-Nrg3 #6144 serum (1:250) was then diluted in blocking buffer without detergent, applied to the tissue sections, and incubated overnight at 4°C. Sections were then washed 3 times for 10 min with PBS, fixed again with 4% paraformaldehyde for 10 min, washed 3 times for 10 min with PBS, and then incubated with blocking buffer containing

0.01% Triton X-100 for 1 hour at room temperature. The anti-Nrg3 #6144 serum (1:250) and anti-MAP2 (1:1000) or anti-GAD65 (1:500) were diluted in blocking buffer without detergent, applied to the tissue sections, and incubated overnight at 4°C. Secondary incubation and visualization were done in the same manner described above and in the section

Immunocytochemistry. Images were collected using a Nikon TE2000 inverted microscope (as described above).

2.2.12 *In Situ* Hybridization:

***All *in situ* hybridization experiments reported in Chapter 3 of this thesis were conducted by Janet Weber and Dr. Cary Lai.

For experiments visualizing Nrg3 mRNA expression in Chapter 3, coronal and sagittal tissue sections for hybridization were prepared from Sprague Dawley rats of ages E17, E19, P3, P7, P20, and P25. Embryos were removed via cesarean section and fixed in 4% paraformaldehyde in 0.1M sodium borate buffer, pH 9.5. Postnatal rats were first deeply anesthetized with Nembutal and then transcardially perfused with 4% paraformaldehyde in 0.1M sodium borate buffer, pH 9.5. A 766 bp Nrg1 (Type III) cDNA fragment (bp 555-1321 in accession #AF194438) and a 750 bp Nrg2 cDNA fragment (bp 586-1336 in accession #D89996) were amplified and subcloned into EcoRI/BamH1 cut pBluescript (-). The plasmids were linearized with EcoRI to generate antisense RNAs using T3 RNA polymerase. A 563 bp Nrg3 cDNA fragment (bp 940-1503 in accession #NM_008734) was amplified and subcloned into pCR2.1. The plasmid was linearized with Hind III to generate antisense primers using T7 RNA polymerase. Transcriptions were performed using 125 Ci ³³P-UTP (2,000-4,000 Ci/mmol, either NEN or ICN). The pre- and post-hybridization procedures closely followed those of (Simmons, Arriza, & Swanson, 1989). This procedure was slightly modified to include additional pre-hybridization steps, and were passed through dehydration steps prior to dipping into

photographic emulsion, as developed and previously described in (Anne L. Prieto, Weber, Tracy, Heeb, & Lai, 1999). The slides were exposed to the emulsion in the absolute dark, between 7-20 days prior to development. Hybridization signals were considered background when accumulation of silver grains were not associated with a particular area in the tissue and when the distribution of the grain appeared uniform both under dark field and bright field illumination. The hybridization signals were visualized on an Olympus BX51 microscope and photographed using a Nikon Coolpix 4300 digital camera. Images were converted to black and white and were not modified other than relative adjustments to brightness and contrast.

2.2.13 Neurite Outgrowth Measurements:

To perform quantitative neurite outgrowth measurements in the experiments presented in Chapter 4, untransfected cortical neurons or cortical neurons overexpressing ErbB4/mCherry or overexpressing the EGFP-N1 control vector were cultured in the presence of GST or GST-Nrg factors for 2 or 5 days depending on the experiment (as described under **Nrg activation**). After this period, the neurons were fixed and immunostained (as described in **Immunocytochemistry**), and imaged using 10X or 40X objectives on a Nikon TE2000 microscope.

Neurite outgrowth analyses were carried out using the “Freehand Line” and “Measure” tools available in the n ImageJ 1.48v software, subsequent to setting the scale on the program (using 10X or 40X objective rulers). For each cell we measured (in μm): the length of all primary neurites, the length of the longest primary neurite (the axon), and the average length of the primary neurites excluding the longest one. A primary neurite was defined as any process extending directly from the cell body. Measurements were taken by tracing a neurite as it connects to the cell body (the base) to its very tip. Other morphological analyses included: counts of the number of neurites per cell, a breakdown of the proportion of cells expressing one

neurite, two neurites, three neurites, four neurites, five neurites, or more than five neurites, and proportions of cells displaying secondary neurites. Secondary neurites were defined as any extension from a primary neurite.

For neurite outgrowth measurements of GABAergic interneurons expressing ErbB4 either endogenously or overexpressing ErbB4 after transfection, measurements from 3 (independent neuronal preparations (experiments) were taken. For each experiment, 25 cells were imaged and measured from three different coverslips for a total of 225 cells/condition. A neuron was measured only if it was positive for both ErbB4 (mCherry in overexpression condition) and GABA.

For GABA positive interneurons in which neurites that were Ankyrin-G (+) were measured, 15 cells per coverslip were imaged from one coverslip from three different experiments (45 cells/condition total). Neurites in a neuron were measured only if it was positive for GABA and also unequivocally expressed Ankyrin-G.

For neurite outgrowth measurements of β -tubulin (+) and ErbB4 (-) neurons, 25 cells per coverslip were imaged from one coverslip from three different experiments (75 cells/condition total). A neuron was measured only if it was positive for β -tubulin and negative for ErbB4.

For neurite outgrowth measurements of GABA (+) and ErbB4 (-) interneurons, 25 cells per coverslip were imaged from one coverslip from three different experiments (75 cells/condition total). A neuron was measured only if it was positive for GABA and negative for ErbB4.

For neurite outgrowth measurements on control experiments in GABAergic interneurons overexpressing the pEGFP-N1 vector, 25 cells per coverslip were imaged from one coverslip

from three different experiments (75 cells/condition total). A neuron was measured only if it was positive for GABA and EGFP.

2.2.14 Statistical Analyses:

Analyses of neurite outgrowth in Chapter 4 and densitometry in Chapter 5 were compared between conditions for statistical significance using one-way ANOVAs with Tukey post hoc analyses, with $p \leq 0.05$ being considered significant. All analyses were done using the SPSS 25 statistics software.

For some experiments in Chapter 4 where the means of only two groups were compared (GST vs. Nrg1), statistical significance was determined using a two-tailed independent samples t-test, with $p \leq 0.05$ being considered significant.

For all experiments in Chapter 4, the median value was taken from each coverslip. In experiments that encompassed 3 coverslips/experiment, the median values were averaged to obtain one mean value for each experiment. Data is reported as the average of three experiments \pm SEM.

Chapter 3: Developmental Expression of Neuregulin-3 in the Rat Central Nervous System

Portions of this chapter have been published

Rahman, A., Weber, J., Labin, E., Lai, C., & Prieto, A. L. (2019). Developmental expression of Neuregulin-3 in the rat central nervous system. *Journal of Comparative Neurology*, 527(4), 797-817.

3.1 INTRODUCTION:

The Nrgs (Nrg1-4), including Nrg3 have been shown to play important roles in the developing and mature nervous system (Birchmeier & Bennett, 2016; Grieco, Holmes, & Xu, 2019; Mei & Nave, 2014; Mei & Xiong, 2008). Among the Nrgs, Nrg1 and its isoforms are the most extensively studied and Nrg1 expression has been well-characterized. However, more recently, Nrg3 has received attention as it has also emerged as a candidate risk gene for several neuropsychiatric disorders including bipolar disorder and SZ (Avramopoulos, 2018; P.-L. Chen et al., 2009; Hayes et al., 2016; Loos et al., 2014; Paterson et al., 2017). Recent studies have also indicated that Nrg3 plays important roles in cortical development (Bartolini et al., 2017) and glutamatergic neurotransmission (Y.-N. Wang et al., 2018). Along with studies on Nrg2 as a regulator of dopaminergic and glutamatergic function (K.-H. Lee et al., 2015; Vullhorst et al., 2015; L. Yan et al., 2018), the current evidence supports the concept that Nrgs 1, 2, and 3 perform distinct functions in the CNS. In order to gain an improved understanding of the roles played by these factors in the nervous system, it is essential to characterize their developmental expression patterns. In this chapter, we provide a comprehensive description of the developmental expression of Nrg3, an understudied Nrg in the rat CNS.

NRG3 has been associated with an increased risk for SZ, and multiple behavioral and cognitive abnormalities (Avramopoulos, 2018). Genetic studies have reported a consistent

relationship between SNPs located within the first intron of *Nrg3* and the SZ endophenotype of delusional behavior (Morar et al., 2011). The characterization of *Nrg3* $-/-$ mice further revealed behaviors that are consistent with animal models of SZ, showing increased levels of novelty-induced hyperactivity, impaired pre-pulse inhibition and a reduction in fear conditioning (Hayes et al., 2016). Increased levels of *Nrg3* expression in mice correlate with impulsivity, with the opposite effect seen in *Nrg3*-deficient mice (Loos et al., 2014). Paterson and Law (Paterson & Law, 2014) also reported that injection of *Nrg3* at an early postnatal age resulted in increased anxiogenic-like behavior and reduced sociability in adult mice. In at least two studies (Meier et al., 2013; Morar et al., 2011), *NRG3* variants have also been associated with attention deficits observed in SZ. Other studies have also linked specific *NRG3* SNPs with increased risk for Alzheimer's disease (K.-S. Wang et al., 2014) and nicotine dependence (Turner et al., 2014; Zhou et al., 2018).

An improved understanding of *Nrg3* signaling at the cellular and systems level should continue to provide insights into how its dysregulation contributes to these neuropathological conditions. A recent study has identified *Nrg3* as a regulator of glutamatergic neurotransmission (Y.-N. Wang et al., 2018). Deletion of *Nrg3* in pyramidal neurons resulted in enhanced neurotransmission as evidenced by an increase in glutamate release. Increased levels of *Nrg3* led to the opposite result with a decrease in glutamatergic neurotransmission. These observations provide one mechanism to explain how alterations in *Nrg3* mRNA levels (Kao et al., 2010; Paterson et al., 2017) underlie changes in glutamatergic neurotransmission associated with these pathological conditions (Cappellini et al., 2006; R. Gao & Penzes, 2015).

Studies in rodent and human have provided evidence that *Nrg3* is involved in cortical development and function. The earliest reported expression of *Nrg3* is at E12.5 in the anti-hem, a structure in the lateral neuroepithelium that gives rise to the cerebral cortex (Assimacopoulos, Grove, & Ragsdale, 2003). At E16, Zhang et al (D. Zhang et al., 1997) observed that *Nrg3* was

predominantly expressed in neural tissue with high levels detected in the cortical plate. A recent effort has provided a detailed characterization of Nrg3 expression throughout early cortical development (E13.5 to P4) (Bartolini et al., 2017). These investigators have determined that Nrg3 serves to regulate the migration of interneuronal precursors into distinct cortical layers. Although the information regarding Nrg3 expression in the postnatal period is more limited (Anton et al., 2004; Marines Longart et al., 2004), it is evident that Nrg3 is more widely expressed than either Nrg1 type III or Nrg2.

In order to provide a framework for future studies on Nrg3 function in the CNS, we have sought to provide a comprehensive analysis of the spatiotemporal distribution of Nrg3 mRNA and protein in the embryonic and postnatal rat brain. We have observed that Nrg3 is widely expressed throughout the CNS during both embryonic and postnatal ages. Expression is largely confined to neurons with low to background levels detected in white matter tracts. We further characterized the subcellular localization of Nrg3 in Neuro2a cells and cortically derived cell cultures. In neurons, Nrg3 was localized to the plasma membrane of the cell soma, neurites, and Golgi apparatus. In glia, Nrg3 detection was limited to the Golgi apparatus. Nrg3 was highly expressed and widely distributed in the brain, compared to Nrg1 Type III and Nrg2. Our observations are consistent with and extend those of Longart et al. (2004), Anton et al. (2004), and Bartolini et al. (2017). Our findings have identified regions throughout the rodent CNS in which Nrg3 may play functional roles and highlight potential cellular model systems to study Nrg3 in health and disease.

3.2 RESULTS:

3.2.1 Characterization of Anti-Nrg3 Antibodies

3.2.1.1 Antibody Specificity

To study the spatio-temporal expression of Nrg3 in the rat nervous system, we raised antibodies (serum 6144) against epitopes contained in the EGF-like domain and adjacent sequences of Nrg3. We characterized the ability of these antibodies to recognize Nrg3 by Western blotting, immunocytochemistry, and immunohistochemistry.

We first tested the ability of the antibodies to recognize Nrg3 by Western blotting on detergent extracts from untransfected Neuro2a (N2a) cells (U in Fig. 3.1A and B), N2a cells transfected with Nrg3 (N2a/Nrg3; N3 in Fig. 3.1A and B), and from adult rat brain homogenates (Br in Fig. 3.1A). We tested both serum 6144 (Fig. 3.1A, panels 1 and 2) and affinity-purified anti-Nrg3 from serum 6144 (Fig. 3.1A, panels 3 and 4; Fig. 3.1B, panel 3). The 6144 serum reacted with a major band of approximately 80 kDa in the N2a/Nrg3 samples (Fig. 3.1A, panel 1, lane N3) which was absent in the untransfected cells (Fig. 3.1A, panel 1, lane U) and a band of approximately 97 kDa in the brain extracts (Fig. 3.1A, panel 1, lane Br). The affinity-purified 6144 antibodies, also reacted with the 80 kDa band in the N2a/Nrg3 extracts and a 97 kDa band in the brain extracts (Fig. 3.1A, panel 3, lane N3 and Br respectively). A minor band of approximately 90 kDa was detected by serum 6144 in both untransfected and Nrg3 transfected N2a samples (Fig. 3.1A, panel 1, lanes U and N3) but was not detected even at long exposures when testing the affinity-purified antibodies (Fig. 3.1A, panel 3). Preabsorption of the 6144 serum (Fig. 3.1A, panel 2) and affinity-purified antibodies (Fig. 3.1A, panel 4) with the immunizing antigen (GST-Nrg3) eliminated the immunoreactivity to all bands. The inability to detect additional bands in the N2a/Nrg3 cell and brain extracts indicates that these antibodies specifically recognize Nrg3.

To determine if the anti-Nrg3 antibody cross-reacts with Nrg1 and/or Nrg2, we prepared detergent extracts of N2a cells transfected with cDNAs encoding Nrg1, Nrg2, and Nrg3 (Fig. 3.1B, panels 1, 2 and 3, lanes N1, N2, N3 respectively). To demonstrate that Nrg1 and Nrg2 are expressed in cell extracts derived from N2a/Nrg1 and N2a/Nrg2 transfected cells, we blotted with affinity-purified anti-Nrg1 antibodies (Fig. 3.1B, panel 1) and affinity-purified anti-Nrg2 antibodies (Fig. 3.1B, panel 2). The anti-Nrg1 antibodies (Fig. 3.1B, panel 1) recognized several bands in the Nrg1 (N1 lane) extract but did not react with bands in the Nrg2 (N2 lane) or the Nrg3 (N3 lane) transfected cells. Similarly, the anti-Nrg2 antibodies (Fig. 3.1B, panel 2) recognized a major band of approximately 110 kDa and several minor bands in the Nrg2 (N2 lane) transfected cells and an unspecific band of approximately 50 kDa in all cell extracts. Anti-Nrg2 antibodies did not detect any major bands with molecular weights corresponding to either Nrg1 or Nrg3 (Fig. 3.1B, panel 2, lanes N1 and N3 respectively). When the affinity-purified anti-Nrg3 antibodies were tested (6144) (Fig. 3.1B, panel 3), they recognized a major band of 80 kDa in the N2a/Nrg3 (N3 lane) cell extracts but did not cross-react with bands corresponding to Nrg1 and Nrg2 (Fig. 3.1B, lanes N1 and N2). These results indicate that the anti-Nrg3 antibodies are specific for Nrg3 and do not cross-react with Nrg1 or Nrg2.

3.2.1.2 Developmental Expression of Nrg3 in Whole Brain Lysates and Cortical Cultures

To establish a developmental time frame of Nrg3 expression, we used detergent extracts prepared from whole E18 to adult (A) rat brains (Fig. 3.1C) to perform Western blotting using the anti-Nrg3 affinity-purified antibodies. At embryonic and early postnatal stages, relatively low levels of Nrg3 were detected compared to later stages. Nrg3 expression increased steadily between P0 and P11, a period consistent with a potential role in dendritic elaboration and synaptogenesis (Aghajanian & Bloom, 1967). Nrg3 expression peaked at P14 and remained high throughout adulthood. We also established a developmental time frame of Nrg3 expression in primary cortical cultures derived from E17-18 rat cortices by using detergent extracts

prepared from cultures from 1-24 DIV (Fig. 3.1D) and performing Western blotting using anti-Nrg3 affinity-purified antibodies. Cultures grown for 1 DIV showed background levels of Nrg3, with its levels steadily increasing from when it was first detected at 3 DIV to 12 DIV. Nrg3 expression declined at later stages, peaked back at 21 DIV, and then declined back down at 24 DIV, suggesting dynamic roles for Nrg3 during development.

3.2.1.3 Enzymatic Deglycosylation of Nrg3

We also explored the glycosylation state of Nrg3 since it has a mucin-like region enriched in serine and threonine residues, which can potentially be O-linked glycosylated (Hanisch, 2001; Tran & Ten Hagen, 2013; Zhang et al., 1997). We used enzymes having de-glycosylating activities to monitor changes in the molecular weight of Nrg3 in cortical E18 and P25 extracts. As shown in Fig. 3.1E, panel 1, treatment of E18 cortical extracts with a combination of O-glycosidase and neuraminidase resulted in a small but noticeable reduction in molecular weight. No significant reductions in molecular weight were observed for treatments using only one of the two enzymes. In contrast, treatment of P25 cortical extracts (Fig. 3.1E, panel 2) with a combination of O-glycosidase and neuraminidase resulted in a significant molecular weight reduction in Nrg3 from approximately 80 kDa to approximately 60 kDa. This molecular weight reduction was greater than the decrease caused by treatment with neuraminidase alone, which also was significant. In contrast, N-Glycosidase F (PNGase F) and Endoglycosidase H (Endo-H), which act on N-linked sugars, had no effect on Nrg3's molecular weight (Fig. 3.1E). This is consistent with the absence of N-linked glycosylation sites in the Nrg3 amino acid sequence (Zhang et al., 1997). These results support the conclusion that Nrg3 is O-linked glycosylated and that its glycosylation state changes over the course of development.

Figure 3.1

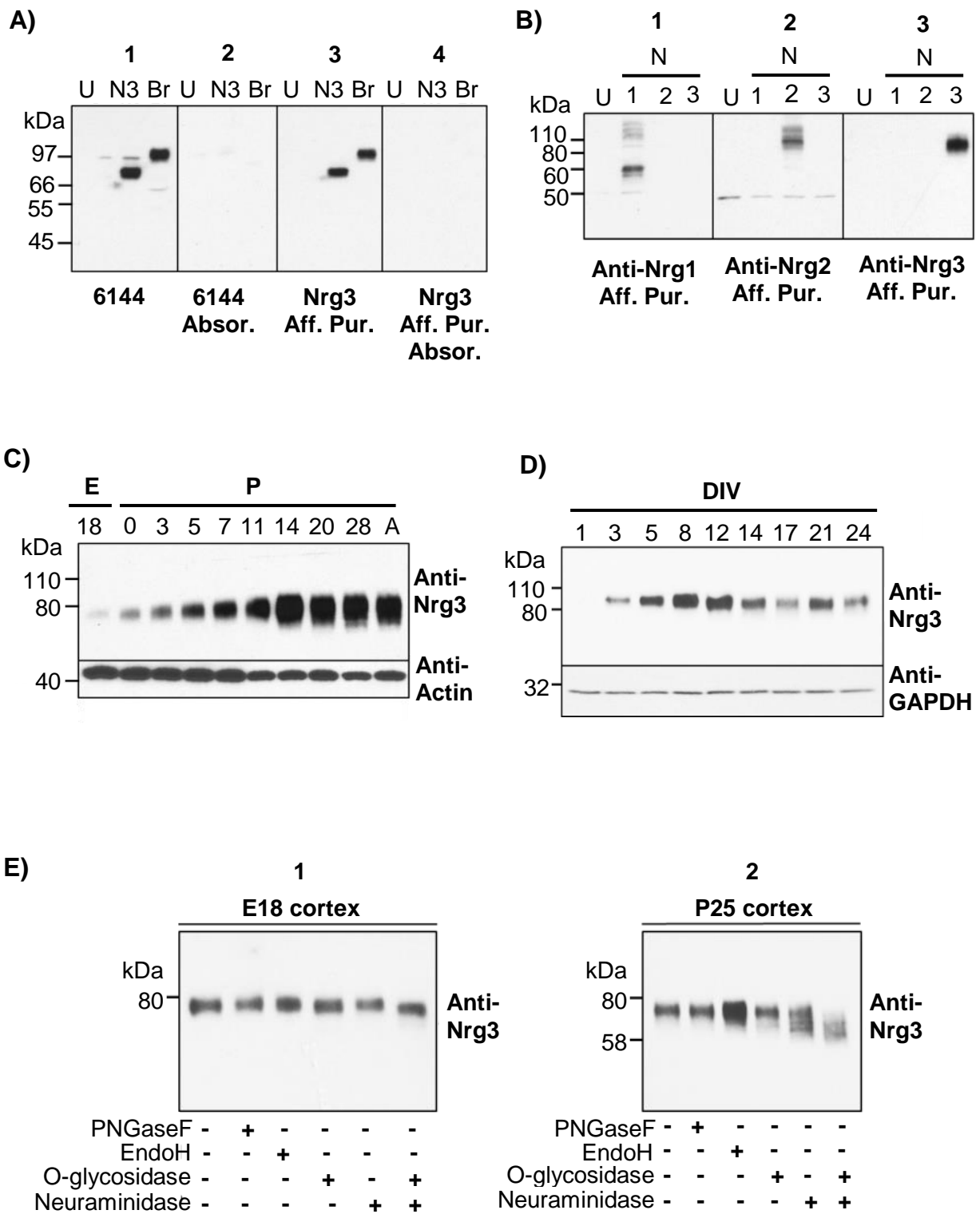


Figure 3.1: Characterization of Specific Nrg3 Antibodies.

A) For Western blotting, detergent extracts corresponding to 50 µg of protein per lane of N2a control (**lane U**), N2a/Nrg3 (**lane N3**), and adult rat brain extracts (**lane Br**) were analyzed by SDS-PAGE using 8% Tris-glycine gels followed by Western blotting. The blots were probed with: **panel 1**, serum #6144 (1:2,000); **panel 2**, serum #6144 (1:2,000) preabsorbed with GST-Nrg3 (1.46 µg); **panel 3**, affinity-purified anti-Nrg3 (0.27 µg/ml); **panel 4**, affinity-purified anti-Nrg3 (0.27 µg/ml) pre-absorbed with GST-Nrg3 (1.46 µg).

B) Anti-Nrg3 was tested for cross-reactivity against Nrg1 and Nrg2. Detergent extracts (50 µg of protein / lane) of N2a control (**lane U**), N2a/Nrg1 (**lane N1**), N2a/Nrg2 (**lane N2**), and N2a/Nrg3 (**lane N3**) were analyzed by SDS-PAGE using 4-20% Tris-glycine gels followed by Western blotting. Blots were probed with: **panel 1**, affinity-purified anti-Nrg1 (0.27 µg/ml); **panel 2**, affinity-purified anti-Nrg2 (0.28 µg/ml); and **panel 3**, affinity-purified anti-Nrg3 (0.27 µg/ml).

C) Whole brain detergent extracts corresponding to 50 µg of protein per lane of embryonic (E)18, postnatal (P) day 0, P3, P5, P7, P11, P14, P20, P28 and P50 (A), were analyzed by SDS-PAGE using 8% Tris-glycine gels followed by Western blotting. The blots were probed with affinity-purified anti-Nrg3 (0.27 µg/ml, top panel) and β-actin (1:5,000, bottom panel).

D) Detergent extracts corresponding to 50 µg of protein per lane of primary cortical cultures grown for 1, 2, 5, 8, 12, 14, 17, 21, and 24 DIV, were analyzed by SDS-PAGE using 4-20% Tris-glycine gels followed by Western blotting. The blots were probed with affinity-purified anti-Nrg3 (0.27 µg/ml, top panel) and GAPDH (1:5,000, bottom panel).

E) Detergent extracts (15 µg/lane) from E18 (**panel 1**) and P25 (**panel 2**) rat cortices were incubated overnight with or without PNGase F, endoH, O-glycosidase (O-gly), neuraminidase (N), or an O-gly/N mixture (O-gly/N). SDS-PAGE was performed using 8% Tris-glycine gels followed by Western blot analysis using affinity-purified anti-Nrg3 antibodies (0.27 µg/ml).

3.2.2 Compartmentalization of Nrg3 by Immunocytochemistry

3.2.2.1 Nrg3 Expression in N2a/Nrg3 Cells

To determine the subcellular localization of Nrg3, we compared the immunoreactivity of the Nrg3 antibodies on N2a cells transfected with Nrg3 (N2a/Nrg3 in Fig. 3.2) and untransfected N2a cells (UNT in Fig. 3.2). Because Nrg3 is a transmembrane protein (Vullhorst et al., 2017; D. Zhang et al., 1997), we performed immunocytochemistry both in the absence (Fig. 3.2A–H, I–Q) and presence of detergent (0.01% Triton X- 100) (Fig. 3.2A”–H”, I”–Q”). Nrg3 immunoreactivity with serum 6144 in the absence of detergent (Fig. 3.2B, C, O, Q) was detected on the plasma membrane of N2a/Nrg3 cells of both the soma and processes. Consistent with these observations, the affinity-purified anti-Nrg3 antibodies also stained the plasma membrane and cell processes (Fig. 3.2F, G). In the presence of detergent, the cell surface staining was less evident while the cytoplasmic staining became more pronounced with strong perinuclear Nrg3 immunoreactivity with both serum 6144 (Fig. 3.2B”, C”, O”, Q”) and the affinity-purified anti-Nrg3 antibodies (Fig. 3.2F”, G”). The Nrg3 staining was eliminated when serum 6144 (Fig. 3.2D, D”) and the affinity-purified anti-Nrg3 (Fig. 3.2H, H”) were preabsorbed with the immunizing antigen (GST-Nrg3), both in the absence and presence of detergent. In contrast, untransfected N2a cells were only weakly stained by the 6144 antiserum (Fig. 3.2A, A”) in the presence and absence of detergent. N2a/Nrg3 transfected cells incubated with secondary antibody alone showed background to very low fluorescence under both detergent conditions (Fig. 3.2E, E”).

3.2.2.2 Anti-Nrg3 Antibodies do not Cross-React with Nrg1 and Nrg2 in Transfected N2a Cells

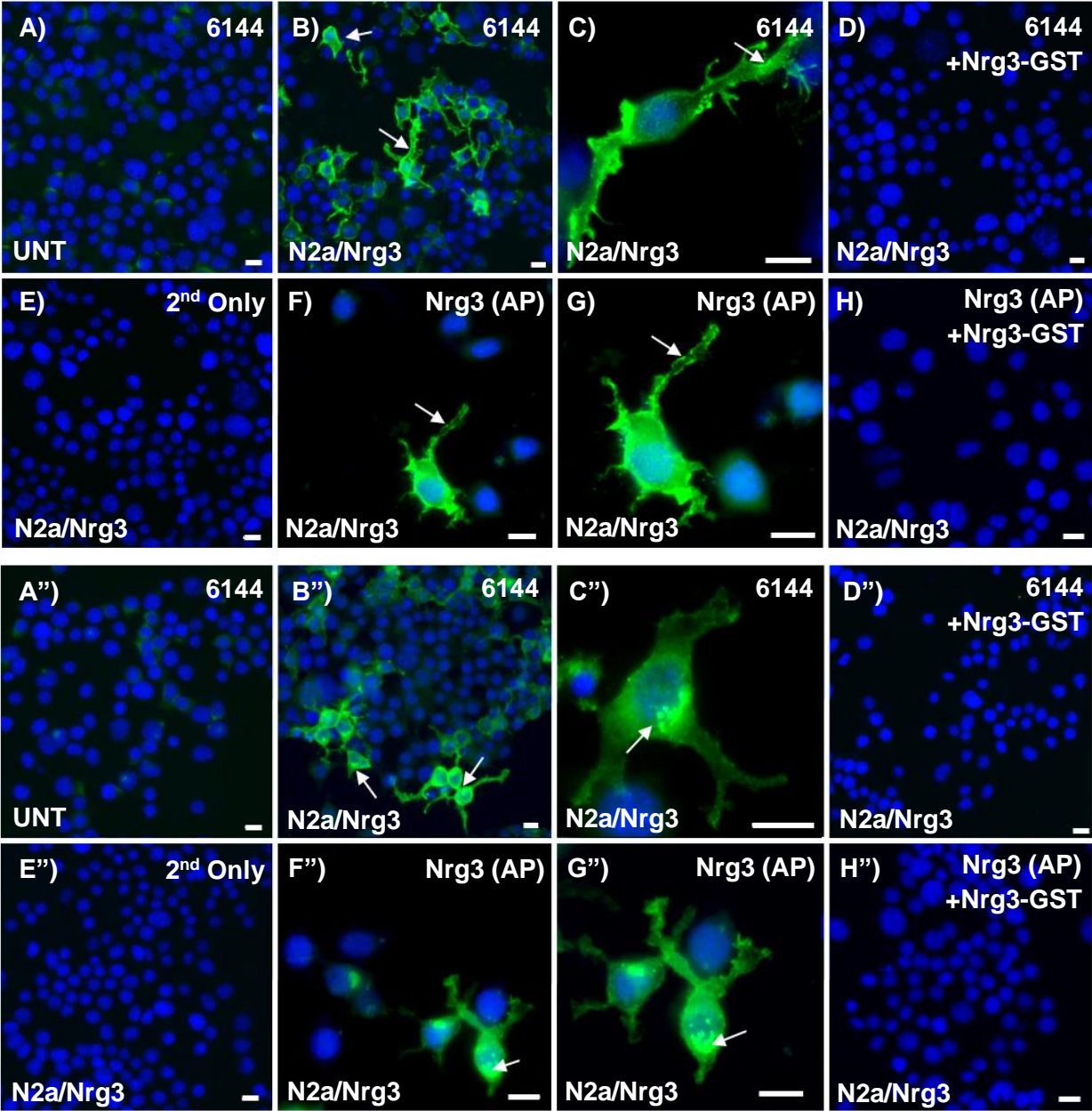
To determine if the anti-Nrg3 antibody cross-reacts with Nrg1 or Nrg2 by immunocytochemistry, we compared the immunoreactivity of the Nrg3 serum 6144 on N2a cells transfected with 0.25µg of Nrg1 (Fig. 3.2I–K, I”–K”), Nrg2 (Fig. 3.2L–N, L”–N”) or Nrg3 (Fig. 3.2O–

Q, O"–Q"). We also cotransfected with 0.25µg of a cDNA encoding mCherry to visualize the transfected cells (Fig. 3.2J, J", M, M", P, P"). We performed immunocytochemistry both in the absence (Fig. 3.2I–Q) and presence (Fig. 3.2I"–Q") of detergent (0.01% Triton X-100). We first quantified our transfections by imaging five fields within three coverslips per condition. We observed an average of 314±74 cells/field for Nrg1, 205±32 cells/field for Nrg2, and 309±24 cells/field for Nrg3. We also counted the mCherry positive (+), Nrg3 (+) and mCherry/Nrg3 (+) cells on each field and calculated averages for all three experiments. The numbers are presented as the means and standard deviations of three experiments for each condition. For the Nrg3/mCherry transfections 80.3 ± 3.0% of the mCherry positive cells also expressed Nrg3 (23.9 ± 1.1 mCherry (+) cells per field and 19.2 ± 1.2 Nrg3 (+) cells per field for all three experiments). We did not detect any anti-Nrg3 (+) cells on the Nrg1/mCherry transfections (23.5 ± 3.2 mCherry (+) cells per field and 0 Nrg3 (+) cells per field for all three experiments). As observed for the Nrg1 transfectants, we did not detect any Nrg3 (+) cells in the Nrg2/mCherry transfections (14.9 ± 1.9 mCherry (+) cells per field and 0 Nrg3 (+) cells per field for all three experiments).

As can be observed by our immunocytochemistry data (Fig. 3.2I–Q), Nrg3 immunoreactivity was only detected in the cells transfected with Nrg3 (Fig. 3.2O–Q, Q"–Q"). Nrg3 immunoreactivity was not observed in the N2a/Nrg1/mCherry (Fig. 3.2I–K, I"–K") or in the N2a/Nrg2/mCherry expressing cells (Fig. 3.2L–N, L"–N") above that observed in the untransfected cells (Fig. 3.2A, A"). To verify that the lack of anti-Nrg3 immunoreactivity in the Nrg1 and Nrg2 transfectants was not due to lack of expression of these polypeptides, we also performed a parallel transfection experiment analyzed by Western blotting that allowed us to determine that there was expression of Nrg1, Nrg2, and Nrg3 in these transfectants (Fig. 3.2R, lanes N1, N2, and N3 respectively). Bands corresponding to Nrg1, Nrg2, and Nrg3 were not observed in untransfected N2a cells or N2a cells transfected with an EGFP-N1 vector control

and mCherry (Fig. 3.2R, lanes U and V respectively). These observations allow us to conclude that our anti-Nrg3 antibodies do not cross-react with Nrg1 and Nrg2 both by Western blotting (Fig. 3.1B) and immunocytochemistry (Fig. 3.2I-N, I''-N'').

Figure 3.2



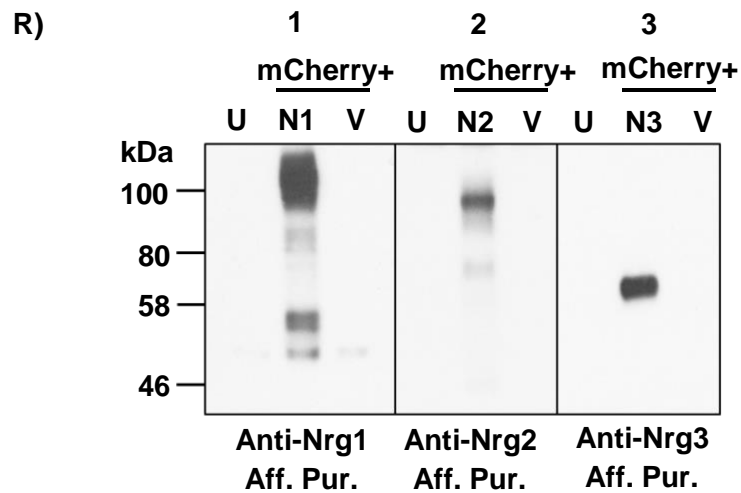
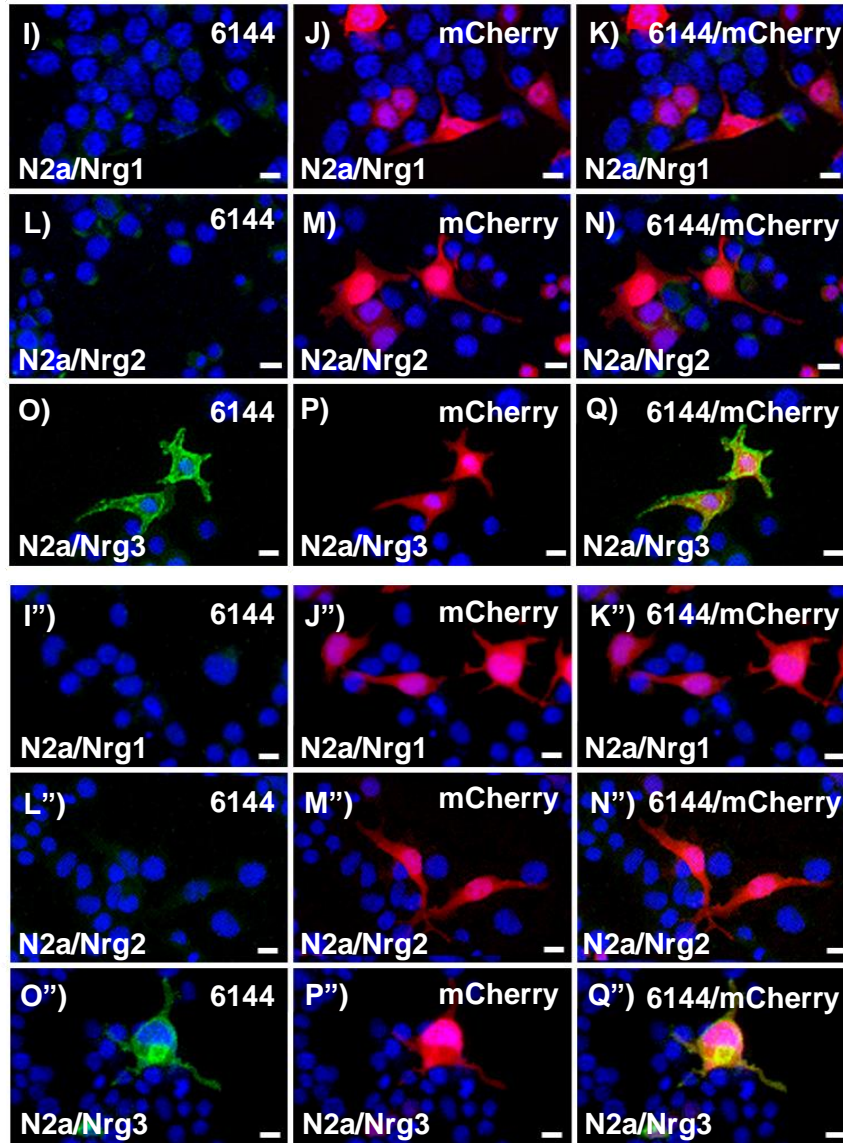


Figure 3.2 Compartmentalization of Nrg3 by Immunocytochemistry.

Anti-Nrg3 antibodies were used to detect the localization of Nrg3 by immunocytochemistry in the absence of **(panels A-Q)** and in the presence of 0.01% Triton X-100 **(panels A''-Q'')**.

Immunofluorescence staining of untransfected (UNT) N2a cells **(panels A and A'')** and N2a/Nrg3 cells **(panels B-H, B''-H'', O-Q, and O''-Q'')** was performed using: #6144 antisera (1:250, **panels A-C, A''-C'', O-Q, and O''-Q''**); #6144 antisera (1:250) preabsorbed with GST-Nrg3 (0.75 µg, **panels D and D''**); affinity-purified antiNrg3 antibodies (2.16 µg/ml, **panels F, G, F'', and G''**); affinity-purified anti-Nrg3 antibodies (2.16 µg/ml) pre-absorbed with GST-Nrg3 (0.75 µg, **panels H and H''**) and secondary antibodies only (1:300, **panels E and E''**). N2a cells shown in panels I-Q and I''-Q'' were transfected with either Nrg1, 2 or 3 and cotransfected with an mCherry encoding plasmid. Immunofluorescence staining of N2a/Nrg1/mCherry **(panels I-K and I''-K'')**, N2a/Nrg2/mCherry cells **(panels L-N and L''-N'')** and N2a/Nrg3/mCherry cells **(panels O-Q and O''-Q'')** was performed using #6144 antisera (1:250). The mCherry expressing cells appear in red. Anti-Nrg3 antibodies were visualized with Alexa Fluor 488 coupled goat anti-rabbit antibodies (in green) at 1:300 dilution. The nuclei were visualized using either DAPI **(panels A-H and A''-H'')** or Hoechst 33342 **(panels I-Q and I''-Q'')** (both in blue). Scale bar = 15 µm for all panels.

R) N2a cells were transfected with Nrg1, Nrg2, Nrg3, or EGFP-N1 control vector and cotransfected with a mCherry encoding plasmid **(panels 1-3)**. For Western blotting, detergent extracts corresponding to 50 µg of protein per lane of N2a control **(lane U)**, N2a/Nrg1/mCherry **(lane N1)**, N2a/Nrg2/mCherry **(lane N2)**, N2a/Nrg3/mCherry **(lane N3)**, and N2a/EGFP-N1-mCherry vector control **(lane V)** were analyzed by SDS-PAGE using 8% Tris-glycine gels followed by Western blotting. The blots were probed with: **panel 1**, affinity-purified anti-Nrg1 (0.27 µg/ml); **panel 2**, affinity-purified anti-Nrg2 (0.28 µg/ml); and **panel 3**, affinity-purified anti-Nrg3 (0.27 µg/ml).

3.2.2.3 Nrg3 is Enriched in the Golgi Apparatus

To determine whether the perinuclear Nrg3 immunostaining in the detergent-permeabilized samples corresponded to the Golgi apparatus, we performed double-labeling immunocytochemistry with serum 6144 and an antibody directed against GM-130, a resident molecule of the cis-Golgi apparatus (Nakamura et al., 1995). As shown in Figure 3.3A-C, anti-Nrg3, and anti-GM-130 showed overlapping immunoreactivity in the perinuclear region of N2a/Nrg3 cells. This overlap was also observed in the Golgi apparatus of cortical neurons expressing endogenous Nrg3 (Fig. 3.3D-F). Nrg3 immunostaining of the Golgi apparatus was not detected in the untransfected N2a cells (Fig. 3.3A-C, unt [arrow]), indicating that the Nrg3 staining within the Golgi was not due to a crossreacting antigen also present in the untransfected cells. We also detected co-localization of Nrg3 and GM-130 in detergent-treated P7 rat cortical tissue sections expressing endogenous Nrg3 (Figure 3.3H-J), which was not observed in our secondary-only negative control (Fig. 3.3K). These results indicate that Nrg3 is primarily expressed in the plasma membrane and in the Golgi apparatus, not only in Nrg3-transfected cells, but also in primary cortical neurons cultured *in vitro* and in neurons present in cortical tissue sections.

Figure 3.3

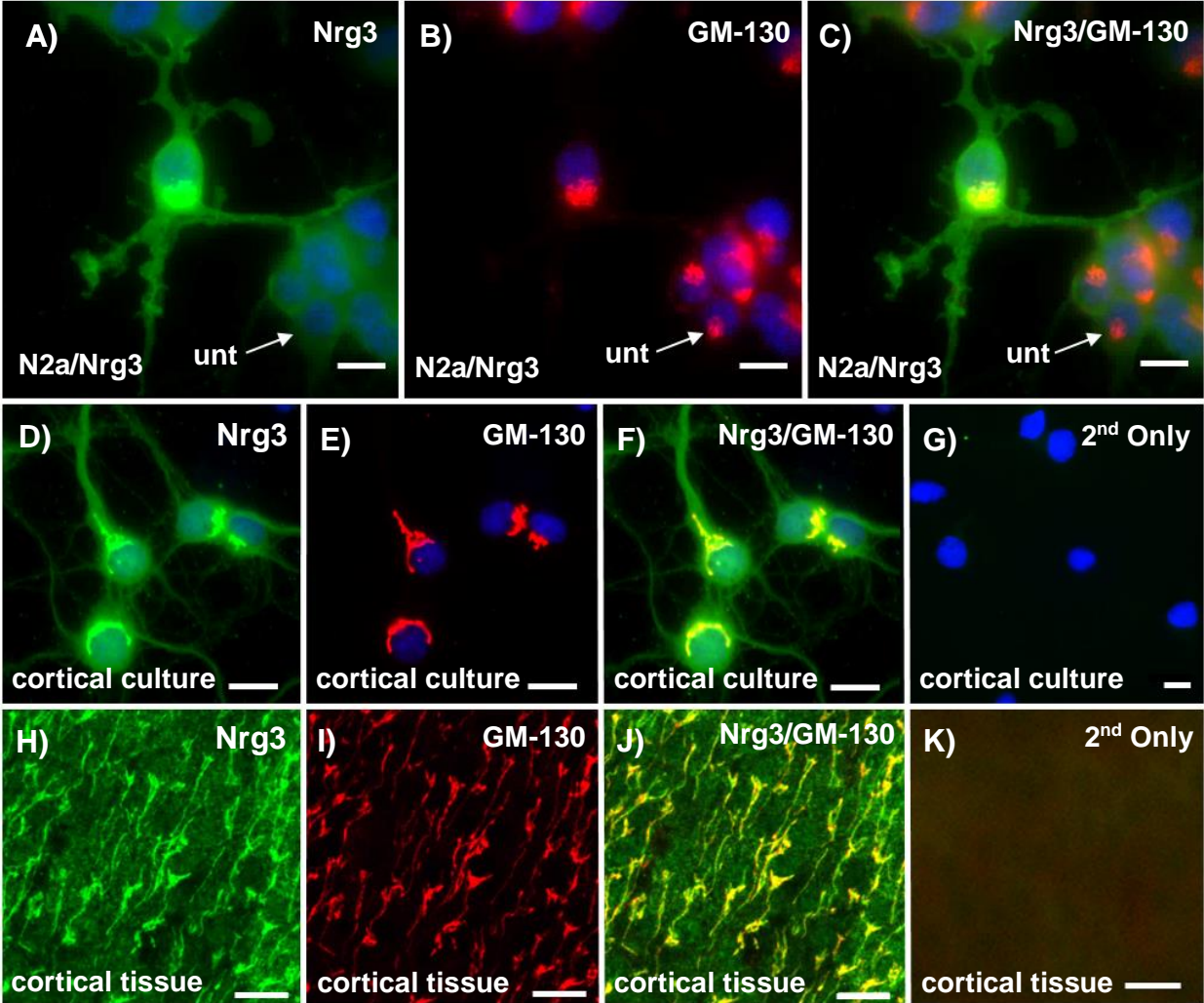


Figure 3.3: Nrg3 is Enriched in the Golgi Apparatus.

Double immunofluorescent staining using #6144 antiserum (1:250, **panels A, D, and H**) and anti-GM-130 (1:500, **panels B, E, and I**) was performed on N2a/Nrg3 transfected cells (**panels A-C**), cortical neurons expressing endogenous Nrg3 (**panels D-G**), and Cx coronal sections (15 μ m) of P7 rats expressing endogenous Nrg3 (**panels H-K**). Merged images are shown in **panels C, F, J, and K**. Cortical neurons (**panel G**) and Cx coronal sections (15 μ m) of P7 rats (**panel K**) were stained with secondary antibodies only (1:300). Arrows in **panels A-C** point to N2a untransfected cells that were negative for Nrg3 but stained with anti-GM-130. For all panels the staining was performed in the presence of 0.01% Triton X-100 detergent. Anti-GM-130 antibodies were detected with anti-mouse secondary antibodies coupled with AlexaFluor 594 (in red) and anti-Nrg3 antibodies were detected using anti-rabbit secondary antibodies coupled to Alexa Fluor 488 (in green) both at 1:300 dilution. The nuclei were visualized using DAPI (in blue). Scale bar = 15 μ m for all panels.

3.2.3 Expression of Nrg3 in Primary Cortical Neurons and Glia *in vitro*

3.2.3.1 Nrg3 is Abundantly Expressed in Cortical Neurons

To identify the cell types expressing Nrg3 in the rat brain, we performed immunocytochemistry on isolated cells from rat E17-E18 cortices and immunohistochemistry on tissue sections using markers to identify different neuronal and glial subtypes. As shown in Figure 3.4, Nrg3 immunoreactivity was detected in both the cell bodies and processes of neurons that expressed the neuronal marker microtubule associated protein 2 (MAP2) (Fig. 3.4A-C). Immunofluorescence staining in P4 tissue sections also shows Nrg3 expression on MAP2 expressing cortical neurons (Fig. 3.4D-F). Nrg3 was also observed in cells expressing the enzyme glutamic acid decarboxylase (GAD-65), a marker of inhibitory GABAergic interneurons (Fig. 3.4G-L) (Benson, Watkins, Steward, & Banker, 1994) both in neuronal cultures (Fig. 3.4G-I) and P4 tissue sections (Fig. 3.4J-L). This is of interest since GABAergic interneurons express the Nrg3 receptor ErbB4 (Vullhorst et al., 2009; Yau et al., 2003). As ErbB4 is preferentially expressed in the parvalbumin-positive subset of cortical interneurons, we performed immunofluorescence staining in P7 tissue sections and identified Nrg3 in parvalbumin-expressing neurons (Fig. 3.4M-O). The Nrg3 immunostaining was observed throughout the dendritic compartment as well as in the soma of parvalbumin positive interneurons. In the presence of detergent, the Nrg3 cell surface staining was reduced as observed in cultured cells (Fig. 3.2).

Figure 3.4

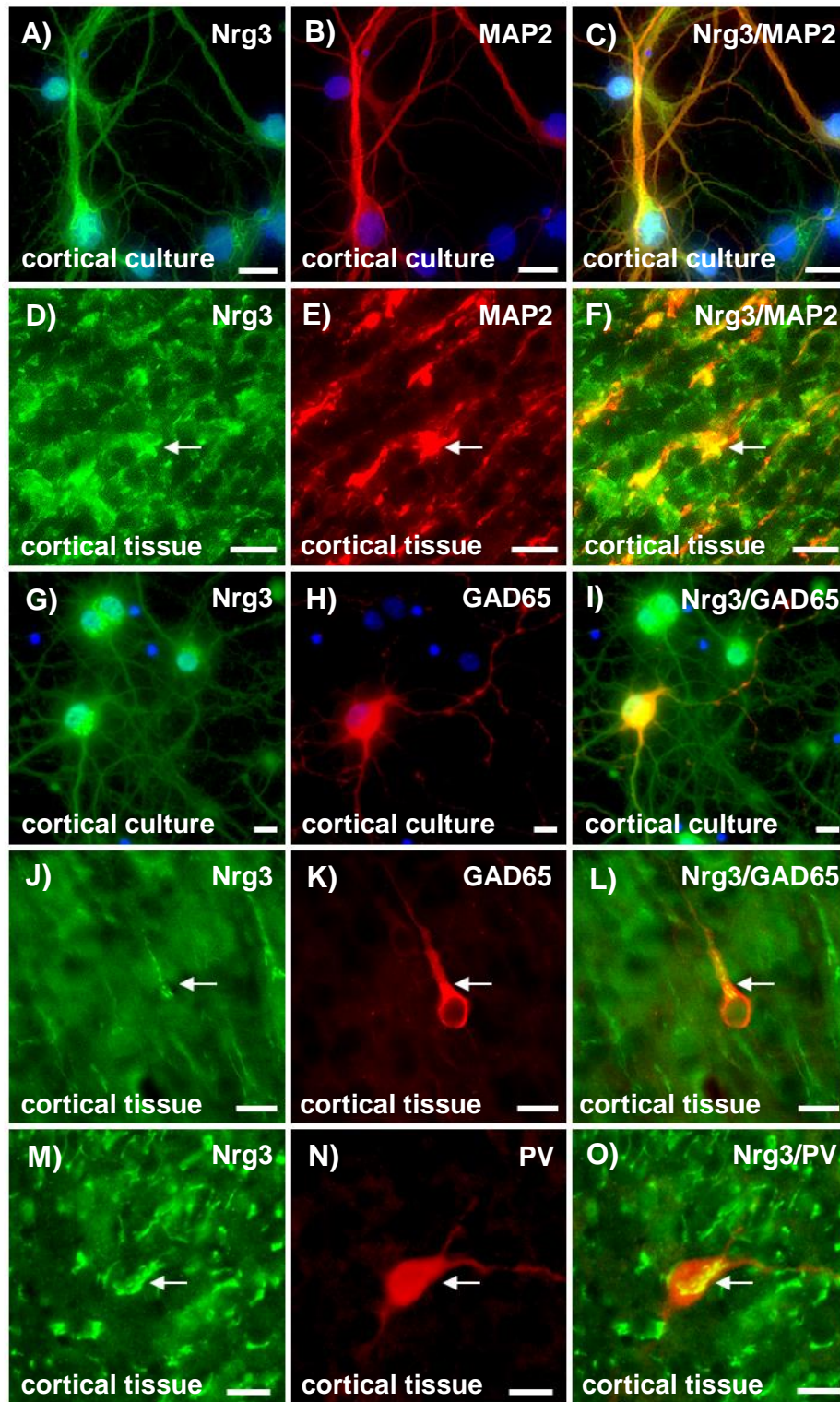


Figure 3.4: Expression of Nrg3 in Neurons.

Dissociated cortical cell cultures (8 days in vitro) (**panels A-C and G-I**) and 15 μ m coronal sections of P4 (**panels D-F and J-L**) and P7 rat brain (**panels M-O**) were double stained with Nrg3 6144 antiserum (1:250, **panels A, D, G, J, and M**), and with anti-MAP2 antibodies (1:1,000, **panels B and E**), anti-GAD-65 antibodies (1:25,000, **panels H and K**) or anti-parvalbumin (1:1,000, **panel N**) in the presence of 0.01% Triton-X 100 (all panels). The anti-Nrg3 antibodies were visualized with AlexaFluor 488 goat anti-rabbit antibodies (in green) and the anti-MAP2, anti-GAD-65, and anti-parvalbumin antibodies with AlexaFluor 594 goat anti-mouse antibodies (in red) both at 1:300 dilution. The nuclei were visualized using DAPI (in blue). Scale bar = 15 μ m for all panels.

3.2.3.2 Nrg3 is Expressed at Low to Background Levels in Glia

We also examined the expression of Nrg3 in glial cells (Fig. 3.5) present in dissociated cortical cultures (Fig. 3.5A-C, G-I) and in sections of P3 and P7 cerebral cortices (Fig. 3.5D-F, J-L respectively). To determine whether Nrg3 was expressed in astrocytes and oligodendrocytes, we performed immunocytochemistry using an antibody against GFAP (Fig. 3.5A-F) and O4 (Fig. 3.5G-I), a marker of oligodendrocytic precursors. We used the myelin enzyme 20,30-cyclic nucleotide 3'-phosphodiesterase (CNPase) to identify oligodendrocytes in cortical tissue sections (Fig. 3.5J-L). For both the GFAP (Fig. 3.5A-C) and O4-positive cells (Fig. 3.5G-I), Nrg3 staining was primarily detected in the perinuclear region consistent with its potential localization to the Golgi apparatus. We observed very low to background levels of Nrg3 staining at the cell surface and also in the cytoplasm of both cell types. These findings were confirmed in tissue sections, with Nrg3 staining only overlapping with GFAP (Fig. 3.5D-F) and CNPase (Fig. 3.5J-L) at the perinuclear region. These observations suggest that the location of Nrg3 in glia may be restricted to the Golgi apparatus, a finding that differs from neurons where Nrg3 is present in the soma as well as in the processes.

Figure 3.5

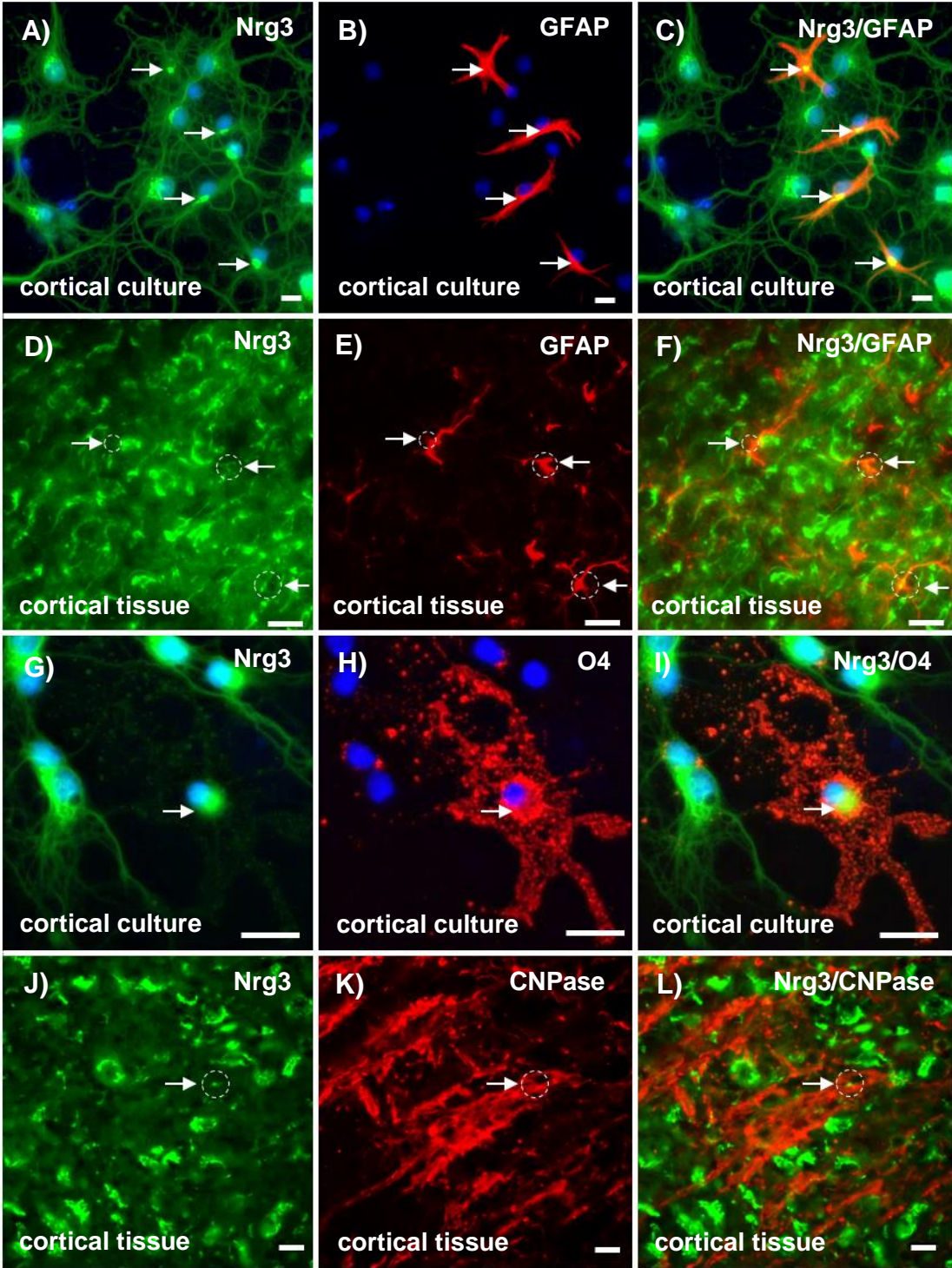


Figure 3.5: Expression of Nrg3 in Glia.

Dissociated cortical cell cultures (8 days in vitro) (**panels A-C and G-I**), 15 μ m coronal sections of P3 rat brain (**panels D-F**), and 15 μ m coronal sections of P7 rat brain (**panels J-L**), were double stained with Nrg3 6144 antiserum (1:250, **panels A, D, G, J**), with anti-GFAP (1:500, **panels B,E**), anti-O4 antibodies (1:1,000, **panel H**), and anti CNPase (1:500, **panel K**) in the presence of 0.01% Triton X-100 for all panels. The anti-Nrg3 antibodies were visualized with AlexaFluor 488 goat anti-rabbit antibodies (in green) and anti-GFAP, anti-O4, and anti-CNPase antibodies were visualized with AlexaFluor 594 goat anti-mouse antibodies (in red) both at 1:300 dilution. The nuclei were visualized using DAPI (in blue). Scale bar = 15 μ m for all panels.

3.2.4 Overall Expression of Nrg3 mRNA in the Rat CNS

To characterize the spatio-temporal expression of Nrg3 in the rat CNS, we performed immunohistochemistry and *in situ* hybridization studies in tissues derived from rats ranging in age from E19 to P20. We focused on late embryonic and early postnatal stages given the extensive developmental changes that take place during this period. In sagittal sections from E19 rat embryos (Fig. 3.6J), we observed high levels of Nrg3 mRNA hybridization in the developing cortical plate and also low but detectable levels of hybridization in the ventricular zone (VZ) and subventricular zones (SVZ) (also see Fig. 3.7A). We also observed hybridization in the developing hippocampal formation (Hi) and detected high levels of Nrg3 hybridization within the developing thalamic region (Th). In contrast, very low to background levels of Nrg3 hybridization were detected in the developing striatum (CPu). More posteriorly, we observed generalized Nrg3 mRNA hybridization in the mesencephalon, with extensive hybridization observed in the dorsal structures such as the superior and inferior colliculi (SC and IC, respectively), and also in the more ventral structures. We also observed generalized hybridization throughout the hindbrain, with a prominent signal in the pontine nucleus (Pn). At E19, Nrg3 hybridization in the cerebellum (Cb) was still sparse, in contrast to later developmental stages as shown in Figure 3.6H and K, in Figure 3.8, and in Figure 3.10I.

We also conducted *in situ* hybridization on coronal sections of P7 rat brain (Fig. 3.6A-I). Within the olfactory bulb Nrg3 was detected in the anterior olfactory nucleus (AON) and the mitral (Mi) and glomerular cell layers (Gl) (Fig. 3.6A). Low levels of Nrg3 hybridization were detected in the internal granule layer (IGr). Nrg3 was also expressed at high levels throughout the frontal (Fr), orbital (Orb), cingulate (Cg), and piriform cortex (Pir) (Fig. 3.6B,C). The widespread high levels of hybridization throughout all cortical layers were maintained in both anterior and posterior regions. As shown in Figure 3.6D, the caudate/putamen (CPu) showed overall very low levels of hybridization with some areas showing higher mRNA levels resulting in

an overall patched appearance (Figs. 3.6D and 3.10G). High levels of Nrg3 mRNA were also observed in the tenia tecta (TT) and the lateral septal nucleus (LSN) (Fig. 3.6D). In addition, Nrg3 mRNA was observed at high levels in the thalamus including the medial-dorsal (MD) and ventral thalamic nuclei (VP) (Fig. 3.6E). In the hippocampal formation, Nrg3 mRNA was expressed in the CA1-CA3 regions with lower levels of hybridization detected in the dentate gyrus (DG) at this developmental stage (Figs. 3.6E-G, 3.9, and 3.10H). Nrg3 mRNA was detected in the medial habenula (Mhb), the dorsal endopiriform nucleus (DEn), the posterolateral cortical amygdaloid nucleus (PLCo) (Fig. 3.6E), and the basolateral (BLA) and basomedial (BMA) amygdala (Fig. 3.6F). The ventral cochlear nucleus (VCA), as well as the superior (SC) and inferior colliculi (IC), also showed high levels of Nrg3 mRNA (Fig. 3.6G, H). As observed at E19, there was particularly high expression of Nrg3 mRNA in the pontine nucleus (Pn) (Fig. 3.6I).

In situ hybridization of Nrg3 mRNA in sagittal sections of P20 rat brains showed that Nrg3 mRNA levels remained high and widely distributed throughout the CNS (Fig. 3.6K). As observed in earlier stages of development, high levels of Nrg3 mRNA hybridization were observed throughout the cortex as well as the anterior olfactory nucleus (AON) in the olfactory bulb (Fig. 3.6K). The striatum (CPu) showed higher levels of Nrg3 hybridization than at earlier stages. At this stage, the hippocampal formation is fully developed with Nrg3 mRNA present in areas CA1-CA3 and also within the dentate gyrus (DG). Nrg3 expression remained high within the thalamic region, as observed by the strong hybridization signal detected within the ventrolateral (VL), ventral posteromedial (VPM), and lateral posterior (LP) nuclei of the thalamus. In the cerebellum, Nrg3 mRNA was detected in the Purkinje cell layer (PCL), the granule cell layer (GL), and the cerebellar nuclei (CerN) (Fig. 3.6K and 3.8). In the hindbrain, a signal was clearly distinguished in the facial nucleus (Fig. 3.6K labeled "7"). At all ages examined we observed very low to background levels of Nrg3 hybridization within the white

matter as illustrated by the low Nrg3 mRNA hybridization signal in the corpus callosum (cc) (Fig. 3.6D, K), the internal capsule (ic) (Fig. 3.6K), and cerebellar white matter (wm) (Fig. 3.6H, K).

Figure 3.6

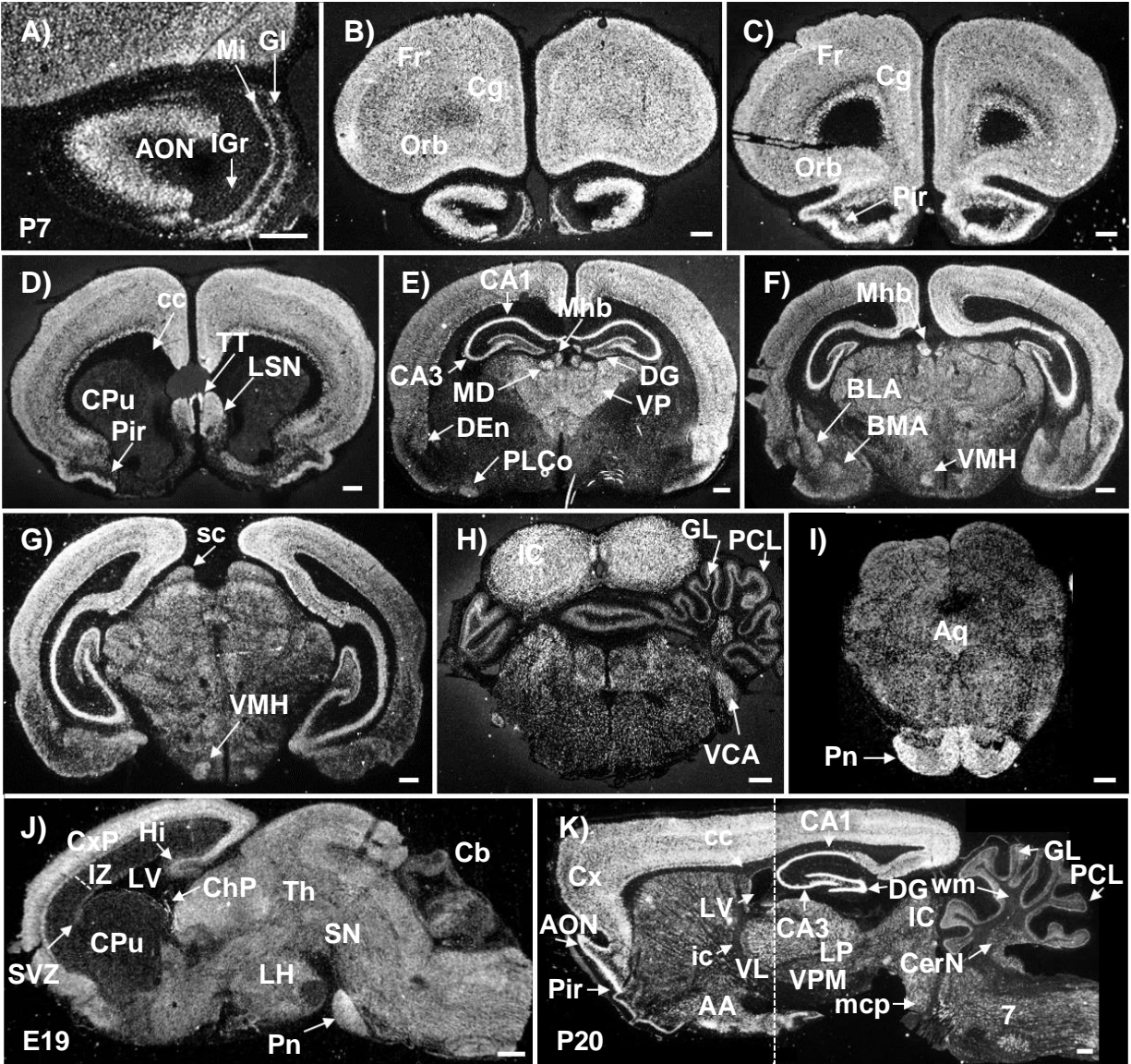


Figure 3.6: Overall Distribution of Nrg3 mRNA by *in situ* hybridization.

In situ hybridization was performed using antisense probes for Nrg3 mRNA on 30 µm sagittal sections of E19 (**panel J**) and P20 rat brain (**panel K**) and on coronal sections of P7 rat brain (**panels A-I**). Abbreviations in alphabetical order: 7, facial nucleus; AA, anterior amygdaloid area; AON, anterior olfactory nucleus; Aq, aqueduct; BLA, basolateral amygdaloid nucleus; BMA, basomedial amygdaloid nucleus; CA1, CA1 field of the hippocampus; CA3, CA3 field of the hippocampus; CPu, caudate-putamen; Cb, cerebellum; ChP, choroid plexus; Cg, cingulate cortex; cc, corpus callosum; Cx, cortex; CxP, cortical plate; DG, dentate gyrus; DEn, dorsal endopiriform nucleus; Fr, frontal cortex; Gl, glomerular layer of the olfactory bulb; GL, granule cell layer; Hi, hippocampus; IC, inferior colliculus; ic, internal capsule; IZ, intermediate zone; IGr, internal granule layer of the olfactory bulb; CerN, cerebellar nucleus; LH, lateral hypothalamic area; LP, lateral posterior nucleus of the thalamus; LSN, lateral septal nucleus; LV, lateral ventricle; Mhb, medial habenula; MD, mediodorsal thalamic nucleus; mcp, middle cerebellar peduncle; Mi, mitral cell layer of the olfactory bulb; Orb, orbital cortex; Pir, piriform cortex; Pn, pontine nuclei; PLCo, posteromedial amygdaloid nucleus; PCL, Purkinje cell layer; SN, substantia nigra; SVZ, subventricular zone; SC, superior colliculus; TT, tenia tecta; Th, thalamus; VCA, ventral cochlear nucleus; VPM, ventral posteromedial nucleus of the thalamus; VL, ventrolateral nucleus of the thalamus; VMH, ventromedial hypothalamic nucleus; VP, ventroposterior nucleus of the thalamus; wm, white matter. Scale bar = 125 µm for A and J; 160 µm for B-I and K.

3.2.5 Developmental Localization of Nrg3 in the Cortex

To examine the developmental expression of Nrg3 in the cortex, we performed *in situ* hybridization as well as immunofluorescent staining. As shown in Figure 3.7A, *in situ* hybridization of Nrg3 at E17 showed strong hybridization throughout the cortical plate both anteriorly and posteriorly (Fig. 3.7A). Nrg3 mRNA was also detected in the ventricular and subventricular zones (VZ and SVZ) (Fig. 3.7A). These findings were consistent with those observed by immunohistochemical staining (Fig. 3.7B) showing clear anti-Nrg3 staining in the cortical plate, and lighter staining in the intermediate zone (IZ). We also observed Nrg3 expression along the ventricular lining (VZ) (Fig. 3.7B, C). At this stage (E17) Nrg3 staining was observed in the soma and neuronal processes extending radially within the cortical plate (see arrows in Fig. 3.7D). Within the upper cortical layers there was extensive co-localization of Nrg3 with the neuronal marker MAP2 (Fig. 3.7E-G). The Nrg3-expressing cells were not restricted to the cortical plate as cells in the subplate (SP) and intermediate zones (IZ) also expressed Nrg3 (Fig. 3.7E). At P3, a developmental stage in which the cortex is undergoing dynamic changes in connectivity and cellular differentiation, we observed continued expression of Nrg3 mRNA and protein throughout all cortical layers (Fig. 3.7H, I) as was also seen at P7 (Fig. 7J, K). As shown in the sagittal sections of the P20 brain (Fig. 3.6K), the expression of Nrg3 mRNA remained elevated at late postnatal stages throughout the brain.

Figure 3.7

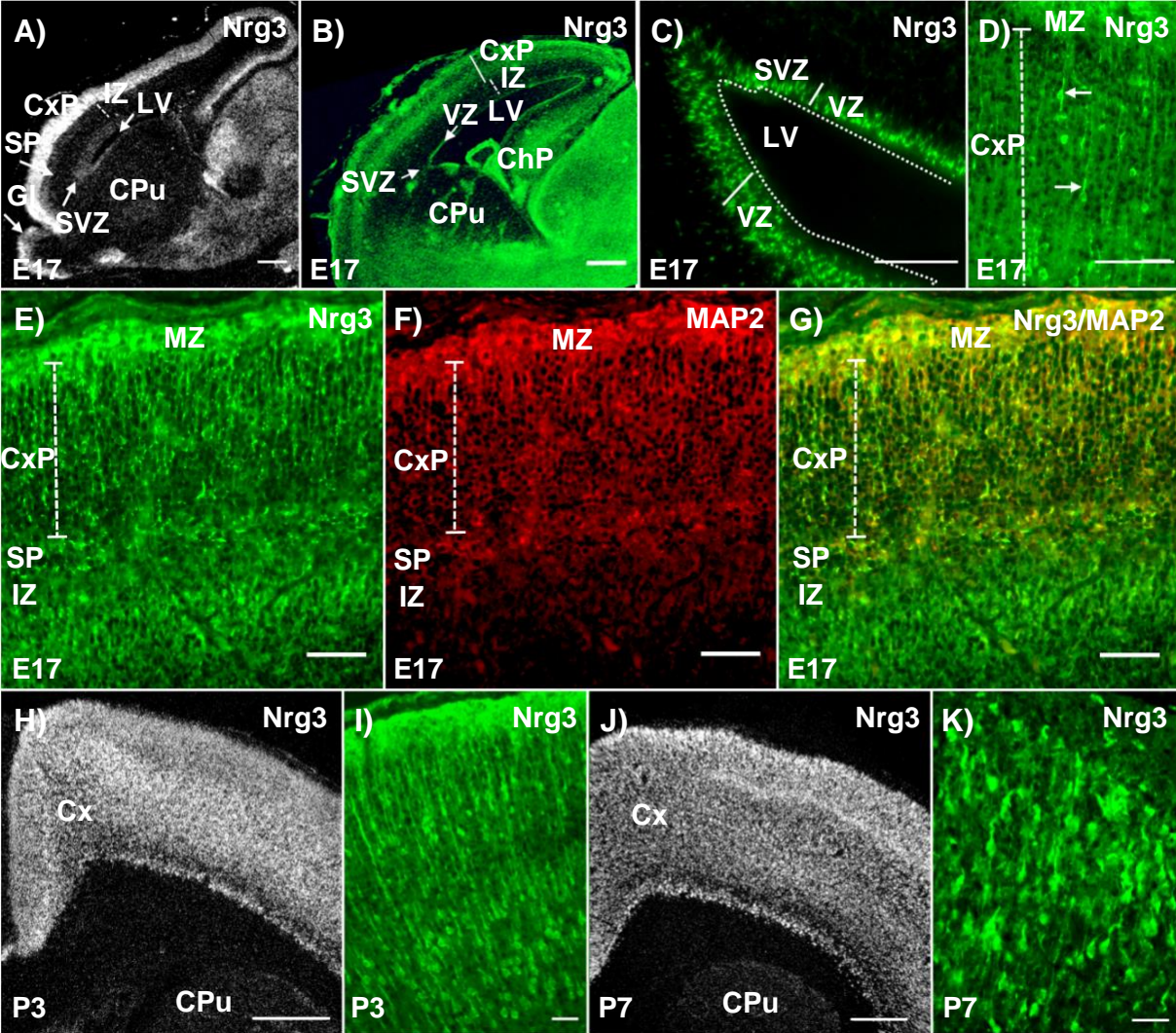


Figure 3.7: Nrg3 Expression in the Cortex.

In situ hybridization was performed using antisense probes for Nrg3 mRNA on 30 μm parasagittal sections of E17 (**panel A**), coronal sections of P3 (**panel H**) and P7 (**panel J**). Immunofluorescent staining was performed on 15 μm parasagittal sections of E17 (**panels B-G**) rat brain, and coronal sections of P3 (**panel I**) and P7 (**panel K**) cerebral cortices. The immunofluorescence staining was performed with Nrg3 6144 antiserum (1:250, **panels B-E, G, I, and K**) and anti-MAP2 (1:1,000, **panel F**) in the presence of 0.01% Triton X-100. The anti-Nrg3 antibodies were visualized with AlexaFluor 488 goat anti-rabbit antibodies (in green) and MAP2 antibodies were visualized with AlexaFluor 594 goat anti-mouse antibodies (in red) both at 1:300 dilution. Abbreviations in alphabetical order: CPu, caudate-putamen; Cx, cortex; CxP, cortical plate; Gl, glomerular layer of the olfactory bulb; IZ, intermediate zone; LV, lateral ventricle; MZ, marginal zone; SP, subplate; SVZ, subventricular zone; VZ, ventricular zone. Scale bar = 100 μm for A and B; 50 μm for C-G, I and K; 220 μm for H; and 175 μm for J.

3.2.6 Developmental Localization of Nrg3 in the Cerebellum

We analyzed the expression of Nrg3 in the cerebellum at three developmental stages that represent distinct stages of cerebellar maturation P3, P7, and P20. Unlike the cortex and many other brain structures, the development of the cerebellum occurs largely in the postnatal period (Caceres, Banker, Steward, Binder, & Payne, 1984). At P3, the expression of Nrg3 mRNA in the external granule cell layer (EGL) is at background levels (Fig. 3.8A). However, a low level of Nrg3 expression was observed in the internal granule cell layer (IGL). At this stage, the cells in the EGL are actively proliferating and the resulting neuroblasts are beginning to migrate internally past the Purkinje (PC) neurons to form the internal granule cell layer (IGL) (Fig. 3.8A). At P7, when the generation of granule neurons in the EGL is at its peak, we observed low levels of Nrg3 expression in the EGL but much higher levels of Nrg3 mRNA in the granule neurons that had migrated into the IGL (Fig. 3.8B). We also compared the localization of Nrg3 mRNA to that of Nrg1 Type III mRNA at P7 (Fig. 3.8C). Unlike Nrg3 mRNA, Nrg1 Type III shows low levels of expression in the IGL and EGL but high levels of hybridization in large neurons consistent with its localization to Golgi neurons. These differences suggest distinct biological functions for Nrg3 and Nrg1 Type III in the cerebellum at this stage. It was difficult to determine from these *in situ* hybridization experiments whether the PC neurons expressed Nrg3 mRNA. To address this question we performed immunofluorescence staining (Fig. 3.8E-G) and determined that Nrg3 was expressed in PC neurons as demonstrated by colocalization of Nrg3 with calbindin (Fig. 3.8G), a Ca²⁺-binding protein expressed by these neurons. We further analyzed whether Nrg3 was expressed in astrocytes and Bergmann glia (BG) using GFAP as a marker. Consistent with our observations in cortical cultures and cortical sections, only low to background levels of Nrg3 were observed in glia (Figs. 3.5A-F and 3.8H). We also analyzed the distribution of Nrg3 at P20 (Fig. 3.8D), a stage in which the migration of the granule neurons into the IGL is complete. At this stage, the expression of Nrg3 mRNA in the Purkinje cell layer (PCL) was evident by *in situ* hybridization with lower but clearly detectable levels in the IGL. In

contrast, the molecular layer (ML) at this stage, which is composed mainly of granule neuron axons and the dendritic arbors of PC neurons, showed low to background levels of Nrg3 mRNA (Fig. 3.8D).

Figure 3.8

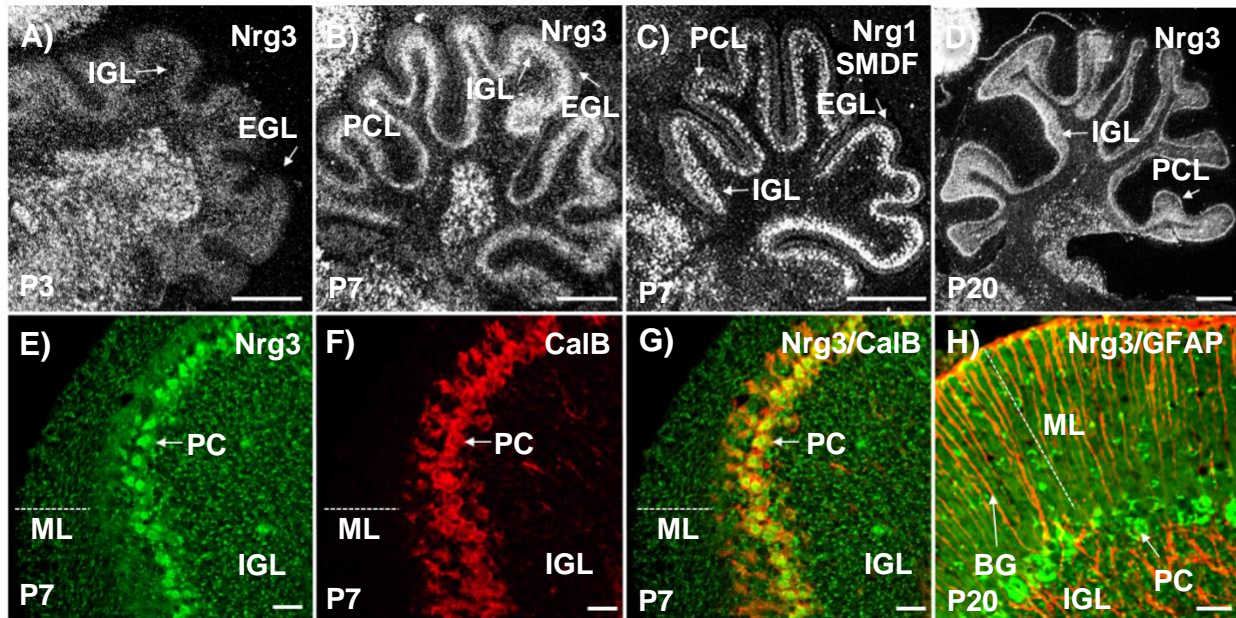


Figure 3.8: Developmental Expression of Nrg3 in the Cerebellum.

In situ hybridization was performed using antisense probes for Nrg3 (**panels A, B, and D**) or Nrg1 type III mRNA (**panel C**) on 30 μm coronal sections of P3 (**panel A**), P7 (**panels B and C**), or parasagittal P20 sections (**panel D**). Immunofluorescent staining was performed on 15 μm coronal sections of P7 (**panels E-G**) or sagittal sections of P20 (**panel H**) rat brains using Nrg3 6144 antiserum (1:250, **panels E and H**), anti-calbindin (Calb) antibodies (1:1,000, **panels F and G**) or anti-GFAP antibodies (1:500, **panel H**) in the presence of 0.01% Triton X-100 for all panels. The anti-Nrg3 antibodies were visualized with AlexaFluor 488 goat anti-rabbit antibodies (in green) and anti-calbindin and anti-GFAP antibodies were visualized with AlexaFluor 594 goat anti-mouse antibodies (in red) both at 1:300 dilution. Abbreviations: BG, Bergman glia; EGL, external granule cell layer; IGL, internal granule cell layer; ML, molecular layer; PC, Purkinje cell; PCL, Purkinje cell layer. Scale bar = 160 μm for A and B; 200 μm for C and D; and 15 μm for E-H.

3.2.7 Developmental Localization of Nrg3 in the Hippocampus

We examined the developmental expression of Nrg3 in the hippocampus. As shown in Figure 3.9, *in situ* hybridization showed that Nrg3 mRNA was present throughout areas CA1-3 at the three developmental stages examined P3, P7, and P25 (Fig. 3.9A-C, respectively). The dentate gyrus (DG), unlike areas CA1-3, is primarily formed during the postnatal period and the Nrg3 mRNA hybridization levels closely reflect this developmental pattern of maturation. At P3 (Fig. 3.9A), low levels of hybridization were observed in the DG anlagen, progressively increasing through P25 (Fig. 3.9C). At P25, the Nrg3 mRNA hybridization signal in the DG matches or exceeds that observed in areas CA1-3 (Fig. 3.9C). Consistent with the mRNA localization, immunofluorescence also showed Nrg3 labelling of cell processes and the soma of neurons in these areas (CA1 shown in Fig. 3.9D, E; the dentate gyrus shown in Fig. 3.9F, G).

Figure 3.9

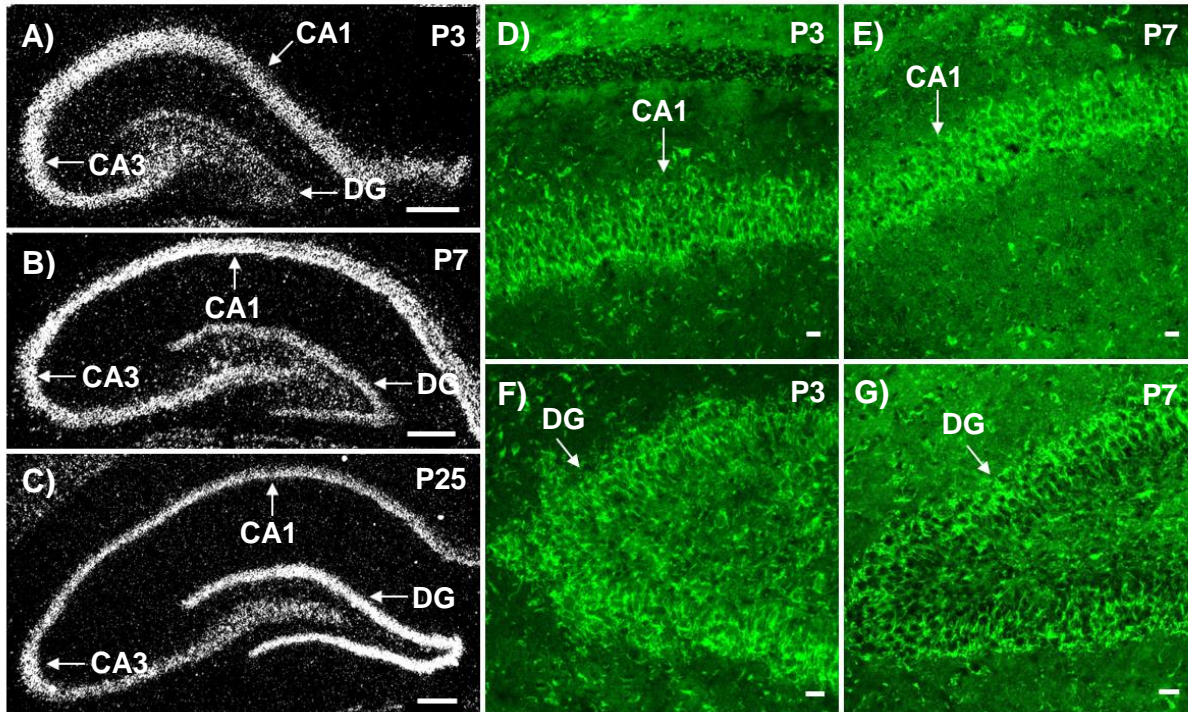


Figure 3.9: Nrg3 Expression in the Hippocampal Formation.

In situ hybridization was performed using antisense probes for Nrg3 mRNA on 30 μm coronal sections of P3, P7, and P25 rat brains (**panels A-C, respectively**). Immunofluorescent staining was performed on 15 μm coronal sections of P3 (**panels D and F**) and P7 (**panels E and G**) rat brains with Nrg3 6144 antiserum (1:250) in the presence of 0.01% Triton X-100 for all immunofluorescent staining. The anti-Nrg3 antibodies were visualized with AlexaFluor 488 goat anti-rabbit antibodies (in green) at 1:300 dilution. Abbreviations: CA1, CA1 field of the hippocampus; CA3, CA3 field of the hippocampus; DG, dentate gyrus. Scale bar = 80 μm for A and B; 100 μm for C; and 15 μm for D-G.

3.2.8 Comparison of the Localization of Nrg1 Type III, Nrg2, and Nrg3 mRNAs in P7 Rat Brain

To identify areas in which the Nrgs, including Nrg3, could have unique or shared functions, we compared the distribution of Nrg3 to that of Nrg1 Type III and Nrg2 mRNAs in P7 rat brains by *in situ* hybridization. Nrg3 showed high levels of hybridization throughout all cortical layers, as previously described (Bartolini et al., 2017; Marines Longart et al., 2004) (Figs. 3.6 and 3.7 and in Fig. 3.10G, H). Nrg2 mRNA hybridization was detected throughout the cortex with the highest levels concentrated in the upper cortical layers (Fig. 3.10D, E). Nrg1 Type III mRNA hybridization was also observed throughout the cortex, with the highest levels detected in the upper cortical layers. It was particularly prominent in layer V (Fig. 3.10A, B). In the hippocampus, although all three Nrgs were present throughout areas CA1-3, they exhibited clear differences. Nrg1 Type III mRNA had a more prominent expression in area CA3 than in CA1 or the DG (Fig. 3.10B), while both Nrg2 and Nrg3 seemed evenly distributed among the CA1-3 regions at this stage (Fig. 3.10E, H, respectively). In the DG, the hybridization levels of Nrg2 were comparable to those in areas CA1-CA3 while those of Nrg1 Type III and Nrg3 were less intense than those detected at CA1-3 at this developmental stage (Fig. 3.10E, B, H, respectively). Nrg3 and Nrg2 mRNAs were widely distributed throughout the thalamic region (Fig. 3.10E, H) while NRG1 Type III showed a more selective expression in the medial habenula (Mhb) and the reticular nuclei of the thalamus (Rt) (Fig. 3.10B). As previously described, only background levels of Nrg3 mRNA hybridization were observed in the striatum (CPu), however, higher levels of Nrg2 were observed in this region (Fig. 3.10G, D, respectively and Fig. 3.6D). Nrg1 Type III also showed clear hybridization in the arcuate nucleus (Arc) and the paraventricular nucleus of the thalamus (Pa) (Fig. 3.10B), unlike Nrg2 and Nrg3. At P7, in the cerebellum, Nrg2 and Nrg3 (Fig. 3.10F, I) were expressed in the internal granule cell layer (IGL) while Nrg1 Type III expression was restricted to the Golgi neurons and possibly Bergmann glia, as previously described (Figs. 3.8C and 3.10C). Immunofluorescent staining with an antibody

specific to Nrg1 Type III is required to unambiguously determine Nrg1 Type III expression in this glia. Overall, Nrg2 and Nrg3 were expressed in a greater number of brain regions than Nrg1 Type III, whose expression was more restricted.

Figure 3.10

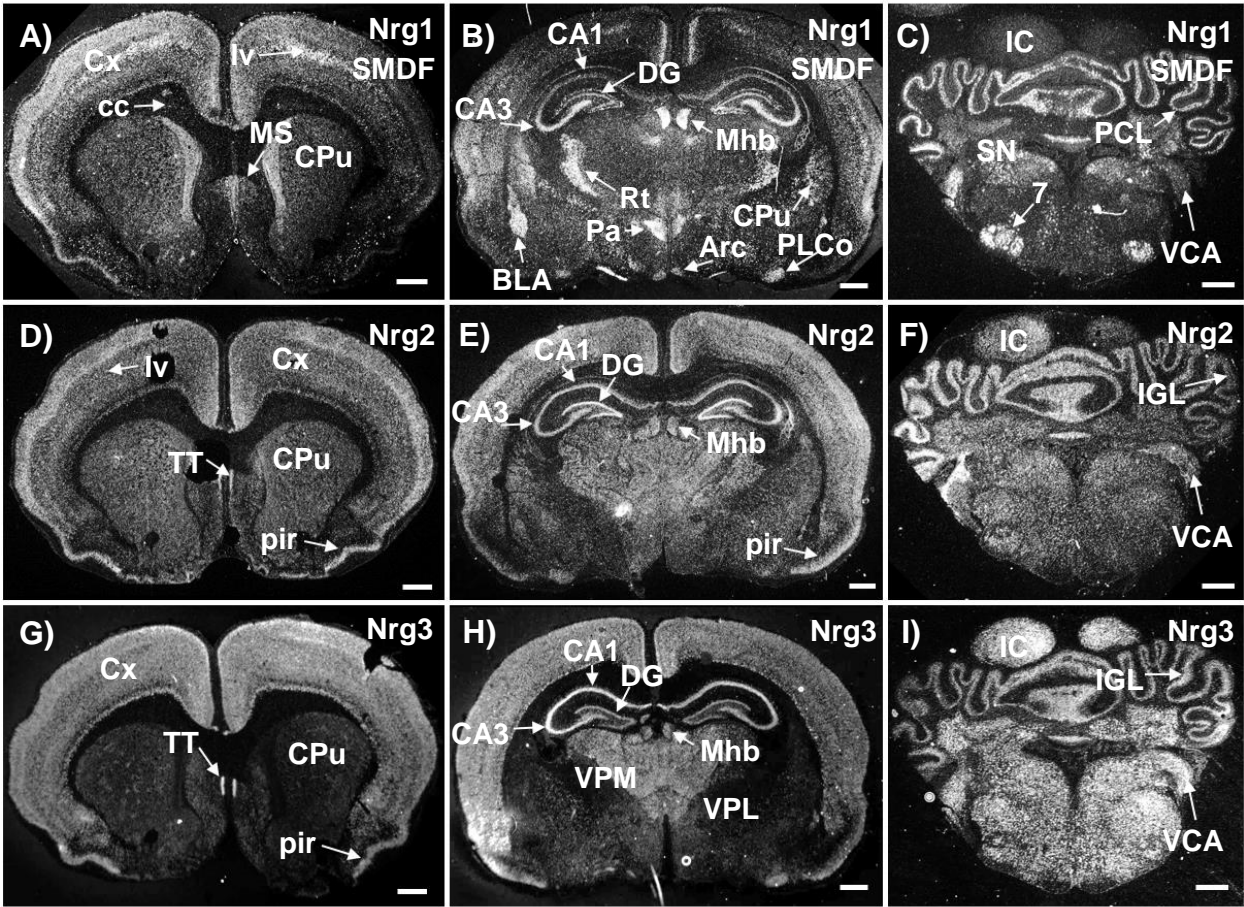


Figure 3.10: Comparison of Nrg1 Type III, Nrg2, and Nrg3 mRNA Distribution.

In situ hybridization was performed using antisense probes against Nrg1 Type III (**panels A-C**), Nrg2 (**panels D-F**), and Nrg3 mRNAs (**panels G-I**) on 30 μm coronal sections of P7 rat brain.

Abbreviations in alphabetical order: 7, facial nucleus; Arc, arcuate hypothalamic nucleus; BLA, basolateral amygdaloid nucleus; CA1, CA1 field of the hippocampus; CA3, field of the hippocampus; CPu, caudate-putamen; cc, corpus callosum; Cx, cortex; Iv, cortical layer V; DG, dentate gyrus; IC, inferior colliculus; IGL, internal granule cell layer; Mhb, medial habenula; MS, medial septal nucleus; Pa, paraventricular hypothalamic nucleus; pir, piriform cortex; PLCo, posteromedial amygdaloid nucleus; PCL, Purkinje cell layer; Rt, reticular nucleus of the thalamus; SN, substantia nigra; TT, tenia tecta; VCA, ventral cochlear nucleus; VPL, ventral posterolateral nucleus of the thalamus; VPM, ventral posteromedial nucleus of the thalamus.

Scale bar = 160 μm for A and I; and 200 μm for B-H.

3.3 DISCUSSION:

The Nrgs and their receptors the ErbBs play diverse and important roles in the PNS and CNS. In this chapter, we have characterized the developmental expression and localization of Nrg3 in the rat CNS in order to gain insight into its possible functions. Previous studies have also suggested that Nrg3 is more widely expressed than the other Nrgs. However, as these studies have been limited in scope, we sought to provide a more extensive description of the localization of Nrg3 by *in situ* hybridization and immunohistological analyses.

Our study provides additional support for the widespread expression of Nrg3, a pattern that is more extensive than that observed for either Nrg1 (M. S. Chen et al., 1994; Corfas, Rosen, Aratake, Krauss, & Fischbach, 1995; Xihui Liu et al., 2011; Marchionni et al., 1993; Meyer et al., 1997; Pinkas-Kramarski et al., 1994) or Nrg2 (Marines Longart et al., 2004). Regions with particularly notable levels of expression included the cortical plate, the mature cerebral cortex, hippocampus, thalamus, cerebellum, and the brain stem. In contrast to the other Nrgs, Nrg3 remains high at later stages of development suggesting that it plays a role in the mature brain (Fig. 3.10).

At the subcellular level, Nrg3 was observed in the plasma membrane of the neuronal cell body and dendritic compartment, with very prominent localization to the Golgi apparatus. Its expression in neurons was more prominent than that observed in glial cells. These immunocytochemical observations are consistent with those reported by Wang et al (Y.-N. Wang et al., 2018) that showed expression of Nrg3 in lysates of cultured neurons but not in those of astrocytes. The expression of Nrg1 is not limited to neurons and there are multiple reports showing Nrg1 in brain astrocytes (Kerber et al., 2003; Xihui Liu et al., 2011; Pinkas-Kramarski et al., 1994; Tokita et al., 2001), suggesting unique roles for these Nrgs.

The expression of Nrg3 was not restricted to glutamatergic neurons but was also identified in GABAergic neurons in culture and in tissue sections. In addition to its expression in GABAergic Purkinje neurons, Nrg3 was detected in parvalbumin-positive neurons, a finding consistent with single cell transcriptome studies (Tasic et al., 2016). We also detected the presence of Nrg3 in dendrites, a compartment critical for integrating synaptic inputs. Two recent observations have shown that Nrg3 can also function within the axonal compartment. In one study, overexpression of Nrg3 resulted in its accumulation in axonal varicosities (Vullhorst et al., 2017). Using biochemical approaches, a separate study showed that Nrg3 is present in postsynaptic density fractions and that it associates with components of the pre- but not postsynaptic terminals, specifically with the SNARE complex (Y.-N. Wang et al., 2018). As a consequence of this association, Nrg3 influences synaptic function. The deletion of Nrg3 in GFAP-Nrg3^{f/f} mice increased glutamatergic transmission whereas increased levels of Nrg3 led to a reduction in transmission. Intriguingly, these roles for Nrg3 appear to be independent of ErbB4 (Y.-N. Wang et al., 2018).

One of the most significant observations to emerge from this study is that in addition to its plasma membrane expression, Nrg3 is prominently expressed in the Golgi apparatus. Even in glial cells that only exhibit low levels of expression, Nrg3 was detected in a perinuclear compartment consistent with localization to the Golgi apparatus. Like other secreted and transmembrane proteins, this localization is likely to reflect its transit from the endoplasmic reticulum to the Golgi. In addition to trafficking, the Golgi is also important for post-translational modifications, such as glycosylation and proteolytic cleavage. Like Nrg1 type III, Nrg3 has an amino-terminal transmembrane (TM_N) domain and a carboxyl-terminal transmembrane (TM_C) domain (D. Zhang et al., 1997). Recent work has shown that the protease, BACE1, can proteolytically cleave Nrg3 at a site between the TM_C and the EGF-like domain (Vullhorst et al., 2017). This yields a transmembrane form of Nrg3 that remains tethered to the membrane by its

TM_N domain, with its N-terminus located inside of the cell and with its EGF-like domain displayed outside of the cell. This cleavage event was thought to occur in the Golgi as mutations that prevented the proteolytic processing resulted in increased levels of Nrg3 in this compartment. Similar mutations in Nrg1 type III did not lead to accumulation in the Golgi, but instead resulted in its dispersion throughout the cell. These findings suggested that the role of the Golgi in Nrg3 post-translational processing may differ from that of Nrg1 type III (Vullhorst et al., 2017). Proteolytic processing in the Golgi is not limited to Nrg3 and Nrg1 type III as it has also been reported for other Nrg1 subtypes (Ben Halima et al., 2016; Fleck et al., 2013; Loeb et al., 1998; Montero et al., 2007; J. Y. Wang et al., 2001; Yokozeki et al., 2007).

One of the possible explanations for the prevalence of Nrg3 in the Golgi apparatus is that Nrg3 undergoes O-linked glycosylation. Unlike N-linked glycosylation that occurs co-translationally in the endoplasmic reticulum with subsequent remodeling in the Golgi, the enzymes that perform O-linked glycosylation are localized within the Golgi (Hang & Bertozzi, 2005; Hanisch, 2001; Kudelka, Ju, Heimbürg-Molinaro, & Cummings, 2015). In this chapter, we demonstrated that treatment of P25 cerebral cortical extracts with a combination of neuraminidase and O-glycanase resulted in a substantial reduction in its molecular weight. A more limited reduction was detected in Nrg3 from E18 cortex. These data indicate a developmental shift in the sugar content for Nrg3. O-glycanase requires the removal of peripheral branches before it can cleave the core GalNAc/GlcNAc disaccharide linking the sugar chains to the serine/threonine residues on the core protein (Hanisch, 2001). Consistent with this fact, neuraminidase treatment alone resulted in a molecular weight reduction of Nrg3, which was further enhanced by co-incubation with O-glycanase. In contrast, O-glycanase by itself did not result in a significant reduction in Nrg3 molecular weight. PNGase did not reduce the molecular weight of Nrg3, in agreement with the prediction by Zhang et al (D. Zhang et al., 1997) that Nrg3 lacks potential N-linked glycosylation sites. This same group described a region

near the amino-terminal end of Nrg3, corresponding to a sequence rich in serines and threonines such as that found in mucins (mucin-like). These stretches concentrate GalNAc-based glycans since they can be subject to serial O-linked glycosylation (Hang & Bertozzi, 2005). An alternatively spliced form of human NRG3 appears to contain β -N-acetyl galactosamine based on its ability to interact with soybean agglutinin, which preferentially binds to Gal NAc-containing sugars (Carteron, Ferrer-Montiel, & Cabedo, 2006). This human NRG3 variant lacks the mucin-like stretch, suggesting that Nrg3 can undergo O-linked glycosylation at sites other than within the mucinlike region. It will be important to identify what residues are glycosylated in Nrg3 as well as the developmental time course of these modifications. Other Nrgs have been shown to be both N- and O-linked glycosylated (Cabedo, Carteron, & Ferrer-Montiel, 2004; Loeb et al., 1998; Lu et al., 1995; Peles et al., 1992; Shamir & Buonanno, 2010; J. Y. Wang et al., 2001; D. Wen et al., 1994). The developmental differences in Nrg3 glycosylation likely influence its functional properties. O-linked glycosylation has been previously shown to modify protein structure, affect the availability of proteolytic cleavage sites, modulate protein-protein interactions, and alter protein compartmentalization and trafficking.

Nrg3 is highly abundant and widely expressed in the cerebral cortex from early stages of development into adulthood as shown in Figure 3.7 and as described in previous studies (Bartolini et al., 2017; Marines Longart et al., 2004; D. Zhang et al., 1997). This distribution differs from that of Nrg2 and Nrg1 type III (Fig. 3.10), as these Nrgs are expressed more prominently in the upper cortical layers than in the lower layers (also see (M. S. Chen et al., 1994; Corfas et al., 1995; Marines Longart et al., 2004; Meyer et al., 1997)). In layer V, the expression of Nrg1 type III is particularly notable. In contrast to previous studies, we show for the first time, by both in situ hybridization and immunohistochemistry, that Nrg3 is expressed in cells lining the ventricular surface. The localization of Nrg3 in the ventricular zone (VZ) suggests potential roles in the proliferation of neuronal and glial precursors, differentiation (such as radial

glial differentiation), and in neuroblast migration. Previous studies have identified the presence of Nrgs in neuroblasts. Nrgs1 and 2 have been detected in neuroblasts present in the postnatal anterior subventricular zone (SVZ) (H T Ghashghaei et al., 2006). In addition, Nrg1 has been shown to induce the proliferation of neural progenitor cells derived from E11 mouse cortex (Y. Liu, Ford, Mann, & Fischbach, 2005). Our observations showing the presence of Nrg3 in the VZ raises the possibility that Nrg3 could play a proliferative role in cells expressing ErbB4 in the VZ.

The earliest description of Nrg3 expression in cortical development at E12.5 (Assimacopoulos et al., 2003) supports the hypothesis of a potential role of Nrg3 acting by itself or synergistically with Nrg1 in the establishment of radial glia. At this stage Nrg3, Nrg1, and TGF α are expressed in the anti-hem, an area flanking the lateral neuroepithelium that gives rise to the cerebral cortex. Another structure, the hem, which acts as an organizing center, also flanks the neuroepithelium but on its medial aspect (Subramanian, Remedios, Shetty, & Tole, 2009). As elimination of the anti-hem results in loss of the radial glial palisade at the pallial-subpallial boundary (A. S. Kim, Anderson, Rubenstein, Lowenstein, & Pleasure, 2001; Stenman, Yu, Evans, & Campbell, 2003; Yun, Potter, & Rubenstein, 2001), it has been proposed that expression of Nrg1 in the anti-hem contributes to the formation and maintenance of this radial glial palisade at this early developmental stage (Subramanian et al., 2009). The contribution of each Nrg (1 and 3) at the anti-hem in the establishment and maintenance of the radial glia palisade at this early age remains to be determined. Nrg1/ErbB2/4 signaling has been implicated in the establishment and maintenance of the radial glia phenotype in the cortex (Anton et al., 1997; Schmid et al., 2003) and the cerebellum (Rio et al., 1997), however the role of the ErbB2 and ErbB4 in this process has been challenged (see Barros et al (Barros et al., 2009)).

A newly identified role for Nrg3 is in the guidance of migrating interneurons in the developing cortex. These cells express ErbB4 and it has been previously shown that they

migrate tangentially from the ganglionic eminences into the cortex. This process is influenced by distinct isoforms of Nrg1, which serve as both short- and long-range attractants (Bartolini et al., 2017; Flames et al., 2004). When the migrating cells have completed their tangential migration, Nrg3 serves as an important factor that helps to guide GABAergic interneurons as they migrate radially into their appropriate final laminar destination in the cortex (Bartolini et al., 2017).

In the hippocampus, Nrg3 is the most abundantly expressed Nrg. We observed Nrg3 in areas CA1-CA3 and in the granule neurons of the dentate gyrus (DG). Expression in the hippocampal formation was high throughout development and remained high at P25, suggesting that Nrg3 may play roles both during development and in the mature hippocampus. In contrast, the developmental expression of both Nrg1 type III and Nrg2 in CA1-3 differs significantly from that of Nrg3. Previously, Longart et al (Marines Longart et al., 2004) reported that the expression of Nrg2 in CA1-CA3, is transient showing a bell-shaped expression pattern. It increases from P0 to P7 and then decreases significantly by P25 (Marines Longart et al., 2004). In contrast, Nrg1 type III shows its highest expression levels in the CA3 region with only low to background levels in the CA1 at P7. Thus at the mRNA level, it appears that Nrg3 is the primary Nrg expressed in CA1, while in CA3 it is expressed along with Nrg1 type III. As the DG matures, its granule neurons express significant levels of both Nrg3 and Nrg2 at late postnatal stages, while Nrg1 type III levels are much lower. There have been multiple studies highlighting the role of Nrgs in hippocampal function and plasticity (Buonanno, 2010; Mei & Nave, 2014; Mei & Xiong, 2008) and it will be interesting to determine if Nrg3 plays a similar role in these processes.

In the cerebellum, Nrg3 was expressed in the granule cell layer and in Purkinje neurons in a pattern resembling that of Nrg2 (Marines Longart et al., 2004). The expression of Nrg1 in the cerebellum is isoform dependent with types I and II reported in cerebellar granule and Purkinje neurons (Corfas et al., 1995; Kerber et al., 2003; Rio et al., 1997). Nrg1 type III differs

from these isoforms and is detected in Golgi type I neurons (see Fig. 3.8), as has been previously reported (Corfas et al., 1995; Marines Longart et al., 2004). In addition, we also observed detectable hybridization of Nrg1 type III in cells near the border of the molecular layer. Antibody staining will be required to ascertain the identity of these cells. In view of the aforementioned role of Nrg3 in cortical interneuronal migration (Bartolini et al., 2017), it will be of interest to determine whether it also plays a role in the migration of cerebellar granule neurons. Nrg1 has been previously shown to promote granule cell migration via an interaction with ErbB4, which is expressed on Bergmann glial fibers (Rio et al., 1997). Although the expression of ErbB4 by cerebellar granule cells has been controversial (Bean et al., 2014), our studies (not shown) and those of others (Klaus Elenius et al., 1997; Pinkas-Kramarski et al., 1997), have provided evidence supporting its expression in granule neurons both in tissue sections and in vitro (Rieff et al., 1999; Rio et al., 1997; Xie, Padival, & Siegel, 2007). Perez-Garcia (Perez-Garcia, 2015) and our own unpublished work, have observed ectopic clusters of granule neurons at the surface of the EGL in ErbB4 deficient mice. These observations also support a role for ErbB4 in cerebellar granule cell migration. Nrg1/ErbB4 signaling has also been shown to promote an increase in dendritic outgrowth of cerebellar granule neurons in vivo (Rieff & Corfas, 2006; Rieff et al., 1999). In view of the role of Nrg3 in GABAergic cell migration in the cortex (Bartolini et al., 2017), it is possible that it also plays a developmental role in the migration of cerebellar granule neurons.

Although they have partially overlapping patterns of expression, each of the Nrgs is expressed in a distinct manner. In addition to the brain regions discussed in the preceding paragraphs, Nrg3 is broadly expressed in a number of thalamic and hypothalamic nuclei and throughout the brain stem, a pattern distinct from the other Nrgs. Furthermore, the hybridization levels detected for Nrg3 were significantly higher than the other Nrgs. These observations suggest that the Nrgs serve different functions in the nervous system. Nrg1 plays an essential

role in peripheral myelination, a role not shared by either Nrg2 or Nrg3 (Birchmeier & Bennett, 2016; Mei & Nave, 2014). In neurons in the CNS, ErbB4 is the most readily detected ErbB and it has largely been assumed that ErbB4-expressing neurons are the likely target of activation by Nrgs 1, 2, and 3. A recent report, however, has revealed that Nrg3 can regulate glutamatergic neurotransmission in an ErbB4-independent manner (Y.-N. Wang et al., 2018). This finding leads to the speculation that other Nrgs may have functions that do not require activation of an ErbB receptor. Indeed, this has been reported for Nrg2, which has been shown to regulate GABAR alpha 1 expression. In this case, ErbB4 is required but it functions in a manner that does not require its tyrosine kinase activity (Mitchell et al., 2013). The identification of an ErbB4-independent role for Nrg3 provides an additional layer of complexity, as one can no longer simply compare its expression profile to the known sites of ErbB expression in order to identify potential targets of Nrg3 activity.

In summary, Nrg3 is the most abundantly expressed Nrg in the brain and an improved understanding of its site of expression should facilitate our ability to identify novel functional roles for this molecule.

Chapter 4: The Neuregulins and ErbB4 Developmentally Regulate Neurite Outgrowth of Cortical GABAergic Interneurons

4.1 INTRODUCTION:

During the development of the nervous system, neuronal differentiation unfolds following a series of stages including initiation of neurite extension, axonal and dendritic specification, target selection, and synaptogenesis (Nicolas & Hassan, 2014; Stiles & Jernigan, 2010). Members of the neuregulin (Nrg) family of growth factors and their receptors, the ErbBs are among several molecules that can affect diverse aspects of neuronal differentiation, including neural outgrowth [reviewed in (Mei & Nave, 2014)]. In order to gain an improved understanding of the roles that Nrg1-3 and their receptor ErbB4 play in neuronal differentiation, we sought to analyze the effects of these molecules in several aspects of neurite outgrowth in cortical GABAergic interneurons.

During cortical development, the majority of interneurons are born in the ganglionic eminences and tangentially migrate to their final positions in the cortical plate (Lim, Mi, Llorca, & Marín, 2018). Nrg1 and Nrg3 have previously been shown to play both chemoattractive and chemorepulsive roles in guiding the migration of GABAergic interneurons to their proper positions in the cortex (Bartolini et al., 2017; Flames et al., 2004; H. Li et al., 2012). After migration, neurons must undergo neurite outgrowth prior to their integration in functioning neural circuits. Nrg1 has been reported to mediate neurite outgrowth and extension in several neuronal populations, including neurons of the rodent retina, hippocampus, cerebral cortex, midbrain, spinal cord, and cerebellum, as well as in the PC12 cell line (Anton et al., 1997; Audisio et al., 2012; Bermingham-McDonogh et al., 1996; M E Cahill et al., 2012; Y. Chen et al., 2010; Gamett & Cerione, 1994; Gamett et al., 1995; García et al., 2013; Kimberly M Gerecke et al., 2004; Krivosheya et al., 2008; Mòdol-Caballero et al., 2017; Rieff et al., 1999; Tal-Or et al., 2006;

Vaskovsky et al., 2000; Villegas et al., 2000; R. Xu et al., 2013; L. Zhang et al., 2004; Q. Zhang et al., 2017, 2016). In one such example, in cultured primary cortical neurons, the extracellular and intracellular domains of Nrg1 Type III have been shown to have unique effects on axonal extension and dendritic outgrowth, respectively (Y. Chen et al., 2010). The roles of Nrg2 in neurite outgrowth are less understood, but it was previously reported that Nrg2 secreted from astrocytes promoted neurite outgrowth and survival of hippocampal neurons (Nakano et al., 2016). There are currently no reports on the effects of Nrg3 on neurite outgrowth in any neuronal population.

In the CNS, expression of the Nrg receptor ErbB4 is limited to GABAergic interneurons, with preferential expression in the parvalbumin (PV)-positive subtype of GABAergic cells (Fazzari et al., 2010; Krivosheya et al., 2008; Neddens et al., 2011; Vullhorst et al., 2009; Woo et al., 2007). In the cerebral cortex, GABAergic interneurons encompass a heterogeneous group of cells that can be divided into three large classes based on the expression of the neuropeptide somatostatin (SST), the serotonin receptor 3A (Htr3A), and the calcium-binding protein PV, which is the most abundant class and widespread of cortical interneurons (Kelsom & Lu, 2013; Rudy et al., 2011). The PV-expressing subset can be further categorized into three main cell types: chandelier cells, basket cells, and the relatively rare fast-spiking translaminal cells. Postmortem brain studies and rodent models have linked stunted neurite formation and abnormal neuronal differentiation of cortical GABAergic interneurons with the disease presentation of schizophrenia (SZ) (Badea, Nicholls, Johnson, & Wetsel, 2007; Black et al., 2004; Broadbelt, Byne, & Jones, 2002; Kalus, Bondzio, Federspiel, Müller, & Zuschratter, 2002; Matricon et al., 2010; Q. Zhang et al., 2016). In parallel, the biological functions of Nrg1, Nrg3, and their receptor ErbB4 have received noteworthy attention due to several studies identifying them as SZ susceptibility genes (P.-L. Chen et al., 2009; Hahn et al., 2006; Mei & Nave, 2014; Norton et al., 2006; Silberberg et al., 2006; Stefansson et al., 2002; Y.-C. Wang et al., 2008)

and linking them to other mental illnesses [reviewed in (Mei & Nave, 2014)]. In order to better understand the roles of the Nrgs and their receptors in disease and also their role in normal development, it is crucial to understand their effects in the differentiation of GABAergic interneurons.

The main growth factor known to induce differentiation of GABAergic interneurons both *in vivo* and *in vitro*, is brain derived neurotrophic factor (BDNF), acting through its receptor TrkB (Cohen-Cory, Kidane, Shirkey, & Marshak, 2010; Jin, Hu, Mathers, & Agmon, 2003; Pozas & Ibáñez, 2005; Wirth, Brun, Grabert, Patz, & Wahle, 2003). Aside from BDNF, the study of other factors that can regulate GABAergic development including dendritogenesis have been lacking. In addition to the role BDNF, several studies have previously implicated Nrg1 signaling in the development of GABAergic interneurons (M E Cahill et al., 2012; Krivosheya et al., 2008). Nrg1-ErbB4 signaling has been shown to promote dendritic outgrowth in mature cortical interneurons dependent on kalirin-7 phosphorylation, a dendritic Rac1-GEF whose mutation has also been linked to the onset of SZ. Furthermore, cortical cultures from ErbB2/ErbB4 knockout mice have shown that interneurons, but not pyramidal neurons, exhibit reduced dendritic length compared to cultures from wild-type controls (M E Cahill et al., 2012). Consistent with these observations of dendritic outgrowth, Nrg1 treatment of hippocampal interneurons overexpressing ErbB4 resulted in an increase in the number of primary neurites; however, these cells displayed a loss of mature and elongated dendrites (Krivosheya et al., 2008). Given the selective expression of ErbB4 in GABAergic interneurons and prior reports of Nrg1 on neurite outgrowth, we wanted to compare and contrast the effects of Nrg2 and Nrg3 to the effects of Nrg1 in GABAergic neuronal differentiation, which remain largely unexplored.

Towards these goals we characterized and compared the roles of Nrg1-3 and of their receptor ErbB4 in neurite outgrowth, in primary cortical GABAergic interneurons. We observed that all three Nrgs (GST-Nrg1-3) enhanced neurite outgrowth of ErbB4/GABA (+) interneurons,

and that this effect was limited to interneurons expressing ErbB4. Several parameters of neurite outgrowth were affected by GST-Nrg treatment, including the number of primary neurites, sprouting of secondary neurites, and neurite length. Interneurons treated for 2 days showed increased lengths of all neurites, while further treatment to day 5 showed additional enhancement in axonal growth, but not of the other neurites. These results indicate that Nrg treatment can accelerate neurite outgrowth and has a sustained effect on axonal growth. Consistent with the effect of Nrgs on axonal growth, their receptor ErbB4 was expressed in the axon at both 2 and 5 days *in vitro* but its expression gradually decreased with GABAergic cell maturation. The overexpression of mCherry/ErbB4 enhanced the length of the axon and the number of primary neurites in cortical interneurons, independent of Nrg treatment. However, treatment with Nrg1-3 further enhanced neurite outgrowth of mCherry/ErbB4 overexpressing interneurons. These findings suggest that Nrg2 and Nrg3, similar to Nrg1, can enhance neurite outgrowth of ErbB4-expressing GABAergic cells. These results broaden our understanding of the molecular mechanisms regulating neurite outgrowth of GABAergic interneurons and expand our understanding, at a cellular and molecular level, of disorders (such as SZ) in which the Nrgs have been linked to and where neurite outgrowth may be compromised.

4.2 RESULTS:

4.2.1 Characterization of Primary Cortical Cultures and GST-Nrg Activation

The main goal of our study was to compare and characterize the potential effect of the different Nrgs on the neurite outgrowth properties of neurons expressing the receptor ErbB4 in the cerebral cortex. Previous studies have reported that ErbB4 is expressed primarily in γ -Aminobutyric acid (GABA) expressing interneurons, with preferential expression in a parvalbumin (PV)-positive subset of this class of neurons (Neddens & Buonanno, 2010; Neddens et al., 2011; Yau et al., 2003). To determine whether, in our primary rat cortical neuronal cultures, we could detect ErbB4 in PV-positive GABAergic interneurons, we quantified the expression of GABA, PV, and ErbB4 cells. We performed immunocytochemistry for GABA and ErbB4 in cortical cultures at 2 days *in vitro* (DIV) (Fig. 4.1A-C) and 5 DIV (Fig. 4.1D-G). Our results show that ErbB4 co-localizes with GABA-expressing cells (Fig. 4.1C and F) at both 2 and 5 DIV, and we observed that $18.01\% \pm 2.45\%$ (14.60 ± 1.85 cells) of total cells were ErbB4 (+), $20.85\% \pm 3.62\%$ (16.80 ± 1.94 cells) of total cells were GABA (+), and $17.18\% \pm 2.44\%$ of total cells (13.90 ± 1.51 cells) were both ErbB4 (+)/GABA (+). We also determined that of the GABA expressing cells, $84.61 \pm 6.27\%$ (average \pm SD) also expressed ErbB4 at 5 DIV (Fig. 4.1H), showing that that the majority of GABAergic neurons also express ErbB4. We did not detect any cells that were ErbB4 (+) and GABA (-) (Fig. 4.1H).

Since ErbB4 has been reported to be preferentially expressed in the PV (+) subtype of interneurons (Neddens et al., 2011; Vullhorst et al., 2009), we further determined ErbB4 expression in PV+ interneurons in our cultures. Because the PV protein is not detectable at 2 and 5 DIV [(Benson et al., 1994) and our own data not shown] and is first expressed at late developmental stages, we performed our analysis in cortical cells cultured for 21 DIV. As shown in Fig. 4.1I, we found that all (100%) PV-expressing neurons in our primary cortical cultures also

expressed ErbB4 and that a majority of ErbB4 (+) cells ($64.73 \pm 11.09\%$) are PV (+) interneurons (Fig. 4.1I). We further observed that on average $18.99 \pm 4.63\%$ (average \pm SD) of total cells (15.50 ± 2.50 cells) were ErbB4 (+), $12.46 \pm 3.94\%$ of total cells (10.17 ± 2.88 cells) were PV (+), and $12.46 \pm 3.94\%$ of total cells (10.17 ± 2.88 cells) were both ErbB4(+)/PV(+). Overall, our quantification of ErbB4 (+), GABA (+), and PV (+) neurons in rat cortical cultures derived from E17-E18 embryos are in general agreement with previous reports on the expression of GABAergic interneurons in the rat cortex (Feldman & Peters, 1978; Kawaguchi & Kubota, 1997; Markram et al., 2004; Peters & Kara, 1985), as well as the co-expression of ErbB4 with GABA and PV in both rodent and monkey cerebral cortex (Neddens et al., 2011; Yau et al., 2003).

Since for our neurite outgrowth studies we prepared GST-Nrg1-3 factors, we tested them for their ability to induce ErbB4 receptor phosphorylation in our primary cortical cultures (5 DIV). As shown in Figure 4.1G (top panel), GST-Nrg1-3, but not GST control, induced ErbB4 tyrosine phosphorylation (Fig. 4.1G, lane N1, N2, and N3 respectively). These results demonstrate that our GST-Nrg factors can activate ErbB4 expressed in cultured primary cortical cells and are biologically active.

Fig. 4.1

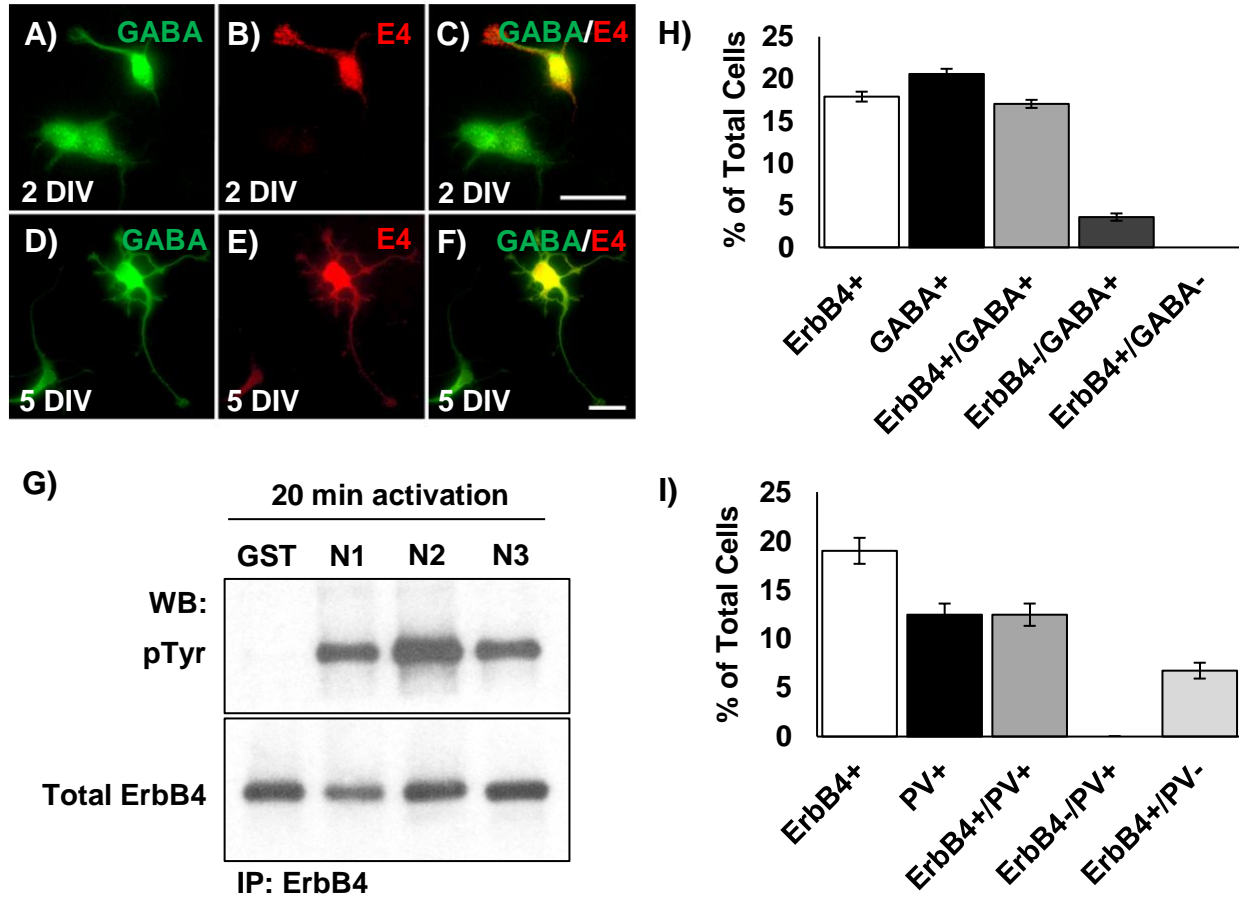


Fig. 4.1: Characterization of Primary Cortical Cultures and GST-Nrg Activation.

A-F) ErbB4 and GABA expression and co-localization in primary cortical cultures. Primary cortical cultures were grown on coverslips for 2 (**panels A-C**) or 5 (**panels D-F**) days *in vitro* (DIV). Cells stained with anti-GABA antibodies (**panels A and D**, 1:1000 dilution) and anti-ErbB4 antibodies (**panels B and E**, 1:250 dilution). The anti-GABA antibodies were visualized with Alexa Fluor 488 goat anti-rabbit antibodies (in green) and the anti-ErbB4 antibodies were visualized with Alexa Fluor 594 coupled goat anti-mouse antibodies (in red) both at 1:300 dilution. Merged images are shown in **panels C and F**. Scale bar = 30 μ m for all panels.

G) GST-Nrg factors were tested for their ability to activate ErbB4. Samples were then analyzed by SDS-PAGE using 4-20% Tris-glycine gels followed by Western blotting. The blots were

probed with anti-phospho-tyrosine (pTyr) PY99 and PY20 (**top panel**, 1:5000 dilution for both) and anti-ErbB4 616 sera (**bottom panel**, 1:7500 dilution).

H) Primary cortical cultures (5 DIV) were quantified for their expression of GABAergic interneurons and neurons expressing ErbB4. Four different fields per coverslip from three different experiments (for a total of 12 fields) were analyzed and counted for total number of cells that expressed ErbB4 (ErbB4+), cells that expressed GABA (GABA+), cells that expressed both GABA and ErbB4 (ErbB4+/GABA+), cells that expressed GABA but not ErbB4 (ErbB4-/GABA+), and cells that expressed ErbB4 but not GABA (ErbB4+/GABA-). Data is reported in the graph as % total of cells (\pm SEM) as determined through Hoechst nuclei staining.

I) Primary cortical cultures (21 DIV) were quantified for their expression of parvalbumin (PV)-positive (+) interneurons and neurons expressing ErbB4. Four different fields per coverslip from three different experiments (for a total of 12 fields) were analyzed and counted for total number of cells that expressed ErbB4 (ErbB4+), cells that expressed PV (PV+), cells that expressed both PV and ErbB4 (ErbB4+/PV+), cells that expressed PV but not ErbB4 (ErbB4-/PV+), and cells that expressed ErbB4 but not PV (ErbB4+/PV-). Data is reported in the graph as % total of cells (\pm SEM) as determined through Hoechst nuclei staining.

4.2.2 GST-Nrg1-3 Factors Enhance Neurite Outgrowth in ErbB4/GABA Positive Interneurons Following 2 Days of Treatment

To study the effects of the Nrgs on the neurite outgrowth of cortical ErbB4/GABAergic interneurons, we treated cortical cultures with 500 ng/mL of GST, GST-Nrg1, GST-Nrg2, or GST-Nrg3 at the time of plating and further cultured the cells for 2 days (2 DIV). We then performed immunocytochemistry against ErbB4/GABA and performed morphometric analyses on individual neurons.

Our morphometric analyses (Fig. 4.2) of ErbB4/GABA (+) interneurons showed that a 2 day GST-Nrg treatment resulted in substantial increase in neurite outgrowth compared to the GST control. As shown in Fig. 4.2A and A", treatment with the GST-Nrgs resulted in an overall average increase between 85-94% in the length of all neurites compared to the GST control (baseline was considered 100% for GST control with an average length of $26.26 \pm 1.10 \mu\text{m}$, 94% increase for GST-Nrg1 with an average length of $51.07 \pm 0.72 \mu\text{m}$, 85% increase for GST-Nrg2 with an average length of $48.55 \pm 3.67 \mu\text{m}$, and 98% increase for GST-Nrg3 with an average length of $51.93 \pm 1.36 \mu\text{m}$; Fig. 4.2A and A"). Differences in average length of all neurites between GST-Nrg1, GST-Nrg2, and GST-Nrg3 conditions were not statistically significant (Fig. 4.2A and A").

We further investigated the possibility that each of the Nrgs may play distinct or preferential roles in neurite outgrowth. We measured two parameters for each cell analyzed: the length of the longest neurite and the average length of the neurites excluding the longest one. Our data, as shown in Fig. 4.2B and B", revealed that the ErbB4/GABA (+) neurons cultured with GST-Nrgs showed an overall average increase in length ranging from 116-120% for the longest neurite compared to the GST control (baseline was considered 100% for GST control with an average length of $31.89 \pm 1.67 \mu\text{m}$, 116% increase for GST-Nrg1 with an average length

of $68.74 \pm 0.37 \mu\text{m}$, 116% increase for GST-Nrg2 with an average length of $68.70 \pm 7.54 \mu\text{m}$, and 120% increase for GST-Nrg3 with an average length of $70.11 \pm 3.34 \mu\text{m}$; Fig. 4.2B and B"). This increase in length of the longest neurite exceeded the measurements observed when all neurites were analyzed together (Fig. 4.2A and A"). Differences in the average length of the longest neurite between GST-Nrg1, GST-Nrg2, and GST-Nrg3 conditions were not statistically significant (Fig. 4.2B and B").

To determine whether the GST-Nrgs affected the extension of all neurites or favored that of the longest neurite, we compared the average length of neurites excluding the longest neurite. As shown in Fig. 4.2C and C"), we found that the ErbB4/GABA (+) neurons cultured with GST-Nrgs showed an overall average increase ranging from 100-120% in the length of neurites excluding the longest compared to the GST control (baseline was considered 100% for GST control with an average length of $19.13 \pm 1.04 \mu\text{m}$, 113% increase for GST-Nrg1 with an average length of $40.92 \pm 2.65 \mu\text{m}$, 100% increase for GST-Nrg2 with an average length of $38.60 \pm 3.39 \mu\text{m}$, and 120% increase for GST-Nrg3 with an average length of $42.12 \pm 1.55 \mu\text{m}$; Fig. 4.2C and C"). There were no significant differences between the GST-Nrg1, GST-Nrg2, and GST-Nrg3 conditions when analyzing the average length of neurites excluding the longest neurite (Fig. 4.2C and C"). Overall, our data show that the GST-Nrg growth factors significantly increase neurite outgrowth in ErbB4/GABA (+) interneurons after 2 days of treatment in cultures grown for 2 DIV. Our findings also show that Nrg1, Nrg2, and Nrg3 have similar roles *in vitro* in promoting neurite outgrowth of ErbB4/GABA (+) interneurons at this early stage of differentiation.

We further analyzed the neurite outgrowth properties of the Nrgs by quantifying the average number of neurites per cell for each condition and calculating the proportions of cells with 1, 2, 3, or more than 3 neurites. Our results showed (Fig. 4.2D) an overall average increase from 2.11 neurites observed for the GST control to 3.0-3.3 neurites observed for the GST-Nrgs.

(GST control, average: 2.11 ± 0.09 neurites; GST-Nrg1, average: 3.33 ± 0.16 neurites; GST-Nrg2, average: 3.22 ± 0.09 neurites; and GST-Nrg3, average: 3.0 ± 0.00 neurites; Fig. 4.2D). There were no significant differences in the average number of primary neurites between the GST-Nrg1, GST-Nrg2, and GST-Nrg3 conditions (Fig. 4.2D).

We also determined the effect of the Nrgs or GST on the proportion of cells displaying 1, 2, 3, or more than 3 neurites. As shown in Fig. 4.2E, in the GST only treated cultures, neurons with 1 and 2 neurites were more prevalent than in the GST-Nrg treated cultures (GST average: $16.33 \pm 4.25\%$, $57.0 \pm 1.89\%$ respectively; GST-Nrg1 average: $1.33 \pm 0.72\%$, $22.33 \pm 5.68\%$ respectively; GST-Nrg2 average: $2.67 \pm 1.09\%$, $21.33 \pm 4.28\%$ respectively; and GST-Nrg3 average: $1.0 \pm 0.82\%$, $23.33 \pm 3.14\%$ respectively; Fig. 4.2E). In contrast, in the GST-Nrg treated cultures the neurons with 3 and more than 3 neurites were more prevalent than in the GST only treated cultures (GST average: $18.67 \pm 3.60\%$, $7.0 \pm 1.25\%$ respectively; GST-Nrg1 average: $30.33 \pm 6.62\%$, $34.0 \pm 6.60\%$ respectively; GST-Nrg2 average: $30.0 \pm 1.25\%$, $46.0 \pm 1.25\%$ respectively; and GST-Nrg3 average: $38.0 \pm 2.94\%$, $35.33 \pm 4.72\%$ respectively; Fig. 4.2E). Furthermore, these GST-Nrg treated cultures also presented neurons with more secondary neurites (GST average: $21.33 \pm 3.07\%$; GST-Nrg1 average: $77.67 \pm 1.96\%$; GST-Nrg2 average: $70.0 \pm 3.86\%$; and GST-Nrg3 average: $72.67 \pm 3.41\%$; Fig. 4.2E). Our morphological analyses did not show any differences between the GST-Nrg1, GST-Nrg2, and GST-Nrg3 conditions (Fig. 4.2E). Overall, our data show that ErbB4/GABA (+) cells cultured for 2 days in the presence of GST-Nrg1, GST-Nrg2, or GST-Nrg3 factors demonstrate an increase in neurite outgrowth in all parameters that were measured, compared to the GST control.

Fig. 4.2

ErbB4/GABA (+) Neurons, 2 Day Treatment:

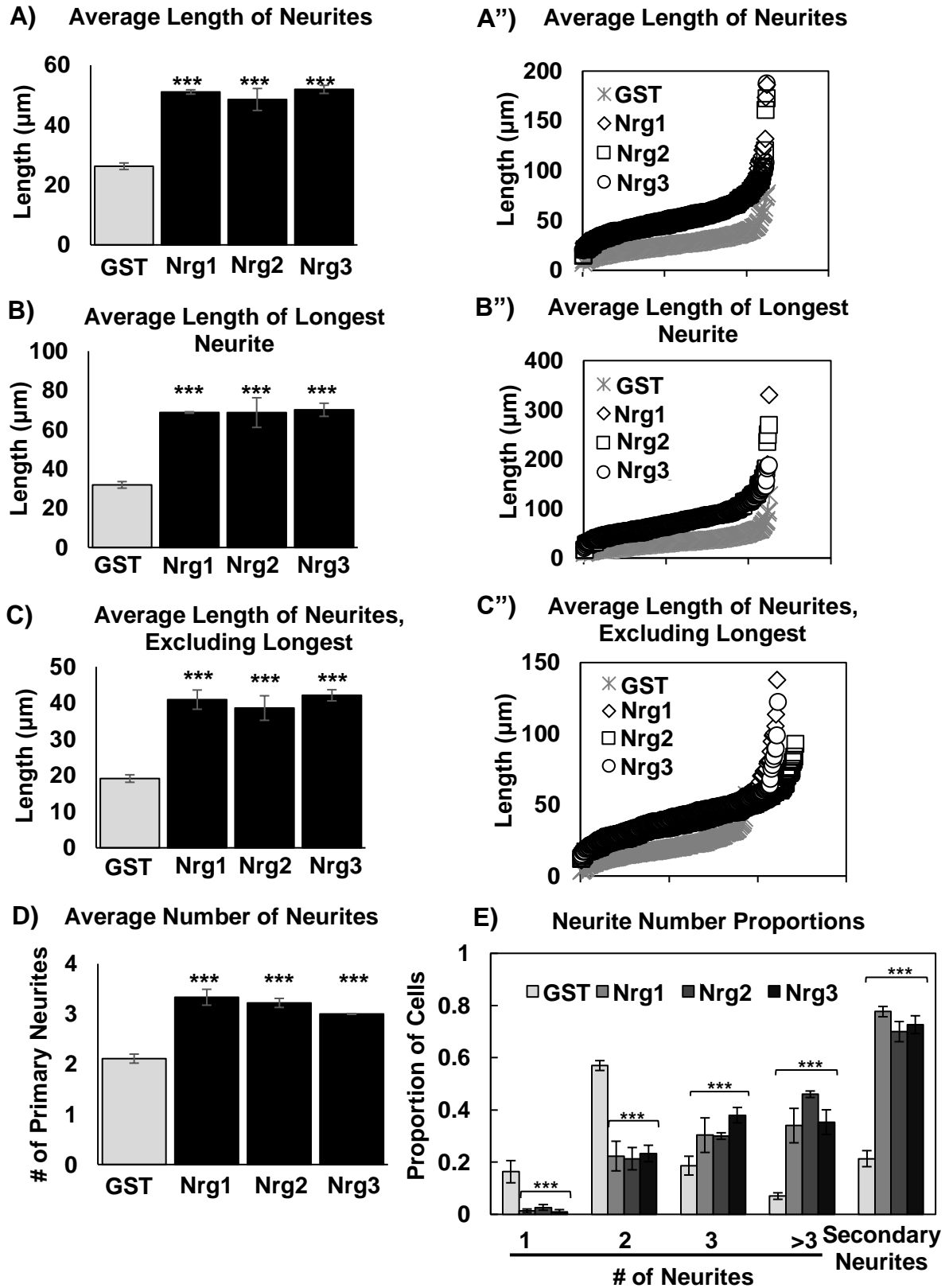


Fig. 4.2: GST-Nrg1-3 Factors Enhance Neurite Outgrowth in ErbB4/GABA Positive Interneurons Following 2 days of Treatment.

Morphometric analyses of primary cortical neurons treated for 2 days with 500 ng/mL of GST-Nrg1, GST-Nrg2, or GST-Nrg3 demonstrate a significant increase in neurite outgrowth in ErbB4/GABA positive cells compared to those treated with 500 ng/mL of GST control. GST-Nrg1-3 treated neurons had significantly greater average lengths of primary neurites (**panels A and A' for all data points**), average lengths of the longest neurite (**panels B and B' for all data points**), average lengths of neurites excluding the longest (**panels C and C' for all data points**), and average number of neurites (**panel D**). Neurons were further characterized (**panel E**) into four groups according to the number of neurites protruded: 1 neurite, 2 neurites, 3 neurites, and >3 neurites. The proportion of cells which displayed secondary neurites was also measured. Cells cultured with GST showed greater number of cells with one or two neurites compared to GST-Nrg conditions, whereas cells cultured with GST-Nrg1-3 had a greater number of cells with three neurites, greater than three neurites, and proportion of cells with secondary neurites compared to the GST control condition. Bars represent the average \pm SEM; n = a total of 3 independent experiments (75 cells/experiment for each condition); ***p = <0.001

4.2.3 GST-Nrg1-3 Enhance Neurite Outgrowth of ErbB4/GABA Positive Interneurons

Following 5 Days of Treatment

To determine if the effects of Nrg-induced neurite outgrowth are sustained at a later developmental time point, we analyzed their effects on neurite outgrowth following 5 days of treatment using the same methodology as for 2 days of treatment.

As observed for 2 days of treatment, GST-Nrg1, GST-Nrg2, and GST-Nrg3 treatment for 5 days continued to show a marked increase in neurite outgrowth compared to the GST control (Fig. 4.3). As shown in Fig. 4.3A and A", ErbB4/GABA (+) interneurons treated with the GST-Nrgs showed an increase ranging from 32-46% in the average length of all neurites compared to the GST control (baseline considered 100% for GST control with an average length of $53.88 \pm 2.14 \mu\text{m}$, 46% increase for GST-Nrg1 with average length of $78.74 \pm 3.46 \mu\text{m}$, 32% increase for GST-Nrg2 with average length of $71.27 \pm 2.09 \mu\text{m}$, and 41% increase for GST-Nrg3 with an average length of $76.15 \pm 4.94 \mu\text{m}$; Fig. 4.3A and A"). When compared to the measurements obtained at 2 DIV the lengths of the neurites increase approximately 54-105% relative to the length observed for the neurites at 2 DIV (Table 4.1). We did not detect any statistically significant differences in average length of neurites between the GST-Nrg1, GST-Nrg2, and GST-Nrg3 conditions (Fig. 4.3A and A").

We also determined the length of the longest neurite and the average length of all neurites excluding the longest. When we only consider the changes observed for the longest neurite, after 5 days (Fig. 4.3B and B") we continued to observe that all three GST-Nrgs showed an increase ranging from 86-96% in the average length of the longest neurite compared to the GST control (baseline considered 100% for GST control with an average length of $95.30 \pm 3.47 \mu\text{m}$, 96% increase for GST-Nrg1 with an average length of $186.85 \pm 4.33 \mu\text{m}$, 85% increase for GST-Nrg2 with an average length of $177.21 \pm 7.99 \mu\text{m}$, and 92% increase for GST-Nrg3 with an

average length of $183.31 \pm 7.26 \mu\text{m}$; Fig. 4.3B and B"). When compared to the measurements obtained at 2 DIV, the lengths of the neurites increased approximately 171-199% relative to the length observed for the neurites at 2 DIV. Differences in the average length of the longest neurite between GST-Nrg1, GST-Nrg2, and GST-Nrg3 conditions were not statistically significant (Fig. 4.3B and B").

To determine whether the changes extended to all neurites or were only confined to the longest neurite, we compared the average length of the neurites excluding the longest one. In contrast to our observations at 2 days of GST-Nrg treatment (Fig. 4.2C and C" and Table 4.1), after 5 days of Nrg treatment we did not observe differences with the GST control (GST control, average length of $36.37 \pm 1.49 \mu\text{m}$; GST-Nrg1, average length of $44.06 \pm 0.69 \mu\text{m}$; GST-Nrg2, average length of $43.39 \pm 1.79 \mu\text{m}$; or GST-Nrg3, average length of $47.44 \pm 4.36 \mu\text{m}$; Fig. 4.3, C and C"). When compared to the measurements obtained at 2 DIV the lengths of the neurites in the cultures treated with GST-Nrgs increased approximately 8-13% relative to the lengths observed for the neurites at 5 DIV (Table 4.1). An exception was observed for the cells treated with GST control. The neurites in these cells continued to grow, and increased approximately 90% relative to the length observed for the neurites at 2 DIV (Table 4.1). This indicates that only the neurites (excluding the longest) in the GST control treated neurons continued to grow and approached the lengths reached by the neurites of the Nrg treated cells at 5 DIV. Because the neurites in the Nrg treated samples only extended by 8-13% when compared to 2 DIV (Table 4.1), one possible conclusion is that the Nrgs accelerated the growth of the neurites, achieving their near maximal effect close to 2 DIV. Further exposure to the Nrgs until 5 DIV only minimally affected their length, with the exception of the longest neurite which continued to respond to the Nrg treatment significantly until at least 5 DIV. Differences in the average length of neurites excluding the longest one between the GST-Nrg conditions were also not statistically significant

(Fig. 4.3, C and C”), suggesting a redundant role of the Nrgs in the growth of the longest neurite at this time point.

We further quantified the average number of neurites per cell for each GST-Nrg treatment condition and further calculated the proportion of cells that have 3 or fewer neurites, 4 neurites, 5 neurites, or more than 5 neurites. As shown in Fig. 4.3D, ErbB4/GABA (+) interneurons cultured in the presence of GST-Nrgs for 5 days showed an overall average increase in the number of primary neurites ranging from 5.11-5.56 neurites compared to the average of 3.78 neurites observed for the GST control (GST average: 3.78 ± 0.18 neurites; GST-Nrg1 average: 5.56 ± 0.36 neurites; GST-Nrg2 average: 5.44 ± 0.33 neurites; and GST-Nrg3 average: 5.11 ± 0.33 neurites; Fig. 4.3D). These findings were similar to those observed at 2 days of treatment (Fig. 4.2D and Table 4.1). In comparison to the cells analyzed after 2 days of treatment (Fig. 4.2D and Table 4.1), there was an overall increase in the number of primary neurites at 5 days for all conditions (Fig. 4.3D), consistent with the normal stages of neuronal development in culture (Dotti et al., 1988). The differences between the numbers of primary neurites among the GST-Nrg conditions were not significant (Fig. 4.3D).

We also determined the effect of the Nrgs or GST on the proportion of cells displaying 3 or fewer neurites, 4 neurites, 5 neurites, or more than 5 neurites. As shown in Fig. 4.3E, in the GST only treated cultures, neurons with 3 or fewer neurites were more prevalent than in the GST-Nrg cultures (GST average: $37.67 \pm 6.42\%$; GST-Nrg1 average: $9.33 \pm 5.62\%$; GST-Nrg2 average: $8.33 \pm 2.37\%$; and GST-Nrg3 average: $9.33 \pm 3.34\%$; Fig. 4.3E). In contrast, in the GST-Nrg treated cultures, the neurons with more than five neurites were more prevalent (GST only average: $10.33 \pm 4.46\%$; GST-Nrg1 average: $46.67 \pm 12.13\%$; GST-Nrg2 average: $50.67 \pm 9.27\%$; and GST-Nrg3 average: $44.0 \pm 8.60\%$; Fig. 4.3E). Our morphological analyses did not show any differences between the GST-Nrg1, GST-Nrg2, and GST-Nrg3 conditions (Fig. 4.3E). We also did not observe any statistically significant differences between any of the groups

(including the GST control) when analyzing the proportions of cells displaying 4 neurites or 5 neurites (Fig. 4.3E). Overall, our data show that ErbB4/GABA (+) cells cultured for 5 days in the presence of GST-Nrg1, GST-Nrg2, or GST-Nrg3 factors demonstrate an increase in neurite outgrowth of the longest neurite and an increase in the number of primary neurites, compared to the GST control.

Fig. 4.3

ErbB4/GABA (+) Neurons, 5 Day Treatment:

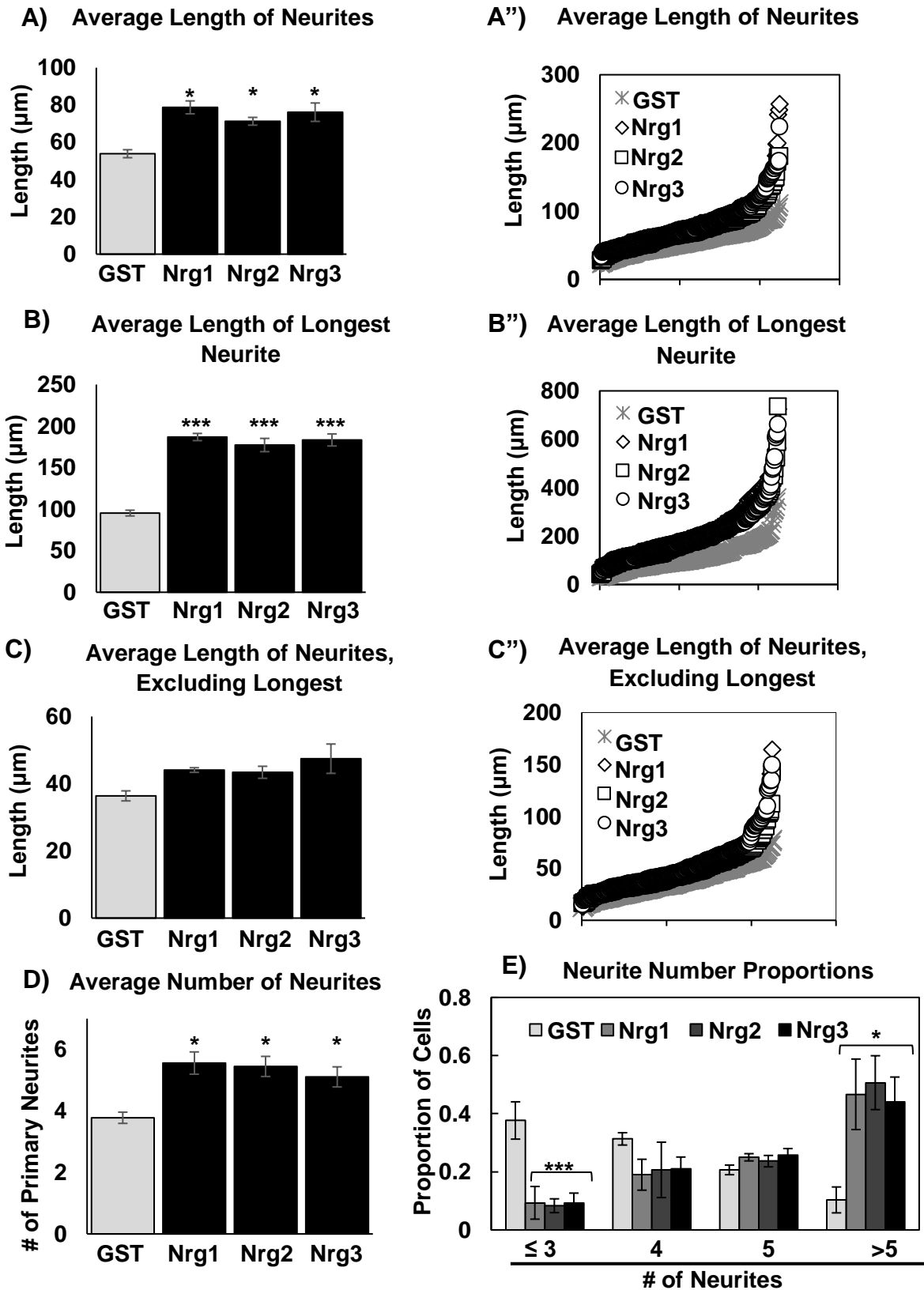


Fig. 4.3: GST-Nrg1-3 Factors Enhance Neurite Outgrowth in ErbB4/GABA Positive Interneurons Following 5 Days of Treatment.

Morphometric analyses of primary cortical neurons treated for 5 days with 500 ng/mL of GST, GST-Nrg1, GST-Nrg2, or GST-Nrg3 demonstrate a significant increase in certain measures of neurite outgrowth in ErbB4/GABA (+) cells compared to those treated with 500 ng/mL of GST control (**panels A, B, D and A''-C''**). GST-Nrg1-3 treated neurons had significantly greater average lengths of primary neurites (**panels A and A'' for all data points**), average lengths of the longest neurite (**panels B and B'' for all data points**), and average number of neurites (**panel D**). When excluding the length of the longest neurite, the average lengths of neurites between groups were not significant (**panels C and C'' for all data points**). **Panel E.** Neurons were further characterized into four groups according to the number of neurites protruded: ≤ 3 neurites, 4 neurites, 5 neurites, and >5 neurites. Cells cultured with GST showed greater number of cells with ≤ 3 neurites compared to GST-Nrg conditions, whereas cells cultured with GST-Nrg1-3 had a greater number of cells with >5 neurites compared to the GST control condition. Bars represent the average \pm SEM; n = a total of 3 independent experiments (75 cells/experiment for each condition); *p = <0.05 , ***p = <0.001

Table 4.1

Table 4.1 Neurite Outgrowth Measures Following GST or GST-Nrg Treatment for 2 or 5 Days				
Average Length of Neurites (in μm)				
	GST	Nrg1	Nrg2	Nrg3
Day 2	26.26 \pm 1.10	51.07 \pm 0.72	48.55 \pm 3.67	51.93 \pm 1.36
Day 5	53.88 \pm 2.14	78.74 \pm 3.46	71.27 \pm 2.09	76.15 \pm 4.94
Average Length of the Longest Neurite (in μm)				
	GST	Nrg1	Nrg2	Nrg3
Day 2	31.89 \pm 1.67	68.74 \pm 0.37	68.70 \pm 7.54	70.11 \pm 3.34
Day 5	95.30 \pm 3.47	186.85 \pm 4.33	177.21 \pm 7.99	183.31 \pm 7.26
Average Length of Neurites, Excluding Longest (in μm)				
	GST	Nrg1	Nrg2	Nrg3
Day 2	19.13 \pm 1.04	40.92 \pm 2.65	38.60 \pm 3.39	42.12 \pm 1.55
Day 5	36.37 \pm 1.49	44.06 \pm 0.69	43.39 \pm 1.79	47.44 \pm 4.36
No. of Primary Neurites				
	GST	Nrg1	Nrg2	Nrg3
Day 2	2.11 \pm 0.09	3.33 \pm 0.16	3.22 \pm 0.09	3.0 \pm 0.0
Day 5	3.78 \pm 0.18	5.56 \pm 0.36	5.44 \pm 0.33	5.11 \pm 0.33

Table 4.1: Neurite Outgrowth Measures Following GST or GST-Nrg Treatment for 2 or 5 Days.

Shown here is a chart comparing the average length of neurites, average length of the longest neurite, average length of neurites excluding the longest, and number of primary neurites in ErbB4/GABA (+) cells after treatment with GST, GST-Nrg1, GST-Nrg2, or GST-Nrg3 for 2 or 5 days. Data is presented as the average \pm SEM.

4.2.4 GST-Nrg Treatment Enhances the Growth of the Axon of Cortical Interneurons

Following 5 Days of Treatment

We showed that following 5 days of treatment (5 DIV), the Nrgs continue to enhance the growth of the longest neurite in ErbB4/GABA (+) cells, but not of the other neurites (Fig. 4.3). To determine whether this longest neurite corresponds to the axon, we performed immunocytochemistry with GABA and the axonal marker ankyrin-G, a scaffolding protein responsible for the organization of the axon initial segment (AIS; Fig. 4.4A-L). As shown in Figure 4.4, we quantified the effects of GST and GST-Nrg1 on neurite length of cortical GABAergic neurons by measuring the length of the ankyrin-G positive neurite (axon) and the length of the longest neurite for each cell. For these assays we only treated with either GST control or GST-Nrg1 factor since we found no significant difference among the GST-Nrgs on their effects on neurite outgrowth. For all cells analyzed, except for one, we observed that the longest neurite corresponded to the ankyrin-G expressing axon (Fig. 4.4A-L and data not shown). As shown in Fig. 4.4M, after 2 days of treatment, GABA (+) interneurons treated with GST-Nrg1 had an average axon length of $126.442 \pm 2.66 \mu\text{m}$ which was 27.7% longer than that measured for the GST control ($99.0 \pm 1.43 \mu\text{m}$) (Fig. 4.4M). These lengths for the longest neurite differed from those obtained at 2 DIV presented in Fig. 4.2B and B". They are longer for both the GST ($99.0 \pm 1.43 \mu\text{m}$ (Fig 4.4M)) compared to $31.89 \pm 1.67 \mu\text{m}$ (Fig. 4.2B)) and the GST-Nrg1 ($126.442 \pm 2.66 \mu\text{m}$ (Fig 4.4M)) compared to $68.74 \pm 0.37 \mu\text{m}$ (Fig. 4.2B)) conditions. One possibility is that at day 2 only a subset of GABAergic cells expressed ankyrin-G, which was a necessary condition for us to unequivocally establish which neurite was the axon. These ankyrin-G (+) cells had (on average) longer neurites than the overall population of GABAergic cells that, at this early stage, did not present sufficient ankyrin-G expression to unequivocally assign a specific neurite as an axon.

When we compared the effects of GST and GST-Nrg1 treatment on axonal elongation at 5 DIV (Fig. 4.4M), the GABA (+) interneurons treated with GST-Nrg1 had an average axon length of $179.17 \pm 1.83 \mu\text{m}$ which was 76.05% longer than that measured for the GST control ($101.77 \pm 5.18 \mu\text{m}$) ($p < 0.001$; Fig. 4.4M). In contrast to what we observed at 2 DIV, the average axon lengths (Fig. 4.4M), for both the GST and GST-Nrg1 treated neurons coincide with those shown in Fig. 4.3B and B". Overall, these data together with that in Figs. 4.2 and 4.3 show that the longest neurite corresponds to the axon and that the Nrgs enhance axonal growth in GABAergic interneurons at 2 and 5 days of treatment, the last day we monitored their effect.

Fig. 4.4

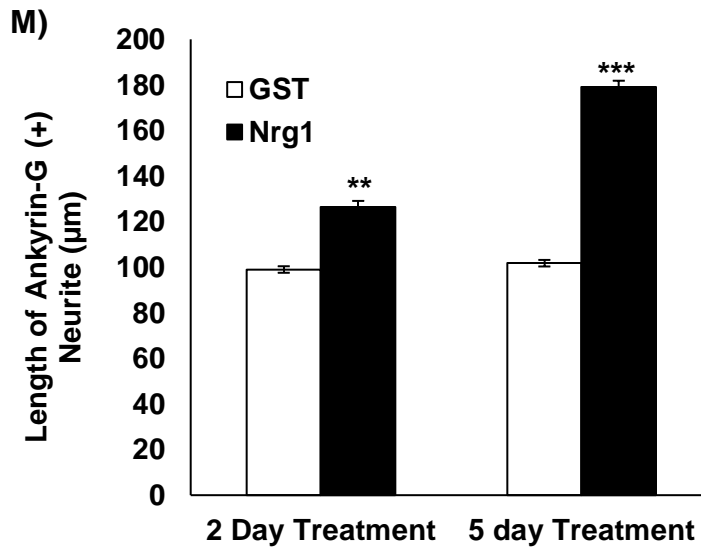
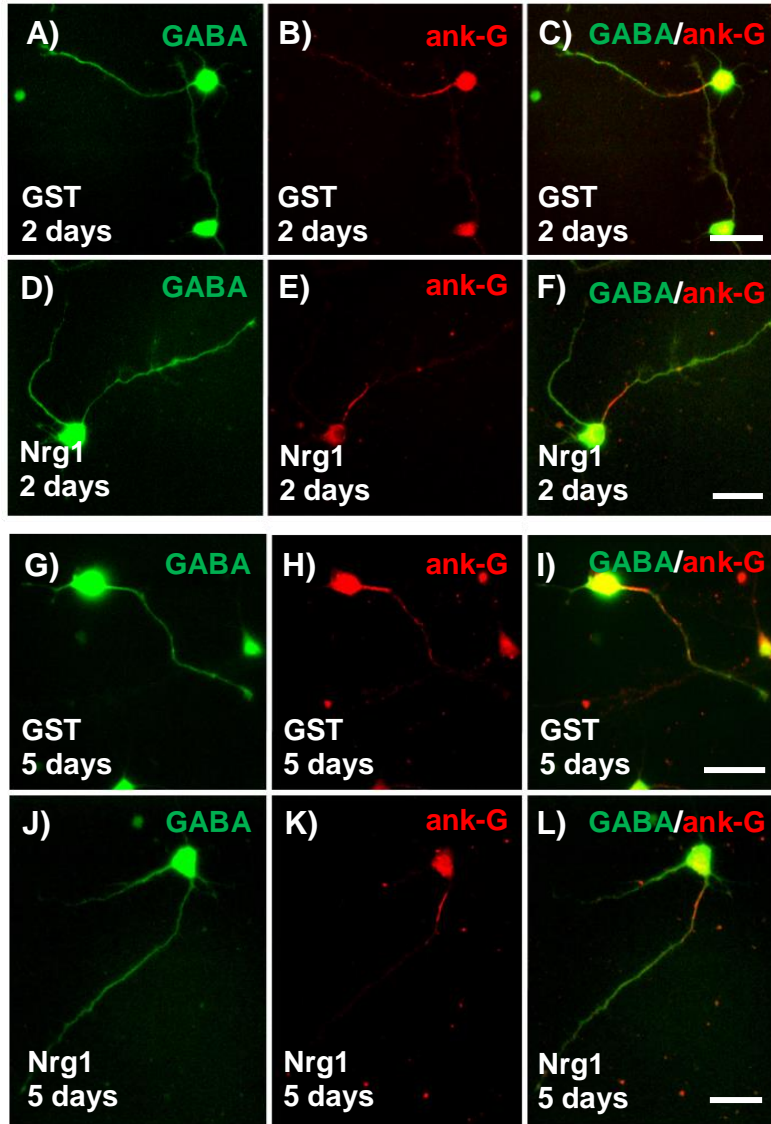


Fig. 4.4: GST-Nrg Treatment Enhances the Growth of the Axon of Cortical Interneurons Following 5 Days of Treatment.

Primary cortical cultures derived from E17 rat embryos were grown on coverslips in the presence of 500 ng/mL of GST (**panels A-C and G-I**) or GST-Nrg1 (**panels D-F and J-L**) for 2 (**panels A-F**) or 5 (**panels G-L**) DIV. Cells were then fixed and stained with anti-GABA antibodies (**panels A, D, G, and J**, 1:1000 dilution) and anti-ankyrin-G (ank-G) antibodies (**panels B, E, H, and K**, 1:500 dilution). The anti-GABA antibodies were visualized with Alexa Fluor 488 goat anti-rabbit antibodies (in green) and the anti-ank-G antibodies were visualized with Alexa Fluor 594 coupled goat anti-mouse antibodies (in red) both at 1:300 dilution. Merged images are shown in **panels C, F, I, and L**. Scale bar = 30 μm for all panels. **Panel M.**

Measurements of the length of the axon (ank-G (+) neurites) in GABA (+) interneurons. GABA (+) neurons treated with 500 ng/mL of GST-Nrg1 showed an increase in the length of the axon compared to those treated with 500 ng/mL of GST after both 2 and 5 days of treatment. Bars represent the average \pm SEM; n = a total of 3 independent experiments (15 cells/experiment for both conditions); **p = <0.01, ***p = <0.001

4.2.5 Axonal Expression of ErbB4 is Transient

Since we determined that the Nrgs play a role in neurite elongation including the axon, we characterized the role of ErbB4. First, to determine whether ErbB4 expression is developmentally regulated, we performed a time course of ErbB4 expression in GABAergic interneurons at 2, 5, 8, 12, 16, and 21 DIV. To identify the axon we performed double immunocytochemistry for ErbB4 and ankyrin-G. At 2 and 5 days (Fig. 4.5C and F), we observed high levels of ErbB4 expression in the axon (Fig. 4.5A-F); while at later developmental stages, ErbB4 expression progressively decreased becoming undetectable in the axon by 21 DIV (Fig. 4.5J-R). In contrast, the expression of ErbB4 remained high in the soma and dendrites in the mature neurons, becoming more punctate, consistent with previous findings (Vullhorst et al., 2009). These data support the conclusion that at days 2 and 5, ErbB4 is well positioned to mediate Nrg induced neurite outgrowth of all neurites including the axon.

Fig. 4.5

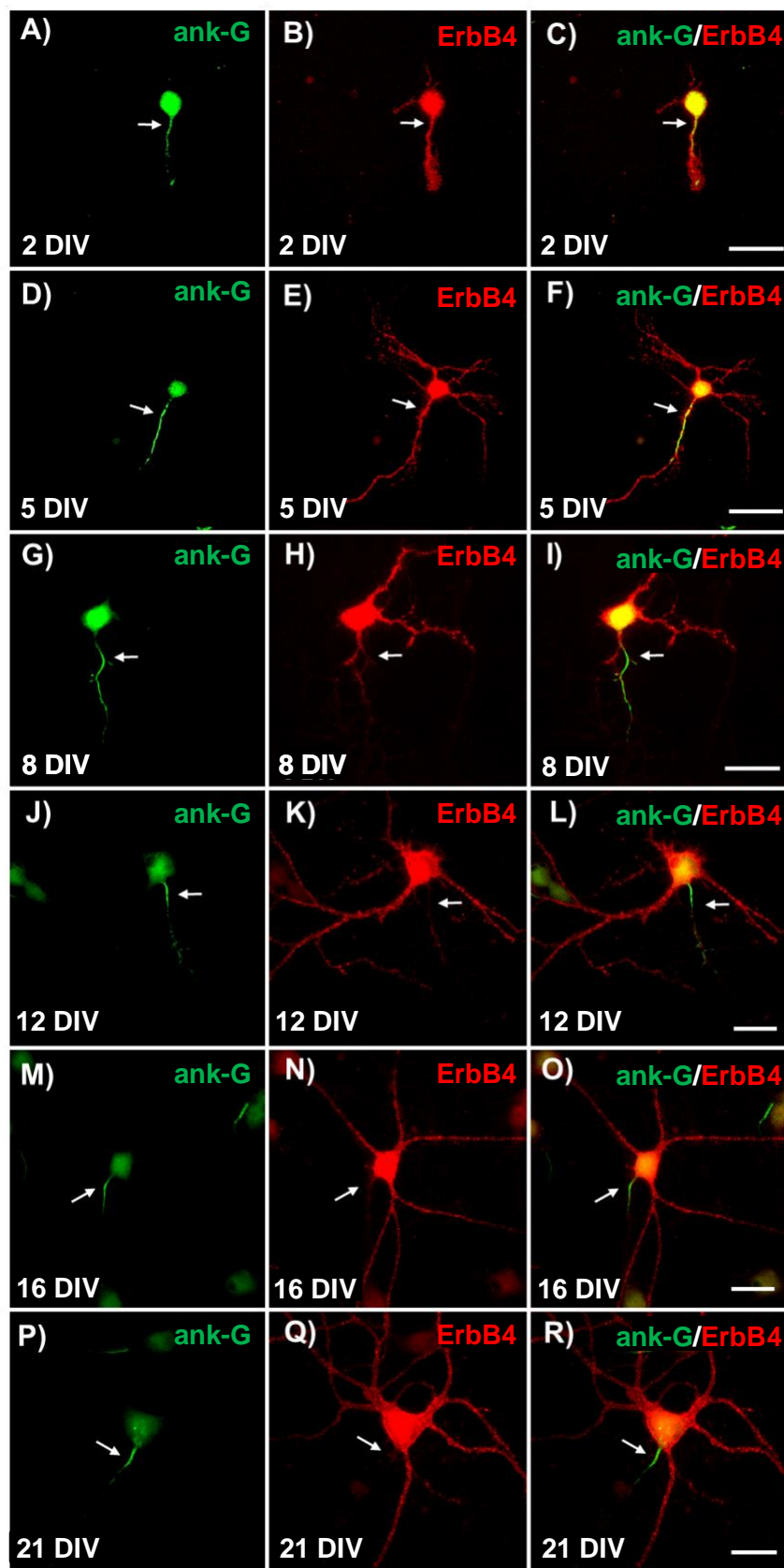


Fig. 4.5: Axonal Expression of ErbB4 is Transient.

ErbB4 and the axon initial segment (AIS) protein ankyrin-G (ank-G) expression and co-localization in primary cortical cultures. Primary cortical cultures derived from E17-E18 rat embryos were grown on coverslips for 2 (**panels A-C**), 5 (**panels D-F**), 8 (**panels G-I**), 12 (**panels J-L**), 16 (**panels M-O**), or 21 (**panels P-R**) DIV. Cells were then fixed and stained with anti-ank-G antibodies (**panels A, D, G, J, M, and P**, 1:500 dilution) and anti-ErbB4 antibodies (**panels B, E, H, K, N, and Q**, 1:250 dilution). The anti-ank-G antibodies were visualized with Alexa Fluor 488 goat anti-rabbit antibodies (in green) and the anti-ErbB4 antibodies were visualized with Alexa Fluor 594 coupled goat anti-mouse antibodies (in red) both at 1:300 dilution. Merged images are shown in **panels C, F, I, L, O, R**. Arrows indicate the ank-G (+) axon. Scale bar = 30 μ m for all panels

4.2.6 Nrg-Induced Neurite Outgrowth is Limited to ErbB4-Expressing GABAergic Interneurons

We next assessed whether the effects of the Nrgs on neurite outgrowth was limited to neurons expressing ErbB4. For these experiments we performed neurite outgrowth measurements on cultured neurons that did not express ErbB4 (2 and 5 days of treatment), but were positive for the neuron specific protein β -tubulin. We analyzed the average length of all primary neurites (Fig. 4.6A and A" for 2 days; Fig. 4.7A and A" for 5 days), average length of the longest primary neurite (Fig. 4.6B and B" for 2 days; Fig. 4.7B and B" for 5 days), average length of primary neurites excluding the longest neurite (Fig. 4.6C and C" for 2 days; Fig. 4.7C and C" for 5 days), and total number of primary neurites (Fig. 4.6C for 2 days; Fig 4.7D for 5 days). We further investigated the proportion of cells expressing secondary neurites (Fig. 4.6E for 2 days) and proportion of cells expressing 3 or fewer neurites, 4 neurites, 5 neurites, or more than 5 neurites (Fig. 4.6E for 2 days; Fig. 4.7E for 5 days). We did not observe any significant differences between any conditions (including the GST control) for all parameters measured after both 2 and 5 days of treatment (Figs. 4.4 and 4.5 respectively). These observations suggest that the effect of the Nrgs is limited to neurons expressing ErbB4.

We also determined the effect of the GST-Nrgs on ErbB4 (-) and GABA (+) neurons, compared to GST control after 5 days of treatment. We chose to do these measures as GABA (+) / ErbB4 (-) cells represent a small proportion of the β -tubulin labeled neurons ($20.85 \pm 3.62\%$ of the total neurons; Fig. 4.1H) and would likely not be represented in the group. Measurements were limited to GABAergic/ErbB4 (-) cells. As in our previous experiments, we measured the average length of all primary neurites (Fig. 4.8A and A"), the length of the longest primary neurite (Fig. 4.8B and B"), the average length of the primary neurites excluding the longest one (Fig. 4.8C and C"), and total number of primary neurites (Fig. 4.8D). We further investigated proportion of cells expressing 3 or fewer neurites, 4 neurites, 5 neurites, or more than 5 neurites

(Fig. 4.8E). Our findings showed that there were no significant differences between any conditions (including the GST control) for all parameters measured ($p > 0.05$; Fig. 4.8), further supporting the conclusion that Nrg-induced neurite outgrowth is limited to ErbB4 expressing GABAergic interneurons.

Fig. 4.6

ErbB4 (-) / β -Tubulin (+) Neurons, 2 Day Treatment:

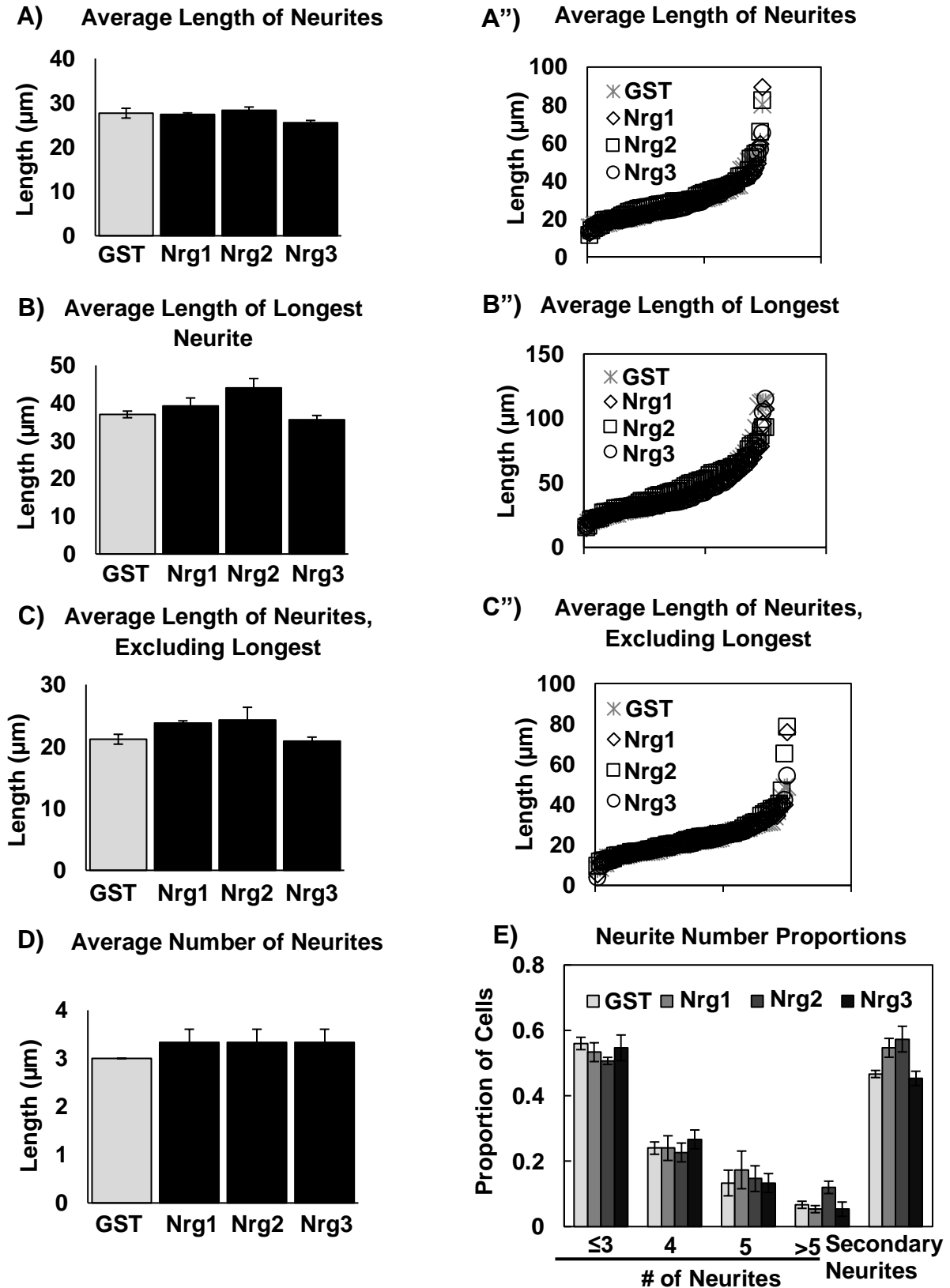


Fig. 4.6: GST-Nrg1-3 Factors do not Enhance Neurite Outgrowth of ErbB4(-)/ β -tubulin(+) Cortical Neurons Following 2 Days of Treatment.

Morphometric analyses of primary cortical neurons treated for 2 days with 500 ng/mL of GST, GST-Nrg1, GST-Nrg2, or GST-Nrg3 reveal no significant differences between any groups in the average length of neurites (**panels A and A'' for all data points**), average length of the longest neurite (**panels B and B'' for all data points**), average length of neurites excluding the longest (**panels C and C'' for all data points**), and average number of neurites (**panel D**) in ErbB4 (-)/ β -tubulin(+) cells. **Panel E.** Neurons were further characterized into four groups according to the number of neurites present: ≤ 3 neurites, 4 neurites, 5 neurites, and >5 neurites. The proportion of cells which displayed secondary neurites was also measured. No significant differences were observed between the GST and GST-Nrg1-3 conditions in any groups or in the proportion of secondary neurites. Bars represent the average \pm SEM; n = a total of 3 independent experiments (25 cells/experiment for each condition); p = >0.05

Fig. 4.7

ErbB4 (-) / β -Tubulin (+) Neurons, 5 Day Treatment:

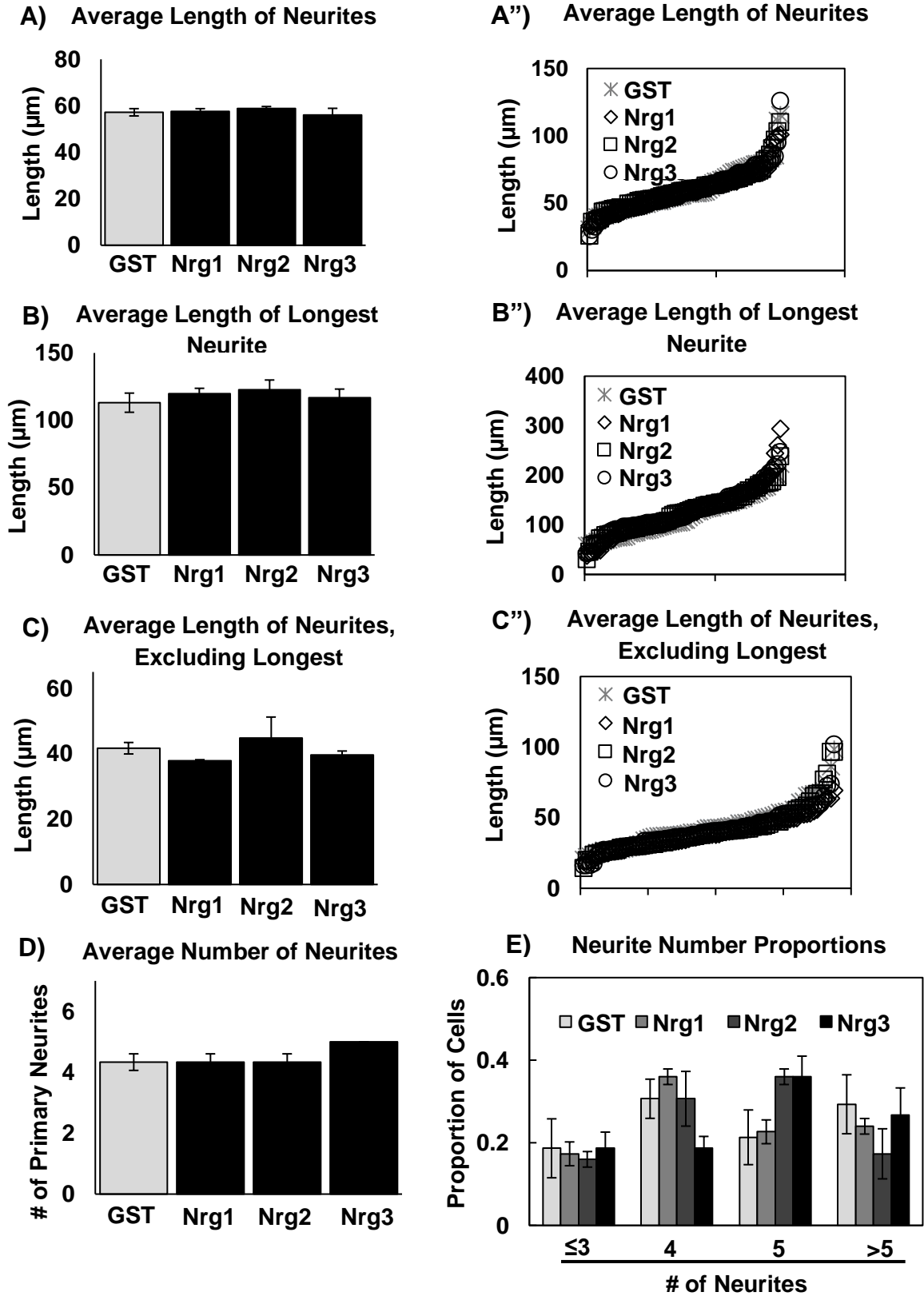


Fig. 4.7: GST-Nrg1-3 Factors do not Enhance Neurite Outgrowth of ErbB4(-)/ β -tubulin(+) Cortical Neurons Following 5 Days of Treatment.

Morphometric analyses of primary cortical neurons treated for 5 days with 500 ng/mL of GST, GST-Nrg1, GST-Nrg2, or GST-Nrg3 reveal no significant differences between any groups in the average length of neurites (**panels A and A'' for all data points**), average length of the longest neurite (**panels B and B'' for all data points**), average length of neurites excluding the longest (**panels C and C'' for all data points**), and average number of neurites (**panel D**) in ErbB4 (-)/ β -tubulin(+) cells. **Panel E.** Neurons were further characterized into four groups according to the number of neurites present: ≤ 3 neurites, 4 neurites, 5 neurites, and >5 neurites. No significant differences were observed between the GST and GST-Nrg1-3 conditions in any groups. Bars represent the average \pm SEM; n = a total of 3 independent experiments (25 cells/experiment for each condition); p = >0.05

Fig. 4.8

ErbB4 (-) / GABA (+) Neurons, 5 Day Treatment:

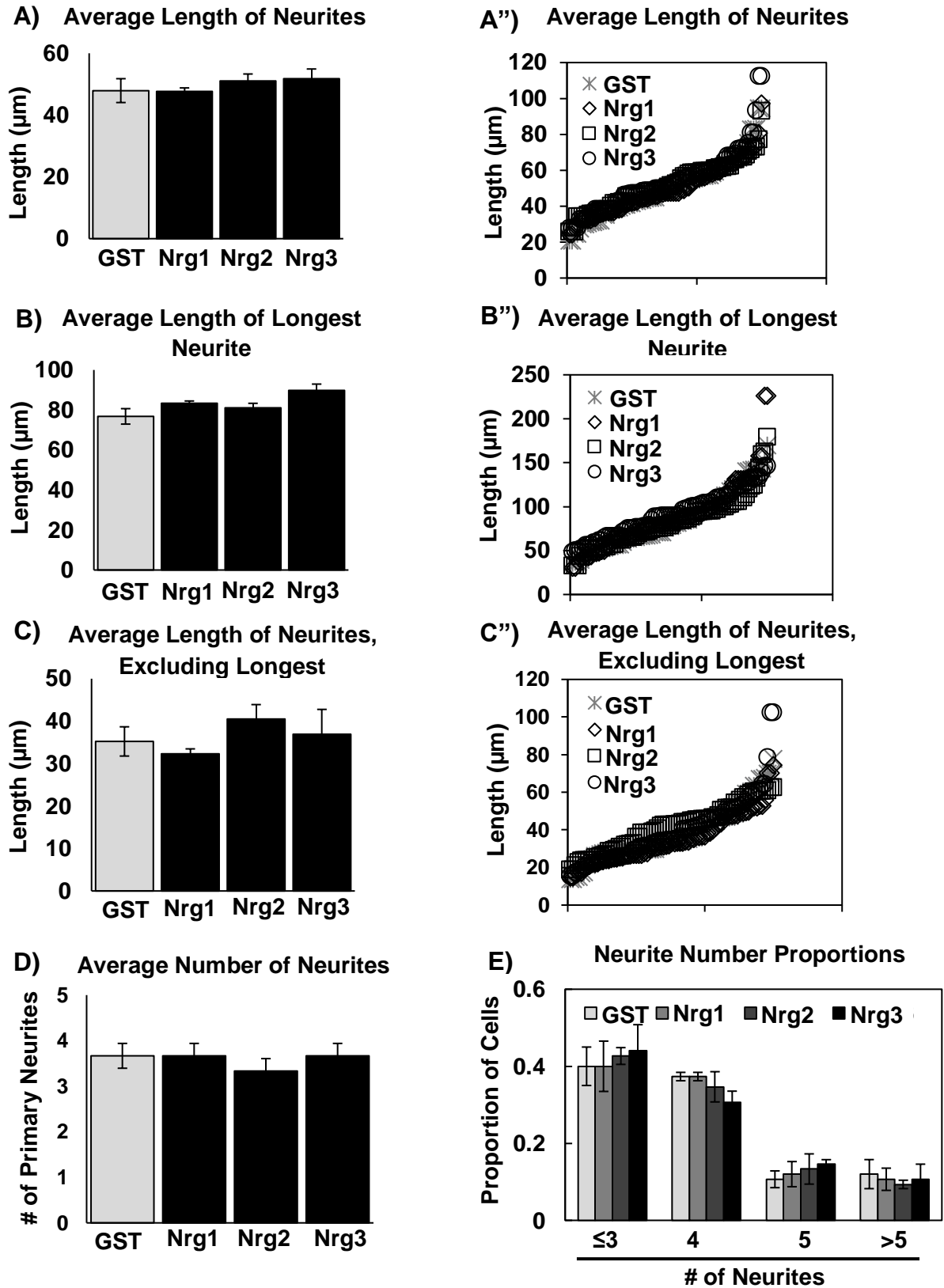


Fig. 4.8: GST-Nrg1-3 Factors do not Enhance Neurite Outgrowth of ErbB4(-)/GABA(+) Cortical Neurons Following 5 Days of Treatment.

Morphometric analyses of primary cortical neurons treated for 5 days with 500 ng/mL of GST, GST-Nrg1, GST-Nrg2, or GST-Nrg3 reveal no significant differences between any groups in the average length of neurites (**panels A and A'' for all data points**), average length of the longest neurite (**panels B and B'' for all data points**), average length of neurites excluding the longest (**panels C and C'' for all data points**), and average number of neurites (**panel D**) in ErbB4 (-)/GABA(+) cells. **Panel E.** Neurons were further characterized into four groups according to the number of neurites present: ≤ 3 neurites, 4 neurites, 5 neurites, and >5 neurites. No significant differences were observed between the GST and GST-Nrg1-3 conditions in any groups. Bars represent the average \pm SEM; n = a total of 3 independent experiments (25 cells/experiment for each condition); p = >0.05

4.2.7 Overexpression of ErbB4 Enhances Neurite Outgrowth in GABAergic Interneurons

We next determined whether the overexpression of ErbB4 in GABAergic interneurons would enhance neurite outgrowth in both the presence and absence of the Nrgs (Table 4.2). For these experiments, we transfected primary cortical cultures at 2 DIV with the EGFP-N1 only (vector control) or ErbB4/mCherry and then treated with GST or GST-Nrg factors for 3 days prior to GABA immunostaining.

As shown in Fig. 4.9A and A", overexpression of ErbB4 resulted in an increase in the average length of all neurites in the samples treated with GST only and the Nrgs. The neurite outgrowth in the ErbB4 overexpressing cells treated with GST was 138% and 42% higher than that observed for the control vector treated with either GST or Nrg1, respectively. This indicates that overexpression of ErbB4 is sufficient for neurite outgrowth and surpasses the effects driven by endogenous expression of ErbB4, even under conditions of Nrg1 activation (GST vector control, average length: $51.60 \pm 0.57 \mu\text{m}$; GST-Nrg1 vector control, average length: $86.83 \pm 1.70 \mu\text{m}$; GST control, average length: $123.22 \pm 3.21 \mu\text{m}$; Fig. 4.9A and A"). We further observed (Fig. 4.9A and A") that in the ErbB4/mCherry overexpressing interneurons, the addition of GST-Nrgs could further enhance the average length of all neurites by 46-66% compared to the GST control (baseline considered 100% for GST control, 46% increase for GST-Nrg1 with an average length of $179.72 \pm 10.78 \mu\text{m}$, 66% increase for GST-Nrg2 with an average length of $204.02 \pm 1.31 \mu\text{m}$, and 49% increase for GST-Nrg3 with an average length of $183.62 \pm 7.31 \mu\text{m}$; Fig. 4.9A and A"). Differences in average length of neurites between GST-Nrg1, GST-Nrg2, and GST-Nrg3 conditions were not statistically significant (Fig. 4.9A and A"). These data suggest that ErbB4 overexpression is sufficient to enhance neurite outgrowth, which can be further increased by Nrg treatment.

We also measured the length of the longest neurite (the axon; Fig. 4.9B and B'') and the average length of all neurites excluding the axon (Fig. 4.9C and C''). As shown in Fig. 4.9B and B'', overexpression of ErbB4, even without the treatment of the Nrgs (GST condition), resulted in a substantial increase in the average length of the longest neurite compared to vector control transfected neurons. The vector control condition treated with GST-Nrg1, expressing endogenous levels of ErbB4, showed an increase of 89.53% in the average length of the longest neurite ($163.25 \pm 4.98 \mu\text{m}$) compared to the vector control condition treated with GST ($86.01 \pm 5.05 \mu\text{m}$; Fig. 4.9B and B''), as also previously shown in Fig. 4.3B and B'' for the untransfected cultures. The ErbB4/mCherry overexpressing GABA (+) interneurons that were cultured with GST-Nrg1, GST-Nrg2, and GST-Nrg3 showed an increase ranging from 92-100% in the average length of the longest neurite compared to the GST control overexpressing ErbB4 (baseline considered 100% for GST control with an average length of $291.31 \pm 8.37 \mu\text{m}$, 99% increase for GST-Nrg1 with an average length of $579.07 \pm 16.84 \mu\text{m}$, 92% increase for GST-Nrg2 with an average length of $559.93 \pm 3.55 \mu\text{m}$, and 100% increase for Nrg3 with an average length of $583.47 \pm 11.11 \mu\text{m}$; Fig. 4.9B and B''). Differences in the average length of the longest neurite between the GST-Nrg1, GST-Nrg2, and GST-Nrg3 conditions were not statistically significant (Fig. 4.9B and B'').

We then compared the average length of neurites excluding the longest one (the axon). As shown in Fig. 4.9C and C'', there were no significant differences in the average length of neurites excluding the longest between the ErbB4/mCherry (+) neurons compared to the vector controls treated with either GST or GST-Nrg1. Furthermore, the average length of neurites excluding the longest between the GST and GST-Nrg1 treated vector controls were also not statistically significant (GST vector control, average length: $40.02 \pm 2.22 \mu\text{m}$; GST-Nrg1 vector control, average length: $45.21 \pm 5.49 \mu\text{m}$; GST control, average length: $62.19 \pm 3.12 \mu\text{m}$; GST-Nrg1, average length: $69.58 \pm 7.38 \mu\text{m}$; GST-Nrg2, average length: $74.69 \pm 10.01 \mu\text{m}$; and

GST-Nrg3, average length: $80.25 \pm 10.21 \mu\text{m}$; Fig 4.9C and C"). Similar to our data observed in our untransfected cultures treated for 5 days expressing endogenous levels of ErbB4 (Fig. 4.3C and C"), we observed no significant differences between the GST and GST-Nrg conditions when analyzing the ErbB4/mCherry overexpressing GABA (+) interneurons (Fig. 4.9C and C"). Overall, these data suggest that ErbB4 plays a role in axonal elongation, which can be further enhanced with Nrg-activation.

We further quantified the average number of neurites per cell for each condition and further broke down the analyses into proportions of cells expressing 3 or fewer neurites, 4 neurites, 5 neurites, or more than 5 neurites. As shown in Fig. 4.9D, cells overexpressing ErbB4 and treated with GST (3.90 ± 0.16 neurites) did not show a significant increase in the overall average number of primary neurites compared to the GST treated vector control (3.33 ± 0.14 neurites). The vector control condition treated with GST-Nrg1, expressing endogenous levels of ErbB4, showed an increase (4.83 ± 0.14 neurites) in the number of primary neurites compared to both GST treated vector (3.33 ± 0.14 neurites) and GST treated ErbB4/mCherry cells (3.90 ± 0.16 neurites). Furthermore, GST-Nrg1 and GST-Nrg3, but not GST-Nrg2, treatments of the ErbB4/mCherry overexpressing interneurons (Fig. 4.9D) showed an overall average increase in the number of primary neurites ranging from 4.9-5.1 neurites compared to the 3.9 neurites observed for the GST treated ErbB4/mCherry neurons (GST control average: 3.90 ± 0.16 neurites; GST-Nrg1 average: 4.93 ± 0.14 neurites; GST-Nrg2 average: 4.67 ± 0.17 neurites; GST-Nrg3 average: 5.10 ± 0.12 neurites; Fig. 4.9D). Differences in the number of primary neurites between the GST-Nrg conditions were not significant (Fig. 4.9D).

We also determined the effect of ErbB4 and the treatment with the Nrgs or GST on the proportion of cells displaying 3 or fewer neurites, 4 neurites, 5 neurites, or more than 5 neurites. As shown in Fig. 4.9E, mCherry/ErbB4 cells treated with GST (36%) did not show a statistically significant difference in the proportion of cells displaying 3 or fewer neurites compared to the

GST treated vector control (52%). The GST treated vector control condition (52%), however, did show a larger proportion of cells with 3 or fewer neurites compared to the GST-Nrg1 vector control condition (22%) and the GST-Nrg treated mCherry/ErbB4 cells (16-21%) (GST vector control average: $51.67 \pm 1.36\%$; GST-Nrg1 vector control average: $21.67 \pm 3.60\%$; GST average: $36.0 \pm 6.55\%$; GST-Nrg1 average: $16.33 \pm 2.68\%$; GST-Nrg2 average: $21.33 \pm 1.36\%$; GST-Nrg3 average: $15.67 \pm 2.84\%$; Fig. 4.9E). There were no statistical differences observed for the proportion of cells displaying 3 or fewer neurites between the GST-Nrg conditions (Fig. 4.9E).

We further observed that the GST treated vector control (12%), the GST-Nrg1 treated vector control (23%), and the GST treated mCherry/ErbB4 conditions (11%) did not show a significant difference in the proportion of cells displaying more than five neurites. However, in the GST-Nrg treated ErbB4/mCherry cells (ranging from 31-42%), neurons with more than five neurites were more prevalent than in the GST treated ErbB4/mCherry cells (11%) and the GST vector control (12%) (GST vector control average: $11.67 \pm 1.36\%$; GST-Nrg1 vector control average: $23.33 \pm 1.36\%$; GST average: $11.0 \pm 1.70\%$; GST-Nrg1 average: $37.66 \pm 2.60\%$; GST-Nrg2 average: $31.0 \pm 3.40\%$; GST-Nrg3 average: $42.33 \pm 2.60\%$; Fig. 4.9E). ErbB4/mCherry (+) neurons treated with GST-Nrg1 (38%) and GST-Nrg3 (42%), but not GST-Nrg2 (31%), also displayed a higher proportion of cells with more than five neurites compared to the GST-Nrg1 treated vector control condition (Fig. 4.9E). There were no significant differences between the GST-Nrg conditions in these morphological analyses (Fig. 4.9E). We also did not observe any statistically significant differences between any of the groups (including controls) when analyzing the proportions of cells displaying 4 neurites or 5 neurites (Fig. 4.9E). Overall, our morphometric analyses show that Nrg1 and Nrg3 can enhance the number of neurites in cells overexpressing ErbB4, compared to GST; however, these effects are not different from Nrg1 treatment of cells endogenously expressing ErbB4.

Fig. 4.9

ErbB4 Overexpression / GABA (+) Neurons, 5 Day Treatment:

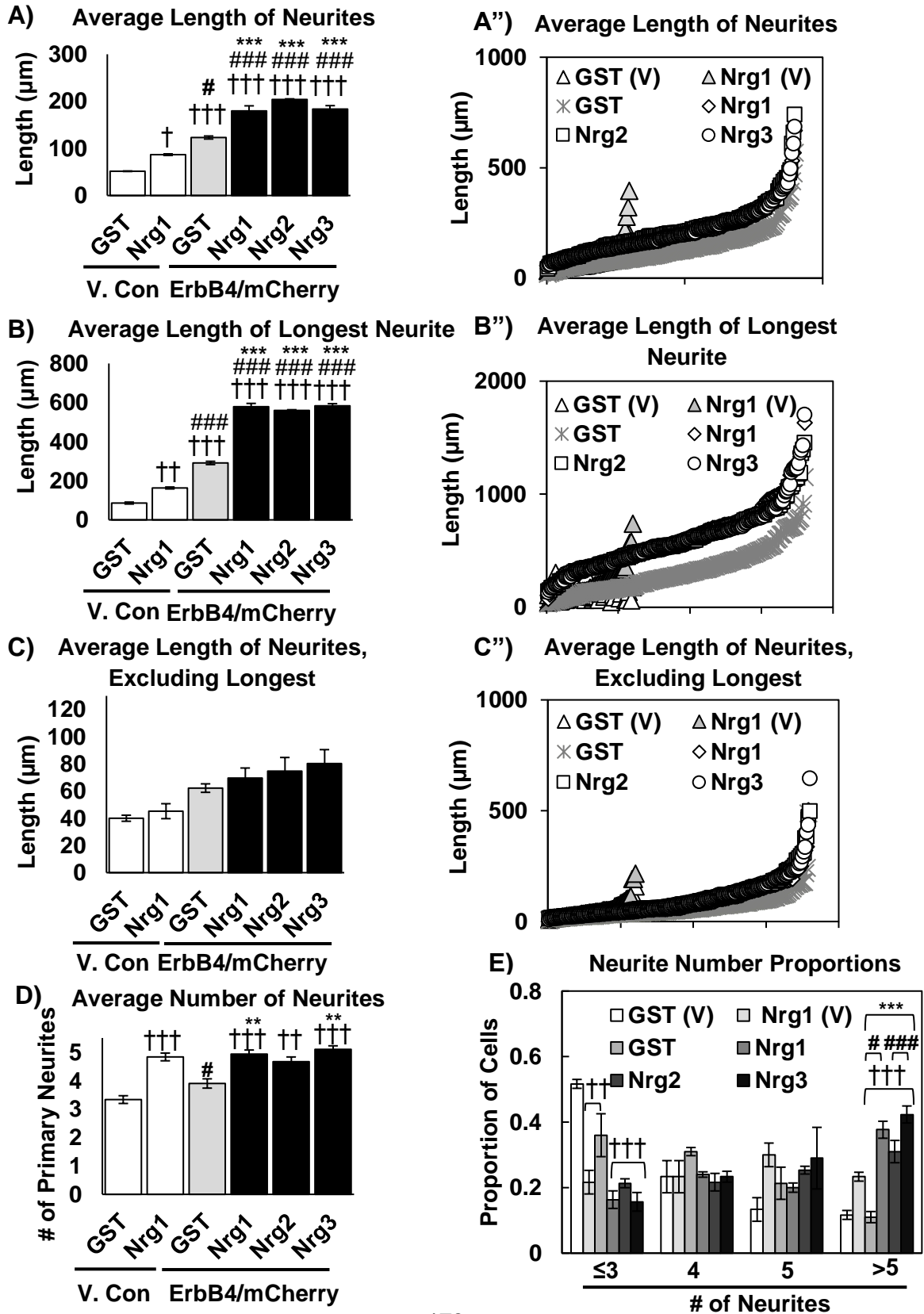


Fig. 4.9: Overexpression of ErbB4 Enhances Neurite Outgrowth in GABAergic Interneurons.

Primary cortical cultures (2 DIV) were transfected with EGFP-N1 vector (V) control or mCherry co-transfected with ErbB4 (ErbB4/mCherry). Cells were then treated for 3 days with 500 ng/mL of GST, GST-Nrg1, GST-Nrg2, or GST-Nrg3. **Panels A and A'' for all data points.** GABAergic neurons overexpressing ErbB4/mCherry had significantly greater average lengths of primary neurites compared to neurons transfected with the V control. V control cells that were treated with GST-Nrg1 showed enhanced average lengths of primary neurites compared to V control cells treated with GST only. ErbB4/mCherry overexpression in conjunction with treatment with the GST-Nrg1-3 factors further enhanced the average lengths of primary neurites compared to those treated with GST only. **Panels B and B'' for all data points.** GABAergic neurons overexpressing ErbB4/mCherry had significantly greater average lengths of the longest neurite (axon) compared to neurons transfected with the V control. V control cells that were treated with GST-Nrg1 showed enhanced average length of the longest neurite compared to V control cells treated with GST only. ErbB4/mCherry overexpression in conjunction with treatment with GST-Nrg1-3 further enhanced the average length of the longest neurite compared to those treated with GST alone. **Panels C and C'' for all data points.** GABAergic neurons overexpressing ErbB4/mCherry were not statistically different compared to neurons transfected with V control when measuring the length of neurites excluding the longest one. The addition of GST-Nrgs did not affect this parameter either. **Panel D.** ErbB4/mCherry overexpressing cells treated with the GST-Nrgs and V control cells treated with GST-Nrg1 showed significantly greater numbers of neurites compared to V control cells treated with GST. ErbB4/mCherry overexpressing cells treated with GST-Nrg1 and GST-Nrg3 and V control cells treated with GST-Nrg1 showed significantly greater number of neurites compared to ErbB4/mCherry overexpressing cells treated with GST. **Panel E.** Neurons were further characterized into four groups according to the

number of neurites present: ≤ 3 neurites, 4 neurites, 5 neurites, and >5 neurites. GABAergic neurons that were transfected with V control and treated with GST showed higher proportion of cells that expressed ≤ 3 neurites compared to V control cells treated with GST-Nrg1 and ErbB4/mCherry overexpressing cells treated with the GST-Nrgs. ErbB4/mCherry overexpressing cells treated with the GST-Nrg factors showed higher proportion of cells that expressed >5 neurites compared to those treated with GST only and also those transfected with V control and then treated with GST. ErbB4/mCherry overexpressing neurons treated with GST-Nrg1 and GST-Nrg3 showed higher proportion of cells that expressed >5 neurites compared to cells transfected with V control and then treated with GST-Nrg1. Bars represent the average \pm SEM; n = a total of 3 independent experiments (75 cells/experiment for GST, GST-Nrg1, GST-Nrg2, and GST-Nrg3 conditions; 25 cells/experiment for V control conditions); †, comparison to GST treated V control (†p = <0.05 , ††p = <0.01 , †††p = <0.001); #, comparison to GST-Nrg1 V control (#p = <0.05 , ###p = <0.001); *, comparison to GST condition (**p = <0.01 , ***p = <0.001)

Table 4.2

Table 4.2 Neurite Outgrowth Measures in EGFP-N1 or ErbB4 Overexpressing Neurons Following GST or GST-Nrg Treatment for 3 Days					
Average Length of Neurites (in μm)					
V Con. G	V Con. N1	GST	Nrg1	Nrg2	Nrg3
51.6 \pm 0.6	86.8 \pm 1.7	123.2 \pm 3.2	179.2 \pm 10.8	204.0 \pm 1.3	183.6 \pm 7.3
Average Length of the Longest Neurite (in μm)					
V Con. G	V Con. Nrg1	GST	Nrg1	Nrg2	Nrg3
86.0 \pm 5.1	163.2 \pm 4.9	291.3 \pm 8.4	579.1 \pm 16.8	559.9 \pm 3.6	583.4 \pm 11.1
Average Length of Neurites, Excluding Longest (in μm)					
V Con. G	V Con. Nrg1	GST	Nrg1	Nrg2	Nrg3
40.0 \pm 2.2	45.2 \pm 5.5	62.1 \pm 3.1	69.6 \pm 7.4	74.7 \pm 10.0	80.2 \pm 10.2
No. of Primary Neurites					
V Con. G	V Con. Nrg1	GST	Nrg1	Nrg2	Nrg3
3.3 \pm 0.1	4.8 \pm 0.1	3.9 \pm 0.2	4.9 \pm 0.1	4.7 \pm 0.3	5.1 \pm 0.1

Table 4.2: Neurite Outgrowth Measures in EGFP-N1 or ErbB4 Overexpressing Neurons Following GST or GST-Nrg Treatment for 3 Days.

Shown here is a chart comparing the average length of neurites, average length of the longest neurite, average length of neurites excluding the longest (axon), and number of primary neurites of cortical neurons transfected with EGFP-N1 (vector control) or ErbB4-N1 at 2 DIV followed by treatment with GST, GST-Nrg1, GST-Nrg2, or GST-Nrg3 for 3 days. Data is presented as the average \pm SEM.

4.3 DISCUSSION:

In this study we have characterized the effects of three Nrgs (Nrgs 1, 2 and 3) on early neurite outgrowth of cortical GABAergic interneurons. Using dissociated cortical neurons, our studies revealed that treatment at early developmental stages (0-5 DIV) with GST-Nrgs 1, 2, and 3 had significant effects on the growth of neurites in GABAergic interneurons, including axonal elongation. Addition of Nrgs1-3 to the cultures from 0-2 DIV increased the length of all neurites, including the axon, as well as increased the average number of neurites per neuron and the proportion of neurons with 3 or more neurites. In cultures treated with Nrgs for 5 days (0-5 DIV), we observed growth mainly of the axons, with the other neurites displaying neurite lengths that were comparable to our observations after 2 days of treatment. We also observed that the average number of neurites were higher in the Nrg treated neurons after 5 days of treatment and that the proportion of cells with 5 or more neurites was more prominent in these cultures. We detected the presence of ErbB4 on all neurites, including the axon, at early stages (2 and 5 DIV). While ErbB4 expression was reduced and eventually eliminated from the axon, it remained present in the rest of the neurites and cell body. We did not observe any neurite outgrowth effects in cells that were GABA (+)/ErbB4 (-), suggesting that these outgrowth effects were limited to neurons expressing ErbB4. Neurite outgrowth was also enhanced in neurons overexpressing ErbB4 in the absence of added Nrgs. This effect was further enhanced by addition of Nrgs to the cultures. These results, collectively, indicate that Nrg1-3 have a potent effect in the enhancement of neurite elongation and enhance neurite number of GABAergic interneurons, which is likely being mediated by its receptor ErbB4.

Prior immunohistochemical studies in rodents and primates (Garcia, Vasudevan, & Buonanno, 2000; K M Gerecke, Wyss, Karavanova, Buonanno, & Carroll, 2001; Y. Z. Huang et al., 2000; M Longart, Chatani-Hinze, Gonzalez, Vullhorst, & Buonanno, 2007; Yau et al., 2003) and *in situ* hybridization studies in rodents (Fox & Kornblum, 2005; K M Gerecke et al., 2001; Y.

Z. Huang et al., 2000; C Lai & Lemke, 1991; Steiner, Blum, Kitai, & Fedi, 1999; Thompson et al., 2007) have indicated that ErbB4 is primarily expressed in GABAergic interneurons. Consistent with those observations, immunocytochemical analyses in our cortical cultures (Fig. 4.1A-F) showed that ErbB4 was expressed only in GABAergic interneurons (Fig. 4.1H). We also determined that, in our cultures, ErbB4 was expressed in approximately $84.61 \pm 6.27\%$ of GABAergic neurons (Fig. 4.1H), of which the vast majority were PV (+) interneurons (Fig. 4.1H and I). Our findings, in conjunction with the previous reports described above, influenced our emphasis on studying the effects of the Nrgs on the differentiation of ErbB4/GABA interneurons and also support the biological relevance of our *in vitro* system.

Our findings in this chapter provide evidence of the roles of the Nrgs in the differentiation of cortical interneurons, a field that has been understudied. Prior experiments in dissociated and organotypic cultures have identified brain derived neurotrophic factor (BDNF) as a growth factor that can affect the maturation of GABAergic neurons from several different origins, including the hippocampus, cerebellum, and cortex (Jin et al., 2003; Pozas & Ibáñez, 2005). Since BDNF has been well-studied in the context of interneuron differentiation, including neurite outgrowth, it will be important to determine whether the Nrgs act synergistically or in a redundant fashion to BDNF. Another possibility could be that BDNF and the Nrgs act on different neuronal populations, creating the necessity for future experiments that compare and contrast the effects of these factors in the differentiation of interneurons in diverse neuronal populations. Furthermore, similar to depolarization-dependent BDNF release which regulates dendritic maturation in cortical interneurons (Jin et al., 2003), it would be interesting to determine whether neuronal activity has the ability to facilitate Nrg-dependent GABAergic maturation. This hypothesis is particularly attractive as Nrgs have been reported to be proteolytically released in response to neuronal activity (Ozaki, Itoh, Miyakawa, Kishida, & Hashikawa, 2004; Vullhorst et al., 2015).

Although the enhancement of a number of neurite outgrowth parameters by Nrg1 have been reported in several neuronal populations, such as neurons of the rodent retina, hippocampus, cerebral cortex, midbrain, spinal cord, and cerebellum (Anton et al., 1997; Audisio et al., 2012; Bermingham-McDonogh et al., 1996; M E Cahill et al., 2012; Y. Chen et al., 2010; Kimberly M Gerecke et al., 2004; Krivosheya et al., 2008; Mòdol-Caballero et al., 2017; Rieff et al., 1999; R. Xu et al., 2013; L. Zhang et al., 2004; Q. Zhang et al., 2017, 2016), the majority of these studies did not use markers to identify the ErbB4-expressing neurons. Our findings greatly expand on these previous studies that analyzed the roles of Nrg1 in neurite outgrowth of cortical neurons, as we demonstrated neurite outgrowth effects of the Nrgs specifically in ErbB4/GABA (+) interneurons (Figs. 4.2 and 4.3), and also compared them to neurons that were ErbB4 (-) (Figs. 4.6-4.8). Our findings also allowed us to compare the neurite outgrowth effects of three different Nrgs (1, 2, and 3), which has not previously been done, and showed that all Nrgs had similar effects on neurite outgrowth in GABAergic neurons *in vitro*. These analyses also demonstrated novel biological roles of Nrg2 and Nrg3, whose roles in the CNS are less understood than Nrg1. There are no prior reports for Nrg3 on neurite outgrowth and only a single report on the effects of Nrg2 on neurite outgrowth and neuronal survival of hippocampal neurons *in vitro*. In that study, however, the identity of the affected cells were not reported (Nakano et al., 2016).

While our findings showed evidence of enhanced neurite length after treatment with the GST-Nrgs for both 2 and 5 days (Fig. 4.2 and 4.3 respectively), the dendritic lengths were comparable between our earlier (2 days) and later (5 days) time points. Interestingly, after 5 days of treatment, the GST-Nrgs enhanced axonal length but not the length of the other neurites (Fig. 4.3A-C and A"-C" and Fig. 4.4). This finding differed from our observations after 2 days of treatment where the GST-Nrgs enhanced the length of all neurites (Fig. 4.2A-C and A"-C"). These findings demonstrated that the GST-Nrgs can accelerate neurite outgrowth but do not

significantly exceed the total length observed with control GST at 5 DIV (Table 4.1). One exception is the growth of the axon, which continues to elongate in response to GST-Nrg treatment at the latest time point that we examined (5 days; Table 4.1). Our findings that the GST-Nrgs enhance axonal elongation in ErbB4 (+) cortical GABAergic interneurons are consistent with previous reports in cultured rat mesencephalic neurons and rat primary sensory neurons (Audisio et al., 2012; L. Zhang et al., 2004). Zhang et al (2004) previously reported that a 9 day treatment of GGF2/Nrg1 in rat primary midbrain cultures, derived from E14 rat ventral mesencephalon, significantly increased the length of the longest neurite and the total number of neurites in TH (+) cells, compared to controls (L. Zhang et al., 2004). Another study done by Audisio et al. (2012) showed that dissociated rat dorsal root ganglion (DRG) cells cultured with Nrg1 for 3 days (3 DIV) showed an increase in the length of the longest neurite (axon), neurite area, and proportion of neurons sprouting neurites. However, unlike our findings showing that GST-Nrg treatment enhanced the number of primary neurites (Fig. 4.2D and E; Fig. 4.3D and E), treatment of DRG neurons with Nrg1 did not enhance the number of neurites (Audisio et al., 2012). This suggests differing roles for the Nrgs or perhaps the preferential activation of specific ErbB dimers in different neuronal populations.

Our findings that GST-Nrg treatment enhances axonal elongation is particularly interesting, as it has previously been reported that the Nrg receptor ErbB4 is highly expressed throughout dendritic branches and spines, but is mainly absent from the axons of cortical and hippocampal interneurons (Mechawar, Lacoste, Yu, Srivastava, & Quirion, 2007; Vullhorst et al., 2009). Our findings (Fig. 4.5) revealed that ErbB4 is in fact expressed in the axon of cortical interneurons but only at early developmental stages, including 2 and 5 DIV, consistent with the our observations on the effects caused by the Nrgs on axonal elongation. We also detected a progressive reduction in axonal ErbB4 expression, being undetectable by 21 DIV (Fig. 4.5P-R). The absence of ErbB4 in the axon in mature GABAergic neurons is consistent with previous

reports (Mechawar et al., 2007; Vullhorst et al., 2009). In contrast to its axonal expression, ErbB4 continued to be highly expressed in the dendrites at all developmental stages examined (Fig. 4.5). Our findings of ErbB4 expression and localization in the axons of GABAergic interneurons represents a significant contribution to the field, since prior studies focused on hippocampal interneurons at 8 DIV and mature cortical interneurons at 28 DIV which, like our studies, indicated that ErbB4 was not present in the axon. The conclusions from prior studies that state that Nrg1-ErbB4 ligand-receptor pairs play a role in dendritic outgrowth and development but not in axonal elongation (M E Cahill et al., 2012; Krivosheya et al., 2008) need to be revisited based on our observations of dynamic ErbB4 expression in the axon.

Our findings showing that overexpression of ErbB4 is sufficient to promote neurite outgrowth, even in the absence of Nrg treatment, is consistent with overexpression-induced ligand independent activation. There is substantial evidence of ligand-independent activation of overexpressed receptor tyrosine kinases (RTKs), especially within their roles in tumorigenesis (Appert-Collin et al., 2015; Guo et al., 2015; Kolibaba & Druker, 1997; Roskoski, 2004). Among the ErbB receptors, EGFR/ErbB1 and ErbB2 are well-characterized oncogenes that are overexpressed in several types of human cancers, including breast and ovarian cancers, and can engage in ligand-independent dimerization and activation (Adelsman, Huntley, & Maihle, 1996; Brennan, Kumogai, Berezov, Murali, & Greene, 2000; Mishra, Hanker, & Garrett, 2017; Stern, 2008; Z. Wang, 2017). Several studies have also reported the overexpression of ErbB4 in breast and ovarian cancers and the ligand-independent activation of overexpressing ErbB4 (JM-a CYT-2) in breast cancer cells (Hollmén & Elenius, 2010; Määttä et al., 2006; Z. Wang, 2017). Taking this into account, it is possible that our observations of neurite outgrowth in cells overexpressing ErbB4/mCherry (Fig. 4.9) are partly due to ligand-independent activation of ErbB4. However, it is also possible that the overexpression of ErbB4 resulted in a greater number of available receptors that could be activated by Nrg secreted or produced

endogenously within our cultures. This hypothesis is consistent with our observations (Fig. 4.9) that the addition of GST-Nrgs could further enhance the neurite outgrowth of ErbB4/mCherry expressing cells.

Although ErbB4 overexpression, in the absence of GST-Nrg treatment (GST condition), resulted in an increase in axonal length (Fig. 4.9B and B”), ErbB4 overexpression was not sufficient to cause an increase in the number of primary neurites (Fig. 4.9D). The addition of the Nrg factors, however, in both ErbB4/mCherry cells and vector control cells did increase the number of neurites compared to our GST controls (Fig. 4.9D). Our findings are consistent with a previous report in cultured hippocampal cells, showing that the overexpression of ErbB4-HA was not sufficient to enhance the number of primary neurites, compared to the GFP-transfected control. However, prolonged Nrg1 treatment in the ErbB4-HA overexpressing cells increased neurite number, an effect that was not observed in the GFP-transfected control cells (Krivosheya et al., 2008). These findings, in conjunction with our results in Fig. 4.9D, suggest that Nrg activation of ErbB4 is necessary for the enhancement of the number of neurites. It is possible that the signaling events initiated by ErbB4 overexpression may not have been sufficient to drive neurite initiation, and that either additional or more prolonged signaling events triggered by Nrg activation are required for an increase in neurite numbers. Further studies are necessary to determine if the molecular mechanisms driving neurite number are independent than those set in motion for neurite elongation.

Our studies in dissociated neurons provided several benefits that are challenging to accomplish with *in vivo* studies. They allowed us to directly compare the neurite outgrowth effects of 3 different Nrgs under controlled media and growth conditions, as well as allowing the overexpression of ErbB4 in these cells. In spite of these advantages, however, there are significant limitations of our studies since they were performed *in vitro*. In such a system, the circuitry is perturbed and also the cell density and cell-to-cell interactions may not replicate

those present *in vivo*. Furthermore, alterations of the growth conditions imposed by the tissue culture media, as well as the cell density and composition may have caused a loss of complexity or introduced variables that may differ from the effects of Nrg mediated neurite outgrowth of GABAergic neurons that would have been obtained *in vivo*. Future experiments using neurons derived from ErbB4 knockout and wild type animals should be performed to compare the expression of ErbB4 on different types of GABAergic interneurons and to determine the impact of the loss of ErbB4 on the morphology of these specific sub-types of GABAergic cells. An aspect that would be important for these experiments would be timing at which these studies are performed, as we have reported a previously unrecognized expression of ErbB4 in the axon at early developmental stages (Fig. 4.5). In addition, studies further exploring the impact of the Nrgs on other aspects of GABAergic interneuron differentiation were not explored. As prior studies analyzing the effect of Ig-Nrg1 in dissociated cerebellar granule neurons resulted not only in an increase of neurite outgrowth but also in the expression of GABA receptor subunits and GABA receptors (Rieff et al., 1999), it would be of interest to analyze the impact of the Nrgs on these aspects of differentiation in cortical GABAergic neurons.

Taken together, our findings show that all three Nrgs can accelerate neurite outgrowth and the elongation of axons of GABAergic interneurons *in vitro*, most likely being mediated by ErbB4. These findings identify novel biological roles for Nrg2 and Nrg3 and improve our understanding of Nrg-ErbB4 signaling in cortical interneuron differentiation.

Chapter 5: Activation-Dependent Association of ErbB4 with Members of the Par Polarity Complex

5. 1 INTRODUCTION:

Neurons are highly polarized cells that asymmetrically partition their structural components, giving rise to multiple dendrites and one axon that are functionally and molecularly distinct (Banker, 2018; Craig, Jareb, & Banker, 1992; Dotti et al., 1988; Goslin & Banker, 1989; Hansen, Duellberg, Mieck, Loose, & Hippenmeyer, 2017; Kon, Cossard, & Jossin, 2017; Laumonnerie & Solecki, 2018; Yogev & Shen, 2017). The establishment of neuronal polarity is pivotal for the morphogenesis of the brain and the development of functional circuitry. Neuronal polarity underlies several hallmark events essential for the establishment of neuronal circuits, including axonal specification, axonal pathfinding, neuronal migration, and the generation and elongation of axons and dendrites (Hansen et al., 2017; Kon et al., 2017; Laumonnerie & Solecki, 2018; Yogev & Shen, 2017). An important regulator of neuronal polarity is the Par polarity complex, consisting of the proteins Par6, Par3, aPKC, and Cdc42/Rac1. In the developing CNS, members of the Par complex have been shown to be important in specifying the apical polarity of radial glial cells, the initiation of axonal specification, and the regulation of neuronal migration (Arimura & Kaibuchi, 2005; Bultje et al., 2009; Cappello et al., 2006; L. Chen et al., 2006; Chou et al., 2018; Costa et al., 2008; Ghosh et al., 2008; Hapak, Rothlin, et al., 2018; Takashi Nishimura et al., 2005; Solecki et al., 2006; Yokota et al., 2010). In addition, members of the Par complex also play roles in dendritic maturation through the formation and maintenance of dendritic spines (H. Zhang & Macara, 2006, 2008). In this Chapter, we show that ErbB4 associates with members of the Par polarity complex, and furthermore, that activation by Nrg1-3 enhances their association in N2a cells and primary cortical neurons. These findings represent the first description of links between ErbB4 signaling and the Par polarity complex.

A series of studies have recognized Nrg1, Nrg3, and ErbB4 as schizophrenia (SZ) susceptibility genes (P.-L. Chen et al., 2009; Mei & Nave, 2014; Norton et al., 2006; Silberberg et al., 2006; Stefansson et al., 2002; Y.-C. Wang et al., 2008), a disorder that has been linked with abnormalities in neuronal polarity, including aberrant patterns of neuronal migration during cortical development and decreased dendritic spine density (Bunney, 2000; Glantz & Lewis, 2000; Glausier & Lewis, 2013; Moyer, Shelton, & Sweet, 2015; Muraki & Tanigaki, 2015). Previous studies have suggested several roles for Nrg-ErbB signaling in events mediating neuronal migration and the establishment and maintenance of the radial glial scaffold (Anton et al., 1997; Louhivuori et al., 2018; Mei & Nave, 2014; Schmid et al., 2003), which are discussed in more detail in the sections below.

Nrg-ErbB signaling in migration. Nrg-ErbB4 signaling has been demonstrated to regulate the migration of developing GABAergic interneurons from their place of birth to their final position in the cerebral cortex (Bartolini et al., 2017; Flames et al., 2004; H. Li et al., 2012). It has previously been reported that ErbB4 is expressed in the medial ganglionic eminence, a birthplace for GABAergic interneurons, as early as E13 in rats. These interneurons migrate into the cerebral cortex and also express ErbB4 (Yau et al., 2003) which appear to be required for the proper migration of these cells. Studies using ErbB4^{-/-} HER^{heart} mice or mice expressing a dominant-negative form of ErbB4 in the medial ganglionic eminence (MGE) show a reduction in the number of GABAergic interneurons that migrate into the rodent cortex (Fisahn et al., 2009; Flames et al., 2004; H. Li et al., 2012). The ErbB4 ligands, Nrg1 and Nrg3, have also been shown to regulate cortical interneuronal migration (Bartolini et al., 2017; Flames et al., 2004; H. Li et al., 2012). Nrg1 Type I can act as a chemoattractant and divert the normal route of migration of ErbB4 (+) migrating interneurons from the MGE (Flames et al., 2004). Similarly, Nrg3 expressed by pyramidal neurons can also attract and guide ErbB4 (+) cortical interneurons into the developing mouse cortical plate (Bartolini et al., 2017). The Nrgs and ErbB4 have also

been shown not only to have attractant roles in cell migration but also to have an opposite effect on migration. Evidence has been presented that Nrg1 Type I, Nrg1 Type III, and Nrg3 can act as repellents for migrating ErbB4 (+) MGE interneurons, creating barriers that define migratory pathways that funnel the GABAergic interneurons to their final destination in the cortex (H. Li et al., 2012).

Nrg-ErbB signaling in the establishment of the radial glial scaffold. In addition to its role in guiding GABAergic interneuron migration, Nrg1 has also previously been shown to aid the migration of excitatory cortical neurons and cerebellar granule neurons along radial glial fibers, as well as regulate the morphology and differentiation of radial glia (Anton et al., 1997; Rio et al., 1997). Radial glial cells are highly polarized cells and are a transient population of cells which differentiate into astrocytes once cortical development is completed. Radial glia have their soma positioned at the ventricular surface with radial fibers reaching upward into the marginal zone. During neurodevelopment, neuroblasts migrate from the germinal layers to their final destination along these radial glial fibers (Chou et al., 2018). Cortical imprint assays have revealed that Nrg1 signaling by ErbB2 promotes the maintenance of radial glia elongation and morphology, as well as enhances the migration of neurons along radial glial fibers (Anton et al., 1997). The downregulation of ErbB2 in radial glia contributes to their transformation into astrocytes (Schmid et al., 2003). Furthermore, the generation of radial glial cells is severely impaired in Nrg1^{-/-} mice, a phenotype that can be rescued by treatment with exogenous Nrg1 (Schmid et al., 2003). In a recent study by Louhivuori et al (2018), it was reported that Nrg1 treatment of cortical neurospheres resulted in the elongation of radial glial fibers. Blocking ErbB4 in these neurospheres inhibited radial glial process extension which could not be restored by Nrg1 treatment (Louhivuori et al., 2018). These studies suggest that Nrg1 signaling of ErbB2/4 can induce morphological changes which enhance radial glial generation and consequently alter neuronal migration.

The Par polarity complex: Roles in the CNS. The Par polarity complex is a protein complex resulting from interactions between Par6, Par3, aPKC, and Cdc42/Rac1. This complex is a key player in the regulation of cytoskeletal elements which can affect the front-rear polarity of migrating cells, establishment and maintenance of apicobasal polarity in epithelial cells, and neuronal polarity (Etienne-Manneville, 2008; Goldstein & Macara, 2007; Atsushi Suzuki & Ohno, 2006). In neurons, the Par polarity complex is critical for axon specification via the localization of Par complex members at the tip of the future axon (Insolera, Chen, & Shi, 2011; Takashi Nishimura et al., 2004; S.-H. Shi et al., 2003; Wiggin, Fawcett, & Pawson, 2005). As demonstrated for Nrg1-ErbB2/4 signaling, members of the Par complex have also been shown to play a role in the development and maintenance of the radial glial scaffold. In radial glial progenitors, the Par complex localizes to the apical adherens junctions and this assembly is important for regulating asymmetric cell division, extension of radial glial fibers, and the branching of radial glial endfeet (Bultje et al., 2009; Cappello et al., 2006; L. Chen et al., 2006; Costa et al., 2008; Ghosh et al., 2008; Yokota et al., 2010). In addition to their roles in early brain morphogenesis, both Nrg-ErbB signaling and members of the Par polarity complex are required for the formation and maturation of dendritic spines (Barros et al., 2009; Y.-J. J. Chen et al., 2008; Goda & Davis, 2003; Hering & Sheng, 2001; B. Li et al., 2007; Sheng & Hoogenraad, 2007; Yin, Chen, et al., 2013; H. Zhang & Macara, 2006, 2008).

Previous studies have also recognized the Nrg-ErbB signaling network and the Par polarity complex as key players in epithelial polarity, both in mammary morphogenesis and also in mammary malignancies (B. Howard et al., 2005; Kogata et al., 2013; Lelièvre, 2010; Muraoka-Cook et al., 2008; Rejon, Al-Masri, & McCaffrey, 2016; Stern, 2008; Troyer & Lee, 2001; Wiesen, Young, Werb, & Cunha, 1999). In epithelial cells of the mammary gland it was previously demonstrated that ErbB2 can associate with two members of the Par complex, Par6-aPKC ϵ , (Aranda et al., 2006). ErbB2 overexpression and activation in breast epithelial cells

resulted in ErbB2 association with Par6-aPKC ζ . This inhibited Par6-aPKC ζ binding to Par3 and also disrupted epithelial polarity (Aranda et al., 2006).

Due to the roles of Nrg-ErbB2/4 signaling in polarity-driven events, the association of members of the Nrg-ErbB4 signaling network to an increased risk of developing SZ, the overlapping biological roles of Nrg-ErbB signaling and the Par polarity complex, and the association of ErbB2 with members of the Par polarity complex, we analyzed whether ErbB4, a binding partner of ErbB2, could also associate with members of the Par complex in the context of the developing cortex. Using biochemical and immunocytochemical techniques, we show a novel Nrg1-3-dependent association between ErbB4 and Par6, Par3, and aPKC ζ , members of the Par polarity complex, in transfected N2a cells and cortical neurons. We also demonstrated that ErbB4 did not directly associate with Cdc42 but ErbB4 did interact with Cdc42 when Par6 was expressed. We further observed that Par6 and ErbB4 co-localize in transfected primary cortical neurons and that activation with Nrg1 resulted in an increase in Par6/ErbB4 (+) puncta. We also conducted preliminary studies to determine the site of ErbB4 and Par6/Par3 interaction and concluded that Par6 and Par3 do not interact with ErbB4 within the last 204 amino acids of the ErbB4 receptor. These results help further our understanding of the molecular mechanisms regulating neuronal polarity and may contribute to the development of therapies for disorders demonstrating aberrant neuronal polarity, such as SZ.

5.2 RESULTS:

In order to begin studies to test the hypothesis that the regulation of neuronal migration, radial glia polarity, or dendritic spine morphogenesis mediated by Nrg/ErbB4 signaling involves the engagement of ErbB4 with members of the Par polarity complex, we first validated and characterized a series of reagents necessary to perform our experiments.

5.2.1 Characterization of ErbB4 and Par Complex cDNA Plasmid Constructs, Antibodies, and GST-Nrg Fusion Proteins

To characterize our reagents which included antibodies for specific immunoblotting detection, antibodies for immunoprecipitation (IP), and cDNA constructs encoding ErbB4 and members of the Par polarity complex for cell transfections, we performed IPs and Western blotting experiments. For these experiments we used untransfected or transfected N2a cells and lysates of cortical cultures (8 DIV) or cortical tissue (P7) as positive controls.

First, we determined the suitability of our ErbB4 antibodies for immunoblotting. As shown in Fig. 5.1A, we detected a band of approximately 185 kDa with anti-ErbB4 serum #616, which recognizes the C-terminus of ErbB4. This can be observed in the lanes corresponding to the N2a/ErbB4 (lane E4), P7 brain lysate (lane Br), and N2a/ErbB4 IP (lane E4^{IP}) samples. The size of the observed band matches that predicted for ErbB4 (Plowman et al., 1993). No bands corresponding to ErbB4, or any additional bands were recognized in the untransfected N2a condition (lane UNT), suggesting the N2a cell line does not endogenously express ErbB4 at the levels detectable by this technique (Fig. 5.1A).

For some of our experiments we used anti-myc tag antibodies to detect constructs expressing the Par6, Par3, and Cdc42 proteins fused to a myc tag. For this we first tested the specificity of our myc-tag antibodies and their ability to IP or immunoblot myc-tagged constructs.

Using N2a untransfected cells and N2a cells transfected with myc-Par6 (as an example of a myc-tagged construct), we detected a band of approximately 37 kDa which corresponds with the predicted size of Par6 (T. J. Hung & Kemphues, 1999) (Fig. 5.1B, lanes corresponding with N2a/myc-Par6 (lane myc) and N2a/myc-Par6 IP (lane myc^{IP} Par6)). No bands were observed in the untransfected condition (lane UNT). These results demonstrate that the myc antibodies were suitable for IP and Western blotting (Fig. 5.1B). Figure 5.1E and F also demonstrate myc-Cdc42 and myc-Par3 anti-myc IPs respectively, providing further evidence of the antibody's specificity to detect myc-tagged constructs.

As shown in Fig. 5.1C, we tested the ability of Par6 antibodies to IP or detect endogenous Par6 expressed in P7 brain lysate (positive control) and myc-Par6 transfected into N2a cells. We observed immunoreactivity of a band approximately 37kDa, a size consistent with that reported for Par6 (Fig. 5.1C, left panel), in lanes corresponding to N2a/myc-Par6 (lane Par6), P7 brain lysate (lane Br), and N2a/myc-Par6 IP (lane Par6^{IP}) samples. At long exposures, endogenous Par6 was not observed in N2a untransfected cells (left panel, lane UNT). However, when we doubled the amount of protein loaded from N2a untransfected lysates, we were able to detect low levels of Par6 (compare Fig. 5.1C, right panel, lane UNT 2X to lane Par6). These results indicate that N2a cells express very low endogenous levels of Par6.

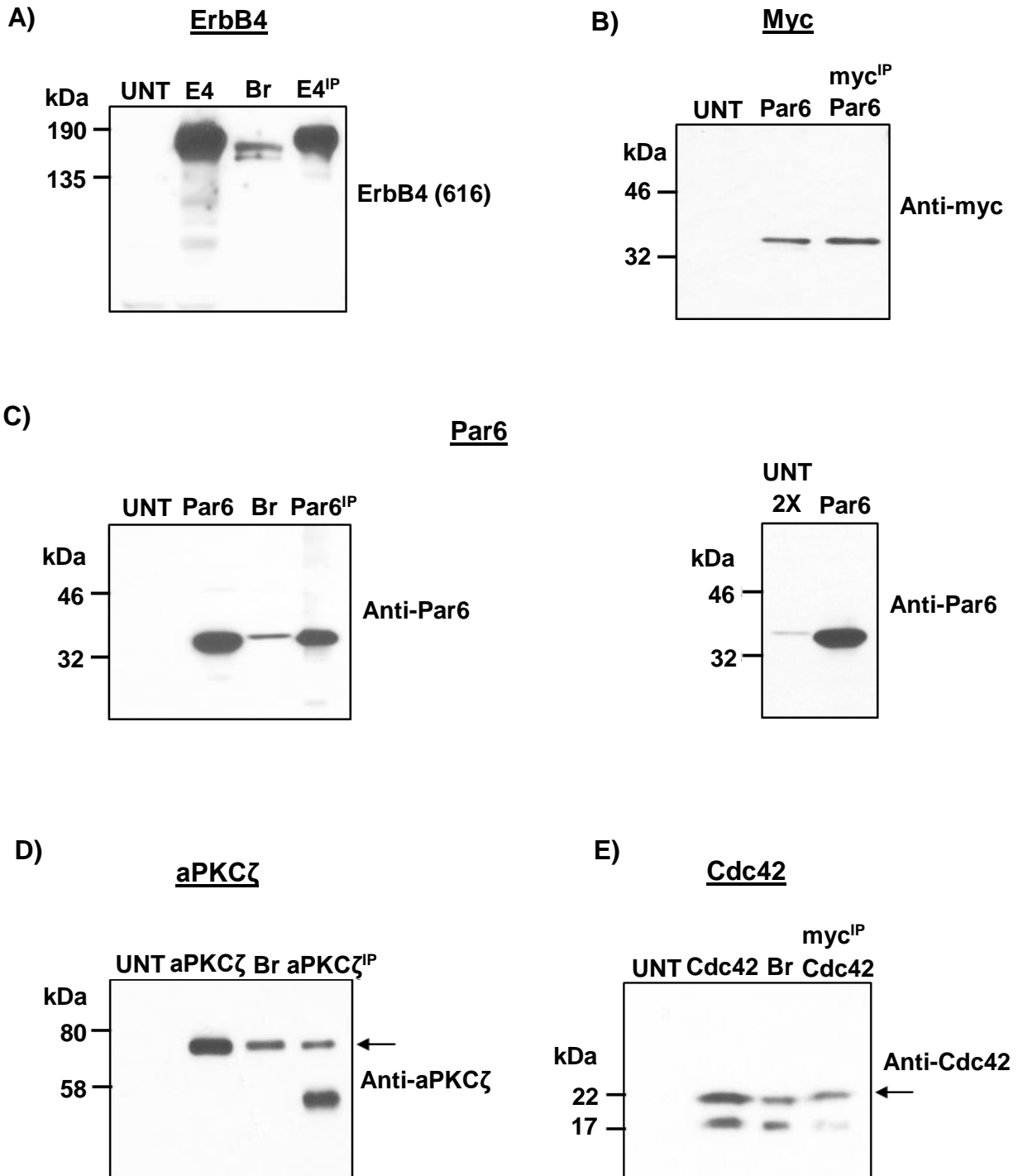
We then further analyzed the reagents used to detect the expression of the other members of the Par complex. As shown in Fig. 5.1D (lane aPKC ζ , lane CN, and lane aPKC ζ ^{IP}), a strong band was detected at approximately 76 kDa using antibodies for the PKC isoform, aPKC ζ , that matched the size reported for aPKC ζ (Wetsel et al., 1992). As a positive control, we used freshly lysed primary rat cortical neurons cultured for 8 DIV (Fig. 5.1D). No bands were detected in lysates from N2a untransfected cells (lane UNT), suggesting that aPKC ζ is not expressed at detectable levels in N2a cells (Fig. 5.1D).

We also characterized the ability of anti-Cdc42 (Figure 5.1E) to specifically detect Cdc42 expressed endogenously in P7 brain lysate (lane Br) or by transfection (lane Cdc42 and lane myc^{IP} Cdc42). Our Cdc42 antibodies were also suitable for IP, as shown in Fig. 5.4B, D, and F. A band at 21 kDa corresponding to the predicted size of Cdc42 (Munemitsu et al., 1990), and a band at 18 kDa were observed for these conditions. No bands were observed for N2a untransfected cells (lane UNT), suggesting that the N2a cells do not endogenously express Cdc42 at detectable levels (Figure 5.1E).

Next, we characterized our Par3 antibodies and cDNA expression constructs encoding a myc-tagged Par3 construct (Figure 5.1F). The *PARD3* gene gives rise to three isoforms of Par3, with molecular weights of 180, 150, and 100 kDa. For our transfections we used a cDNA clone encoding a Par3 isoform corresponding to the 150 kDa isoform of Par3 (L. Gao, Macara, & Joberty, 2002). Immunoblotting with an antibody directed towards all three isoforms of Par3, we observed two strong bands (between 150 and 180 kDa) in lysates from N2a/myc-Par3 cells (Fig 5.1F, left panel, lane Par3 and lane myc^{IP} Par3, short film exposure). Since our N2a/myc-Par3 cells were transfected with a plasmid corresponding to the 150 kDa isoform, the higher band (approximately 180 kDa) may represent Par3 that has undergone post-translational modifications, such as glycosylation (Fig. 5.1F, lane Par3). We used myc antibodies to IP for Par3 since our Par3 antibodies were not suitable for IP. For the N2a untransfected lysates (Figure 5.1F, right panel, lane UNT), a longer film exposure (Fig. 5.1F, right panel) revealed three bands between 100-180 kDa. The levels of the Par3 isoforms showed clear differences between cortical brain tissue and the N2a cells. In P7 brain lysates, a strong band was observed at 150 kDa, a weaker band at 180 kDa, and a weak band at 100 kDa (Figure 5.1F, right panel, lane Br). We also observed an unspecific band at about 245 kDa in all conditions, as well as two other unspecific bands between 100 and 150 kDa in N2a/myc-Par3 lysates (Figure 5.1F, left panel, lane Par3).

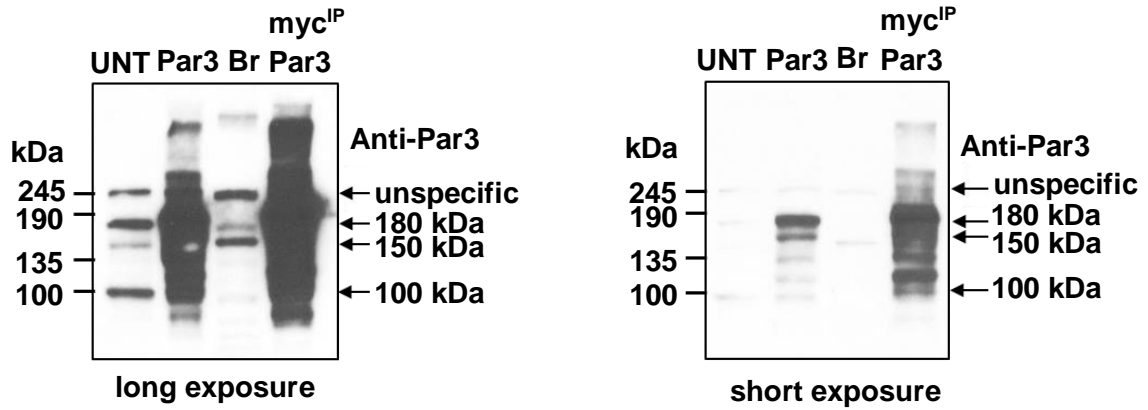
We next sought to ensure that our GST-Nrg factors were able to activate ErbB4. Towards this goal, we activated N2a/ErbB4 cells with 500 ng/mL of GST, GST-Nrg1, GST-Nrg2, and GST-Nrg3 for 15 minutes. As shown in Figure 5.1G, activation with these factors resulted in the increase in anti-pTyr immunoreactivity, relative to the GST-activated control. This band was approximately 185 kDa, corresponding to the predicted size of ErbB4. These results indicate that the GST-Nrgs factors activate the ErbB4 receptor in N2a/ErbB4 cells.

Fig. 5.1



F)

Par3



G)

GST-Nrg Activation

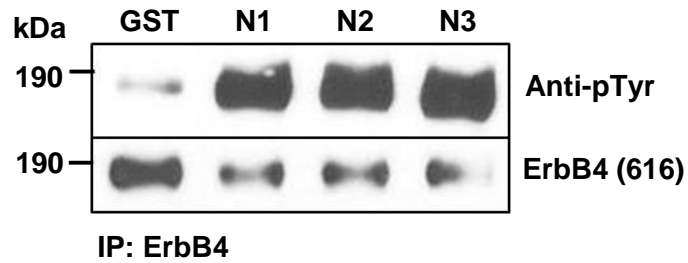


Figure 5.1: Characterization of ErbB4 and Par Complex cDNA Plasmid Constructs, Antibodies, and GST-Nrg Fusion Proteins.

A) Lysates from untransfected N2a cells (**lane UNT**), N2a cells transiently transfected with 2 µg of ErbB4 (N2a/ErbB4; **lane E4** and **lane E4^{IP}**), and P7 cortical rat brain extracts (**lane Br**) were prepared. After protein normalization, half of the N2a/ErbB4 lysate was IP'ed with 0.2 µg of anti-ErbB4 (**lane E4^{IP}**). Detergent extracts were analyzed by SDS-PAGE using 4-20% gels followed by Western blotting. The blot was probed with anti-ErbB4 serum #616 (1:5,000).

B) Lysates from untransfected N2a cells (**lane UNT**) and N2a cells transiently transfected with 2 µg of myc-Par6 (N2a/myc-Par6; **lane Par6** and **lane myc^{IP} Par6**) were prepared. After protein normalization, half of the N2a/myc-Par6 lysate was IP'ed with 0.2 µg of anti-myc (**lane myc^{IP} Par6**). Detergent extracts were analyzed by SDS-PAGE using 4-20% gels followed by Western blotting. The blot was probed with anti-myc (1:2,000). All blots are representative of at least three experiments.

C) Lysates from untransfected N2a cells (**lane UNT** and **lane UNT 2X**), N2a cells transiently transfected with 2 µg of myc-Par6 (N2a/myc-Par6; **lane Par6** and **lane Par6^{IP}**), P7 cortical rat brain extracts (**lane Br**) were prepared. After protein normalization, half of the N2a/myc-Par6 lysate was IP'ed with 0.2 µg of anti-Par6 (**lane Par6^{IP}**). To detect Par6 in untransfected N2a lysates, twice the amount of lysate was loaded (**lane UNT 2X**) compared to N2a/myc-Par6 lysate (**lane Par6**). Detergent extracts were analyzed by SDS-PAGE using 4-20% gels followed by Western blotting. The blot was probed with anti-Par6 (1:2,000). All blots are representative of at least three experiments.

D) Lysates from untransfected N2a cells (**lane UNT**), N2a cells transiently transfected with 2 µg of FLAG-aPKCζ (N2a/FLAG-aPKCζ; **lane aPKCζ** and **lane aPKCζ^{IP}**), and primary cortical cells cultured for 8 DIV (**lane CN**) were prepared. After protein normalization, half of the N2a/FLAG-

aPKC ζ lysate was IP'ed with 0.2 μ g of anti-aPKC ζ (**lane aPKC ζ ^{IP}**). Detergent extracts were analyzed by SDS-PAGE using 4-20% gels followed by Western blotting. The blot was probed with anti-aPKC ζ (1:2,000). All blots are representative of at least three experiments.

E) Lysates from untransfected N2a cells (**lane UNT**), N2a cells transiently transfected with 2 μ g of myc-Cdc42 (N2a/myc-Cdc42; **lane Cdc42** and **lane myc^{IP} Cdc42**), and P7 cortical rat brain extracts (**lane Br**) were prepared. After protein normalization, half of the N2a/myc-Cdc42 lysate was IP'ed with 0.2 μ g of anti-myc (**lane myc^{IP} Cdc42**). Detergent extracts were analyzed by SDS-PAGE using 4-20% gels followed by Western blotting. The blot was probed with anti-Cdc42 (1:2,000). All blots are representative of at least three experiments.

F) Lysates from untransfected N2a cells (**lane UNT**), N2a cells transiently transfected with 2 μ g of myc-Par3 (N2a/myc-Par3; **lane Par3** and **lane myc^{IP} Par3**), and P7 cortical rat brain extracts (**lane Br**) were prepared. After protein normalization, half of the N2a/myc-Par3 lysate was IP'ed with 0.2 μ g of anti-myc (**lane myc^{IP} Par3**). Detergent extracts were analyzed by SDS-PAGE using 4-20% gels followed by Western blotting. The blot was probed with anti-Par3 (1:2,000). To clearly observe the 180, 150, and 100 kDa isoforms (arrows) of Par3 in untransfected N2a cells (**lane UNT**) and in N2a/myc-Par3 cells (**lane Par3** and **lane myc^{IP} Par3**), a short film exposure (**left panel**) and a longer film exposure (**right panel**) were both included. All blots are representative of at least three experiments.

G) GST-Nrg factors were tested for their ability to induce phosphorylation of ErbB4 in N2a/ErbB4 cells. N2a/ErbB4 cells were activated with 500 ng/mL of GST, GST-Nrg1, GST-Nrg2, or GST-Nrg3 for 20 min. After protein normalization, lysates were IP'ed with 0.2 μ g of anti-ErbB4. Samples were then analyzed by SDS-PAGE using 4-20% Tris-glycine gels followed by Western blotting. The blots were probed with anti-phospho-tyrosine (pTyr) PY99 and PY20 (**top panel**, 1:5,000 dilution for both) and anti-ErbB4 using serum #616 (**bottom panel**, 1:5,000

dilution) to detect total levels of ErbB4. The top and bottom panels are from separate blots but from the same samples. All blots are representative of at least three experiments.

5.2.2 ErbB4 Associates with Par6 and Par3 in a Nrg and Time Dependent Manner

Aranda et al previously demonstrated that ErbB2 could associate with Par6-aPKC ζ in rodent mammary epithelia (Aranda et al., 2006). To determine whether ErbB4, a heterodimerization partner for ErbB2, can associate with members of the Par complex in the CNS, we performed experiments using a stably transfected N2a cell line expressing ErbB4 (N2a/ErbB4; Figs. 5.2-5.4) and also primary cortical neurons (Fig. 5.6). When necessary, we transiently transfected members of the Par polarity complex to assess potential interactions with ErbB4. To begin our investigations (Fig. 5.2), we transiently transfected N2a/ErbB4 cells with myc-Par6 (N2a/ErbB4/myc-Par6) prior to activation with 500 ng/mL of GST-Nrg1, GST-Nrg2, or GST-Nrg3 for 0, 5, 15, 30, or 60 min. Cell lysates were then IP'ed for both ErbB4 (Fig. 5.2A-A", C-C", E-E", and G) and myc (myc-Par6; Fig. 5.2B-B", D-D", and F-F") and Western blotted for Par3 (endogenous), myc to detect myc-Par6, and ErbB4 (Fig. 5.2).

Upon activation with GST-Nrg1 (Fig. 5.2A-A" and B-B"), GST-Nrg2 (Fig. 5.2C-C" and D-D"), and GST-Nrg3 (Fig. 5.2E-E" and F-F"), we observed a time-dependent increase in the association between ErbB4 with myc-Par6 and endogenous Par3. Based on the densitometric analyses of our Western blots, activation with GST-Nrg1 for 30 or 60 min (Fig. 5.2A' and B') showed a statistically significant increase in ErbB4-myc-Par6 association compared to unactivated cells (0 min; Fig. 5.2A' and B') or cells activated with GST-Nrg1 for only 5 min (Fig. 5.2A'). Activation with GST-Nrg2 (Fig. 5.2C' and D') and GST-Nrg3 (Fig. 5.2E' and F') showed a statistically significant increase in ErbB4-myc-Par6 association upon activation ranging from 15 min (Fig. 5.2C', E' and F') to 60 min (Fig. 5.2C', D', E', and F'), compared to unactivated cells (0 min; Fig. 5.2C', D', E' and F') or cells activated for a shorter period of time (Fig. 5.2C', D', and F'). We also observed that the association of Par3 and ErbB4 significantly increased in a Nrg-activation and time-dependent manner in our cells (Fig. 5.2A, A", C, C", E, and E"). Our densitometric analyses revealed a statistically significant increase in ErbB4-Par3 association

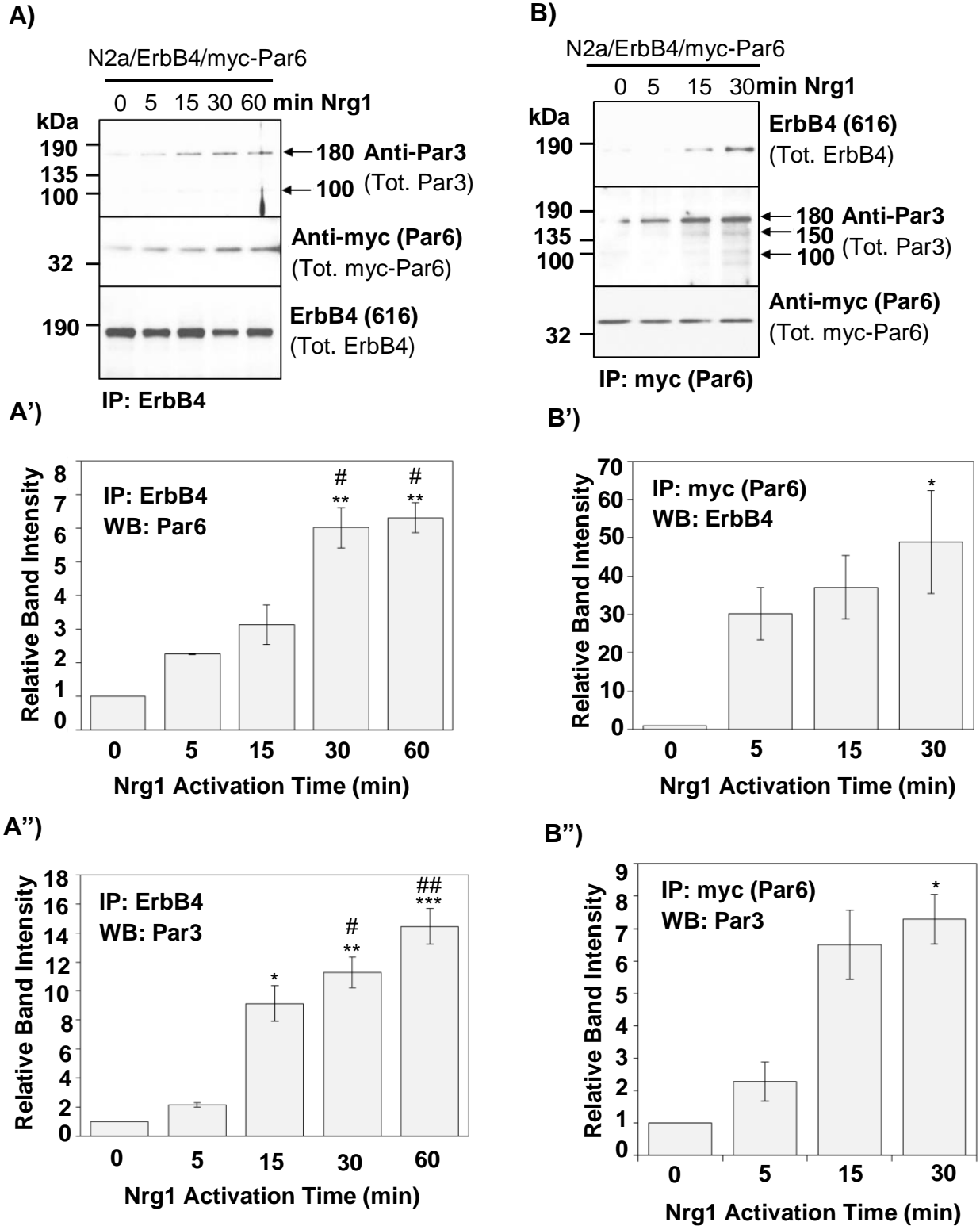
within 15 min of activation with all three GST-Nrgs, compared to unactivated cells (0 min) or cells activated less than 15 min (Fig. 5.2A", C", and E"). The association of the 180 kDa isoform of Par3 with ErbB4 steadily increased upon activation with all three GST-Nrgs (Fig. 5.2A, C, and E). However, the 150 kDa isoform of Par3 associated with ErbB4 after 30 mins of activation with GST-Nrg2 (Fig. 5.2 C) and GST-Nrg3 (Fig. 5.2E), but was not observed in samples activated with GST-Nrg1 (Fig. 5.2A). Association of the 100 kDa isoform of Par3 with ErbB4 was unique because it was dependent on the identity of the GST-Nrg used for activation (Fig. 5.2A, C, and E). Activation with GST-Nrg2 (Fig. 5.2C) resulted in a robust increase in the association between the 100 kDa isoform of Par3 with ErbB4, while activation with GST-Nrg1 and GST-Nrg3, resulted only in a slight increase in the association (Fig. 5.2A and E). Without any activation (0 min), we detected low levels of both endogenous Par3 and myc-Par6 association with ErbB4 (Fig. 5.2A and E). Our control mouse IgG IPs did not pull down any of the Par proteins or ErbB4 (Fig. 5.2G). These findings suggest that activation with individual Nrgs induces differential association of Par3 isoforms with ErbB4.

Our findings that ErbB4 associates with Par3 in an activation-dependent manner is interesting and unexpected since it has previously been reported that ErbB2 does not associate with Par3 (Aranda et al., 2006). In fact, that same study reported that ErbB2 association with Par6-aPKC γ resulted in the disruption of Par3 binding to Par6. Therefore, we sought to determine if activation of ErbB4 resulted in a disruption of the Par complex or if ErbB4 could associate with the entire Par complex. Towards this goal, we activated N2a/ErbB4/myc-Par6 cells with the GST-Nrgs (as described above) and IP'ed for myc-Par6 to detect potential changes in association with Par3 (Fig. 5.2B-B", D-D", and F-F"). Without any activation (0 min), we detected association of myc-Par6 with the 180 kDa isoform of Par3 and ErbB4 (Fig. 5.2B and F). Upon activation with GST-Nrgs (Fig. 5.2B for GST-Nrg1; Fig. 5.2D for GST-Nrg2; and Fig. 5.2F for GST-Nrg3), the association between myc-Par6 and Par3 steadily increased with

activation time, peaking at 30 min (Fig. 5.2B, B", D, D", F, and F"). Densitometric analyses revealed that activation with GST-Nrg1 (Fig. 5.2B") or GST-Nrg2 (Fig. 5.2D") for at least 30 min or GST-Nrg3 (Fig. 5.2F") for at least 15 min resulted in a significantly greater association between myc-Par6 and Par3 compared to unactivated cells (0 min; Fig. 5.2B", D", and F"). This was also the case for the association between myc-Par6 and ErbB4 (Fig. 5.2B, B', D, D', F, and F'), consistent with our observations made with ErbB4 IPs (Fig. 5.2A, A', C, C', E, and E'). Activation with the GST-Nrgs resulted in a more robust association of the 180 kDa isoform of Par3 and myc-Par6 than the other two Par3 isoforms (Fig. 5.2B, D, and F). Unlike our observations shown in Fig 5.2C which demonstrated a strong Nrg2-dependent association with the 100 kDa isoform of Par3 with ErbB4, we did not observe this association between Par3 (100 kDa) and myc-Par6 (Fig. 5.2D). On the contrary, activation with GST-Nrg1 and GST-Nrg3 showed low levels of association between the 100 kDa isoform of Par3 with myc-Par6 (Fig. 5.2B and F); however, GST-Nrg2 activation did not result in the association between these two proteins (Par3-myc-Par6) (Fig. 5.2D). These findings suggest that there might be competition between the interaction of the 100 kDa isoform of Par3 with ErbB4 and Par6, dependent on Nrg2 activation. It also suggests that ErbB4 may be interacting with Par3 and Par6 independently of the Par complex (Fig. 5.2H). Overall, our findings show that ErbB4 can interact with myc-Par6 and Par3 (Fig. 5.2H) in a Nrg- and time-dependent manner.

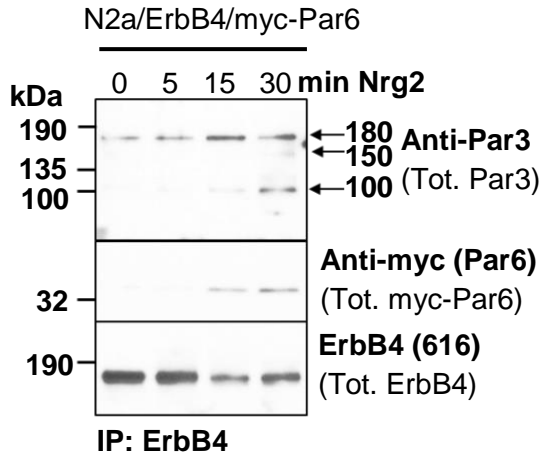
Fig. 5.2

GST-Nrg1 Activation

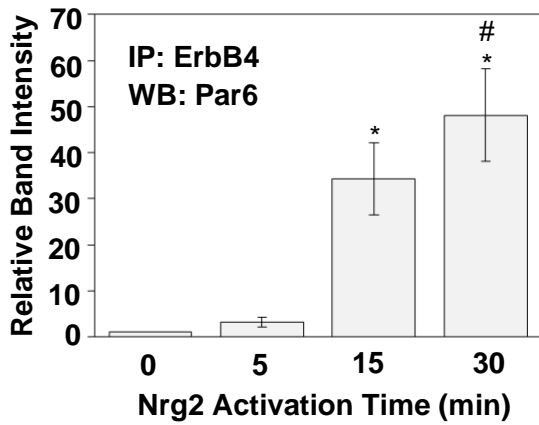


GST-Nrg2 Activation

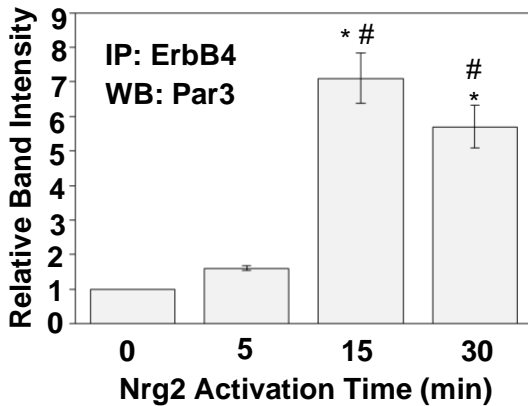
C)



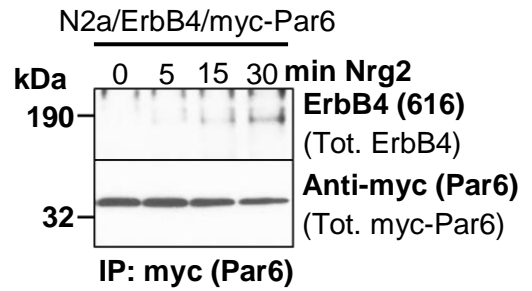
C')



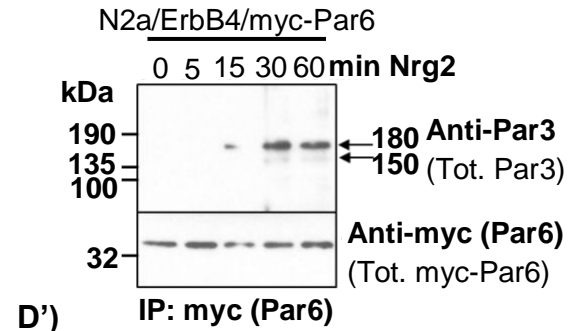
C'')



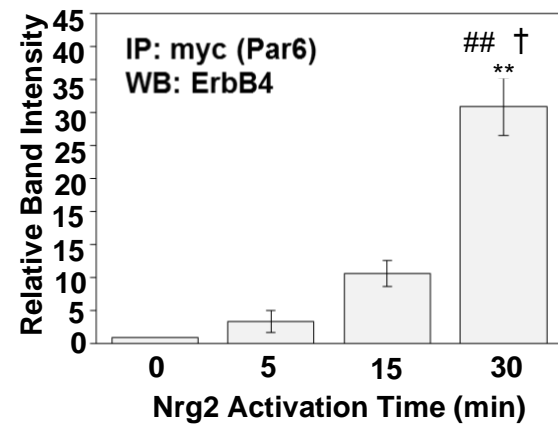
D)



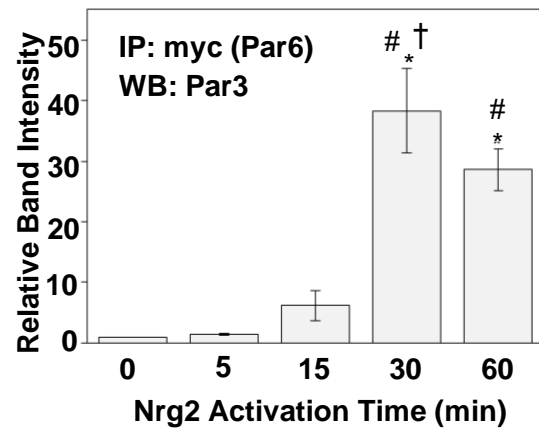
D')



D'')

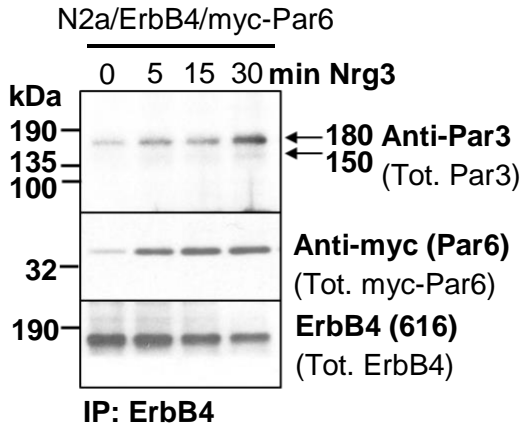


D''')

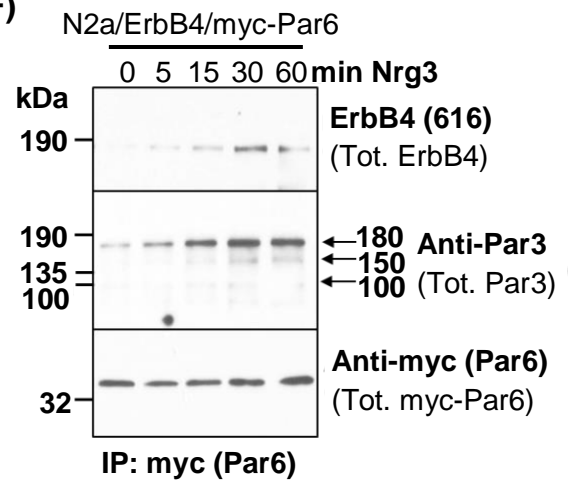


GST-Nrg3 Activation

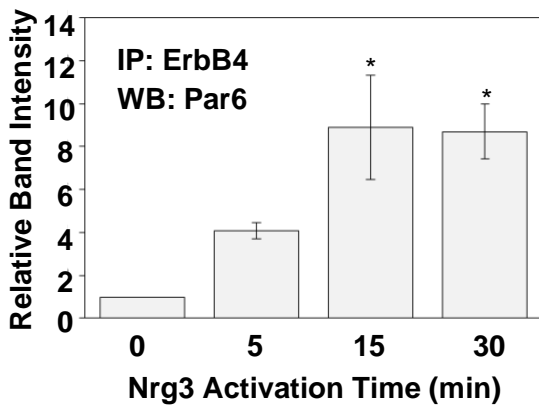
E)



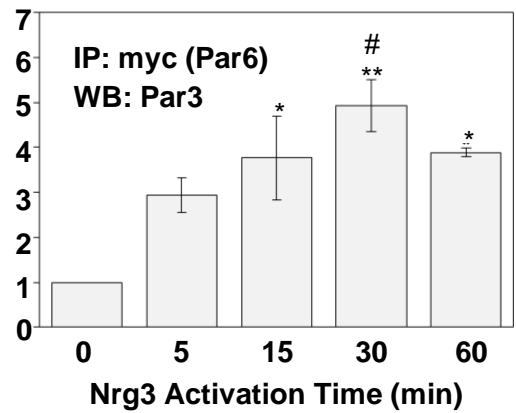
F)



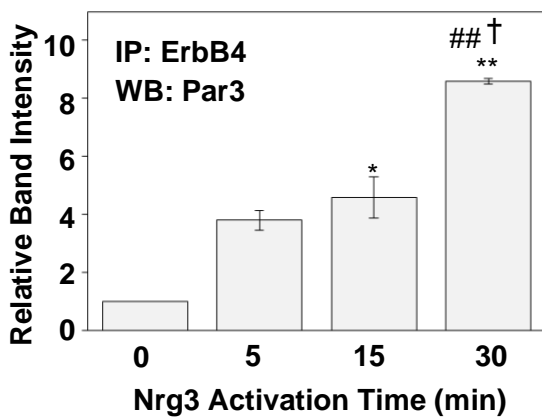
E')



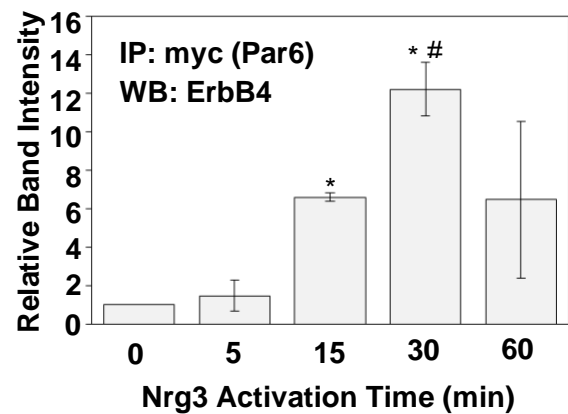
F')



E'')

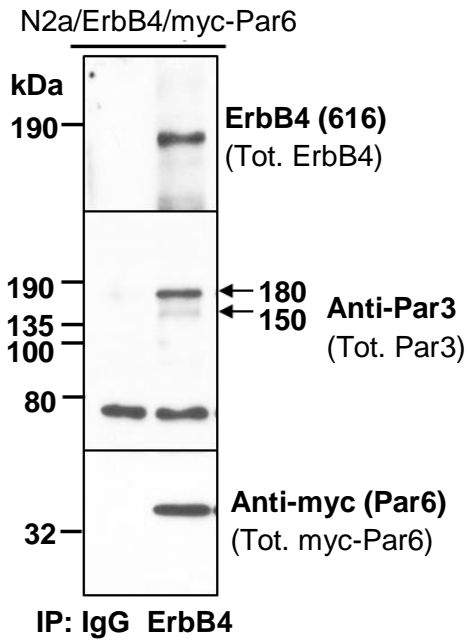


F'')



G)

Control IPs



H)

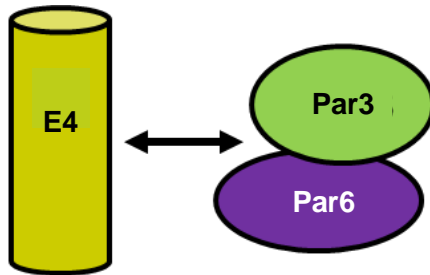


Figure 5.2: ErbB4 Associates with Par6 and Par3 in a Nrg and Time Dependent Manner in N2a/ErbB4/myc-Par6 Cells.

A-F) The association between ErbB4 and Par6 and between ErbB4 and Par3 increases in a Nrg and time dependent manner. N2a/ErbB4 cells were transiently transfected with 2 µg of myc-Par6. The cells were then activated with 500 ng/mL of GST-Nrg1 (**panels A and B**), GST-Nrg2 (**panels C and D**), or GST-Nrg3 (**panels E and F**) for 0, 5, 15, 30, or 60 min. After protein normalization, the extracts were IP'ed with ErbB4 (**panels A, C, and E**) or myc (for myc-Par6) (**panels B, D, and F**). Samples were analyzed by SDS-PAGE using 4-20% gels followed by Western blotting. Membranes were probed with anti-ErbB4 using serum #616 (1:5,000), anti-Par3 (1:2,000), and anti-myc (for myc-Par6; 1:2,000) to detect their interaction. These blots are representative of five experiments.

A'-F' and A''-F'') Band intensities were quantified from at least two experiments by densitometric analysis and used to calculate the ratios of myc-Par6/ErbB4 (total ErbB4; **panels A', C', and E'**), Par3 180 kDa/ErbB4 (total ErbB4; **panels A'', C'', and E''**), ErbB4/myc-Par6 (total myc-Par6; **panels B', D', and F'**) and Par3 180 kDa/myc-Par6 (total myc-Par6; **panels B'', D'', and F''**). The bars ("relative band intensity") represent the fold change from control (0 min of activation) which was considered 1. *, comparison to 0 min of activation (*p = <0.05, **p = <0.01, ***p = <0.001); #, comparison to 5 min of activation (#p = <0.05, ##p = <0.01); †, comparison to 15 min of activation (†p = <0.05). n=2 for A', A'', B'', C', C'', D', D'', E'', F, and F'' and n=3 for B' and E'.

G) Control mouse IgG IPs do not pull down ErbB4, Par6, or Par3. N2a/ErbB4 cells were transiently transfected with 2 µg of myc-Par6. The cells were then activated with 500 ng/mL of GST-Nrg1 for 10 min. After protein normalization, the extracts were IP'ed with either ErbB4 (**lane ErbB4**) or mouse IgG isotype (**lane IgG**) as a control. Samples were analyzed by SDS-

PAGE using 4-20% gels followed by Western blotting. The membranes were probed with anti-ErbB4 using serum #616 (1:5,000), anti-Par3 (1:2,000), and anti-myc (for myc-Par6; 1:2,000). These blots are representative of three experiments.

H) Schematic representation of possible ErbB4, Par6, and Par3 interactions. Our data demonstrate that Par6 and Par3 co-IP with ErbB4, showing that these members of the Par complex associate with the receptor. Par6 and Par3 may be individually interacting with ErbB4 or could be interacting together as a Par3-Par6 complex. It is important to note that the arrow does not necessarily represent a direct interaction or the site of interaction between ErbB4 with Par6 and Par3. The interaction of the Par proteins and ErbB4 may involve other intermediary molecules or adapter proteins not yet identified.

5.2.3 ErbB4 Associates with aPKC ζ in a Nrg and Time Dependent Manner in aPKC ζ Overexpressing Cells

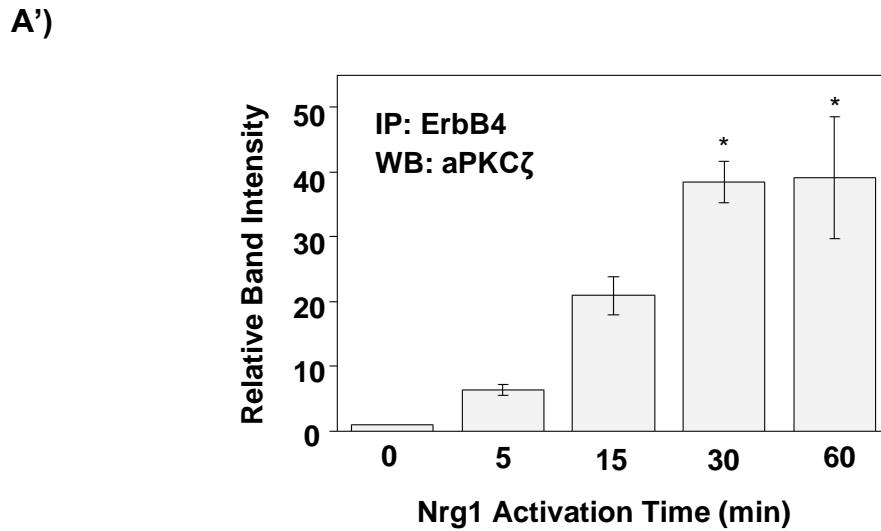
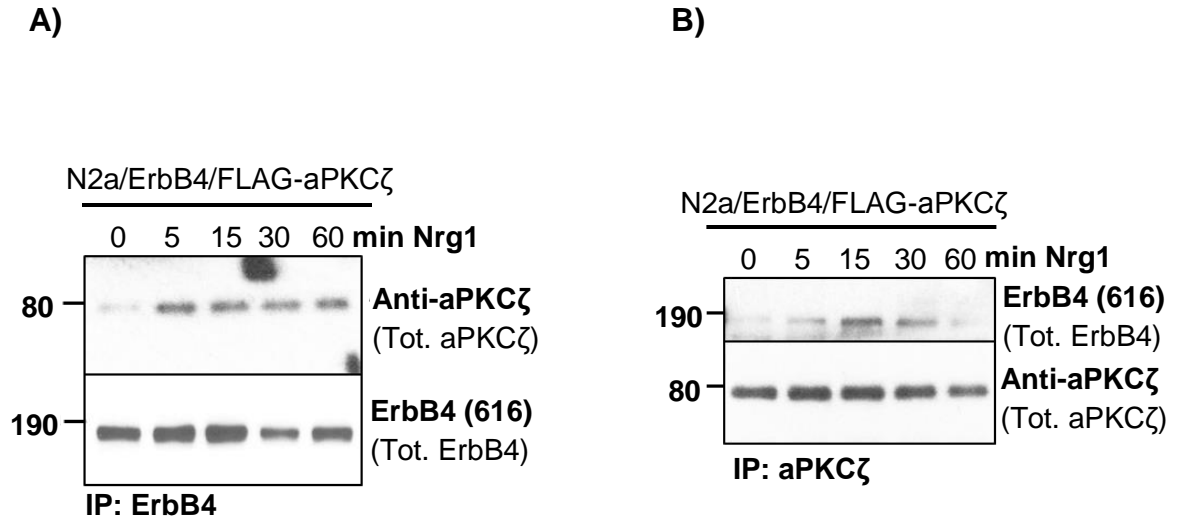
We have shown that ErbB4 can interact with Par3 and Par6, two members of the Par polarity complex (Fig. 5.2). In addition to Par3 and Par6, the Par polarity complex includes aPKC ζ and Cdc42. In order to investigate whether ErbB4 can associate with the other two members of the Par complex, we determined if ErbB4 and aPKC ζ could co-IP with one another in N2a/ErbB4 cells transiently transfected with FLAG-aPKC ζ (N2a/ErbB4/FLAG-aPKC ζ). These aPKC ζ expressing cells were activated with 500 ng/mL of GST-Nrg1 (Fig. 5.3A, A', and B), GST-Nrg2 (Fig. 5.3C, C', and D), and GST-Nrg3 (Fig. 5.3E, E', and F) for 0, 5, 15, 30, or 60 min. Cells were lysed and IP'ed for ErbB4 (Fig. 5.3A, A', C, C', E, and E') and aPKC ζ (Fig. 5.3B, D, and F), followed by immunoblotting for both ErbB4 and aPKC ζ .

Activation with GST-Nrg1 (Fig. 5.3A, A', and B), GST-Nrg2 (Fig. 5.3C, C', and D), and GST-Nrg3 (Fig. 5.3E, E', and F) resulted in an increase in ErbB4 association with aPKC ζ (Fig. 5.3). This pattern of GST-Nrg-regulated association of ErbB4-aPKC ζ was observed in both ErbB4 and aPKC ζ IPs (Fig. 5.3A, A', C, C', E, and E' and Fig. 5.3B, D, and F respectively). Densitometric analyses revealed that activation with GST-Nrg1 (Fig. 5.3A') for at least 30 min, GST-Nrg2 (Fig. 5.3C') for at least 15 min, or GST-Nrg3 (Fig. 5.3E') for at least 60 min resulted in a significantly greater association between ErbB4 and aPKC ζ compared to unactivated cells (0 min; Fig. 5.3A', C', and E'). Without activation (0 min), we observed low levels of ErbB4 association with aPKC ζ (Fig. 5.3A-F). We did not detect ErbB4 or aPKC ζ in our mouse IgG control IPs (Fig. 5.4G, lane IgG). Since in these cells there are low levels of endogenous Par6 (Fig. 5.1C, right panel) and higher levels of endogenous Par3 (Fig. 5.1F, right panel), it is possible that ErbB4 can associate with the Par6-aPKC ζ or Par6-aPKC ζ -Par3 complexes in the aPKC ζ overexpressing cells (N2a/ErbB4/FLAG-aPKC ζ cells; Fig. 5.3H). Whether ErbB4 and aPKC ζ are interacting independently of Par6 could be addressed by performing a knockdown of

Par6 expression in these cells and observing whether the interaction between ErbB4 and aPKC ζ is affected. Overall, these results show that ErbB4 and aPKC ζ can associate (Fig. 5.3H) in aPKC ζ overexpressing cells (N2a/ErbB4/FLAG-aPKC ζ cells) and that this association can be regulated by GST-Nrg activation.

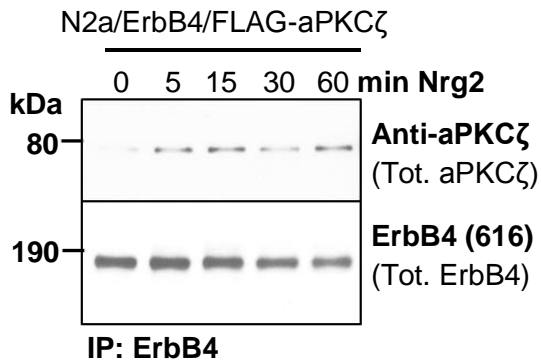
Fig. 5.3

GST-Nrg1 Activation

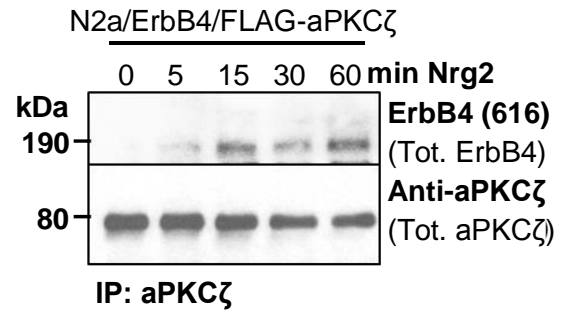


GST-Nrg2 Activation

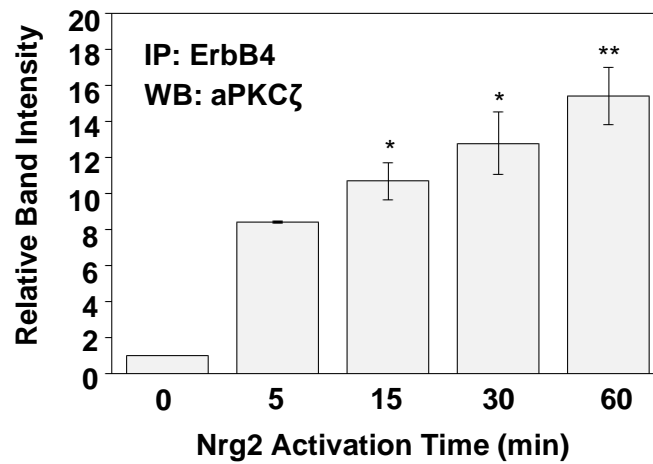
C)



D)

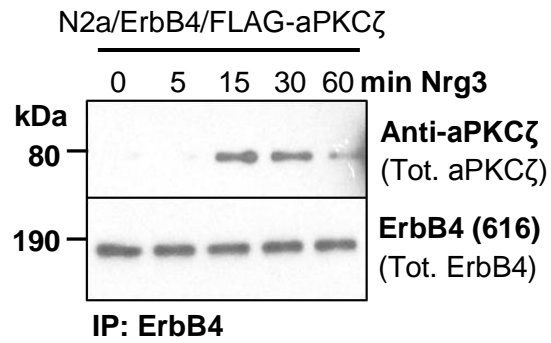


C')

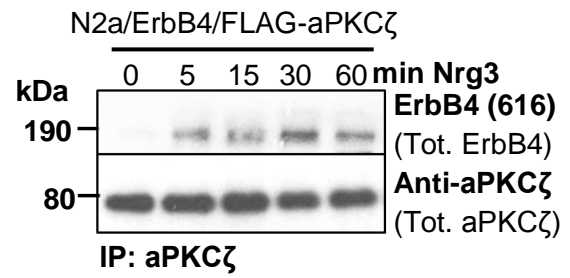


GST-Nrg3 Activation

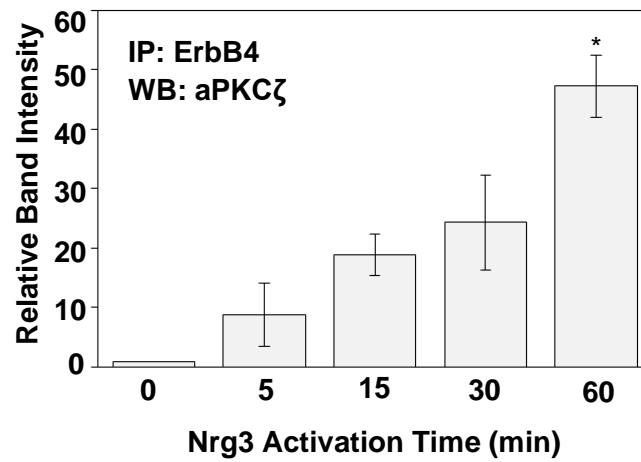
E)



F)

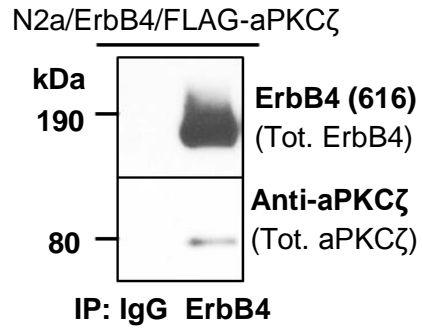


E')



G)

Control IP



H)

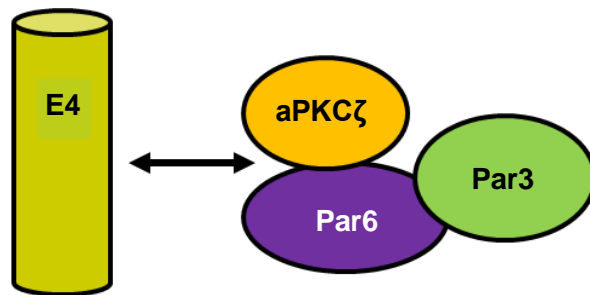


Figure 5.3: ErbB4 Associates with aPKCζ in a Nrg and Time Dependent Manner.

A-F) ErbB4 can associate with aPKCζ in a Nrg and time dependent manner. N2a/ErbB4 cells were transiently transfected with 2 μg of FLAG-aPKCζ. The cells were then activated with 500 ng/mL of GST-Nrg1 (**panels A and B**), GST-Nrg2 (**panels C and D**), or GST-Nrg3 (**panels E and F**) for 0, 5, 15, 30, or 60 min. After protein normalization, the extracts were IP'ed with either ErbB4 (**panels A, C, and E**) or aPKCζ (**panels B, D, and F**). Samples were analyzed after SDS-PAGE using 4-20% gels followed by Western blotting. The membranes were probed with anti-ErbB4 using serum #616 (1:5,000) and anti-aPKCζ (1:2,000) to detect their interaction. These blots are representative of four experiments.

A', C', and E') Band intensities were quantified from three experiments by densitometric analysis and used to calculate the ratios of aPKCζ/ErbB4 (total ErbB4; **panels A', C', and E'**). The bars ("relative band intensity") represent the fold change from control (0 min of activation) which was considered 1. *, comparison to 0 min of activation (*p = <0.05, **p = <0.01, n=3).

G) Control mouse IgG IPs do not pull down ErbB4 or aPKCζ. As an immunoprecipitation control, N2a/ErbB4 cells were transiently transfected with 2 μg of FLAG-aPKCζ. The transfected cells were then activated with 500 ng/mL of GST-Nrg1 for 10 min. After protein normalization, the extracts were IP'ed with either ErbB4 (**lane ErbB4**) or mouse IgG isotype (**lane IgG**) as a control. Samples were analyzed after SDS-PAGE using 4-20% gels followed by Western blotting. The membranes were probed with anti-ErbB4 using serum #616 (1:5,000) and anti-aPKCζ (1:2,000). These blots are representative of three experiments.

H) Schematic representation of possible ErbB4 interactions with members of the Par polarity complex. Our data demonstrate that Par6, Par3, and aPKCζ co-IP with ErbB4, showing that these members of the Par complex associate with the receptor. Members of the Par complex may be individually interacting with ErbB4 or could be interacting together as a complex. Further

experiments need to be conducted to determine if aPKC ζ can interact with ErbB4 independently of the Par complex (dotted line). It is important to note that the arrows do not necessarily signify a direct interaction or the location of interaction between ErbB4 with Par6, Par3, or aPKC ζ and may involve other molecules or adapter proteins yet to be identified.

5.2.4 ErbB4 Does Not Directly Associate with Cdc42 but Can Indirectly Associate Through Par6

Both Rac1 and Cdc42 have been shown to bind with Par6 in the Par polarity complex and are associated with neuronal polarization (Joberty et al., 2000; Lin et al., 2000; Takashi Nishimura et al., 2005; Qiu et al., 2000; Schwamborn & Püschel, 2004). However, Cdc42 is reported to be a stronger binding partner for Par6 than Rac1 (Johansson et al., 2000; Lin et al., 2000). Therefore, our focus for the following experiments was to determine whether ErbB4 associates with Cdc42, as we have determined for the associations between ErbB4 with Par3, Par6, and aPKC ζ . Towards this goal, we used N2a/ErbB4 cells transiently transfected with myc-Cdc42 (N2a/ErbB4/myc-Cdc42; Fig. 5.4A-C). Cdc42 overexpressing cells (N2a/ErbB4/myc-Cdc42 cells) were activated for 15 min with 500 ng/mL of GST or GST-Nrgs (Fig. 5.4A and B, GST, lane GST; GST-Nrg1, lane N1; GST-Nrg2, lane N2; GST-Nrg3, lane N3) for 0, 5, 15, 30, or 60 min. Cells were then lysed and IP'ed for ErbB4 (Fig. 5.4A and C) and myc (myc-Cdc42; Fig. 5.4B) prior to immunoblotting for ErbB4 and Cdc42. As shown in Fig. 5.4A and B, we did not detect ErbB4 association with Cdc42, even upon activation with the GST-Nrgs (Fig. 5.4A and B). We also monitored the potential association of ErbB4 with Cdc42 at additional time points using GST-Nrg1 (Fig. 5.4C) for activation, and also failed to observe Cdc42 co-IP with ErbB4.

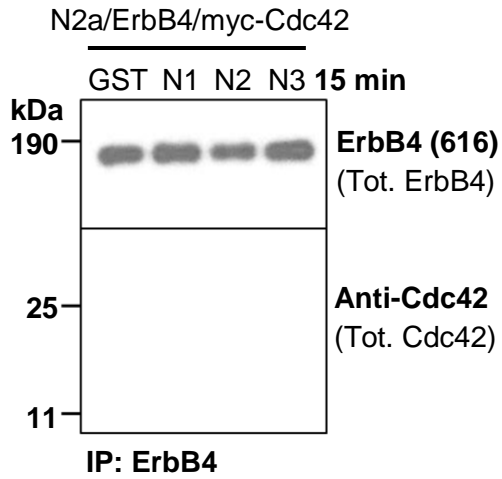
It has previously been shown that Par6 directly interacts with Cdc42 through a partial CRIB motif and an adjacent PDZ domain (Garrard et al., 2003). Since we have observed that ErbB4 associates with Par6 (Figs. 5.2), we next sought to determine whether ErbB4 could associate with Cdc42 but in the form of a Par6-Cdc42 complex. Since endogenous levels of Par6 are low in N2a cells, we used N2a/ErbB4 cells doubly transfected with myc-Par6 and myc-Cdc42 (N2a/ErbB4/myc-Par6/myc-Cdc42) for these experiments (Fig. 5.4D-F). Par6 and Cdc42 overexpressing cells were activated with 500 ng/mL of GST or GST-Nrgs (Fig. 5.4D and E, GST, lane GST; GST-Nrg1, lane N1; GST-Nrg2, lane N2; GST-Nrg3, lane N3). Cells were lysed

and IP'ed for Cdc42 (Fig. 5.4D) and Par6 (Fig. 5.4F) and then immunoblotted for ErbB4, Cdc42, and Par6. In these experiments we were unable to IP using a myc antibody since both Par6 and Cdc42 constructs are myc-tagged, therefore we utilized antibodies targeted against the individual proteins. We observed that in both our Cdc42 IPs (Fig. 5.4D) and Par6 IPs (Fig. 5.4E) the two proteins (Par6 and Cdc42) associate with one another and that this association was greater in cells that were activated with the GST-Nrgs (lanes N1, N2, and N3), compared with the GST control (lane GST). As observed previously (Fig. 5.2), ErbB4 was detected in the Par6 IPs (Fig. 5.4E) and this association was greater in cells that were activated with the GST-Nrgs (lanes N1, N2, and N3), compared with the GST control (lane GST). Not only did we detect Par6 in our Cdc42 IPs (Fig. 5.4D, middle panel), but ErbB4 was also detected in our Cdc42 IPs (Fig. 5.4D, top panel). Furthermore, the interaction between ErbB4 and Cdc42 increased upon activation with the GST-Nrgs (Fig. 5.4D, top panel). Neither ErbB4 nor Cdc42 were observed in our control mouse IgG IPs (Fig. 5.4F). Overall, our results show that ErbB4 and Cdc42 do not directly interact with each other (Fig. 5.4G). However, in the presence of Par6, ErbB4 and Cdc42 can interact, most likely indirectly through an interaction that includes both Par6 and Cdc42 (Fig. 5.4G).

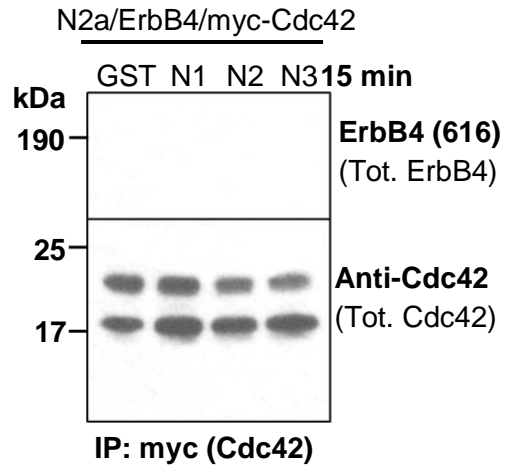
Fig. 5.4

GST-Nrg1-3 Activation

A)

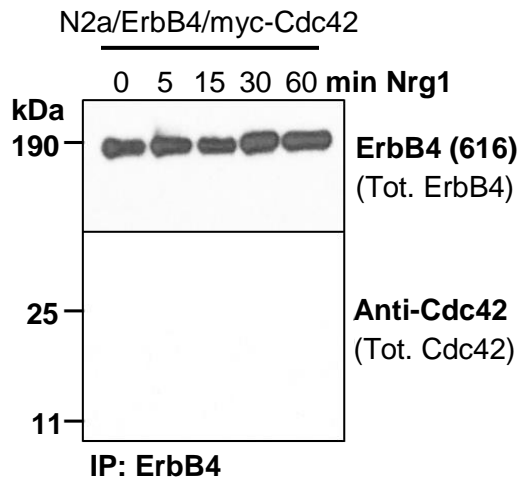


B)



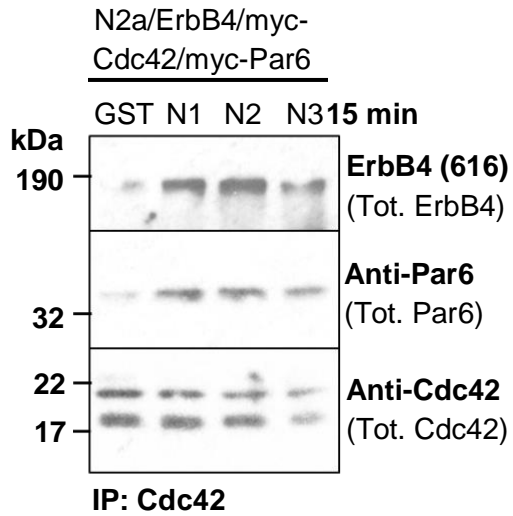
C)

GST-Nrg1 Activation

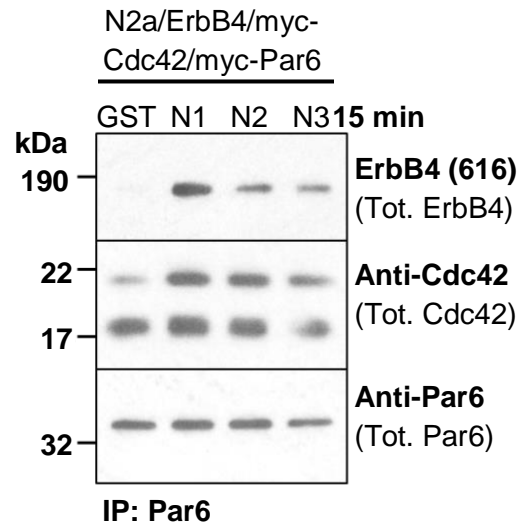


GST-Nrg1-3 Activation

D)

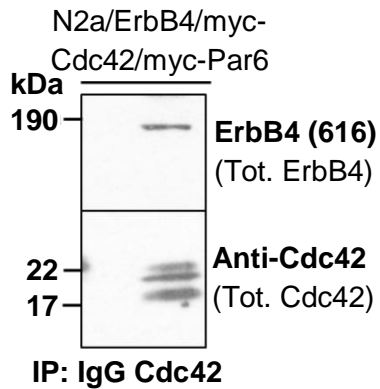


E)



F)

Control IP



G)

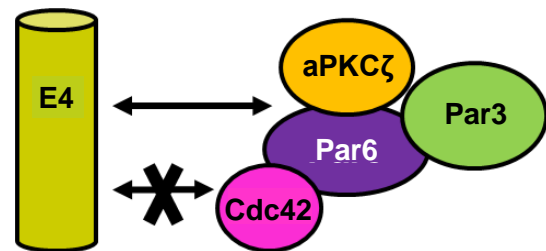


Figure 5.4: ErbB4 Does Not Directly Associate with Cdc42, But Can Indirectly Associate Through Par6.

A-C) ErbB4 and Cdc42 do not co-IP, even upon GST-Nrg activation. N2a/ErbB4 cells were transiently transfected with 2 µg of myc-Cdc42. The cells were then activated with 500 ng/mL of GST, GST-Nrg1, GST-Nrg2, or GST-Nrg3 for 15 min (**panels A and B**) or for 0, 5, 15, 30, or 60 min (**panels C**). After protein normalization, the extracts were IP'ed with either ErbB4 (**panels A and C**) or Cdc42 (**panel B**). Samples were analyzed after SDS-PAGE using 4-20% gels followed by Western blotting. The membranes were probed with anti-ErbB4 using serum #616 (1:5,000) and anti-Cdc42 (1:2,000) to detect their interaction. These blots are representative of four experiments.

D and E) ErbB4 and Cdc42 indirectly associate through Par6 in a Nrg-dependent manner. N2a/ErbB4 cells were transiently transfected with 1 µg of myc-Cdc42 and 1 µg of myc-Par6. The cells were then activated with 500 ng/mL of GST, GST-Nrg1, GST-Nrg2, or GST-Nrg3 for 15 min. After protein normalization, the extracts were IP'ed with either Cdc42 (**panel D**) or Par6 (**panel E**). Samples were analyzed after SDS-PAGE using 4-20% gels followed by Western blotting. The membranes were probed with anti-ErbB4 using serum #616 (1:5,000), anti-Cdc42 (1:2,000), and anti-Par6 (1:2,000) to detect their interaction. These blots are representative of three experiments.

F) Control mouse IgG IPs do not pull down ErbB4 or Cdc42. As an immunoprecipitation control N2a/ErbB4 cells were transiently transfected with 1 µg of myc-Cdc42 and 1 µg of myc-Par6. The cells were then activated with 500 ng/mL of GST-Nrg1 for 10 min. After protein normalization, the extracts were IP'ed with either Cdc42 (**lane Cdc42**) or mouse IgG isotype (**lane IgG**) as a control. After SDS-PAGE using 4-20% gels and transfer, the membranes were

probed with anti-ErbB4 serum #616 (1:5,000) and anti-Cdc42 (1:2,000). These blots are representative of three experiments.

G) Schematic representation of possible ErbB4 interactions with members of the Par polarity complex. Our data demonstrate that although Par6, Par3, and aPKC ζ may be associating directly or indirectly with ErbB4, Cdc42 does not directly associate with the receptor. Interaction of ErbB4 with Cdc42 requires the Par6-Cdc42 complex. It is important to note that the arrows do not necessarily signify a direct interaction or the location of interaction between ErbB4 with members of the Par complex and may involve other molecules or adapter proteins that may still need to be identified.

5.2.5 ErbB4 Associates with Members of the Par Polarity Complex in Primary Cortical Cultures

Our results so far (Figs. 5.2-5.4) have shown that ErbB4 can interact with the members of the Par polarity complex: Par6, Par3, aPKC ζ , and indirectly with Cdc42. These experiments were performed by transfection causing overexpression of several molecular components under study. Overexpression may lead to protein-protein interactions that may not normally occur *in vivo*. Despite these considerations, these experiments provide a framework for the study of the interactions between ErbB4 in GABAergic neurons and the Par polarity complex in these cells. We next asked whether ErbB4 can interact with members of the Par complex in primary cortical cultures, derived from E17-E18 rat cortices, which have a representation of GABAergic neurons that endogenously express ErbB4 and the Par polarity complex proteins.

Using our primary cortical cultures, we first determined the developmental expression of ErbB4 (Fig. 5.5A), Par3, aPKC ζ , Par6, and Cdc42 (Fig. 5.5B, top panel, second, third and fourth panel respectively). For these experiments, we cultured rat primary cortical cells for 1, 3, 5, 8, 12, 14, 17, 21, and 24 (DIV) and prepared detergent extracts for to Western blotting. Our results (Fig. 5.5A) show that ErbB4 is expressed in our primary cortical cultures as early as 1 DIV. ErbB4 expression steadily increased and peaked at 14 DIV, prior to steadily decreasing and leveling off by 24 DIV (Fig. 5.5A, top panel for short exposure and middle panel for longer exposure).

In addition to these changes in ErbB4, we observed changes in the developmental expression for the members of the Par polarity complex, including changes in the ratios of Par3 isoforms. As shown in the top panel in Fig. 5.5B, we detected high levels of the 180 and 100 kDa isoforms of Par3 at 1 DIV (Fig. 5.5B, top panel). The Par3 180 kDa isoform was the highest isoform expressed at all developmental time points examined. The 100 kDa isoform was at its

highest levels at 1-3 DIV and decreased as development progressed to almost undetectable levels by 24 DIV (Fig. 5.5B, top panel). These findings suggest that the three isoforms of Par3 may play differential roles in neuronal differentiation based on their developmental patterns of expression.

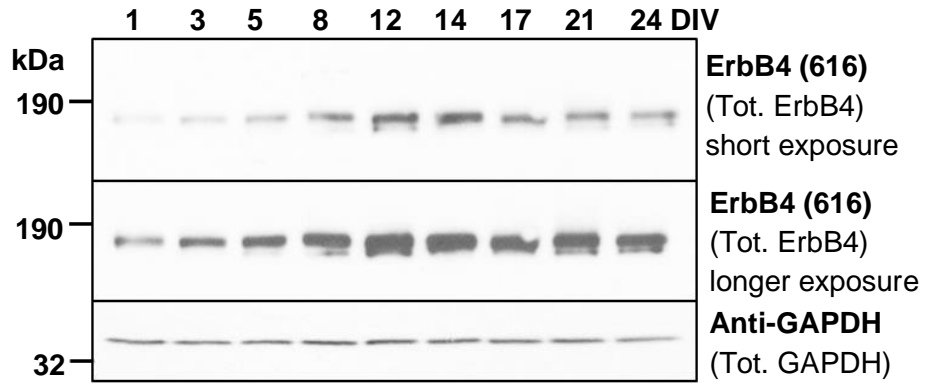
We further analyzed the levels of aPKC ζ protein in our cultures (Fig. 5.5B, second panel). At 1 DIV we detected very low levels of aPKC ζ . However, by 3 DIV, its expression was drastically upregulated, remaining high until 8 DIV. After 8 DIV aPKC ζ expression significantly decreased and by 14 DIV it returned to the low levels observed at 1 DIV.

We next analyzed the expression of Par6 in our cultures (Fig. 5.5B, third panel). We observed that Par6 was expressed at low levels at 1 DIV and steadily increased with time, peaking at 21-24 DIV (Fig. 5.5B, third panel).

Lastly, we analyzed the expression of Cdc42 in our cultures (Fig. 5.5B, fourth panel). The levels of Cdc42 were low in our cultures at the early time points (1-5 DIV) and increased with development. Between 5 and 8 DIV there was a spike in expression with its levels remaining high throughout all time points examined (Fig. 5.5B, fourth panel).

Fig. 5.5

A)



B)

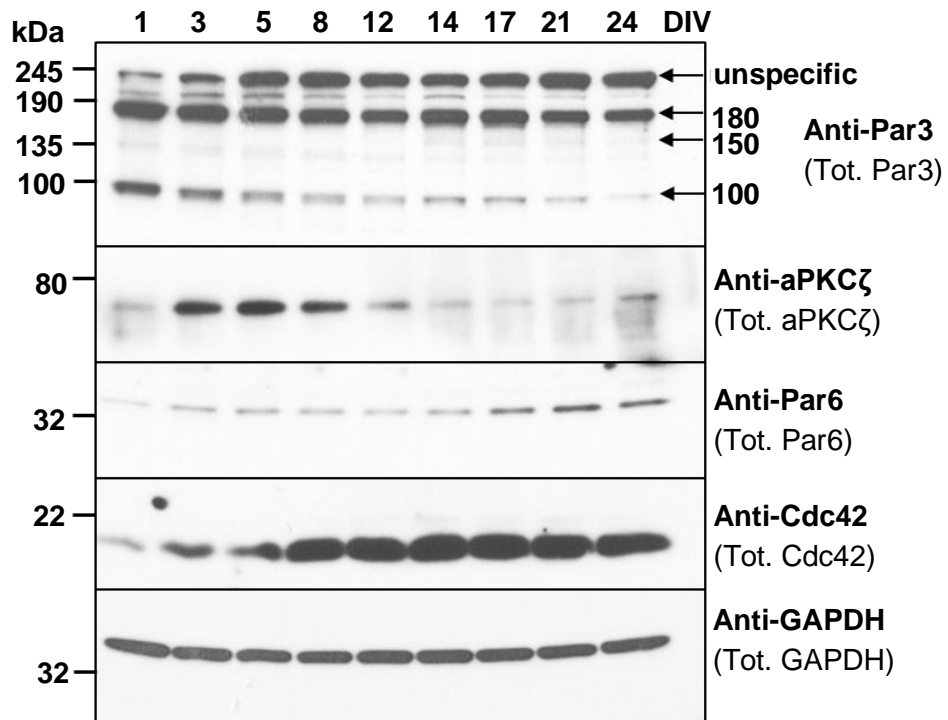


Figure 5.5: Developmental Expression of ErbB4 and Members of the Par Polarity Complex in Primary Cortical Cultures.

Expression of ErbB4 and members of the Par polarity complex are developmentally dynamic. Detergent extracts corresponding to 50 µg of protein per lane of primary cortical cultures grown for 1, 2, 5, 8, 12, 14, 17, 21, and 24 days (DIV), were analyzed by SDS-PAGE using 4-20% Tris-glycine gels followed by Western blotting. The blots were probed with anti-ErbB4 using serum #616 (**panel A, top and middle panels**; 1:5,000), anti-Par3 (**panel B, top panel**; 1:2,000), anti-aPKCζ (**panel B, second panel**; 1:2,000), anti-Par6 (**panel B, third panel**; 1:2,000), anti-Cdc42 (**panel B, fourth panel**; 1:2,000), and GAPDH (**panels A and B, bottom panels**; 1:5,000). These blots are representative of two experiments.

To determine whether ErbB4 and members of the Par complex associate in cortical cells, we utilized primary cortical cultures grown for 5 DIV prior to a 20 min activation with 500 ng/mL of GST or GST-Nrgs. Cells were then lysed and IP'ed for ErbB4 (Fig. 5.6A-G), Par6 (Fig. 5.6H and I), or mouse IgG (as a control; Fig. 5.6A, H, and I) and immunoblotted for ErbB4, Par6, Par3, aPKC ζ , phospho-aPKC ζ , Cdc42, and phospho-Cdc42 (Fig. 5.6). Our findings were consistent with our observations obtained using N2a/ErbB4 cells (Fig. 5.2-5.4). We observed that ErbB4 associated with all members of the Par complex (Par6, Par3, aPKC ζ , and Cdc42) and that these interactions increased upon GST-Nrg activation (Fig. 5.6A-G). These associations were confirmed by densitometric analyses as our measurements also revealed that association of ErbB4 with all members of the Par complex increased upon activation with the GST-Nrgs, compared to the GST activated control (Fig. 5.6B, C, and E). One exception was ErbB4 association with Cdc42. Although we observed a statistically significant increase in ErbB4-Cdc42 association upon activation with GST-Nrg2 and GST-Nrg3, our densitometric analyses revealed no significant differences between the GST-Nrg1 and GST control conditions (Fig. 5.6F). Bands corresponding to our proteins of interest were not observed in our control mouse IgG IPs, providing evidence that the observed associations between ErbB4 and members of the Par complex were not due to background binding or artifacts (Fig. 5.6A, lane C). Furthermore, as shown in Fig. 5.6A-G, all three GST-Nrgs enhanced ErbB4 association with Par6, Par3 (180 kDa), aPKC ζ , and Cdc42, suggesting overlap in their ability to induce ErbB4/Par complex formation among the Nrgs. Our densitometric analyses did not show any statistically significant differences between the GST-Nrg conditions and their ability to enhance ErbB4 association with members of the Par complex (Fig. 5.6B, C, E, and F). We did observe differences in ErbB4 association between the Par3 (150 kDa) and Par3 (100 kDa) isoforms, which was dependent on the identity of the GST-Nrg used for activation. GST-Nrg3 induced the greatest association between ErbB4 and Par3 (150 kDa) (Fig. 5.6A, lane N3). In contrast, GST-Nrg2 induced the greatest association between ErbB4 and Par3 (100 kDa) (Fig. 5.6A, lane N2).

These observations are consistent with those made in N2a/ErbB4 cells (Fig. 5.2), in spite that the levels of interaction in our cortical cultures were significantly lower (Fig. 5.5B, top panel) than in our N2a/ErbB4 cells (Fig. 5.1F, right panel).

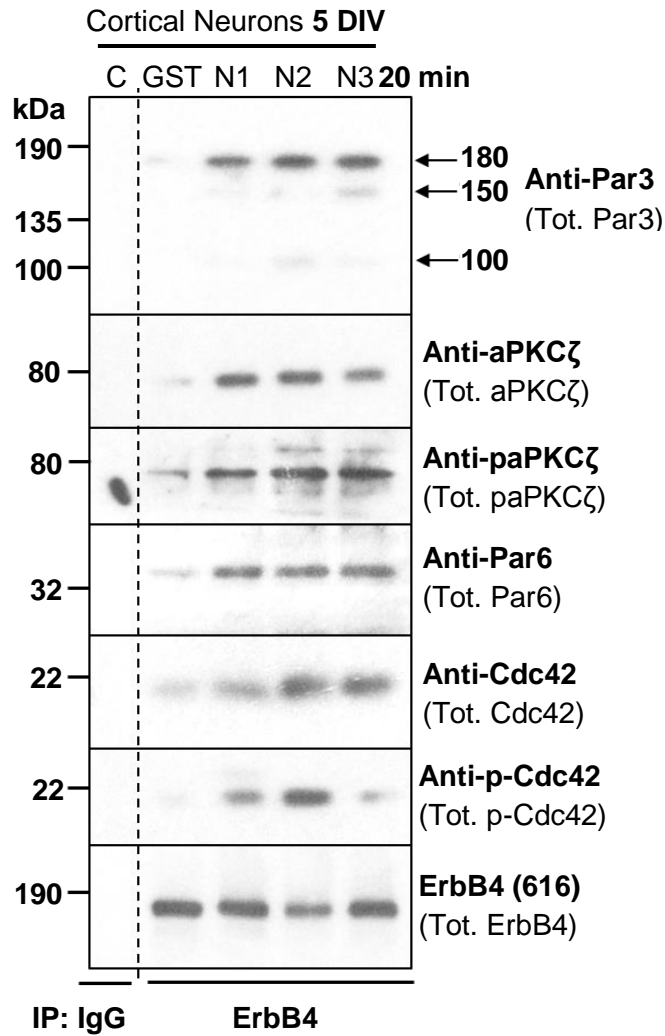
Previous studies have shown that Nrg1 activation can increase the phosphorylation of aPKC ζ in cortical neurons (Pandya & Pillai, 2014). Therefore, we also sought to determine if activation of ErbB4 by Nrg1-3 induced aPKC ζ phosphorylation in our cultures and its association with ErbB4 (Fig. 5.6A). As shown in Fig. 5.6A and D, we observed an increase in ErbB4 association with phospho-aPKC ζ in samples treated with GST-Nrg1-3, compared to samples that were activated with GST only (compare lane GST with lanes N1, N2, and N3). There was no statistically significant differences between ErbB4 and phospho-aPKC ζ association when comparing the different GST-Nrg conditions (Fig. 5.6D). We also explored whether ErbB4 could associate with phosphorylated Cdc42 (Fig. 5.6A and G). Upon activation with the GST-Nrg2, we observed an increase in ErbB4 association with phospho-Cdc42 compared to samples that were activated with the other GST-Nrgs or GST only (Fig. 5.6A and G, compare lane GST, N1, and N3 with N2). This association was confirmed through densitometric analyses (Fig. 5.6G).

Our Par6 IPs (Fig. 5.6H and I) in primary cortical cultures revealed that, in conjunction with an increase in association with ErbB4 upon GST-Nrg activation (Fig. 5.6A, B, and H), Par6 association with all members of the Par complex increased as well (Fig. 5.6H and I, lanes N1, N2, and N3), compared to the GST control (lane GST). Par6 association with Par3 (predominately the 180 kDa isoform), aPKC ζ , and Cdc42 were comparable between GST-Nrg activated samples (Fig. 5.6H and I, lanes N1, N2, and N3), suggesting that all three GST-Nrgs can regulate the association of the Par complex members. We further observed that activation with the GST-Nrgs resulted in an increase in association of Par6 with phosphorylated aPKC ζ and Cdc42 (Fig. 5.6H and I, lanes N1, N2, and N3), compared to the GST-activation control

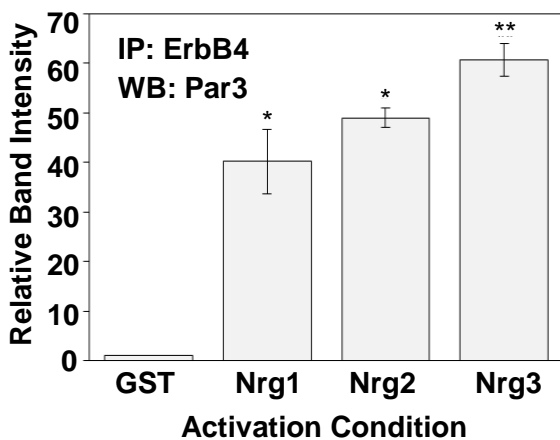
(Fig. 5.6H and I, lane GST). Overall our findings in primary cortical cultures show that GST-Nrg activation can regulate ErbB4 association with members of the Par polarity complex and that GST-Nrg activation also results in enhanced association of Par6 with the other members of the Par complex. These findings (Fig. 5.6) are in agreement with those observed in our N2a/ErbB4 cells (Figs. 5.2-5.4).

Fig. 5.6

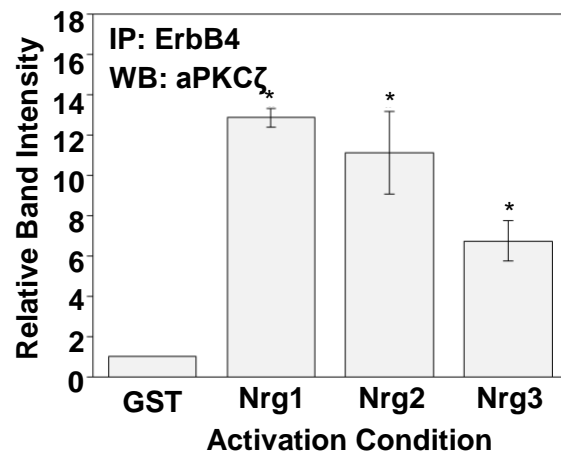
A)



B)



C)



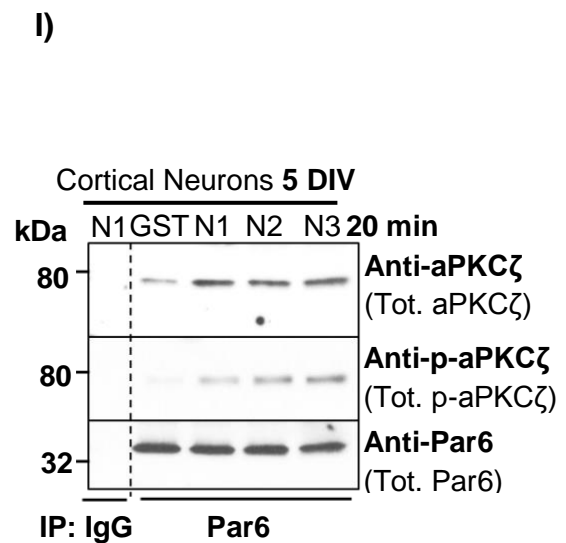
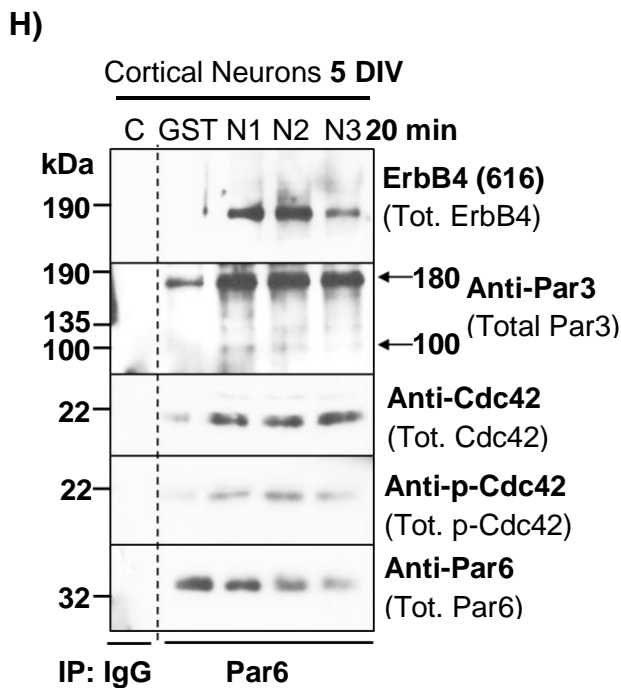
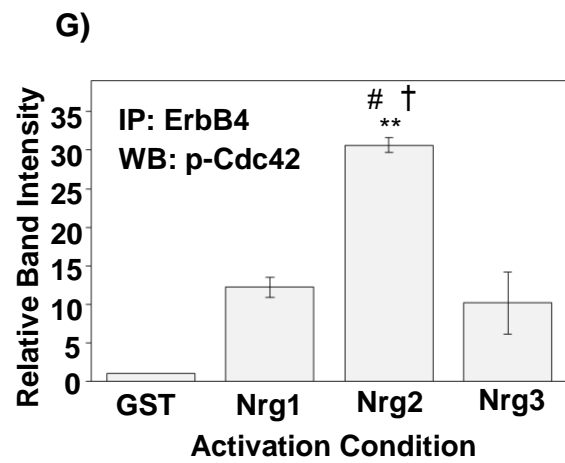
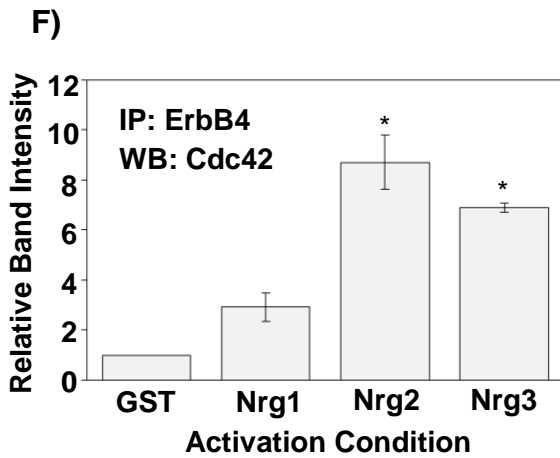
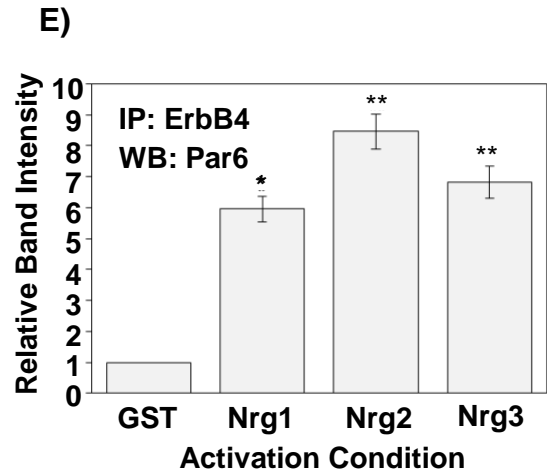
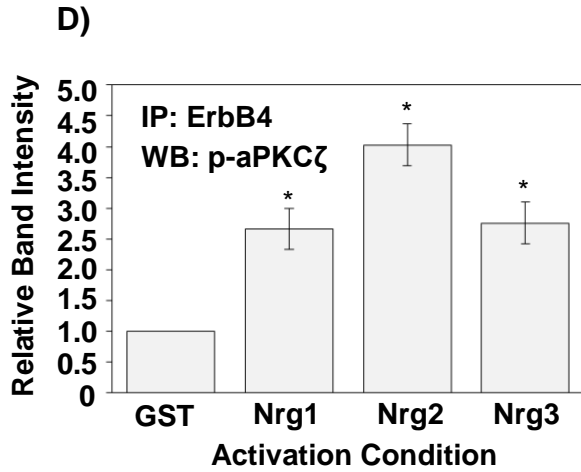


Figure 5.6: ErbB4 and Members of the Par Polarity Complex Associate in Primary Cortical Cultures in a Nrg-Dependent Manner.

A, H, and I) ErbB4 and the Par complex proteins increase their association upon GST-Nrg1-3 activation. Primary cortical cultures (5 DIV) were activated with 500 ng/mL of GST and GST-Nrg1-3 for 20 min. After protein normalization, the extracts were IP'ed with either ErbB4 (**panel A**) or Par6 (**panels H and I**). Samples were analyzed after SDS-PAGE using 4-20% gels followed by Western blotting. The membranes were probed with anti-ErbB4 using serum #616 (1:5,000), anti-Par3 (1:2,000), anti-aPKC ζ (1:2,000), phospho-aPKC ζ (1:1,2000), anti-Par6 (1:2,000), anti-Cdc42 (1:2,000), and anti-phospho-Cdc42 (1:2,000) to detect their interaction. These blots are representative of three experiments.

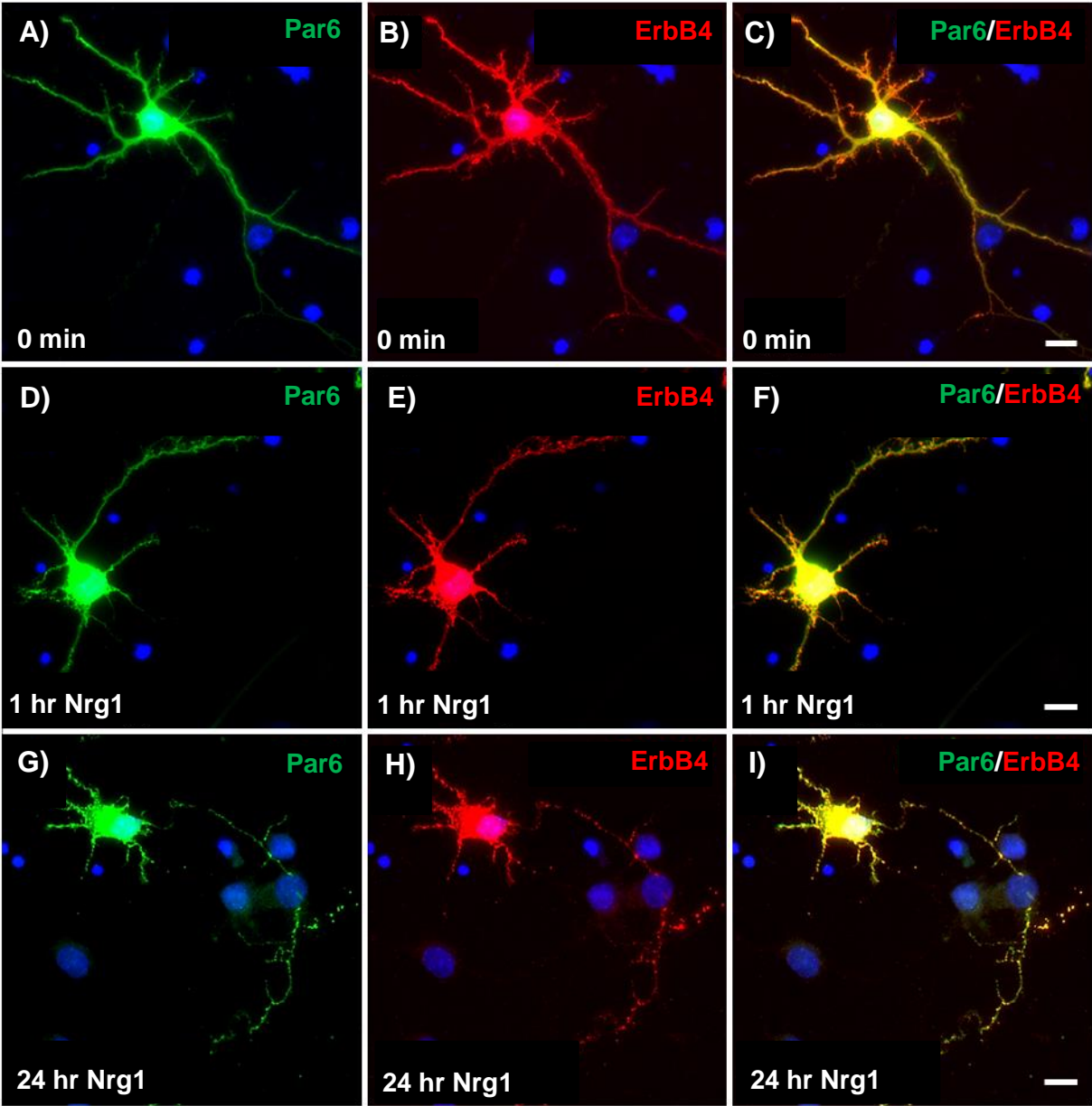
B-G) Band intensities were quantified from three experiments by densitometric analysis and used to calculate the ratios of Par3 180 kDa/ErbB4 (total ErbB4; **panel B**), aPKC ζ /ErbB4 (total ErbB4; **panel C**), p-aPKC ζ /ErbB4 (total ErbB4; **panel D**), Par6/ErbB4 (total ErbB4; **panel E**), Cdc42/ErbB4 (total ErbB4; **panel F**), p-Cdc42/ErbB4 (total ErbB4; **panel G**). The bars ("relative band intensity") represent the fold change from control (GST activation) which was considered 1. *, comparison to GST activation (*p = <0.05, **p = <0.01); #, comparison to GST-Nrg1 activation (#p = <0.05); †, comparison to GST-Nrg3 activation (†p = <0.05); n=3.

5.2.6 Nrg-Dependent ErbB4 and Par6 Co-Localization in Primary Cortical Neurons

The observations that ErbB4 associates with members of the Par polarity complex in a Nrg dependent manner that we described in the preceding sections were performed using biochemical immunoprecipitation experiments (Figs. 5.2-5.4 and 5.6). In these types of experiments, the protein-protein interactions may have been perturbed by the conditions in which the associations are tested, including buffer composition, levels of expression, length of incubation times with various reagents, and perhaps more importantly the spatial relationships between the interacting proteins may have been disturbed. To avoid some of these pitfalls, we also asked whether ErbB4 and Par6 co-localize in intact neurons, by performing immunocytochemistry experiments (Fig. 5.7). Towards this goal we have obtained preliminary data suggesting that Par6-ErbB4 co-localize in primary cortical cultures. We first co-transfected primary cortical cultures with myc-Par6 and ErbB4 at 5 DIV, and performed activation experiments at 8 DIV with GST-Nrg1 for 0 min (Fig. 5.7A-C and J-L), 20 min (data not shown), 1 hr (Fig. 5.7D-F and M-O), 6 hrs (data not shown), 12 hrs (data not shown) and 24 hrs (Fig. 5.7G-I and P-R) prior to staining for Par6 and ErbB4 (Fig. 5.7). At 0 min of activation (Fig. 5.7A-C and J-L) Par6 and ErbB4 were both present throughout the cell body and processes of cortical neurons (Fig. 5.7A-C). Higher magnification images of a neurite at this time point (0 hrs of activation) (Fig. 5.7J-L) showed strong punctate ErbB4 staining, in comparison to Par6 staining which was found in significantly fewer puncta with a more diffuse pattern of staining. We also observed several prominent puncta co-expressing both Par6 and ErbB4, as indicated by the arrows (Fig. 5.7J-L, arrows). When compared to cultures that were activated with GST-Nrg1 for 20 min or longer the neurons appeared to show an increase in the number and intensity of Par6/ErbB4 co-expressing puncta (Fig. 5.7D-I and M-R and data not shown). This increase of Par6/ErbB4 expressing puncta was observed within 20 min of GST-Nrg1 activation (data not shown) and continued to increase in size with activation time (Fig. 5.7D-F and M-O for

1 hr and G-I and P-R for 24 hrs). As can be observed in our higher magnification images (Fig. 5.7J-R), activation with GST-Nrg1 (Fig. 5.7M-R) resulted in strong punctate appearance for the Par6 staining, which was not observed at this level in our non-activated cells (0 min; Fig. 5.7J-L). Our preliminary data shows that activation with GST-Nrg1 induces ErbB4 and Par6 co-localization in the neurites and cell bodies of primary cortical neurons. However, these results must be verified through a quantitative analysis of the extent and intensity of the puncta that co-stain for Par6 and ErbB4.

Fig. 5.7



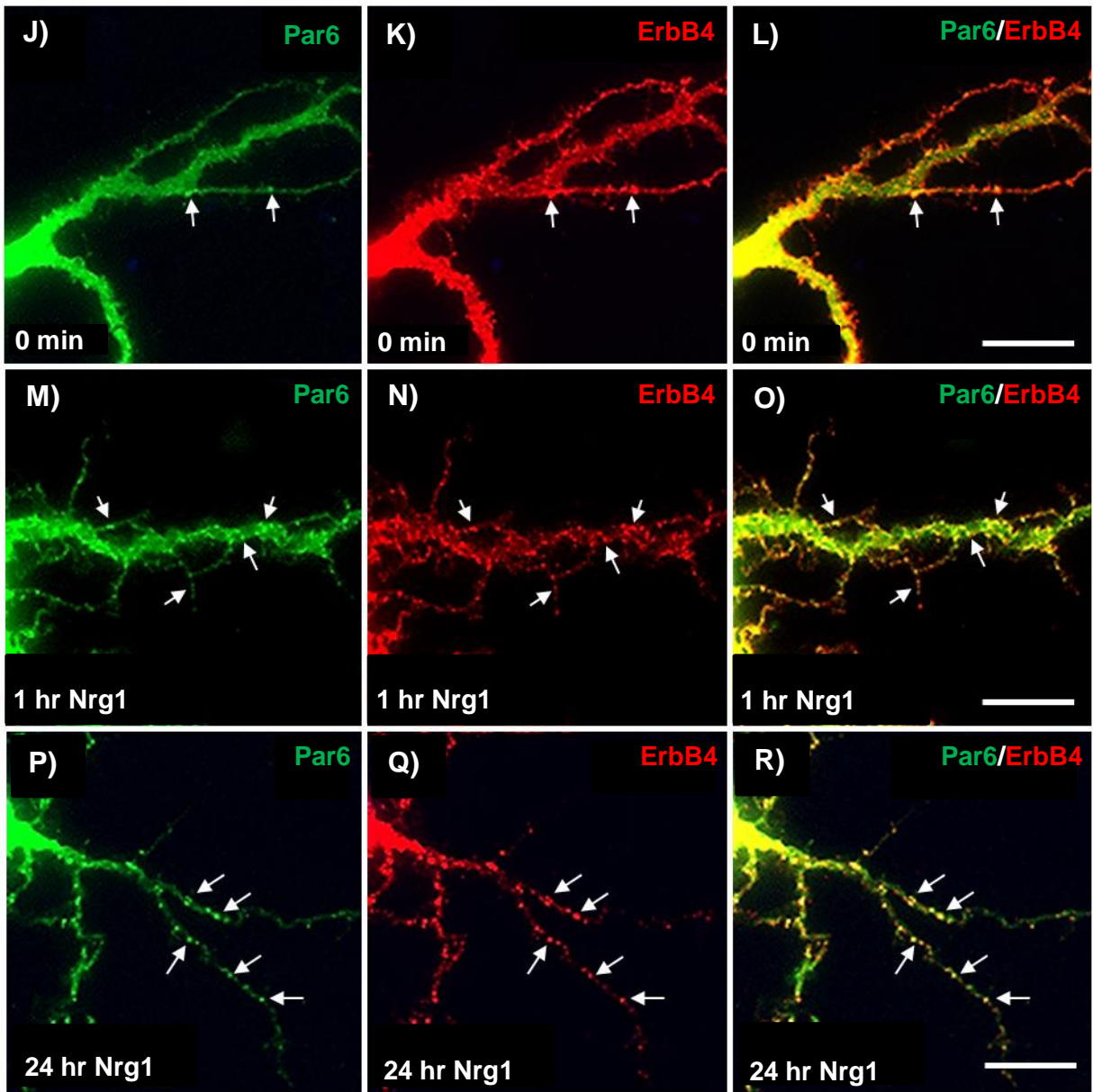


Figure 5.7: ErbB4 and Par6 Co-Localize in Primary Cortical Cultures.

Dissociated cortical cell cultures transfected with 2 μg of myc-Par6 and ErbB4 (8 DIV) were double-stained with anti-Par6 antibodies (1:500, **panels A, D, G, J, M, and P**) and with anti-ErbB4 antibodies (1:500, **panels B, E, H, K, N, and Q**) in the presence of 0.01% Triton X-100. The anti-Par6 antibodies were visualized with Alexa Fluor 488 goat anti-rabbit antibodies (in green) and the anti-ErbB4 antibodies with Alexa Fluor 594 goat anti-mouse antibodies (in red) both at 1:300 dilution. The nuclei were visualized using Hoechst 33342 (in blue, **panels A-I**). Scale bar = 15 μm for all panels.

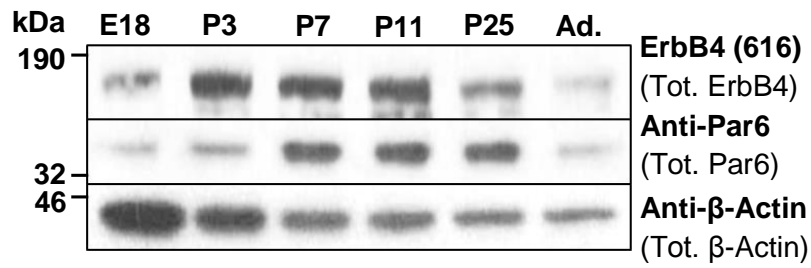
5.2.7 Developmental Expression and Association of ErbB4 and Members of the Par Complex in Cortical Tissue

Based on our observations in N2a/ErbB4 cells (Figs. 5.2-5.4) and primary cortical cultures (Fig. 5.6), we reasoned that ErbB4 should interact with members of the Par polarity complex in cortical brain tissue. Towards this goal, we first conducted a developmental time course of expression for ErbB4 and members of the Par complex in cortical tissue. Our results show that ErbB4 is present (Fig. 5.8A) at E18, the earliest time point that we measured, but at low levels. ErbB4 expression, however, increased substantially by P3 with its levels remained high until P11, prior to steadily decreasing into adulthood (Fig. 5.8A). In comparison, Par6 expression levels were low at E18 and P3 (Fig. 5.8A) and increased to maximal levels at P7, remaining high until P25, prior to decreasing into adulthood (Fig. 5.8A). We also analyzed the developmental expression of Par3 and Cdc42 in these lysates (Fig. 5.8B). Our observations of Par3 expression showed that at E18, the 180 and 100 kDa isoforms of Par3 were abundantly expressed (Fig. 5.8B, top panel), with their levels decreasing significantly as development progressed. By P25 the the 180 and 100 kDa isoforms were practically undetectable (Fig. 5.8B, top panel). We also observed that the Par3 150 kDa isoform was first detected at P3 and peaked at P11, a time when it was the most abundant Par3 isoform (Fig. 5.8B, top panel). After its peak of expression at P11, the expression of the 150 kDa isoform significantly decreased in adulthood (Fig. 5.8B, top panel). The predominant expression of the 150 kDa isoform of Par3 in cortical tissue differed from our *in vitro* observations in primary cortical neurons (Fig. 5.6) in which the 150 kDa isoform was only weakly expressed. We further observed low levels of Cdc42 immunoreactivity in E18 cortical tissue lysates (Fig. 5.8B, middle panel) that increased as development progressed. Cdc42 expression peaked at P7 prior to decreasing at later developmental stages (Fig. 5.8B, middle panel).

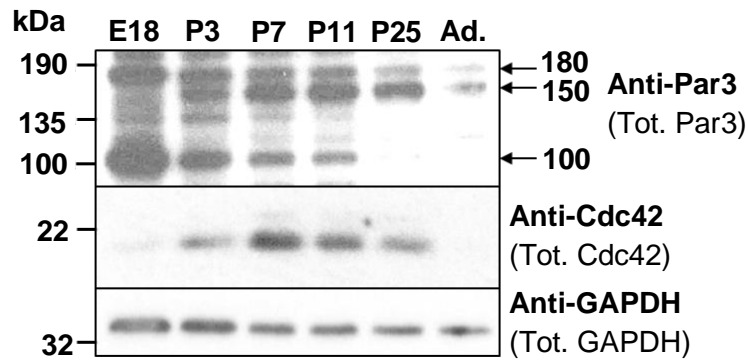
We next determined whether the association between ErbB4 and Par6 could be detected in cortical tissue (Fig. 5.8C and D) as we previously observed in neurons in culture (Fig. 5.6). Towards this goal, we IP'ed for ErbB4 (Fig. 5.8C) and Par6 (Fig. 5.8D) from cortical detergent extracts ranging from E18 to adult. We detected association between ErbB4 and Par6 at several stages of development. Association between ErbB4 and Par6 reached its maximal levels between P3 and P25, as observed for both ErbB4 and Par6 IPs (Fig. 5.8C and D). We did not observe bands corresponding to these two proteins in our control mouse IgG IPs (Fig. 5.8C and D). These results are consistent with our findings detecting ErbB4 and Par6 association in N2a cells (Fig. 5.2) and cortical neurons (Fig. 5.6). Overall, our findings show that ErbB4 and Par6 can interact in cortical tissue and that this interaction is dynamic during development.

Fig. 5.8

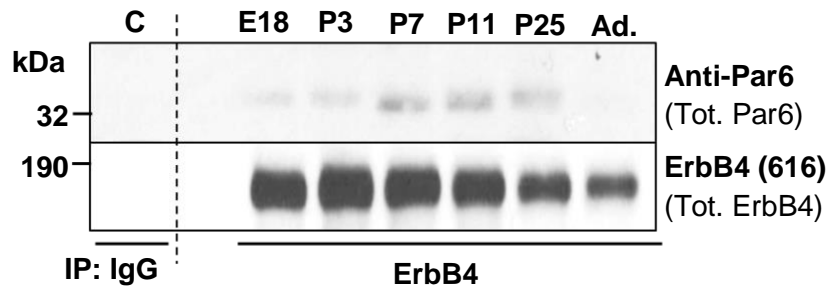
A)



B)



C)



D)

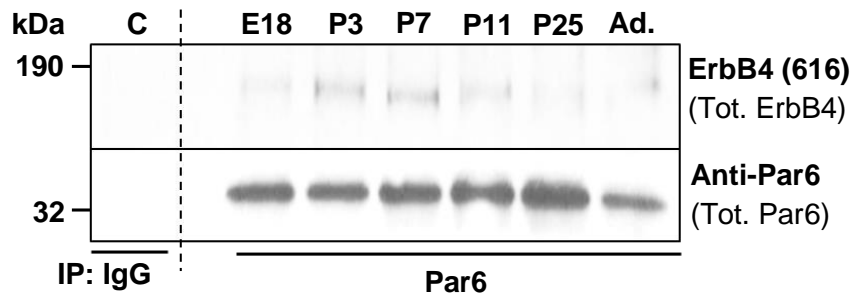


Figure 5.8: Developmental Expression and Association of ErbB4 and Members of the Par Complex in Cortical Tissue.

A and B) Detergent extracts from rat cortex corresponding to 50 µg of protein per lane of embryonic (E)18, postnatal (P) day 3, P7, P11, P25, and P50 (Ad.), were analyzed by SDS-PAGE using 4-20% Tris-glycine gels followed by Western blotting. The blots were probed with anti-ErbB4 using serum #616 (**panel A, top panel**; 1:5,000), anti-Par6 (**panel A, middle panel**; 1:2,000), β-actin (**panel A, bottom panel**; 1:5,000), anti-Par3 (**panel B, top panel**; 1:2,000), anti-Cdc42 (**panel B, middle panel**; 1:2,000), and anti-GAPDH (**panel B, bottom panel**; 1:5,000). These blots are representative of four experiments.

C and D) Detergent extracts from E18, P3, P7, P11, P25 and P50 (Ad.) rat cortices were normalized for protein and then IP'ed for either ErbB4 (**panel C**) or Par6 (**panel D**). The samples were analyzed after SDS-PAGE using 4-20% gels followed by Western blotting. The membranes were probed with anti-ErbB4 using serum #616 (1:5,000) and anti-Par6 (1:2,000) to detect their interaction. These blots are representative of four experiments.

5.2.8 ErbB4- Δ 204 Mutant Can Interact with Par6 and Par3 in N2a Cells

Our observations so far have indicated that ErbB4 and Par6 can interact in cells overexpressing ErbB4 and Par6 (N2a/ErbB4/myc-Par6 cells; Fig. 5.2), primary cortical cultures (Fig. 5.6 and 5.7), and cortical tissue (Fig. 5.8). We next sought to map the site of interaction of Par6 on the ErbB4 molecule. Previous studies have shown that the last four amino acid residues of ErbB4 (N-T-V-V) conform to a consensus motif, known as the PDZ binding (PDZb) domain, that can bind to class 1 PDZ domains (Garcia et al., 2000; A. Y. Hung & Sheng, 2002). This interaction has been documented between the ErbB4 PDZb domain and two class 1 PDZ domains of the post-synaptic density protein PSD-95 (Garcia et al., 2000). In addition, Par6 contains in its sequence a class 1 PDZ domain (Peterson, Penkert, Volkman, & Prehoda, 2004) which may be potentially recruited to associate with ErbB4 upon Nrg-activation.

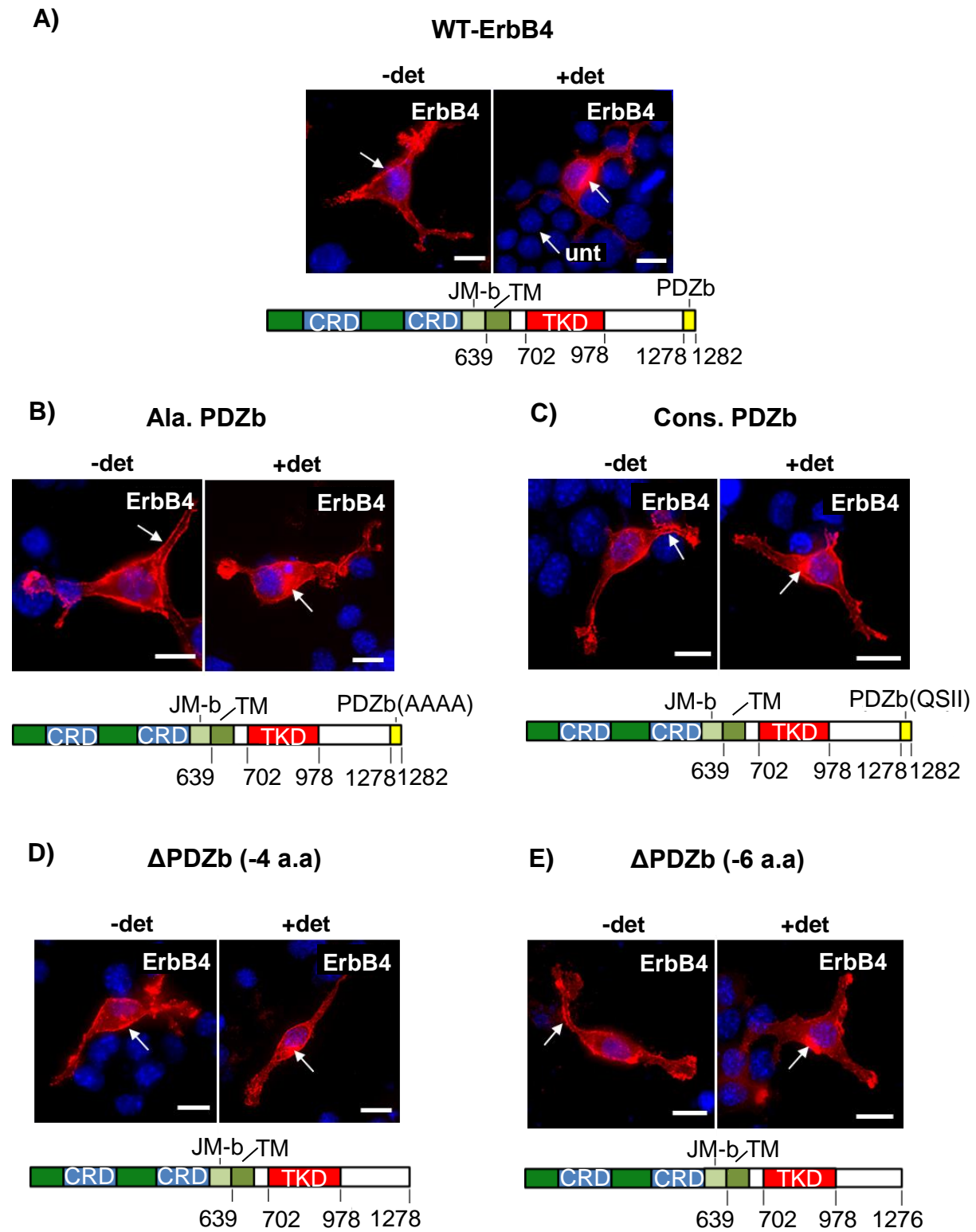
To test the possibility that ErbB4 interacts with Par6 through its PDZ domain, we generated several ErbB4 mutant constructs (Fig. 5.9) and analyzed whether these mutated ErbB4 proteins could still interact/IP with Par6 (Fig. 5.10). If the interaction occurs between the PDZ domain of Par6 and the PDZb domain of ErbB4, we would expect to eliminate their association when mutating the PDZb domain in ErbB4. As shown in the schematic diagrams in Fig. 5.9, we first generated several ErbB4 PDZb mutations including the replacement of the last four amino acid residues to alanines (ErbB4-AlaPDZb; Fig. 5.9B), converting the last four amino acids using conservative amino acid substitutions (amino acids with equivalent biochemical properties) to glutamine, serine, isoleucine, isoleucine (ErbB4-ConsPDZb; Fig. 5.9C), and deleting the last four or six amino acid residues entirely (ErbB4- Δ 4PDZb and ErbB4- Δ 6PDZb; Fig. 5.9D and E respectively). We also generated 2 larger deletion constructs missing the last 103 and 204 C-terminal amino acid residues in the ErbB4 cytoplasmic tail (ErbB4- Δ 103 and ErbB4- Δ 204; Fig. 5.9F and G respectively). After generating and sequencing our ErbB4 mutant constructs, we performed transfection experiments to determine whether the mutant proteins

were expressed and trafficked to the plasma membrane, where they could be activated by the Nrgs from the extracellular space (Fig. 5.9). For these experiments, N2a cells were transfected with wild-type (WT) ErbB4 (Fig. 5.9A) or one of the mutant ErbB4 constructs (Fig. 5.9B-G) prior to immunocytochemical staining for ErbB4. As shown in the immunofluorescence images in Fig. 5.9, for all the ErbB4 mutant constructs (Fig. 5.9B-G), we observed ErbB4 staining at the plasma membrane in the absence of detergent (-det). In the presence of detergent (+det), the ErbB4 staining was more intense within the cell body (Fig. 5.9B-G). The staining pattern for all ErbB4 mutants, both in the presence and absence of detergent, was consistent with that observed for WT ErbB4 (Fig. 5.9A). These findings demonstrate that our cDNAs encoding mutant forms of ErbB4 are competent to express ErbB4 proteins that can be inserted into the plasma membrane. Based on these results we proceeded to determine the site of interaction of ErbB4 and Par6 using these constructs.

To determine whether Par6 could bind to the mutated ErbB4 constructs, we first tested (Fig. 5.10) our largest deletion mutant construct (ErbB4- Δ 204). We reasoned that if Par6 interacted with ErbB4- Δ 204 then their interaction would probably not be mediated by the PDZb domain in ErbB4. Since PSD-95 has been shown to interact with ErbB4 through its PDZb domain (Garcia et al., 2000; A. Y. Hung & Sheng, 2002), we used it as a positive control for ErbB4 PDZb domain interaction. Since ErbB4- Δ 204 lacks the PDZb domain known to bind PSD95, its loss of ability to interact with this mutant would signal that using this construct can be used as a good indicator of a potential association with the PDZb domain in ErbB4. As shown in Fig. 5.10A, N2a cells were co-transfected with FLAG-PSD-95 and WT ErbB4 or ErbB4- Δ 204 prior to activation for 15 min with 500 ng/mL of GST-Nrg1. Our ErbB4 IPs (Fig. 5.10A) show that PSD-95 co-IP'ed with WT ErbB4 (top panel; lane WT) but did not co-IP with ErbB4- Δ 204 (top panel; lane Δ 204). These experiments indicate that the ErbB4- Δ 204 construct lacks its ability to interact with PSD-95 since it lacks the PDZb domain.

We next determined whether Par6 could co-IP with ErbB4- Δ 204 (Fig. 5.10B) by singly transfecting N2a cells with WT ErbB4 or ErbB4- Δ 204 or doubly transfecting N2a cells with myc-Par6 and WT ErbB4 or myc-Par6 and ErbB4- Δ 204. As shown in Fig. 5.10B, Par6 IP'ed with both WT ErbB4 (middle panel; lane WT) and ErbB4- Δ 204 (middle panel; lane Δ 204). These experiments show that Par6 most likely binds to ErbB4 at a site upstream of the carboxyl-terminal deletion which removed the last 204 amino acids in the ErbB4 tail. We further immunoblotted for Par3 in our ErbB4 IPs since all three isoforms of Par3 contain three PDZ domains, albeit they bind preferentially to class II PDZ consensus motifs (Izumi et al., 1998; Renschler et al., 2018). Similar to our findings for Par6, the 180 and 100 kDa isoforms of Par3 (Fig. 5.10B, top panel) co-IPed with both WT ErbB4 (lane WT) and ErbB4- Δ 204 (lane Δ 204). Overall, our findings have shown that ErbB4 does not interact with Par6 and Par3 within its last 204 amino acid residues, but at a site amino-terminal to this section within the ErbB4 cytoplasmic tail.

Fig. 5.9



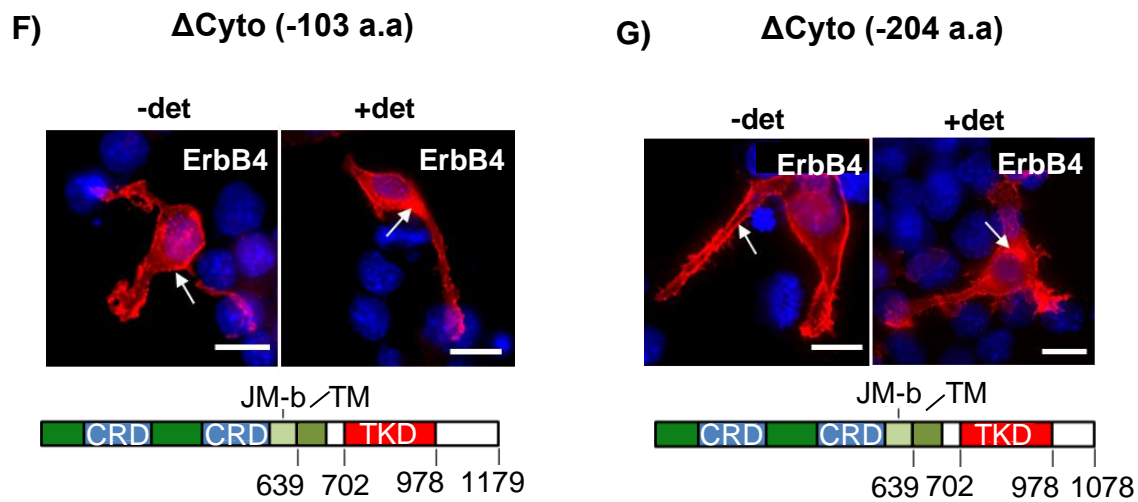


Figure 5.9: Characterization of C-terminal ErbB4 Mutant Constructs.

Anti-ErbB4 antibodies were used to detect the localization and trafficking of wild-type (**panel A**) and mutant ErbB4 constructs (**panels B-G**) by immunocytochemistry in the absence of (-det) and in the presence of 0.01% Triton X-100 (+det). N2a cells (**panel A, unt**) were transfected with 2 μ g of wild-type ErbB4 (**panel A**), ErbB4-AlaPDZb (**panel B**), ErbB4-ConsPDZb (**panel C**), ErbB4- Δ 4PDZb (**panel D**), ErbB4- Δ 6PDZb (**panel E**), ErbB4- Δ 103 (**panel F**), and ErbB4- Δ 204 (**panel G**) prior to staining with anti-ErbB4 (1:500 dilution). Anti-ErbB4 was detected using secondary antibodies coupled to Alexa Fluor 594 (in red) at 1:300 dilution. The nuclei were visualized using Hoechst 33342 (in blue). Scale bar = 15 μ m for all panels. Schematic diagrams summarizing the mutant forms of ErbB4 used are also provided below each panel.

Fig. 5.10

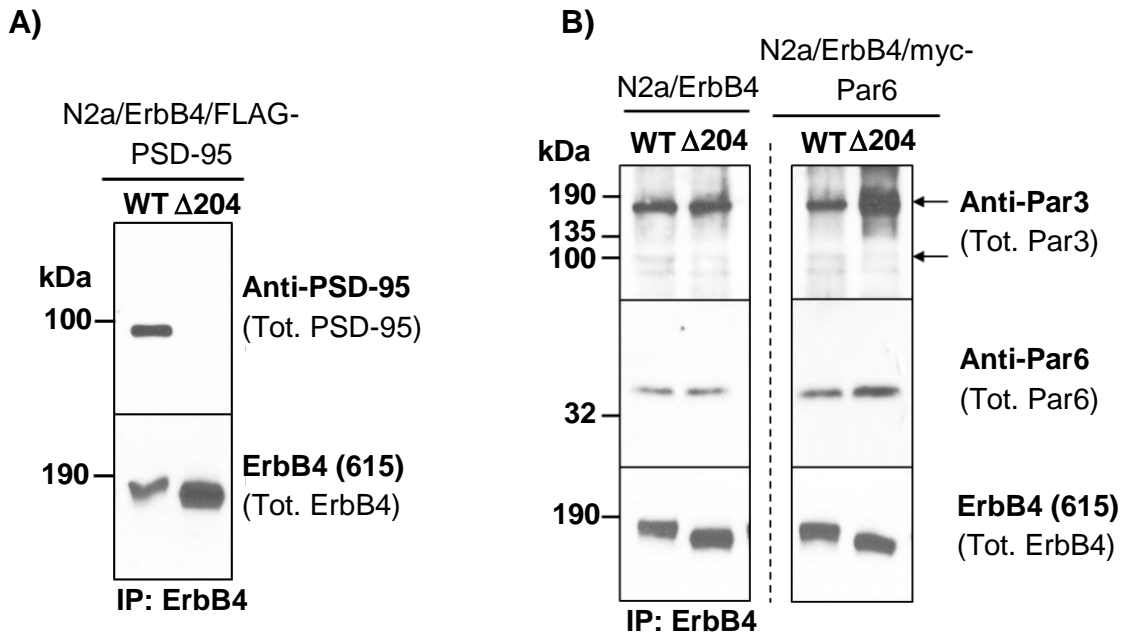


Figure 5.10: ErbB4-Δ204 Does Not Bind to PSD-95 but Can Bind to Par6.

A) N2a cells were doubly transfected with 1 μ g of FLAG-PSD-95 and either 1 μ g of wild-type ErbB4 (lane WT) or 1 μ g of ErbB4-Δ204 (lane Δ204). The cells were activated for 15 min with 500 ng/mL of GST-Nrg1. After protein normalization, the extracts were IP'ed for ErbB4. Samples were analyzed after SDS-PAGE using 4-20% gels followed by Western blotting. The membranes were probed with anti-ErbB4 serum #615 (1:5,000) and anti-PSD-95 (1:2,000).

B) N2a cells were transfected with 1 μ g of wild-type ErbB4 (left panel, lane WT), 1 μ g of ErbB4-Δ204 (left panel, lane Δ204), or doubly transfected with 1 μ g of myc-Par6 and either 1 μ g of wild-type ErbB4 (right panel, lane WT) or 1 μ g of ErbB4-Δ204 (right panel, lane Δ204). The cells were then activated for 15 min with 500 ng/mL of GST-Nrg1. After protein normalization, the extracts were IP'ed for ErbB4. Samples were analyzed after SDS-PAGE using 4-20% gels followed by Western blotting. The membranes were probed with anti-Par6 (1:2,000) and anti-ErbB4 using serum #615 (1:5,000). This blot is representative of two experiments.

5.3 DISCUSSION:

The Nrgs and their receptors, the ErbBs, have previously been shown to regulate biological events that are important for cortical development and neuronal maturation, such as roles in neuronal migration, the development and maintenance of the radial glial scaffold, and dendritic spine morphogenesis (Anton et al., 1997; Barros et al., 2009; Y.-J. J. Chen et al., 2008; Louhivuori et al., 2018; Mei & Nave, 2014; Rio et al., 1997; Schmid et al., 2003; Yin, Sun, et al., 2013). In addition, the Par polarity complex, consisting of the interacting proteins Par6, Par3, aPKC, and Cdc42, is a critical polarity regulator during neuronal morphogenesis and migration as well as a key player in the development of dendritic spines (Arimura & Kaibuchi, 2005; Chou et al., 2018; Hapak, Rothlin, et al., 2018; Insolera et al., 2011; Takashi Nishimura et al., 2004; Sakakibara & Hatanaka, 2015; Sakamoto et al., 2018; S.-H. Shi et al., 2003; H. Zhang & Macara, 2006, 2008). In this study, we have shown a novel Nrg-dependent association between ErbB4 and members of the Par polarity complex, suggesting a molecular mechanism that may be underlying ErbB4 mediated cortical neuronal polarization or dendritic maturation.

It has previously been reported that both Nrg-ErbB signaling and the Par complex play important roles in the establishment and maintenance of the highly polarized radial glial scaffold. The roles of Nrg1 and ErbB2/4 have previously been shown to stimulate the migration of cortical and cerebellar granule neurons along radial glial fibers, promote the elongation of radial glia, and regulate the differentiation of radial glia into astrocytes (Anton et al., 1997; Rio et al., 1997; Schmid et al., 2003). In addition, the Par polarity complex localizes to the apical adherens junctions of radial glia and regulates their asymmetric cell division, as well as facilitates radial glial morphology (Bultje et al., 2009; Cappello et al., 2006; L. Chen et al., 2006; Costa et al., 2008; Ghosh et al., 2008; Yokota et al., 2010). Alterations in the radial glial scaffold can result in aberrancies in migration along radial fibers and deficits in brain morphogenesis. Our findings in this chapter have shown that ErbB4 can associate with the Par complex in cortical neurons and

that this association can be enhanced by Nrg activation (Figs. 5.6 and 5.8). Due to their roles in the formation and maintenance of the radial glial phenotype, it is possible that ErbB4 interaction with the Par complex could play a role in these biological processes, resulting in the regulation of radial glial morphology and ultimately the migration of neurons to the developing cortical plate. It would be of interest to conduct these experiments in animals at E13-E16 when radial migration is at its peak. In addition, analyzing the development of the radial glial scaffold in rodents expressing ErbB4 deficient for Par6 binding would also be a compelling future direction.

A previous study by Aranda et al (2006) showed that the overexpression and activation of ErbB2, in a breast cancer model, resulted in a time-dependent association of ErbB2 with Par6-aPKC ζ . Subsequently, in these cells, Par3 association with Par6-aPKC ζ decreased upon ErbB2 activation and epithelial cell polarity was disrupted (Aranda et al., 2006). In parallel, our findings (Figs. 5.2, 5.3, 5.6, and 5.8) show that ErbB4, a binding partner of ErbB2, interacts with Par6 and associates with aPKC ζ in N2a cells (Figs. 5.2 and 5.3) and cortical neurons (Figs. 5.6 and 5.8), in a Nrg1-3 activation dependent manner. Furthermore, we could detect these interactions in cortical tissue extracts (Fig. 5.8). These findings indicate that ErbB4 can associate with members of the Par complex in a neuronal system. Since ErbB4 expression is mostly limited to GABAergic interneurons and preferentially within the parvalbumin-positive subset (Fazzari et al., 2010; Neddens et al., 2011; Vullhorst et al., 2009), the interactions between ErbB4 and the Par complex could be regulating neuronal polarity in these interneurons.

In contrast to the findings of Aranda et al., we did not observe a disruption of the Par complex upon activation of ErbB4, as Par6 bound to and increased interaction with all members of the Par complex following GST-Nrg activation (Figs. 5.2 and 5.6). There are several reasons why our experiments may not have shown a disruption of the Par complex upon ErbB4 activation by Nrg. Firstly, our findings in primary cortical neurons (Fig. 5.6) were observed in

cells expressing endogenous levels of ErbBs, and not in the context of breast cancer cells that overexpressed ErbB2 as were utilized in Aranda et al. This suggests that disruption of the Par complex upon ErbB2 activation may be unique to the mammary gland or particular tumoral cells overexpressing ErbB2. Another possibility for why we may not have observed a disruption in the Par complex is due to the methods used to activate ErbB4 in our cultures, in comparison to those implemented in Aranda et al. Previous studies have observed that the overexpression of ErbB2, as well as other RTKs, results in ligand-independent dimerization and activation of the receptors [reviewed in (Du & Lovly, 2018)]. The cell lines used in Aranda et al were not only overexpressing ErbB2, but were further activated using an antibody to induce ErbB2 dimerization. In comparison, our N2a/ErbB4 cells (Figs. 5.2-5.4) and primary cortical cultures (Fig. 5.6) were activated using the ErbB4 ligands, Nrg1-3. It is possible that ligand-independent activation of ErbB2 differs in its downstream signaling compared to signaling induced by Nrg-activation, resulting in the disruption or association of the Par complex, respectively. This rationale is based on previous reports that different ErbB receptor combinations can initiate unique receptor phosphorylation and downstream activity (Alroy & Yarden, 1997). It is important to note that our experiments using N2a/ErbB4 cells did overexpress the ErbB4 isoform JM-b CYT-2. However, one report in MCF-7 transfected cells showed that the JM-b CYT-2 isoform does not auto-phosphorylate in a ligand-independent manner, unlike the cleavable ErbB4 JM-a CYT-2 isoform (Määttä et al., 2006), further supporting that our findings of ErbB4 interaction with members of the Par complex were dependent on Nrg-activation.

The Par complex plays a crucial role in axon specification and elongation (Higginbotham, Tanaka, Brinkman, & Gleeson, 2006; Takashi Nishimura et al., 2004, 2005; Schwamborn & Püschel, 2004; S.-H. Shi, Cheng, Jan, & Jan, 2004; S.-H. Shi et al., 2003; Vohra, Fu, & Heuckeroth, 2007; Yi, Barnes, Hand, Polleux, & Ehlers, 2010). As hippocampal or cortical neurons polarize, the subcellular distributions of Par3 and Par6 become asymmetrically

distributed and are selectively enriched at the tip of the future axon, where they can regulate the actin and microtubule cytoskeletons. The disruption of Par3, Par6, and Cdc42 function, either by ectopic expression or downregulation by RNA interference, or the pharmacological inhibition of PKCs generally prevents neurites from differentiating into either dendrites or axons (Insolera et al., 2011; Takashi Nishimura et al., 2005; Schwamborn & Püschel, 2004; S.-H. Shi et al., 2003; Wiggin et al., 2005). Similarly, the overexpression of ErbB4, in conjunction with Nrg1 treatment, in hippocampal interneurons was previously reported to increase the number of primary neurites which failed to develop into mature and elongated dendrites (Krivosheya et al., 2008). These previous reports, in conjunction with our findings in this chapter that show ErbB4-Par complex association, suggest that ErbB4 interaction with the Par complex may play an intimate role together in axon/dendrite differentiation. Future experiments analyzing the differentiation of neurites using rodents expressing ErbB4 deficient for Par6 binding would be necessary to test this hypothesis.

One striking observation we made in these studies was the strong association of the 100 kDa isoform of Par3 with ErbB4 upon GST-Nrg2 activation, which was not observed to be as robust after activation with GST-Nrg1 or GST-Nrg3 (Figs. 5.2 and 5.6). The *Par3A* gene encodes three proteins with varying sizes: the full length 180kDa isoform and the truncated 150kDa and 100kDa variants, all which contain three PDZ domains corresponding to class II PDZ consensus motifs (Izumi et al., 1998; Lin et al., 2000; Renschler et al., 2018). The 100kDa isoform is unique because it lacks the region necessary to bind and phosphorylate aPKC (Lin et al., 2000). Although there are no reports analyzing the functional differences between the alternatively spliced variants of Par3, other than their binding properties, they have been observed to differ in expression profiles (described in detail below), suggesting differences in biological roles (Lin et al., 2000; Takashi Nishimura et al., 2004; Sun, Asghar, & Zhang, 2016; H. Zhang & Macara, 2006).

Previous studies have reported that between E9.5-E14.5 and in adult tissue, the predominant isoform of Par3 is the 180 kDa protein. This is also the case in cultured immature and mature hippocampal neurons. The truncated 100 kDa isoform has also been reported in these tissues as well (Lin et al., 2000; Takashi Nishimura et al., 2004; Sun et al., 2016; H. Zhang & Macara, 2006). These previous reports are consistent with our observations in cultured cortical neurons and E18 cortical tissue (Fig. 5.5 and 5.8). In contrast to previous reports obtained from whole brain, we detected that the most highly expressed form is the 150 kDa Par3 variant (Fig. 5.8) between P7-P25. This pattern of expression is time dependent, as the 150 kDa variant was not observed at E18 and was also detected at low levels in adulthood (Fig. 5.8). These findings further suggest unique functional roles of the Par3 isoforms, where the 150 kDa isoform may be a key regulator of postnatal cortical development and the 180 and 100 kDa isoforms may play a different role during embryonic and postnatal development and regions other than cortex.

Our analyses (Fig. 5.8) of the developmental expression of ErbB4 and members of the Par complex in cortical tissue lysates demonstrated that ErbB4, Par6, Par3 (150 kDa), and Cdc42 expression all peaked at P7, suggesting biological roles for these proteins at this developmental stage. This age (P7) in rodent brain development corresponds to a transient period of rapid growth known as the “brain growth spurt” (Bockhorst et al., 2008; Dobbing & Sands, 1979; Semple, Blomgren, Gimlin, Ferriero, & Noble-Haeusslein, 2013) as well as the peak time of gliogenesis (Catalani et al., 2002; Kriegstein & Alvarez-Buylla, 2009; Semple et al., 2013) and a period of substantial increase in axonal and dendritic density (Baloch et al., 2009; Cowan et al., 2003; Semple et al., 2013). These events rely on the initiation and maintenance of proper cell polarity for normal brain morphogenesis. It would be of interest to test whether the inhibition of ErbB4 binding to the Par complex would result in aberrancies in any of the aforementioned developmental events.

Other than roles in regulating polarity-driven events, ErbB4 and members of the Par complex (Par3 and Par6-aPKC) have also been shown to promote dendritic spine formation and maturation (Barros et al., 2009; Y.-J. J. Chen et al., 2008; Goda & Davis, 2003; Hering & Sheng, 2001; B. Li et al., 2007; Sheng & Hoogenraad, 2007; Yin, Chen, et al., 2013; H. Zhang & Macara, 2006, 2008). The deletion of Nrg1 or the knockdown of Par3 or Par6 results in a reduction in spine morphogenesis on pyramidal neurons. In addition, our preliminary experiments in Fig. 5.7 demonstrated that ErbB4 and Par6 can co-localize within puncta, along dendrites. Nrg1 treatment enhanced ErbB4 and Par6 co-localization forming puncta along the dendrites; however, these data need to be quantified to unambiguously make this assessment. A compelling future direction would be to observe whether ErbB4 association with members of the Par complex is necessary for dendritic maturation and spine formation of GABAergic interneurons. It is important to note, however, that a large proportion of GABAergic cells do not possess spines. Experiments analyzing spine formation could be conducted using rodents or cells expressing an ErbB4 mutant deficient for Par complex binding (discussed further in Chapter 6).

One hypothesis regarding the ErbB4-Par complex interaction was that ErbB4 may be binding to the Par6 class I PDZ domain through its class I PDZ binding motif (PDZb), located within the last four amino acids of the receptor. It has previously been shown that ErbB4 can bind to PDZ domain containing proteins, such as PSD-95 (Garcia et al., 2000; Y. Z. Huang et al., 2000). Contrary to this hypothesis, our findings (Fig. 5.10) showed that ErbB4 and Par6 are not interacting within the last 204 amino acids of ErbB4 (ErbB4- Δ 204), confirming that ErbB4 is not binding to Par6 through its PDZb domain. This raises the question of where ErbB4 is binding to the Par complex and whether they are binding directly. Although there are several possibilities for how and where the Par complex is binding to ErbB4, the hypothesis presented here is particularly striking due to supporting data from previous published reports. ErbB4

contains a number of docking sites along its cytoplasmic tail for the signaling effectors Shc and Grb2 [reviewed in (Wilson, Gilmore, Foley, Lemmon, & Riese, 2009)], which leads to the activation of the MAPK/ERK pathway [reviewed in (Blenis, 1993)]. It has previously been shown in an epithelial cell line that the Grb2-associated-binding protein 1 (Gab1) can bind and stimulate the phosphorylation of Par3 and act as a negative regulator of apical-basal polarity by competing with Par6 for binding of the Par3 PDZ1 domain (Z. Yang et al., 2012). However, in a recent 2018 study, Par3 was observed to simultaneously bind to two Par6 proteins via its PDZ1 and PDZ3 domains (Renschler et al., 2018), suggesting that Par3 could bind to Gab1 at PDZ1 and Par6 at PDZ3. Our ErbB4- Δ 204 mutant construct encompassed a large enough deletion to delete all known Shc and Grb2 binding sites along the cytoplasmic tail (Wilson et al., 2009), except for one Shc binding site which was previously reported by a study to be located within the tyrosine kinase domain (TKD) of ErbB4 (pY733) (Schulze, Deng, & Mann, 2005). It is important to note, however, that this site was not identified as a Shc binding site in a later report (Hause et al., 2012). These conflicting reports raise questions about the ability of this sequence to bind Shc, but the discrepancy could also be explained by methodological differences. It is therefore possible that activation of ErbB4 results in Shc binding to pY733 of ErbB4 initiating the recruitment of Grb2 \rightarrow Gab1/2 \rightarrow Par3/Par6/aPKC/Cdc42 (See Fig. 5.11 for schematic of proposed interaction). To explore if ErbB4 is interacting with the Par complex through this proposed pathway, an ErbB4 construct with a single point mutation at Y733, that would result in the loss of Shc interaction at this site, could be generated and tested for its ability to bind to members of the Par complex.

In summary, ErbB4 interacts with the Par polarity complex in cortical neurons and this interaction can be enhanced upon Nrg activation. These findings identify a potential molecular mechanism that may be regulating cortical neuronal polarity or neuronal maturation, and unveils possible biological targets for therapies where neuronal polarity is abnormal.

Fig. 5.11

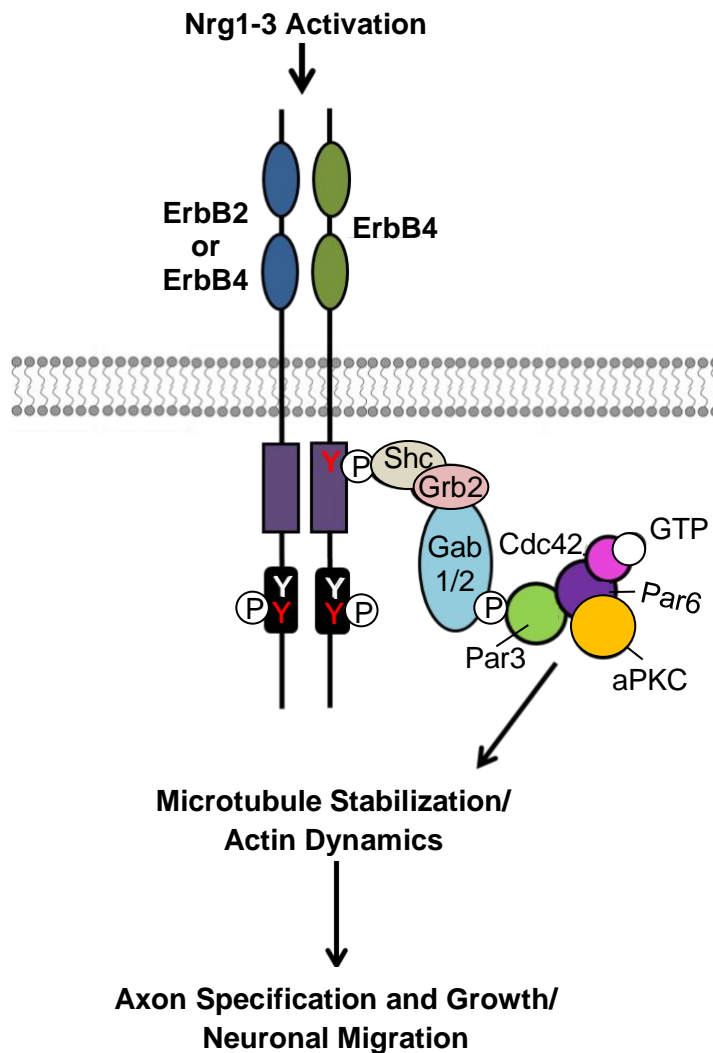


Fig. 5.11: Proposed Interaction of ErbB4 with the Par Polarity Complex.

Activation of ErbB4 by Nrg1-3 results in receptor dimerization and phosphorylation of tyrosine residues. The Shc adaptor protein can bind to pY733 located on the tyrosine kinase domain (TKD) of ErbB4, resulting in the recruitment of Grb2 and Gab1/2. Gab1/2 can then bind to the PDZ1 domain of Par3, resulting in Par3 phosphorylation. Simultaneously, Par3 can recruit Par6/aPKC/Cdc42 through Par6 binding to the PDZ3 domain of Par3. This interaction can result in the activation of pathways responsible for microtubule stabilization and actin dynamics important for regulating axon specification and growth, as well as neuronal migration.

Chapter 6: Discussion and Future Directions

6.1 Summary and Significance

The Nrgs and ErbB4 play important roles in the developing and mature nervous system, including roles in neuronal migration, neuronal differentiation, and synaptogenesis among others. The majority of the studies on Nrg2 function in the CNS and PNS have focused on the roles for Nrg1, while those of Nrg2 and considerably Nrg3 have remained understudied. The results of the experiments described in this thesis strongly suggest that Nrg3 is likely to play important roles in the CNS, given that throughout development and in adulthood it is more widely distributed and more abundantly expressed than both Nrg1 and Nrg2. These studies also delineated previously unrecognized brain regions where Nrg3 could be playing important biological functions and those where the functions of Nrg 1, 2 and 3 could be redundant. Our studies have also contributed with the first description of a potential role for all 3 Nrgs in the differentiation of GABAergic interneurons. We completed an extensive quantitative analysis on the effects that Nrg1, Nrg2, and Nrg3 have on the acceleration of neurite elongation, the increase in the number of neurites, and the increase in the proportion of neurons with higher number of neurites over control. These effects appear to be mediated through activation of ErbB4, which is endogenously expressed in this class of neurons. Finally, for the first time, we report a novel association between ErbB4 and members of the Par polarity complex, a protein complex involved in the establishment of neuronal polarity and also neuronal plasticity. Our studies for the first time provide a link between extracellular activation of an RTK receptor (ErbB4) and the change in association with members of the Par polarity complex in the CNS.

Overall, our findings have provided extensive new knowledge on the localization of a poorly characterized Nrg, Nrg3, in the CNS. We have also addressed several gaps in the literature by describing novel molecular players involved in the differentiation of GABAergic interneurons and

identified proteins in the Par polarity complex as novel molecular players that can underlie Nrg/ErbB4 signaling in the developing nervous system.

6.2 Does the Nrg-ErbB4 Signaling Network Play a Role in Neuronal Polarity and/or Neuronal Morphology?

Nrg-ErbB signaling plays important roles in polarity-driven events during neurodevelopment, such as neuronal migration and differentiation [reviewed in (Mei & Nave, 2014)]. Our contribution from the findings of this thesis suggest that Nrg-ErbB4 signaling may play a role in neuronal polarity or other biological roles associated with the Par polarity complex. We demonstrated a novel Nrg-dependent association of ErbB4 with the Par complex (Chapter 5), a group of proteins that are critical for brain morphogenesis, including roles in axonal formation, neuronal migration, and dendritic spine development (Arimura & Kaibuchi, 2005, 2007; Polleux & Snider, 2010; Takano, Xu, Funahashi, Namba, & Kaibuchi, 2015; Yoshimura, Arimura, & Kaibuchi, 2006; H. Zhang & Macara, 2006, 2008). We also demonstrated that Nrg activation can enhance axonal elongation of ErbB4/GABA (+) interneurons (Chapter 4), an important event during the establishment of neuronal polarity (Arimura & Kaibuchi, 2005, 2007; Yoshimura et al., 2006).

One of the main limitations of our studies, however, is that we did not directly address whether ErbB4-Par complex association was involved in the enhancement of axon growth observed upon Nrg-activation. Several growth factors have been implicated as upstream regulators of the Par complex during axonal growth (Insolera et al., 2011; Polleux & Snider, 2010). It has also previously been shown that the Par complex can mediate the axon outgrowth effects of nerve growth factor (NGF) and netrin-1 in DRG neurons (Hengst, Deglincerti, Kim, Jeon, & Jaffrey, 2009). Given these observations it is possible that Nrg-dependent ErbB4 interaction with the Par complex is also mediating axon growth of GABAergic interneurons. To

address this gap, experiments using ErbB4 mutants identified to be deficient in Par complex binding could be tested for their ability to mediate axonal and dendritic outgrowth in GABAergic interneurons. If ErbB4-Par complex association is involved in Nrg dependent changes of axon/dendritic elongation or neurite number, neurons expressing ErbB4 deficient for Par complex binding should not show an enhancement of neurite length or number, compared to neurons expressing wild-type ErbB4. Although our efforts to identify the Par protein interaction site on ErbB4 were not successful, they allowed us to discard amino acids 1079-1283 corresponding to the last 204 amino acids of the C-terminal tail as Par6 and Par3 binding sites (Fig. 5.10). Further studies using alternative deletion constructs of ErbB4 are required to narrow down the binding site or sites for members of the Par polarity complex. Unfortunately, transfection of N2a cells with larger C-terminal deletion mutants of ErbB4 failed to be inserted in the plasma membrane, as identified by immunocytochemistry (data not shown). Therefore, generating several ErbB4 truncated tagged cytoplasmic domains could be used for transfection experiments and pull down assays for their ability to bind to members of the Par complex *in vivo* or *in vitro* and shed light on a region of ErbB4 that interacts with members of the Par complex. These experiments will also help us determine whether ErbB4 is associating with an assembled Par complex or if ErbB4 is associating with members of the Par complex independently at different or the same binding sites. With the identification of this site or region, ErbB4 mutants deficient in Par complex binding can be used to design experiments *in vivo* to elucidate the phenotypic outcome of such interactions. This can be implemented by performing viral delivery injections or *in utero* electroporation to monitor migration, radial glial morphology and numbers, neurite outgrowth, and synaptogenesis among other effects known to be affected by the polarity complex and ErbB4 (also see below).

It is also possible that ErbB4 association with the Par complex is regulating other aspects of neuronal morphology and maturation other than axonal elongation. For example,

Nrg-ErbB signaling has been shown to play a role in the formation of dendritic spines, small protrusions located within dendrites that receive the majority of excitatory synaptic inputs (Goda & Davis, 2003; Hering & Sheng, 2001; Sheng & Hoogenraad, 2007). Previous studies have reported that deletion of ErbB2/4 from the CNS or deletion of ErbB4 in parvalbumin (PV) interneurons impairs dendritic spine density of pyramidal cells in the hippocampus and prefrontal cortex (Barros et al., 2009; Yin, Sun, et al., 2013). The overexpression of ErbB4 in pyramidal neurons, on the other hand, increases dendritic spine size (B. Li et al., 2007). In addition, several studies have shown that Nrg1 treatment also increases dendritic spine density and size on pyramidal neurons (Barros et al., 2009; Michael E Cahill et al., 2013); whereas, deletion of Nrg1 Type III shows a reduction in spine density (Y.-J. J. Chen et al., 2008). These findings suggest that Nrg-ErbB4 signaling are playing roles in the morphogenesis of dendritic spines. In parallel, members of the Par complex have also been associated with dendritic spine morphogenesis. In particular, Par3 regulates spine formation on hippocampal neurons by binding to the Rac guanine nucleotide exchange factor TIAM1 and changing its compartmentalization into dendritic spines (H. Zhang & Macara, 2006). Interestingly, this is independent of Par3's association with the Par complex. In addition, Par6 also plays a role in dendritic spine morphogenesis in hippocampal neurons which is mediated by its association with aPKC and activation of p190 RhoGAP and RhoA in spines, but independent of its association with Par3 (H. Zhang & Macara, 2008). The knockdown of Par3 or Par6 results in the inhibition of spine morphogenesis (H. Zhang & Macara, 2006, 2008). These findings show that several members of the Par complex, albeit not within the complex, play a role in dendritic spine morphogenesis. Considering that Nrg-ErbB signaling and members of the Par complex play roles in dendritic spine formation, it is possible that their association can regulate spine morphology in GABAergic interneurons. In support of this idea are our findings from our immunocytochemistry experiments in Chapter 5. We revealed that ErbB4 and Par6 co-localize within puncta, observed along dendrites, when they are co-overexpressed in primary cortical

neurons (Fig. 5.7). Furthermore, this interaction appears to increase in size and intensity upon activation with Nrg1 and could be promoting co-localization of Par6 and ErbB4 to dendritic spines. It is important to note, however, that fluorescence intensity of ErbB4 and Par6 co-localization needs to be quantified and markers to identify dendrites and dendritic spines need to be utilized to unambiguously reach this conclusion. Nonetheless, these findings showing co-localization of ErbB4 and Par6 within puncta suggests possible functional roles in dendrite spine morphology. Future immunostaining experiments in ErbB4^{-/-} cultures transfected with ErbB4 mutants deficient in Par6 binding could be used to assess whether Nrg-induced ErbB4-Par6 interaction regulates changes in spine morphology. It would also be of interest to observe if ErbB4 shows the same pattern of association with aPKC and Par3 in these cortical neurons.

6.3 Nrg-ErbB4 Signaling in Neurite Outgrowth: What are Some Potential Downstream Signaling Pathways?

It has previously been shown that Nrg1 plays important roles in neurite outgrowth in several neuronal populations (Anton et al., 1997; Audisio et al., 2012; Bermingham-McDonogh et al., 1996; M E Cahill et al., 2012; Y. Chen et al., 2010; Kimberly M Gerecke et al., 2004; Krivosheya et al., 2008; Mòdol-Caballero et al., 2017; Rieff et al., 1999; Tal-Or et al., 2006; Villegas et al., 2000; R. Xu et al., 2013; Q. Zhang et al., 2017, 2016). A majority of these studies, however, failed to distinguish the neuronal subtypes that respond to Nrg1 stimulation. To address this gap in the literature, our studies compared the effects of Nrg1-3 treatment on ErbB4/GABA (+), ErbB4/ β -tubulin (+), and ErbB4 (-)/GABA (+) cortical neurons. Our findings in Chapter 4 showed redundant effects of the Nrgs in their ability to accelerate neurite outgrowth which was limited to ErbB4/GABA (+) neurons. In addition, these reports are the first, to our knowledge, to compare the effects of all three CNS-expressing Nrgs on neurite outgrowth. Our findings have contributed to the field's knowledge as we have shown that Nrg2 and Nrg3, similar to Nrg1 can also play roles in neuronal differentiation. One limitation of our findings, however, is

that our experiments were performed using dissociated neurons cultured *in vitro*. Whether the Nrgs have these redundant effects *in vivo* needs to be determined in a region specific manner, taking into consideration local expression of the different Nrgs, their isoforms, and their posttranslational modifications, all which can be relevant when evaluating their impact on a specific neuronal function. There are several ways to observe the effects of Nrg treatment *in vivo*, including the use of peripheral injections of Nrg1-3 to deliver them to the CNS for further observation on their effects on neuronal morphology, the use of organotypic cultures for more targeted Nrg delivery using viral or biolistic methods, or conditional CNS Nrg knockouts followed by Nrg treatment to observe potential rescue of phenotypes. These experiments would allow for observations on the *in vivo* consequences of Nrg treatment on neurite outgrowth and conclude whether they are consistent with our *in vitro* observations.

Our studies also did not address multiple modes of Nrg administration, or a more realistic presentation of the Nrgs for ErbB4 activation, as our only method of testing Nrg-dependent neurite outgrowth was by introducing soluble GST-Nrg factors to the culture medium. Therefore, it is possible that the GST-Nrgs were saturating ErbB4 activation in cortical neurons. This raises a concern regarding biological relevance, considering our findings in Chapter 3 show higher levels of Nrg2 and Nrg3 in the cortex than Nrg1. Therefore, it would be valuable to address the effects of neurite outgrowth in cultures from mice deficient for Nrg1, Nrg2, or Nrg3 in the CNS and to observe whether these deficiencies result in redundant decreases in neurite outgrowth or if the deficiency of one Nrg has greater deficits on neurite outgrowth than the others. In addition, since the Nrgs can act as both soluble and membrane-bound proteins, the overexpression of the Nrgs, either via transfections in culture or in utero electroporation, would shed light on whether Nrg-induced neurite outgrowth of ErbB4/GABA (+) interneurons could occur in an autocrine (increase in neurite outgrowth of ErbB4/GABA/Nrg cells) and/or in a juxtacrine or paracrine (increase in neurite outgrowth of ErbB4/GABA cells) manner.

Our findings in Chapter 4 have addressed that Nrg signaling promotes neurite outgrowth of ErbB4 (+) interneurons. However, the mechanisms downstream of Nrg-ErbB4 signaling in regulating neurite outgrowth are not well understood and should be a focus of future studies. Two pathways that can be activated by ErbB4, Ras/MAPK pathway and the PI3K pathway, have previously been shown to be important regulators of neurite outgrowth (Kiryushko et al., 2004; Kumar, Zhang, Swank, Kunz, & Wu, 2005; Read & Gorman, 2009; Rodgers & Theibert, 2002). A previous report by Krivosheya et al (2009) showed that the tyrosine kinase domain of ErbB4 and the activation of the PI3K pathway downstream of ErbB4 were required for Nrg1-induced stimulation of the number of neurites in ErbB4-overexpressing hippocampal neurons. Inhibition of the Ras/MAPK pathway did not abolish the effects of Nrg1-ErbB4 on neurite number, suggesting that this pathway is not involved in Nrg1-induced neurite outgrowth (Krivosheya et al., 2008). This study, however, did not report neurite length and was only measured in cells overexpressing ErbB4. It is possible that signaling pathways regulating neurite number and length may differ or that cells overexpressing ErbB4 might activate different signaling pathways compared to those endogenously expressing ErbB4. It would, therefore, be valuable to treat cortical cultures endogenously expressing ErbB4 with PI3K and Ras/MAPK inhibitors along with treatment with GST or GST-Nrgs and perform neurite outgrowth measurements on ErbB4/GABA interneurons using the methods we used in Chapter 4. This would provide a thorough investigation of the possible roles of these two pathways in Nrg-induced neurite outgrowth and would also help us elucidate whether there were potential differences in the downstream activation of the different Nrgs that regulated neurite outgrowth.

The Trk family of RTKs and their ligands brain-derived neurotrophic factor (BDNF) and NGF have been well-studied in the context of neurite outgrowth in PC12 cells (Colombo, Racchetti, & Meldolesi, 2014; Fuschini et al., 2018; Reichardt, 2006; Schramm et al., 2005; Y. Yan, Eipper, & Mains, 2016). There have been several downstream signaling pathways that

have been proposed to regulate Trk-mediated neurite outgrowth, including the Ras/MAPK and PI3K pathways described above (E. J. Huang & Reichardt, 2003; Tomoko Nishimura, Ishima, Iyo, & Hashimoto, 2008). In addition, Trk receptors have been previously shown to activate the signaling pathway involving PLC γ \rightarrow DAG \rightarrow PKC which can regulate neurite outgrowth (E. J. Huang & Reichardt, 2003; Tomoko Nishimura et al., 2008). Furthermore, and perhaps more relevant to our studies, Pozas et al (2005) described the neurite outgrowth effects of BDNF on GABAergic interneuron migration and neurite outgrowth. Using pharmacological inhibitor experiments, they identified PLC γ as an effector for the BDNF effect on dendritic elongation of GABAergic interneurons (Pozas & Ibáñez, 2005). It has also previously been observed that ErbB signaling can activate PLC γ [(Iwakura & Nawa, 2013; Chen Lai & Feng, 2004) and our own unpublished observations]. One study reported that Nrg1 treatment promoted the proliferation of neural progenitor cells in the hippocampus via the PLC γ -PKC pathway (Chen Lai & Feng, 2004). This study also showed that ErbB4 co-IP'ed with PLC γ in these cells. Although these findings were not in the context of neurite outgrowth, it is possible that this signaling pathway could be regulating other biological mechanisms in more mature cells, such as neurite outgrowth, considering this pathway plays a role in Trk-mediated GABAergic neurite extension. In support of the PLC γ -PKC model of Nrg-induced neurite outgrowth are our findings in cultured primary cortical neurons in Chapter 5 showing that Nrg-activation increased ErbB4 association with activated α PKC ζ (Fig. 5.6). In order to investigate whether this proposed model is valid, future studies would need to use PLC and PKC inhibitors to identify whether the effects of Nrg-induced neurite outgrowth in ErbB4/GABA interneurons is lost.

6.4 Nrg-ErbB4 Signaling in Axonal Elongation: What are Some Potential Downstream Signaling Pathways?

Whereas the roles of Nrg1-ErbB4 signaling in neurite and dendritic outgrowth have been studied, the roles of Nrg signaling in axonal elongation have been addressed to a lesser degree

[see (Audisio et al., 2012; Y. Chen et al., 2010)]. This gap in the literature may be due to the age of neurons in culture utilized in these studies and the transient expression of ErbB4 in the axon that we reported in Fig. 4.5. Our data showed that ErbB4 was highly expressed in the axon of GABAergic interneurons at 2 and 5 DIV, but expression significantly decreased with developmental maturity. This suggests that ErbB4 may be playing transient roles in the developing axon and the rest of the neuron. In support of our immunocytochemical data, we observed that Nrg treatment enhanced the length of the axon of ErbB4/GABA interneurons at both 2 and 5 DIV (Figs. 4.2-4.4). However, one limitation of these studies was that our neurite outgrowth analyses were restricted to cultures no older than 5 DIV due to the extensive nature of the more mature cortical neurons, making it problematic to accurately measure neurites at later stages. Therefore, we are unable to conclude if the Nrgs actually enhance overall axonal elongation or accelerate axonal elongation until the axon has reached its growing potential (similar to what we observed for the other neurites). We were also unable to conclude whether the Nrgs have unique properties in axonal elongation since our measurements were terminated at a point where the axon was still growing (Day 5). It would be of interest to observe whether one Nrg could enhance axonal elongation to a greater degree than the others at longer time points unmasking differences among the Nrgs, or if the Nrgs all possess the same potential in regulating axon growth. The extensive length of the neurites observed in more mature cultures might be countered by plating cells less densely; however, this may compromise the health of the cultures. As an alternative, another form of quantification could be implemented to analyze neurite outgrowth in place of tracing neurite length. For example, a neuron could be overlaid on a grid and neurite outgrowth could be measured by the area of the grid that encompasses the neuron or a particular neurite. This would not provide the exact measurement of the neurite, as neurites can appear wrapped within themselves in culture, but it would shed light on potential functional differences between the Nrgs in their effects on neurite outgrowth. Given that our immunocytochemical data showed very minimal levels of ErbB4 by 8 DIV, it is hypothesized that

Nrg-induced axonal elongation would peak at around 5 DIV. Therefore, to understand the roles of Nrg signaling in axonal elongation, it is imperative to address their effect in axon growth in more mature neurons.

Another key future area of study would be to identify whether Nrg-ErbB4 signaling is playing a role in axon formation. We showed that Nrg treatment could enhance the length of the axon (Chapter 4) and that Nrg stimulation could induce ErbB4 association with members of the Par polarity complex (Chapter 5), a group of proteins that play a pertinent role in axon formation. Therefore, it is possible that the Nrg-ErbB4 signaling network plays a role in axon formation. This could be addressed through culturing cortical neurons from Nrg and ErbB4 conditional knockouts and identifying whether neurites fail to differentiate into axons. A model for axon formation has previously been suggested for BDNF-TrkB signaling, which requires an increase in extracellular BDNF and TrkB internalization via activation of cAMP and PKA and simultaneously the activation of PI3K to transport TrkB to the membrane, creating a feedback loop promoting axon formation (Cosker & Segal, 2014). This signaling pathway differs from what is proposed for axon elongation, which suggests that axon growth requires TrkA internalization via NGF-TrkA signaling through PLC γ , calcineurin, and dynamin1 (Cosker & Segal, 2014). It would, therefore, be interesting to test whether the inhibition of PI3K or PLC γ would eliminate the effects of Nrg-ErbB4 signaling in axon formation or elongation, respectively.

6.5 Could Nrg-ErbB4 Pairs Along with the Par Polarity Complex be a Part of the Positive Feedback Loop Regulating Axon Formation?

Our studies did not identify whether Nrg-ErbB4 signaling plays a role in axon formation; however, we did observe a role for Nrg signaling in axonal elongation which is an important event that occurs in conjunction with axon formation. We also identified ErbB4 association with the Par polarity complex, which is essential for axon specification. It has previously been

suggested that the Par polarity complex may be central to a positive feedback loop that regulates axon specification and growth [reviewed in (Arimura & Kaibuchi, 2007)]. The current model of the positive feedback loop suggests that an extracellular cue activates a receptor which results in downstream signaling following the activation of PI3K → PIP₃ → Cdc42 GEF → Cdc42 → Par complex → Rac GEF (STEF/Tiam1) → Rac → PI3K. This feedback loop then regulates the highly dynamic actin filaments during axonal growth. Based on our findings and this model, it is possible that the Nrgs and ErbB4, at least in a subpopulation of interneurons, are the ligands and receptor that initiate the positive feedback loop that is thought to regulate axonal growth.

One shortcoming of this model incorporating ErbB4 is that the current view supports activation of PI3K as the initiating event in the positive feedback loop. However, our experiments in the stable N2a/ErbB4 cell line (Chapter 5) and experiments overexpressing ErbB4 in primary cortical cultures (Chapter 4) utilized ErbB4 JM-b CYT-2, an isoform of ErbB4 that has not been shown to activate the PI3K pathway. It is possible that in untransfected cortical neurons both CYT-1 and CYT-2 isoforms were interacting with the Par complex, resulting in CYT-1 isoforms that could potentially activate PI3K to initiate the feedback loop (Fig. 6.1). Whereas, CYT-2 isoforms 1) may not be involved in the positive feedback loop and might be interacting with the Par complex to regulate another mechanism to enhance axonal growth or 2) may be initiating the loop by downstream activation of another molecule instead of PI3K (Fig. 6.1). We demonstrated in Chapter 5 that, in cortical cultures, Nrg-activation resulted in increased phosphorylation of Cdc42 and aPKCζ. This increase in phosphorylation was observed not only for aPKCζ and Cdc42 that IP'ed with ErbB4, but total aPKCζ and Cdc42 (data not shown). Therefore, it is possible that ErbB4 activation may trigger the positive feedback loop through the phosphorylation of aPKCζ or Cdc42, which then can regulate PI3K activation.

Future experiments to determine whether Nrg-ErbB4 signaling is regulating axon formation or elongation upstream of PI3K will require the use of PI3K inhibitors.

Fig. 6.1

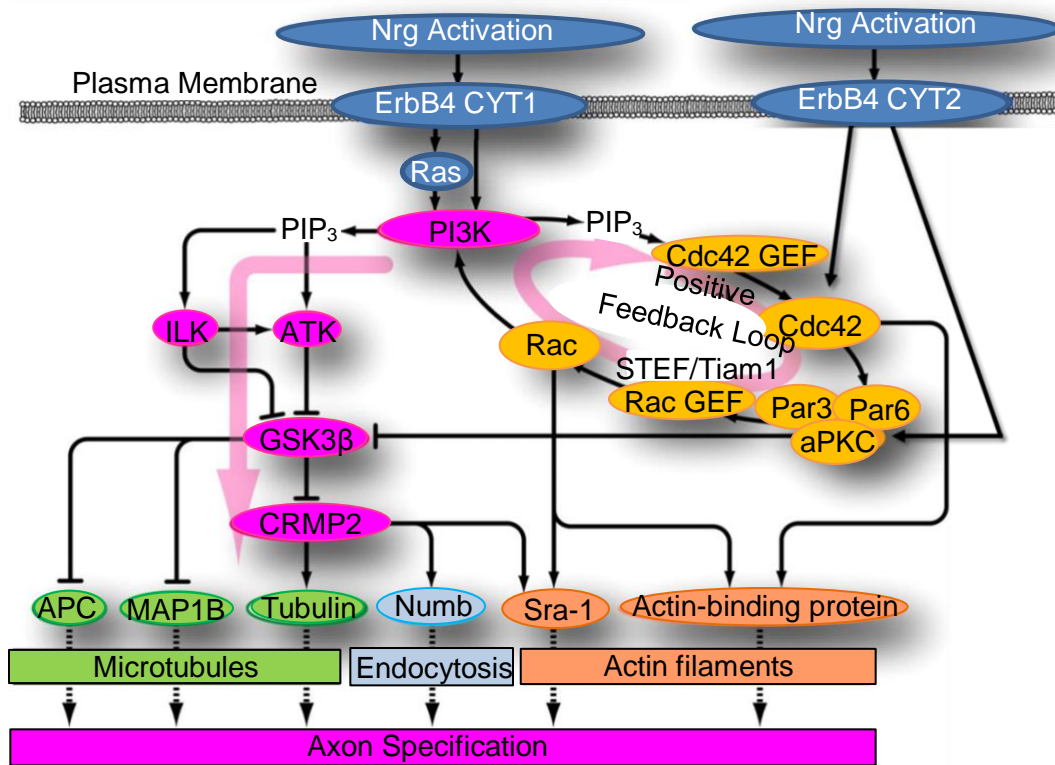


Fig. 6.1: Schematic of Theoretical Positive Feedback Loop Regulating Axon Specification.

Nrg-induced activation of ErbB4 may initiate a positive feedback loop important for axon specification and elongation. Upon Nrg activation ErbB4 CYT-1 variant can activate PI3K, resulting in its product PIP₃ activating Cdc42. Activated Cdc42 associates with the Par complex where Par3 can then interact with the Rac GEF STEF/Tiam1 which activates Rac. Activation of Rac can then start the loop again by activating PI3K. The ErbB4 CYT-2 variant, which does not directly activate PI3K, could possibly initiate the positive feedback loop via activation of Cdc42 or aPKC. The maintenance of this positive feedback loop is thought to play an intimate role in regulating the actin dynamics that are necessary for axon elongation. This figure was taken and modified from (Yoshimura et al., 2006).

6.6 Potential Roles for Nrg Signaling in the Golgi Apparatus

The Golgi apparatus is a trafficking and protein processing center in the cell and plays an important role in the establishment of neuronal polarity, such as regulating the polarized distribution of molecules to axons and dendrites to facilitate growth and function (Fariás, Britt, & Bonifacino, 2016). Therefore, the positioning and architecture of the Golgi are important aspects of proper neuronal development. Our findings in Chapter 3 open several avenues for future study of the Nrgs, particularly Nrg3, in the Golgi apparatus. We revealed striking expression of Nrg3 in the Golgi of N2a/Nrg3 cells, cortical neurons, and in a region consistent with the Golgi in glial cells (Figs. 3.3 and 3.5). Although the abundance of Nrg3 in the Golgi could be accounted by posttranslational modifications occurring within the Golgi, it is also possible that Nrg3 signaling may play functional roles within the organelle. The Golgi itself is a polarized organelle as the proper organization of the functioning Golgi requires the formation of a continuous ribbon of interlocked stacks of flat cisternae known as the Golgi ribbon. It has previously been shown that Par3 and aPKC interact with CLASP2 to regulate Golgi ribbon organization (Matsui et al., 2015). The knockdown of Par3 or aPKC resulted in the accumulation of CLASP2 at the trans-Golgi network (TGN) and consequently disrupted the Golgi ribbon organization, as measured by the circularity index. Our findings in Chapter 5 have shown that ErbB4 can interact with both Par3 and aPKC and that this interaction can be enhanced by the Nrgs, including Nrg3. Since Nrg3 expression in the Golgi is so prominent, it is promising that it may be playing a role in this organelle, possibly through regulating the morphology of the Golgi ribbon via activation of ErbB4. We conducted preliminary experiments (not shown) culturing primary cortical neurons with 500 ng/mL of GST or GST-Nrg3 and measuring the circularity index of the Golgi apparatus to measure disruptions in the Golgi ribbon. Our results did not show any differences between the GST-Nrg3 and GST control conditions. However, in these experiments we did not target the distribution of Nrg3 to the Golgi but bathed the cells with media containing the factor, so it is

possible that our Nrg3 factors did not make it to the Golgi. It is also possible that ErbB4 activation in the Golgi is already saturated since levels of Nrg3 are so high in this organelle; therefore, the addition of Nrg3 factor may have minimal effects within the Golgi. To address the roles of Nrg3-ErbB4 signaling in the formation and maintenance of the Golgi ribbon, Nrg3 or ErbB4 knockdown experiments could be used to assess whether these molecules effect Golgi ribbon morphology.

Another interesting avenue of research would be to address Nrg-ErbB4 signaling in the Golgi in the context of axon formation. From the transition from Stage 2 to Stage 3 (Fig. 1.2), the TGN is reorganized and polarizes the distribution of TGN-derived vesicles to the future axon (Bradke & Dotti, 1997; B. L. Tang, 2001; Yin, Huang, Zhu, & Wang, 2008). It has previously been shown in cultured cerebellar granule neurons and hippocampal pyramidal neurons that the microtubule-organizing center (MTOC), Golgi apparatus, and endosomes cluster and are positioned adjacent to the first neurite that emerges, which usually later becomes the axon (de Curtis, 2007; de Anda et al., 2005; Zmuda & Rivas, 1998). de Anda et al (2005) showed a causal relationship between positioning of the centrosome and axon specification through the use of a cytokinesis inhibitor, resulting in more than one centrosome. The presence of multiple centrosomes resulted in multiple axon-like neurites emerging adjacent to the centrosomes in hippocampal neurons (de Anda et al., 2005). As both Nrg1 and Nrg3 have previously been suggested to act as chemoattractive factors (Bartolini et al., 2017; Flames et al., 2004; B. Howard et al., 2005) and our findings show abundant levels of Nrg3 in the Golgi (Fig. 3.3), it would be compelling to analyze whether polarized Nrg-ErbB signaling could play a role in the positioning/repositioning of the Golgi. These experiments could be done by positioning beads coated with Nrg3 near a neurite that is not adjacent to the position of the Golgi and then analyzing whether the Golgi repositions towards the direction of Nrg3.

6.7 Potential Roles for Nrg3 in the Developing CNS and Schizophrenia

A significant contribution of this thesis to the growing Nrg literature is the in-depth analyses of the vastly understudied Nrg family member, Nrg3. Although several studies have reported on the localization of Nrg3 in the developing rodent brain (Anton et al., 2004; Bartolini et al., 2017; Marines Longart et al., 2004), our studies in Chapter 3 extended these findings to incorporate a more detailed analyses of several stages of development and the identification of a number of brain regions expressing Nrg3 that have not previously been identified. In addition, we observed that although the expression of Nrg1, Nrg2, and Nrg3 overlap in the developing brain in some areas such as the cortex, hippocampus, and cerebellum, there are several regions that the Nrgs differ in their expression intensity and/or compartmentalization, suggesting non-overlapping roles of the Nrgs (Fig. 3.10). Although the identification of brain regions expressing a particular protein does not necessarily reveal its biological role, it does provide a framework for identifying brain regions of interest to detect potential functions of Nrg3 signaling in the developing and mature brain. Our findings showed striking levels of Nrg3 in the developing cortex and hippocampus and are discussed in further detail below. In addition, we identified several biological functions of Nrg3 (as well as Nrg1 and Nrg2) in cortical neurons, including the ability to enhance neurite outgrowth of ErbB4/GABA (+) neurons (including axonal elongation) and promote ErbB4 interaction with members of the Par polarity complex. These findings are of particular interest because *Nrg1*, *Nrg3*, and *ErbB4* have previously been identified as a schizophrenia (SZ) susceptibility genes (P.-L. Chen et al., 2009; Fallin et al., 2003; Faraone et al., 2006; Hahn et al., 2006; Mei & Nave, 2014; Meier et al., 2013; Norton et al., 2006; Silberberg et al., 2006; Stefansson et al., 2002; Y.-C. Wang et al., 2008; Zeledón et al., 2015), a disorder that shows aberrancies in cortical and hippocampal neurite outgrowth and polarity (Badea et al., 2007; Black et al., 2004; Broadbelt et al., 2002; Bunney, 2000; Kalus et al., 2002; Matricon et al., 2010; Muraki & Tanigaki, 2015; Q. Zhang et al., 2016).

6.7.1 The Developing Cortical Plate and the Cerebral Cortex

Several studies have shown evidence suggesting that Nrg3 may play an important role in cortical development and function (Assimacopoulos et al., 2003; Bartolini et al., 2017; D. Zhang et al., 1997). In support, our studies in Chapter 3 have revealed that Nrg3 mRNA and protein expression is widely distributed throughout the developing cortical plate and remains high in the cortex at later stages of development (Fig. 3.6 and 3.7). These data corroborate and expand upon the reports of Longart et al (2004), Anton et al (2004), and Bartolini et al (2017) and further suggest possible functional roles for Nrg3 not only during embryogenesis, but also later stages of development.

Our findings showing that the levels of cortical Nrg3 remain high during development are particularly interesting because it unlocks avenues for potential studies analyzing the roles of Nrg3 at different stages of maturity. For example since Nrg3 has been linked with SZ, one possible avenue of study might be to observe its possible association with the “dual hit” hypothesis of SZ (Datta & Arnsten, 2018). This hypothesis proposes that SZ arises from an initial wave of genetic or environmental insults during perinatal corticogenesis, followed by a second wave of insults during adolescence, resulting in the onset of the overt symptoms of SZ. It is important to note that there are currently no reports linking Nrg3 function to SZ; however, several biological roles of Nrg3 in cortical development and Nrg3^{-/-} mice which exhibit SZ-like symptoms suggest that Nrg3 may play a role in disease presentation (Assimacopoulos et al., 2003; Bartolini et al., 2017; Hayes et al., 2016; Paterson & Law, 2014; D. Zhang et al., 1997). The “dual hit” hypothesis suggests that the initial genetic or environmental insults can alter cortical formation, such as alterations in cortical neuronal migration and differentiation (Datta & Arnsten, 2018; Selemon & Zecevic, 2015). It has previously been shown that Nrg3 expressed in developing pyramidal neurons can act as a chemoattractive factor to guide interneuronal precursors to the developing cortical plate (Bartolini et al., 2017). Our findings in Chapter 4 also revealed that Nrg3, as well as Nrg1 and Nrg2, play a role in neuronal differentiation by

accelerating neurite outgrowth and enhancing axonal elongation of cortical GABAergic interneurons that express ErbB4 (Figs. 4.2 and 4.3). Since defects in the functioning of GABAergic interneurons have been linked with the compromised balance of excitatory and inhibitory neural circuits in patients with SZ (D. A. Lewis, Curley, Glausier, & Volk, 2012), it is possible that Nrg3 expression is associated with the assembly of inhibitory circuits during corticogenesis.

In addition, the “dual hit” hypothesis proposes a second wave of genetic or environmental insults that occur around the time of adolescence. This is thought to transpire during the normal synaptic pruning process that occurs at this stage of development (Datta & Arnsten, 2018). Exacerbations in excitatory synaptic pruning correlate with cortical gray matter loss and have been linked with the onset of mental illness (Bourgeois, Goldman-Rakic, & Rakic, 1994; Cannon, 2015; Cannon et al., 2015; Datta & Arnsten, 2018; Feinberg, 1982; Huttenlocher & Dabholkar, 1997; Petanjek et al., 2011). Considering our reports show that Nrg3 is abundantly expressed in both excitatory and inhibitory neurons (Fig. 3.4) and it has previously been shown that Nrg3 promotes excitatory synapse formation on ErbB4 (+) interneurons (Müller et al., 2018), it is possible that Nrg3 could play a role in the synaptic pruning process. Animal models have shown that ErbB4 activation can enhance excitatory synapses on parvalbumin-positive (PV (+)) interneurons (Mei & Nave, 2014; Rico & Marín, 2011; Ting et al., 2011). Chung et al (2017) previously showed that, in the dorsolateral prefrontal cortex (DLPFC) of primates, excitatory synapses on PV (+) neurons were pruned across adolescence and splicing of ErbB4 may be in part mediating such effects (Chung, Wills, Fish, & Lewis, 2017). This study showed that the most abundant (JM-b CYT-2) ErbB4 variant was preferentially expressed during pre-puberty in primate DLPFC and overexpression of this variant could increase the number of excitatory inputs on PV (+) interneurons in rat cortical cultures. In contrast, the less abundant (JM-a CYT-1) variant was expressed at higher levels right after puberty in primate DLPFC and

that its overexpression did not change the number of excitatory inputs on PV (+) interneurons. There were no changes observed in the overall levels of ErbB4 in these two stages examined. Furthermore, Nrg1 activated the JM-b CYT-2 variant to a greater degree than the JM-a CYT-1 variant in transfected HEK-293 cells, suggesting that the alternative splicing of ErbB4 could be impacting ErbB4 signaling activity during these key stages of development encompassing synaptic pruning (Chung et al., 2017). Interestingly, several studies have also reported that the JM-a CYT-1 variant of ErbB4 is elevated in patients with SZ (Law et al., 2007; Silberberg et al., 2006), without any effects on total levels of ErbB4 (Law et al., 2007). The experiments of Chung et al utilized Nrg1 to activate the ErbB4 variants; however, the expression of Nrg1 in the rat cortex decreases with age (Marines Longart et al., 2004), raising concerns about the biological relevance of Nrg1 activation in cortical neurons during later stages of development. Although we did not analyze the ability of Nrg3 to activate the JM-a CYT-1 variant of ErbB4, our experiments in N2a/ErbB4 (Chapter 4) cells showed that Nrg3 can activate the JM-b CYT-2 variant. Furthermore, since our studies, along with others, have shown that Nrg3 expression remains high in the developing cortex (Figs. 3.6 and 3.7 and (Anton et al., 2004; Bartolini et al., 2017; Marines Longart et al., 2004)), it is possible that Nrg3 activation of JM-b CYT-2 and JM-a CYT-1 variants may play diverse roles around the time of adolescence and during synaptic pruning.

Our studies, however, did not specifically address the expression of Nrg3 in the cortex during the period of adolescence in the rodent model. The adolescent transition in rats occurs between P35-39 (Laviola, Macrì, Morley-Fletcher, & Adriani, 2003; Zoratto et al., 2018); whereas, our analyses of Nrg3 expression in the cortex, due to issues with staining, only encompassed ages up to P20 (post-weaning stage), a stage that would be considered pre-juvenile. There are currently no reports about the cortical expression of Nrg3 during the adolescent stages of development in the rodent model. Therefore, it would be of interest to observe whether the expression of Nrg3 in the cortex steadily increases into adulthood or

fluctuates during later development. Another future direction that would dissect the roles of Nrg3 in the “dual hit” hypothesis of SZ would be to knockdown or overexpress Nrg3 at various ages, such as during embryonic neuronal migration, at a late embryonic stage, prior to adolescence, during adolescence, right after adolescence, and in adulthood. Previous studies have used pharmacological treatments and social isolation to model the “dual hit” hypothesis of SZ (Gaskin, Alexander, & Fone, 2014; Gilabert-Juan et al., 2013), showing that the rodent models can react to these insults and might provide a reliable model for SZ. These manipulations would allow for the comparing and contrasting of cortical morphology and behavioral traits to determine critical time points for Nrg3 activity in the developing brain.

6.7.2 The Developing Hippocampus

One of the major roles of the hippocampus is the encoding and retrieval of declarative memories (Eichenbaum, Otto, & Cohen, 1992). Previous studies have shown roles for Nrg3 signaling in excitatory synaptic transmission in hippocampal neurons (Müller et al., 2018; Y.-N. Wang et al., 2018), suggesting a possible role for Nrg3 in hippocampal activity such as learning and memory. Although these findings, as well as our findings showing abundant levels of Nrg3 in the hippocampus (Fig. 3.9), suggest that Nrg3 may play a role in the hippocampus, behavioral studies have previously shown that the transient neonatal overexposure of Nrg3-EGF through subcutaneous injections does not impact hippocampal-dependent temporal order recognition memory in mice (Paterson & Law, 2014). In addition, it is important to note that even though the previous characterization of the Nrg3^{-/-} knockout mouse revealed certain SZ-like behaviors, no gross morphological brain abnormalities and no deficits in hippocampal-dependent (contextual) fear conditioning were observed (Hayes et al., 2016). However, given the high levels of Nrg3 present in the rodent brain, as reported in Chapter 3, the observation that a complete knockdown of this gene would result in no phenotypic differences needs further examination and interpretation. One possibility for these findings might be that Nrg1 and Nrg2

can compensate for Nrg3 in the Nrg3-deficient mice, as our findings in Chapter 4 and Chapter 5 suggest that the Nrgs can play several redundant roles in cortical neurons. Another possibility might be that even though the expression of Nrg3 is abundant, its role in biological functions regulating brain morphology might be expendable. A more thorough investigation on the roles of Nrg3 in the hippocampus (along with other brain regions) would be valuable, including other hippocampal-dependent tests for memory.

Overall our findings in this thesis have addressed several gaps in the literature, including the expression and biological functions of Nrg3 in the CNS, as well as the roles of the Nrgs in neuronal differentiation and possibly neuronal polarity. These findings advance the knowledge regarding Nrg-ErbB4 signaling in neurodevelopment; however, future experiments are necessary to further elucidate these roles and possibly develop therapeutic interventions for ErbB4-driven neurodevelopmental illnesses.

References

- Abbasy, S., Shahraki, F., Haghightafard, A., Qazvini, M. G., Rafiei, S. T., Noshadirad, E., ... Partovi, R. (2018). Neuregulin1 types mRNA level changes in autism spectrum disorder, and is associated with deficit in executive functions. *EBioMedicine*, *37*, 483–488. doi:10.1016/j.ebiom.2018.10.022
- Abe, Y., Namba, H., Kato, T., Iwakura, Y., & Nawa, H. (2011). Neuregulin-1 signals from the periphery regulate AMPA receptor sensitivity and expression in GABAergic interneurons in developing neocortex. *The Journal of Neuroscience*, *31*(15), 5699–5709. doi:10.1523/JNEUROSCI.3477-10.2011
- Adelsman, M. A., Huntley, B. K., & Maihle, N. J. (1996). Ligand-independent dimerization of oncogenic v-erbB products involves covalent interactions. *Journal of Virology*, *70*(4), 2533–2544.
- Alroy, I., & Yarden, Y. (1997). The ErbB signaling network in embryogenesis and oncogenesis: signal diversification through combinatorial ligand-receptor interactions. *FEBS Letters*, *410*(1), 83–86. doi:10.1016/S0014-5793(97)00412-2
- Alvarez-Buylla, A., & Garcia-Verdugo, J. M. (2002). Neurogenesis in adult subventricular zone. *The Journal of Neuroscience*, *22*(3), 629–634. doi:10.1523/JNEUROSCI.22-03-00629.2002
- Andersen, S. S., & Bi, G. Q. (2000). Axon formation: a molecular model for the generation of neuronal polarity. *Bioessays: News and Reviews in Molecular, Cellular and Developmental Biology*, *22*(2), 172–179. doi:10.1002/(SICI)1521-1878(200002)22:2<172::AID-BIES8>3.0.CO;2-Q
- Andersson, R. H., Johnston, A., Herman, P. A., Winzer-Serhan, U. H., Karavanova, I., Vullhorst, D., ... Buonanno, A. (2012). Neuregulin and dopamine modulation of hippocampal gamma oscillations is dependent on dopamine D4 receptors. *Proceedings of the National Academy of Sciences of the United States of America*, *109*(32), 13118–13123. doi:10.1073/pnas.1201011109
- Ansen-Wilson, L. J., & Lipinski, R. J. (2017). Gene-environment interactions in cortical interneuron development and dysfunction: A review of preclinical studies. *Neurotoxicology*, *58*, 120–129. doi:10.1016/j.neuro.2016.12.002
- Anton, E. S., Ghashghaei, H. T., Weber, J. L., McCann, C., Fischer, T. M., Cheung, I. D., ... Lai, C. (2004). Receptor tyrosine kinase ErbB4 modulates neuroblast migration and placement in the adult forebrain. *Nature Neuroscience*, *7*(12), 1319–1328. doi:10.1038/nn1345
- Anton, E. S., Marchionni, M. A., Lee, K. F., & Rakic, P. (1997). Role of GGF/neuregulin signaling in interactions between migrating neurons and radial glia in the developing cerebral cortex. *Development*, *124*(18), 3501–3510.

- Appert-Collin, A., Hubert, P., Crémel, G., & Bennisroune, A. (2015). Role of erbb receptors in cancer cell migration and invasion. *Frontiers in Pharmacology*, *6*, 283. doi:10.3389/fphar.2015.00283
- Aranda, V., Haire, T., Nolan, M. E., Calarco, J. P., Rosenberg, A. Z., Fawcett, J. P., ... Muthuswamy, S. K. (2006). Par6-aPKC uncouples ErbB2 induced disruption of polarized epithelial organization from proliferation control. *Nature Cell Biology*, *8*(11), 1235–1245. doi:10.1038/ncb1485
- Arimura, N., & Kaibuchi, K. (2005). Key regulators in neuronal polarity. *Neuron*, *48*(6), 881–884. doi:10.1016/j.neuron.2005.11.007
- Arimura, N., & Kaibuchi, K. (2007). Neuronal polarity: from extracellular signals to intracellular mechanisms. *Nature Reviews. Neuroscience*, *8*(3), 194–205. doi:10.1038/nrn2056
- Arteaga, C. L., & Engelman, J. A. (2014). ERBB receptors: from oncogene discovery to basic science to mechanism-based cancer therapeutics. *Cancer Cell*, *25*(3), 282–303. doi:10.1016/j.ccr.2014.02.025
- Assimacopoulos, S., Grove, E. A., & Ragsdale, C. W. (2003). Identification of a Pax6-dependent epidermal growth factor family signaling source at the lateral edge of the embryonic cerebral cortex. *The Journal of Neuroscience*, *23*(16), 6399–6403.
- Audisio, C., Mantovani, C., Raimondo, S., Geuna, S., Perroteau, I., & Terenghi, G. (2012). Neuregulin1 administration increases axonal elongation in dissociated primary sensory neuron cultures. *Experimental Cell Research*, *318*(5), 570–577. doi:10.1016/j.yexcr.2012.01.011
- Aukst Margetic, B., Peitl, V., Vukasović, I., & Karlović, D. (2019). Neuregulin-1 is increased in schizophrenia patients with chronic cannabis abuse: Preliminary results. *Schizophrenia Research*. doi:10.1016/j.schres.2019.02.007
- Avramopoulos, D. (2018). Neuregulin 3 and its roles in schizophrenia risk and presentation. *American Journal of Medical Genetics. Part B, Neuropsychiatric Genetics*, *177*(2), 257–266. doi:10.1002/ajmg.b.32552
- Badea, A., Nicholls, P. J., Johnson, G. A., & Wetsel, W. C. (2007). Neuroanatomical phenotypes in the reeler mouse. *Neuroimage*, *34*(4), 1363–1374. doi:10.1016/j.neuroimage.2006.09.053
- Balciuniene, J., Feng, N., Iyadurai, K., Hirsch, B., Charnas, L., Bill, B. R., ... Selleck, S. B. (2007). Recurrent 10q22-q23 deletions: a genomic disorder on 10q associated with cognitive and behavioral abnormalities. *American Journal of Human Genetics*, *80*(5), 938–947. doi:10.1086/513607
- Baloch, S., Verma, R., Huang, H., Khurd, P., Clark, S., Yarowsky, P., ... Davatzikos, C. (2009). Quantification of brain maturation and growth patterns in C57BL/6J mice via

- computational neuroanatomy of diffusion tensor images. *Cerebral Cortex*, 19(3), 675–687. doi:10.1093/cercor/bhn112
- Banker, G. (2018). The development of neuronal polarity: A retrospective view. *The Journal of Neuroscience*, 38(8), 1867–1873. doi:10.1523/JNEUROSCI.1372-16.2018
- Bao, J., Lin, H., Ouyang, Y., Lei, D., Osman, A., Kim, T.-W., ... Ambron, R. T. (2004). Activity-dependent transcription regulation of PSD-95 by neuregulin-1 and Eos. *Nature Neuroscience*, 7(11), 1250–1258. doi:10.1038/nn1342
- Bao, J., Wolpowitz, D., Role, L. W., & Talmage, D. A. (2003). Back signaling by the Nrg-1 intracellular domain. *The Journal of Cell Biology*, 161(6), 1133–1141. doi:10.1083/jcb.200212085
- Bargmann, C. I., Hung, M. C., & Weinberg, R. A. (1986). The neu oncogene encodes an epidermal growth factor receptor-related protein. *Nature*, 319(6050), 226–230. doi:10.1038/319226a0
- Barros, C. S., Calabrese, B., Chamero, P., Roberts, A. J., Korzus, E., Lloyd, K., ... Müller, U. (2009). Impaired maturation of dendritic spines without disorganization of cortical cell layers in mice lacking NRG1/ErbB signaling in the central nervous system. *Proceedings of the National Academy of Sciences of the United States of America*, 106(11), 4507–4512. doi:10.1073/pnas.0900355106
- Bartolini, G., Sánchez-Alcañiz, J. A., Osório, C., Valiente, M., García-Frigola, C., & Marín, O. (2017). Neuregulin 3 mediates cortical plate invasion and laminar allocation of gabaergic interneurons. *Cell Reports*, 18(5), 1157–1170. doi:10.1016/j.celrep.2016.12.089
- Bean, J. C., Lin, T. W., Sathyamurthy, A., Liu, F., Yin, D.-M., Xiong, W.-C., & Mei, L. (2014). Genetic labeling reveals novel cellular targets of schizophrenia susceptibility gene: distribution of GABA and non-GABA ErbB4-positive cells in adult mouse brain. *The Journal of Neuroscience*, 34(40), 13549–13566. doi:10.1523/JNEUROSCI.2021-14.2014
- Ben Halima, S., Mishra, S., Raja, K. M. P., Willem, M., Baici, A., Simons, K., ... Rajendran, L. (2016). Specific Inhibition of β -Secretase Processing of the Alzheimer Disease Amyloid Precursor Protein. *Cell Reports*, 14(9), 2127–2141. doi:10.1016/j.celrep.2016.01.076
- Benson, D. L., Watkins, F. H., Steward, O., & Banker, G. (1994). Characterization of GABAergic neurons in hippocampal cell cultures. *Journal of Neurocytology*, 23(5), 279–295. doi:10.1007/BF01188497
- Benzel, I., Bansal, A., Browning, B. L., Galwey, N. W., Maycox, P. R., McGinnis, R., ... Purvis, I. (2007). Interactions among genes in the ErbB-Neuregulin signalling network are associated with increased susceptibility to schizophrenia. *Behavioral and Brain Functions*, 3, 31. doi:10.1186/1744-9081-3-31

- Bermingham-McDonogh, O., McCabe, K. L., & Reh, T. A. (1996). Effects of GGF/neuregulins on neuronal survival and neurite outgrowth correlate with erbB2/neu expression in developing rat retina. *Development*, *122*(5), 1427–1438.
- Bertram, I., Bernstein, H.-G., Lendeckel, U., Bukowska, A., Dobrowolny, H., Keilhoff, G., ... Bogerts, B. (2007). Immunohistochemical evidence for impaired neuregulin-1 signaling in the prefrontal cortex in schizophrenia and in unipolar depression. *Annals of the New York Academy of Sciences*, *1096*, 147–156. doi:10.1196/annals.1397.080
- Berzat, A., & Hall, A. (2010). Cellular responses to extracellular guidance cues. *The EMBO Journal*, *29*(16), 2734–2745. doi:10.1038/emboj.2010.170
- Birchmeier, C., & Bennett, D. L. H. (2016). Neuregulin/erbB signaling in developmental myelin formation and nerve repair. *Current Topics in Developmental Biology*, *116*, 45–64. doi:10.1016/bs.ctdb.2015.11.009
- Black, J. E., Kodish, I. M., Grossman, A. W., Klintsova, A. Y., Orlovskaya, D., Vostrikov, V., ... Greenough, W. T. (2004). Pathology of layer V pyramidal neurons in the prefrontal cortex of patients with schizophrenia. *The American Journal of Psychiatry*, *161*(4), 742–744. doi:10.1176/appi.ajp.161.4.742
- Blenis, J. (1993). Signal transduction via the MAP kinases: proceed at your own RSK. *Proceedings of the National Academy of Sciences of the United States of America*, *90*(13), 5889–5892.
- Bockhorst, K. H., Narayana, P. A., Liu, R., Ahobila-Vijjula, P., Ramu, J., Kamel, M., ... Perez-Polo, J. R. (2008). Early postnatal development of rat brain: in vivo diffusion tensor imaging. *Journal of Neuroscience Research*, *86*(7), 1520–1528. doi:10.1002/jnr.21607
- Boucher, A. A., Arnold, J. C., Duffy, L., Schofield, P. R., Micheau, J., & Karl, T. (2007). Heterozygous neuregulin 1 mice are more sensitive to the behavioural effects of Delta9-tetrahydrocannabinol. *Psychopharmacology*, *192*(3), 325–336. doi:10.1007/s00213-007-0721-3
- Bourgeois, J. P., Goldman-Rakic, P. S., & Rakic, P. (1994). Synaptogenesis in the prefrontal cortex of rhesus monkeys. *Cerebral Cortex*, *4*(1), 78–96. doi:10.1093/cercor/4.1.78
- Bradke, F., & Dotti, C. G. (1997). Neuronal polarity: vectorial cytoplasmic flow precedes axon formation. *Neuron*, *19*(6), 1175–1186. doi:10.1016/S0896-6273(00)80410-9
- Brennan, P. J., Kumogai, T., Berezov, A., Murali, R., & Greene, M. I. (2000). HER2/Neu: mechanisms of dimerization/oligomerization. *Oncogene*, *19*(53), 6093–6101. doi:10.1038/sj.onc.1203967
- Brinkmann, B. G., Agarwal, A., Sereda, M. W., Garratt, A. N., Müller, T., Wende, H., ... Nave, K. A. (2008). Neuregulin-1/ErbB signaling serves distinct functions in myelination of the peripheral and central nervous system. *Neuron*, *59*(4), 581–595. doi:10.1016/j.neuron.2008.06.028

- Britto, J. M., Lukehurst, S., Weller, R., Fraser, C., Qiu, Y., Hertzog, P., & Busfield, S. J. (2004). Generation and characterization of neuregulin-2-deficient mice. *Molecular and Cellular Biology*, 24(18), 8221–8226. doi:10.1128/MCB.24.18.8221-8226.2004
- Broadbelt, K., Byne, W., & Jones, L. B. (2002). Evidence for a decrease in basilar dendrites of pyramidal cells in schizophrenic medial prefrontal cortex. *Schizophrenia Research*, 58(1), 75–81. doi:10.1016/S0920-9964(02)00201-3
- Buckley, P. F., Miller, B. J., Lehrer, D. S., & Castle, D. J. (2009). Psychiatric comorbidities and schizophrenia. *Schizophrenia Bulletin*, 35(2), 383–402. doi:10.1093/schbul/sbn135
- Bultje, R. S., Castaneda-Castellanos, D. R., Jan, L. Y., Jan, Y.-N., Kriegstein, A. R., & Shi, S.-H. (2009). Mammalian Par3 regulates progenitor cell asymmetric division via notch signaling in the developing neocortex. *Neuron*, 63(2), 189–202. doi:10.1016/j.neuron.2009.07.004
- Bunney, W. (2000). Evidence for a compromised dorsolateral prefrontal cortical parallel circuit in schizophrenia. *Brain Research Reviews*, 31(2-3), 138–146. doi:10.1016/S0165-0173(99)00031-4
- Buonanno, A. (2010). The neuregulin signaling pathway and schizophrenia: from genes to synapses and neural circuits. *Brain Research Bulletin*, 83(3-4), 122–131. doi:10.1016/j.brainresbull.2010.07.012
- Burgess, T. L., Ross, S. L., Qian, Y. X., Brankow, D., & Hu, S. (1995). Biosynthetic processing of neu differentiation factor. Glycosylation trafficking, and regulated cleavage from the cell surface. *The Journal of Biological Chemistry*, 270(32), 19188–19196.
- Busfield, S. J., Michnick, D. A., Chickering, T. W., Revett, T. L., Ma, J., Woolf, E. A., ... Gearing, D. P. (1997). Characterization of a neuregulin-related gene, Don-1, that is highly expressed in restricted regions of the cerebellum and hippocampus. *Molecular and Cellular Biology*, 17(7), 4007–4014.
- Cabedo, H., Carteron, C., & Ferrer-Montiel, A. (2004). Oligomerization of the sensory and motor neuron-derived factor prevents protein O-glycosylation. *The Journal of Biological Chemistry*, 279(32), 33623–33629. doi:10.1074/jbc.M401962200
- Caceres, A., Banker, G., Steward, O., Binder, L., & Payne, M. (1984). MAP2 is localized to the dendrites of hippocampal neurons which develop in culture. *Brain Research*, 315(2), 314–318.
- Cahill, M E, Jones, K. A., Rafalovich, I., Xie, Z., Barros, C. S., Müller, U., & Penzes, P. (2012). Control of interneuron dendritic growth through NRG1/erbB4-mediated kalirin-7 disinhibition. *Molecular Psychiatry*, 17(1), 1, 99–107. doi:10.1038/mp.2011.35
- Cahill, Michael E, Remmers, C., Jones, K. A., Xie, Z., Sweet, R. A., & Penzes, P. (2013). Neuregulin1 signaling promotes dendritic spine growth through kalirin. *Journal of Neurochemistry*, 126(5), 625–635. doi:10.1111/jnc.12330

- Cannon, T. D. (2015). How schizophrenia develops: cognitive and brain mechanisms underlying onset of psychosis. *Trends in Cognitive Sciences*, 19(12), 744–756. doi:10.1016/j.tics.2015.09.009
- Cannon, T. D., Chung, Y., He, G., Sun, D., Jacobson, A., van Erp, T. G. M., ... North American Prodrome Longitudinal Study Consortium. (2015). Progressive reduction in cortical thickness as psychosis develops: a multisite longitudinal neuroimaging study of youth at elevated clinical risk. *Biological Psychiatry*, 77(2), 147–157. doi:10.1016/j.biopsych.2014.05.023
- Canoll, P. D., Musacchio, J. M., Hardy, R., Reynolds, R., Marchionni, M. A., & Salzer, J. L. (1996). GGF/neuregulin is a neuronal signal that promotes the proliferation and survival and inhibits the differentiation of oligodendrocyte progenitors. *Neuron*, 17(2), 229–243. doi:10.1016/S0896-6273(00)80155-5
- Cao, L., Deng, W., Guan, L., Yang, Z., Lin, Y., Ma, X., ... Hu, X. (2014). Association of the 3' region of the neuregulin 1 gene with bipolar I disorder in the Chinese Han population. *Journal of Affective Disorders*, 162, 81–88. doi:10.1016/j.jad.2014.03.037
- Cappellini, M. D., Cohen, A., Piga, A., Bejaoui, M., Perrotta, S., Agaoglu, L., ... Alberti, D. (2006). A phase 3 study of deferasirox (ICL670), a once-daily oral iron chelator, in patients with beta-thalassemia. *Blood*, 107(9), 3455–3462. doi:10.1182/blood-2005-08-3430
- Cappello, S., Attardo, A., Wu, X., Iwasato, T., Itohara, S., Wilsch-Bräuninger, M., ... Götz, M. (2006). The Rho-GTPase cdc42 regulates neural progenitor fate at the apical surface. *Nature Neuroscience*, 9(9), 1099–1107. doi:10.1038/nn1744
- Carraway, K. L., Weber, J. L., Unger, M. J., Ledesma, J., Yu, N., Gassmann, M., & Lai, C. (1997). Neuregulin-2, a new ligand of ErbB3/ErbB4-receptor tyrosine kinases. *Nature*, 387(6632), 512–516. doi:10.1038/387512a0
- Carteron, C., Ferrer-Montiel, A., & Cabedo, H. (2006). Characterization of a neural-specific splicing form of the human neuregulin 3 gene involved in oligodendrocyte survival. *Journal of Cell Science*, 119(Pt 5), 898–909. doi:10.1242/jcs.02799
- Catalani, A., Sabbatini, M., Consoli, C., Cinque, C., Tomassoni, D., Azmitia, E., ... Amenta, F. (2002). Glial fibrillary acidic protein immunoreactive astrocytes in developing rat hippocampus. *Mechanisms of Ageing and Development*, 123(5), 481–490. doi:10.1016/S0047-6374(01)00356-6
- Chang, H., Riese, D. J., Gilbert, W., Stern, D. F., & McMahan, U. J. (1997). Ligands for ErbB-family receptors encoded by a neuregulin-like gene. *Nature*, 387(6632), 509–512. doi:10.1038/387509a0
- Chen, L., Liao, G., Yang, L., Campbell, K., Nakafuku, M., Kuan, C.-Y., & Zheng, Y. (2006). Cdc42 deficiency causes Sonic hedgehog-independent holoprosencephaly. *Proceedings*

of the National Academy of Sciences of the United States of America, 103(44), 16520–16525. doi:10.1073/pnas.0603533103

- Chen, M. S., Bermingham-McDonogh, O., Danehy, F. T., Nolan, C., Scherer, S. S., Lucas, J., ... Marchionni, M. A. (1994). Expression of multiple neuregulin transcripts in postnatal rat brains. *The Journal of Comparative Neurology*, 349(3), 389–400. doi:10.1002/cne.903490306
- Chen, P.-L., Avramopoulos, D., Lasseter, V. K., McGrath, J. A., Fallin, M. D., Liang, K.-Y., ... Valle, D. (2009). Fine mapping on chromosome 10q22-q23 implicates Neuregulin 3 in schizophrenia. *American Journal of Human Genetics*, 84(1), 21–34. doi:10.1016/j.ajhg.2008.12.005
- Chen, S., Chen, J., Shi, H., Wei, M., Castaneda-Castellanos, D. R., Bultje, R. S., ... Shi, S.-H. (2013). Regulation of microtubule stability and organization by mammalian Par3 in specifying neuronal polarity. *Developmental Cell*, 24(1), 26–40. doi:10.1016/j.devcel.2012.11.014
- Chen, Y. H., Lan, Y. J., Zhang, S. R., Li, W. P., Luo, Z. Y., Lin, S., ... Gao, T. M. (2017). ErbB4 signaling in the prelimbic cortex regulates fear expression. *Translational Psychiatry*, 7(7), e1168. doi:10.1038/tp.2017.139
- Chen, Y., Hancock, M. L., Role, L. W., & Talmage, D. A. (2010). Intramembranous valine linked to schizophrenia is required for neuregulin 1 regulation of the morphological development of cortical neurons. *The Journal of Neuroscience*, 30(27), 9199–9208. doi:10.1523/JNEUROSCI.0605-10.2010
- Chen, Y.-J. J., Johnson, M. A., Lieberman, M. D., Goodchild, R. E., Schobel, S., Lewandowski, N., ... Role, L. W. (2008). Type III neuregulin-1 is required for normal sensorimotor gating, memory-related behaviors, and corticostriatal circuit components. *The Journal of Neuroscience*, 28(27), 6872–6883. doi:10.1523/JNEUROSCI.1815-08.2008
- Chen, Y.-J., Zhang, M., Yin, D.-M., Wen, L., Ting, A., Wang, P., ... Gao, T.-M. (2010). ErbB4 in parvalbumin-positive interneurons is critical for neuregulin 1 regulation of long-term potentiation. *Proceedings of the National Academy of Sciences of the United States of America*, 107(50), 21818–21823. doi:10.1073/pnas.1010669107
- Chou, F.-S., Li, R., & Wang, P.-S. (2018). Molecular components and polarity of radial glial cells during cerebral cortex development. *Cellular and Molecular Life Sciences*, 75(6), 1027–1041. doi:10.1007/s00018-017-2680-0
- Chung, D. W., Volk, D. W., Arion, D., Zhang, Y., Sampson, A. R., & Lewis, D. A. (2016). Dysregulated erbb4 splicing in schizophrenia: selective effects on parvalbumin expression. *The American Journal of Psychiatry*, 173(1), 60–68. doi:10.1176/appi.ajp.2015.15020150

- Chung, D. W., Wills, Z. P., Fish, K. N., & Lewis, D. A. (2017). Developmental pruning of excitatory synaptic inputs to parvalbumin interneurons in monkey prefrontal cortex. *Proceedings of the National Academy of Sciences of the United States of America*, *114*(4), E629–E637. doi:10.1073/pnas.1610077114
- Cohen, B. D., Green, J. M., Foy, L., & Fell, H. P. (1996). HER4-mediated biological and biochemical properties in NIH 3T3 cells. Evidence for HER1-HER4 heterodimers. *The Journal of Biological Chemistry*, *271*(9), 4813–4818.
- Cohen-Cory, S., Kidane, A. H., Shirkey, N. J., & Marshak, S. (2010). Brain-derived neurotrophic factor and the development of structural neuronal connectivity. *Developmental Neurobiology*, *70*(5), 271–288. doi:10.1002/dneu.20774
- Colombo, F., Racchetti, G., & Meldolesi, J. (2014). Neurite outgrowth induced by NGF or L1CAM via activation of the TrkA receptor is sustained also by the exocytosis of enlargosomes. *Proceedings of the National Academy of Sciences of the United States of America*, *111*(47), 16943–16948. doi:10.1073/pnas.1406097111
- Corbin, J. G., Nery, S., & Fishell, G. (2001). Telencephalic cells take a tangent: non-radial migration in the mammalian forebrain. *Nature Neuroscience*, *4 Suppl*, 1177–1182. doi:10.1038/nn749
- Corfas, G., Rosen, K. M., Aratake, H., Krauss, R., & Fischbach, G. D. (1995). Differential expression of ARIA isoforms in the rat brain. *Neuron*, *14*(1), 103–115.
- Cosker, K. E., & Segal, R. A. (2014). Neuronal signaling through endocytosis. *Cold Spring Harbor Perspectives in Biology*, *6*(2). doi:10.1101/cshperspect.a020669
- Costa, M. R., Wen, G., Lepier, A., Schroeder, T., & Götz, M. (2008). Par-complex proteins promote proliferative progenitor divisions in the developing mouse cerebral cortex. *Development*, *135*(1), 11–22. doi:10.1242/dev.009951
- Coussens, L., Yang-Feng, T. L., Liao, Y. C., Chen, E., Gray, A., McGrath, J., ... Francke, U. (1985). Tyrosine kinase receptor with extensive homology to EGF receptor shares chromosomal location with neu oncogene. *Science*, *230*(4730), 1132–1139.
- Cowan, F., Rutherford, M., Groenendaal, F., Eken, P., Mercuri, E., Bydder, G. M., ... de Vries, L. S. (2003). Origin and timing of brain lesions in term infants with neonatal encephalopathy. *The Lancet*, *361*(9359), 736–742. doi:10.1016/S0140-6736(03)12658-X
- Craig, A. M., Jareb, M., & Banker, G. (1992). Neuronal polarity. *Current Biology*, *2*(10), 544. doi:10.1016/0960-9822(92)90027-8
- Datta, D., & Arnsten, A. F. T. (2018). Unique Molecular Regulation of Higher-Order Prefrontal Cortical Circuits: Insights into the Neurobiology of Schizophrenia. *ACS Chemical Neuroscience*, *9*(9), 2127–2145. doi:10.1021/acschemneuro.7b00505

- De Curtis, I. (Ed.). (2007). *Intracellular mechanisms for neuritogenesis*. Boston, MA: Springer US. doi:10.1007/978-0-387-68561-8
- de Anda, F. C., Pollarolo, G., Da Silva, J. S., Camoletto, P. G., Feiguin, F., & Dotti, C. G. (2005). Centrosome localization determines neuronal polarity. *Nature*, *436*(7051), 704–708. doi:10.1038/nature03811
- Deakin, I. H., Law, A. J., Oliver, P. L., Schwab, M. H., Nave, K. A., Harrison, P. J., & Bannerman, D. M. (2009). Behavioural characterization of neuregulin 1 type I overexpressing transgenic mice. *Neuroreport*, *20*(17), 1523–1528. doi:10.1097/WNR.0b013e328330f6e7
- Deakin, I. H., Nissen, W., Law, A. J., Lane, T., Kanso, R., Schwab, M. H., ... Harrison, P. J. (2012). Transgenic overexpression of the type I isoform of neuregulin 1 affects working memory and hippocampal oscillations but not long-term potentiation. *Cerebral Cortex*, *22*(7), 1520–1529. doi:10.1093/cercor/bhr223
- Dehmelt, L., Smart, F. M., Ozer, R. S., & Halpain, S. (2003). The role of microtubule-associated protein 2c in the reorganization of microtubules and lamellipodia during neurite initiation. *The Journal of Neuroscience*, *23*(29), 9479–9490.
- Del Pino, I., García-Frigola, C., Dehorter, N., Brotons-Mas, J. R., Alvarez-Salvado, E., Martínez de Lagrán, M., ... Rico, B. (2013). Erbb4 deletion from fast-spiking interneurons causes schizophrenia-like phenotypes. *Neuron*, *79*(6), 1152–1168. doi:10.1016/j.neuron.2013.07.010
- Dent, E. W., Gupton, S. L., & Gertler, F. B. (2011). The growth cone cytoskeleton in axon outgrowth and guidance. *Cold Spring Harbor Perspectives in Biology*, *3*(3). doi:10.1101/cshperspect.a001800
- Dobbing, J., & Sands, J. (1979). Comparative aspects of the brain growth spurt. *Early Human Development*, *3*(1), 79–83. doi:10.1016/0378-3782(79)90022-7
- Dong, Z., Brennan, A., Liu, N., Yarden, Y., Lefkowitz, G., Mirsky, R., & Jessen, K. R. (1995). Neu differentiation factor is a neuron-glia signal and regulates survival, proliferation, and maturation of rat Schwann cell precursors. *Neuron*, *15*(3), 585–596. doi:10.1016/0896-6273(95)90147-7
- Dotti, C. G., Sullivan, C. A., & Banker, G. A. (1988). The establishment of polarity by hippocampal neurons in culture. *The Journal of Neuroscience*, *8*(4), 1454–1468.
- Dow, L. E., & Humbert, P. O. (2007). Polarity Regulators and the Control of Epithelial Architecture, Cell Migration, and Tumorigenesis (Vol. 262, pp. 253–302). Elsevier. doi:10.1016/S0074-7696(07)62006-3
- Du, Z., & Lovly, C. M. (2018). Mechanisms of receptor tyrosine kinase activation in cancer. *Molecular Cancer*, *17*(1), 58. doi:10.1186/s12943-018-0782-4

- Duffy, L, Cappas, E., Lai, D., Boucher, A. A., & Karl, T. (2010). Cognition in transmembrane domain neuregulin 1 mutant mice. *Neuroscience*, *170*(3), 800–807. doi:10.1016/j.neuroscience.2010.07.042
- Duffy, Liesl, Cappas, E., Scimone, A., Schofield, P. R., & Karl, T. (2008). Behavioral profile of a heterozygous mutant mouse model for EGF-like domain neuregulin 1. *Behavioral Neuroscience*, *122*(4), 748–759. doi:10.1037/0735-7044.122.4.748
- Ehrlichman, R. S., Luminais, S. N., White, S. L., Rudnick, N. D., Ma, N., Dow, H. C., ... Siegel, S. J. (2009). Neuregulin 1 transgenic mice display reduced mismatch negativity, contextual fear conditioning and social interactions. *Brain Research*, *1294*, 116–127. doi:10.1016/j.brainres.2009.07.065
- Eichenbaum, H., Otto, T., & Cohen, N. J. (1992). The hippocampus--what does it do? *Behavioral and Neural Biology*, *57*(1), 2–36. doi:10.1016/0163-1047(92)90724-I
- El-Husseini, A. E., Schnell, E., Chetkovich, D. M., Nicoll, R. A., & Brecht, D. S. (2000). PSD-95 involvement in maturation of excitatory synapses. *Science*, *290*(5495), 1364–1368.
- Elenius, K, Choi, C. J., Paul, S., Santiestevan, E., Nishi, E., & Klagsbrun, M. (1999). Characterization of a naturally occurring ErbB4 isoform that does not bind or activate phosphatidyl inositol 3-kinase. *Oncogene*, *18*(16), 2607–2615. doi:10.1038/sj.onc.1202612
- Elenius, Klaus, Corfas, G., Paul, S., Choi, C. J., Rio, C., Plowman, G. D., & Klagsbrun, M. (1997). A novel juxtamembrane domain isoform of her4/erbb4. *Journal of Biological Chemistry*, *272*(42), 26761–26768. doi:10.1074/jbc.272.42.26761
- Erben, L., He, M.-X., Laeremans, A., Park, E., & Buonanno, A. (2018). A Novel Ultrasensitive In Situ Hybridization Approach to Detect Short Sequences and Splice Variants with Cellular Resolution. *Molecular Neurobiology*, *55*(7), 6169–6181. doi:10.1007/s12035-017-0834-6
- Erickson, S. L., O’Shea, K. S., Ghaboosi, N., Loverro, L., Frantz, G., Bauer, M., ... Moore, M. W. (1997). ErbB3 is required for normal cerebellar and cardiac development: a comparison with ErbB2-and heregulin-deficient mice. *Development*, *124*(24), 4999–5011.
- Esnafoglu, E. (2018). Levels of peripheral Neuregulin 1 are increased in non-medicated autism spectrum disorder patients. *Journal of Clinical Neuroscience*, *57*, 43–45. doi:10.1016/j.jocn.2018.08.043
- Etienne-Manneville, S. (2008). Polarity proteins in migration and invasion. *Oncogene*, *27*(55), 6970–6980. doi:10.1038/onc.2008.347
- Fallin, M. D., Lasseter, V. K., Wolyniec, P. S., McGrath, J. A., Nestadt, G., Valle, D., ... Pulver, A. E. (2003). Genomewide linkage scan for schizophrenia susceptibility loci among Ashkenazi Jewish families shows evidence of linkage on chromosome 10q22. *American Journal of Human Genetics*, *73*(3), 601–611. doi:10.1086/378158

- Falls, D L, Rosen, K. M., Corfas, G., Lane, W. S., & Fischbach, G. D. (1993). ARIA, a protein that stimulates acetylcholine receptor synthesis, is a member of the neu ligand family. *Cell*, *72*(5), 801–815. doi:10.1016/0092-8674(93)90407-H
- Falls, Douglas L. (2003). Neuregulins: functions, forms, and signaling strategies. *Experimental Cell Research*, *284*(1), 14–30. doi:10.1016/S0014-4827(02)00102-7
- Faraone, S. V., Hwu, H.-G., Liu, C.-M., Chen, W. J., Tsuang, M.-M., Liu, S.-K., ... Tsuang, M. T. (2006). Genome scan of Han Chinese schizophrenia families from Taiwan: confirmation of linkage to 10q22.3. *The American Journal of Psychiatry*, *163*(10), 1760–1766. doi:10.1176/ajp.2006.163.10.1760
- Fariás, G. G., Britt, D. J., & Bonifacino, J. S. (2016). Imaging the Polarized Sorting of Proteins from the Golgi Complex in Live Neurons. *Methods in Molecular Biology*, *1496*, 13–30. doi:10.1007/978-1-4939-6463-5_2
- Fazzari, P., Paternain, A. V., Valiente, M., Pla, R., Luján, R., Lloyd, K., ... Rico, B. (2010). Control of cortical GABA circuitry development by Nrg1 and ErbB4 signalling. *Nature*, *464*(7293), 1376–1380. doi:10.1038/nature08928
- Feinberg, I. (1982). Schizophrenia: caused by a fault in programmed synaptic elimination during adolescence? *Journal of Psychiatric Research*, *17*(4), 319–334. doi:10.1016/0022-3956(82)90038-3
- Feldman, M. L., & Peters, A. (1978). The forms of non-pyramidal neurons in the visual cortex of the rat. *The Journal of Comparative Neurology*, *179*(4), 761–793. doi:10.1002/cne.901790406
- Fernandez, P. A., Tang, D. G., Cheng, L., Prochiantz, A., Mudge, A. W., & Raff, M. C. (2000). Evidence that axon-derived neuregulin promotes oligodendrocyte survival in the developing rat optic nerve. *Neuron*, *28*(1), 81–90. doi:10.1016/S0896-6273(00)00087-8
- Fisahn, A., Neddens, J., Yan, L., & Buonanno, A. (2009). Neuregulin-1 modulates hippocampal gamma oscillations: implications for schizophrenia. *Cerebral Cortex*, *19*(3), 612–618. doi:10.1093/cercor/bhn107
- Flames, N., Long, J. E., Garratt, A. N., Fischer, T. M., Gassmann, M., Birchmeier, C., ... Marín, O. (2004). Short- and long-range attraction of cortical GABAergic interneurons by neuregulin-1. *Neuron*, *44*(2), 251–261. doi:10.1016/j.neuron.2004.09.028
- Fleck, D., van Bebber, F., Colombo, A., Galante, C., Schwenk, B. M., Rabe, L., ... Haass, C. (2013). Dual cleavage of neuregulin 1 type III by BACE1 and ADAM17 liberates its EGF-like domain and allows paracrine signaling. *The Journal of Neuroscience*, *33*(18), 7856–7869. doi:10.1523/JNEUROSCI.3372-12.2013
- Flores, A. I., Mallon, B. S., Matsui, T., Ogawa, W., Rosenzweig, A., Okamoto, T., & Macklin, W. B. (2000). Akt-mediated survival of oligodendrocytes induced by neuregulins. *The Journal of Neuroscience*, *20*(20), 7622–7630.

- Flynn, K. C. (2013). The cytoskeleton and neurite initiation. *Bioarchitecture*, 3(4), 86–109. doi:10.4161/bioa.26259
- Flynn, K. C., Hellal, F., Neukirchen, D., Jacob, S., Tahirovic, S., Dupraz, S., ... Bradke, F. (2012). ADF/cofilin-mediated actin retrograde flow directs neurite formation in the developing brain. *Neuron*, 76(6), 1091–1107. doi:10.1016/j.neuron.2012.09.038
- Fornasari, B. E., El Soury, M., De Marchis, S., Perroteau, I., Geuna, S., & Gambarotta, G. (2016). Neuregulin1 alpha activates migration of neuronal progenitors expressing ErbB4. *Molecular and Cellular Neurosciences*, 77, 87–94. doi:10.1016/j.mcn.2016.10.008
- Fox, I. J., & Kornblum, H. I. (2005). Developmental profile of ErbB receptors in murine central nervous system: implications for functional interactions. *Journal of Neuroscience Research*, 79(5), 584–597. doi:10.1002/jnr.20381
- Franco, S. J., & Müller, U. (2013). Shaping our minds: stem and progenitor cell diversity in the mammalian neocortex. *Neuron*, 77(1), 19–34. doi:10.1016/j.neuron.2012.12.022
- Funahashi, Y., Namba, T., Fujisue, S., Itoh, N., Nakamuta, S., Kato, K., ... Kaibuchi, K. (2013). ERK2-mediated phosphorylation of Par3 regulates neuronal polarization. *The Journal of Neuroscience*, 33(33), 13270–13285. doi:10.1523/JNEUROSCI.4210-12.2013
- Fuschini, G., Cotrufo, T., Ros, O., Muhaisen, A., Andrés, R., Comella, J. X., & Soriano, E. (2018). Syntaxin-1/TI-VAMP SNAREs interact with Trk receptors and are required for neurotrophin-dependent outgrowth. *Oncotarget*, 9(89), 35922–35940. doi:10.18632/oncotarget.26307
- Gage, F. H. (2002). Neurogenesis in the adult brain. *The Journal of Neuroscience*, 22(3), 612–613. doi:10.1523/JNEUROSCI.22-03-00612.2002
- Gamett, D. C., & Cerione, R. A. (1994). Oncogenically activated or ligand-stimulated neu kinase stimulates neurite outgrowth in PC12 cells. *FEBS Letters*, 351(3), 335–339.
- Gamett, D. C., Greene, T., Wagreich, A. R., Kim, H. H., Koland, J. G., & Cerione, R. A. (1995). Heregulin-stimulated signaling in rat pheochromocytoma cells. Evidence for ErbB3 interactions with Neu/ErbB2 and p85. *The Journal of Biological Chemistry*, 270(32), 19022–19027.
- Gao, L., Macara, I. G., & Joberty, G. (2002). Multiple splice variants of Par3 and of a novel related gene, Par3L, produce proteins with different binding properties. *Gene*, 294(1-2), 99–107. doi:10.1016/S0378-1119(02)00681-9
- Gao, R., & Penzes, P. (2015). Common mechanisms of excitatory and inhibitory imbalance in schizophrenia and autism spectrum disorders. *Current Molecular Medicine*, 15(2), 146–167. doi:10.2174/1566524015666150303003028

- García, L., Castillo, C., Carballo, J., Rodríguez, Y., Forsyth, P., Medina, R., ... Longart, M. (2013). ErbB receptors and PKC regulate PC12 neuronal-like differentiation and sodium current elicitation. *Neuroscience*, 236, 88–98. doi:10.1016/j.neuroscience.2013.01.026
- Garcia, R. A., Vasudevan, K., & Buonanno, A. (2000). The neuregulin receptor ErbB-4 interacts with PDZ-containing proteins at neuronal synapses. *Proceedings of the National Academy of Sciences of the United States of America*, 97(7), 3596–3601. doi:10.1073/pnas.070042497
- García-Rivello, H., Taranda, J., Said, M., Cabeza-Meckert, P., Vila-Petroff, M., Scaglione, J., ... Hertig, C. M. (2005). Dilated cardiomyopathy in Erb-b4-deficient ventricular muscle. *American Journal of Physiology. Heart and Circulatory Physiology*, 289(3), H1153–60. doi:10.1152/ajpheart.00048.2005
- Garrard, S. M., Capaldo, C. T., Gao, L., Rosen, M. K., Macara, I. G., & Tomchick, D. R. (2003). Structure of Cdc42 in a complex with the GTPase-binding domain of the cell polarity protein, Par6. *The EMBO Journal*, 22(5), 1125–1133. doi:10.1093/emboj/cdg110
- Garratt, A. N., Voiculescu, O., Topilko, P., Charnay, P., & Birchmeier, C. (2000). A Dual Role of *erbB2* in Myelination and in Expansion of the Schwann Cell Precursor Pool. *The Journal of Cell Biology*, 148(5), 1035–1046. doi:10.1083/jcb.148.5.1035
- Garvalov, B. K., Flynn, K. C., Neukirchen, D., Meyn, L., Teusch, N., Wu, X., ... Bradke, F. (2007). Cdc42 regulates cofilin during the establishment of neuronal polarity. *The Journal of Neuroscience*, 27(48), 13117–13129. doi:10.1523/JNEUROSCI.3322-07.2007
- Gaskin, P. L. R., Alexander, S. P. H., & Fone, K. C. F. (2014). Neonatal phencyclidine administration and post-weaning social isolation as a dual-hit model of “schizophrenia-like” behaviour in the rat. *Psychopharmacology*, 231(12), 2533–2545. doi:10.1007/s00213-013-3424-y
- Gassmann, M., Casagrande, F., Orioli, D., Simon, H., Lai, C., Klein, R., & Lemke, G. (1995). Aberrant neural and cardiac development in mice lacking the ErbB4 neuregulin receptor. *Nature*, 378(6555), 390–394. doi:10.1038/378390a0
- Gauthier, M.-K., Kosciuczyk, K., Tapley, L., & Karimi-Abdolrezaee, S. (2013). Dysregulation of the neuregulin-1-ErbB network modulates endogenous oligodendrocyte differentiation and preservation after spinal cord injury. *The European Journal of Neuroscience*, 38(5), 2693–2715. doi:10.1111/ejn.12268
- Geng, H.-Y., Zhang, J., Yang, J.-M., Li, Y., Wang, N., Ye, M., ... Li, X.-M. (2017). Erbb4 Deletion from Medium Spiny Neurons of the Nucleus Accumbens Core Induces Schizophrenia-Like Behaviors via Elevated GABAA Receptor $\alpha 1$ Subunit Expression. *The Journal of Neuroscience*, 37(31), 7450–7464. doi:10.1523/JNEUROSCI.3948-16.2017

- Georgieva, L., Dimitrova, A., Ivanov, D., Nikolov, I., Williams, N. M., Grozeva, D., ... O'Donovan, M. C. (2008). Support for neuregulin 1 as a susceptibility gene for bipolar disorder and schizophrenia. *Biological Psychiatry*, *64*(5), 419–427. doi:10.1016/j.biopsych.2008.03.025
- Gerecke, K M, Wyss, J. M., Karavanova, I., Buonanno, A., & Carroll, S. L. (2001). ErbB transmembrane tyrosine kinase receptors are differentially expressed throughout the adult rat central nervous system. *The Journal of Comparative Neurology*, *433*(1), 86–100.
- Gerecke, Kimberly M, Wyss, J. M., & Carroll, S. L. (2004). Neuregulin-1beta induces neurite extension and arborization in cultured hippocampal neurons. *Molecular and Cellular Neurosciences*, *27*(4), 379–393. doi:10.1016/j.mcn.2004.08.001
- Gerlai, R., Pisacane, P., & Erickson, S. (2000). Heregulin, but not ErbB2 or ErbB3, heterozygous mutant mice exhibit hyperactivity in multiple behavioral tasks. *Behavioural Brain Research*, *109*(2), 219–227. doi:10.1016/S0166-4328(99)00175-8
- Ghashghaei, H T, Weber, J., Pevny, L., Schmid, R., Schwab, M. H., Lloyd, K. C. K., ... Anton, E. S. (2006). The role of neuregulin-ErbB4 interactions on the proliferation and organization of cells in the subventricular zone. *Proceedings of the National Academy of Sciences of the United States of America*, *103*(6), 1930–1935. doi:10.1073/pnas.0510410103
- Ghashghaei, H Troy, Lai, C., & Anton, E. S. (2007). Neuronal migration in the adult brain: are we there yet? *Nature Reviews. Neuroscience*, *8*(2), 141–151. doi:10.1038/nrn2074
- Ghosh, S., Marquardt, T., Thaler, J. P., Carter, N., Andrews, S. E., Pfaff, S. L., & Hunter, T. (2008). Instructive role of aPKCzeta subcellular localization in the assembly of adherens junctions in neural progenitors. *Proceedings of the National Academy of Sciences of the United States of America*, *105*(1), 335–340. doi:10.1073/pnas.0705713105
- Gilabert-Juan, J., Belles, M., Saez, A. R., Carceller, H., Zamarbide-Fores, S., Moltó, M. D., & Nacher, J. (2013). A “double hit” murine model for schizophrenia shows alterations in the structure and neurochemistry of the medial prefrontal cortex and the hippocampus. *Neurobiology of Disease*, *59*, 126–140. doi:10.1016/j.nbd.2013.07.008
- Gilbertson, R., Hernan, R., Pietsch, T., Pinto, L., Scotting, P., Allibone, R., ... Lunec, J. (2001). Novel ERBB4 juxtamembrane splice variants are frequently expressed in childhood medulloblastoma. *Genes, Chromosomes & Cancer*, *31*(3), 288–294. doi:10.1002/gcc.1146
- Glantz, L. A., & Lewis, D. A. (2000). Decreased dendritic spine density on prefrontal cortical pyramidal neurons in schizophrenia. *Archives of General Psychiatry*, *57*(1), 65–73. doi:10.1001/archpsyc.57.1.65
- Glausier, J. R., & Lewis, D. A. (2013). Dendritic spine pathology in schizophrenia. *Neuroscience*, *251*, 90–107. doi:10.1016/j.neuroscience.2012.04.044

- Go, R. C. P., Perry, R. T., Wiener, H., Bassett, S. S., Blacker, D., Devlin, B., & Sweet, R. A. (2005). Neuregulin-1 polymorphism in late onset Alzheimer's disease families with psychoses. *American Journal of Medical Genetics. Part B, Neuropsychiatric Genetics*, 139B(1), 28–32. doi:10.1002/ajmg.b.30219
- Goda, Y., & Davis, G. W. (2003). Mechanisms of synapse assembly and disassembly. *Neuron*, 40(2), 243–264. doi:10.1016/S0896-6273(03)00608-1
- Goes, F. S., Willour, V. L., Zandi, P. P., Belmonte, P. L., MacKinnon, D. F., Mondimore, F. M., ... NIMH Genetics Initiative Bipolar Disorder Consortium. (2009). Family-based association study of Neuregulin 1 with psychotic bipolar disorder. *American Journal of Medical Genetics. Part B, Neuropsychiatric Genetics*, 150B(5), 693–702. doi:10.1002/ajmg.b.30895
- Goldstein, B., & Macara, I. G. (2007). The PAR proteins: fundamental players in animal cell polarization. *Developmental Cell*, 13(5), 609–622. doi:10.1016/j.devcel.2007.10.007
- Goodearl, A. D., Davis, J. B., Mistry, K., Minghetti, L., Otsu, M., Waterfield, M. D., & Stroobant, P. (1993). Purification of multiple forms of glial growth factor. *The Journal of Biological Chemistry*, 268(24), 18095–18102.
- Goslin, K., & Banker, G. (1989). Experimental observations on the development of polarity by hippocampal neurons in culture. *The Journal of Cell Biology*, 108(4), 1507–1516.
- Govek, E.-E., Newey, S. E., & Van Aelst, L. (2005). The role of the Rho GTPases in neuronal development. *Genes & Development*, 19(1), 1–49. doi:10.1101/gad.1256405
- Grant, S., Qiao, L., & Dent, P. (2002). Roles of ERBB family receptor tyrosine kinases, and downstream signaling pathways, in the control of cell growth and survival. *Frontiers in Bioscience*, 7, d376–89.
- Grieco, S. F., Holmes, T. C., & Xu, X. (2019). Neuregulin directed molecular mechanisms of visual cortical plasticity. *The Journal of Comparative Neurology*, 527(3), 668–678. doi:10.1002/cne.24414
- Gu, Z., Jiang, Q., Fu, A. K. Y., Ip, N. Y., & Yan, Z. (2005). Regulation of NMDA receptors by neuregulin signaling in prefrontal cortex. *The Journal of Neuroscience*, 25(20), 4974–4984. doi:10.1523/JNEUROSCI.1086-05.2005
- Guo, G., Gong, K., Wohlfeld, B., Hatanpaa, K. J., Zhao, D., & Habib, A. A. (2015). Ligand-Independent EGFR Signaling. *Cancer Research*, 75(17), 3436–3441. doi:10.1158/0008-5472.CAN-15-0989
- Gupta, R., Qaiser, B., He, L., Hiekkalinna, T. S., Zheutlin, A. B., Therman, S., ... Loukola, A. (2017). Neuregulin signaling pathway in smoking behavior. *Translational Psychiatry*, 7(8), e1212. doi:10.1038/tp.2017.183

- Guy, P. M., Platko, J. V., Cantley, L. C., Cerione, R. A., & Carraway, K. L. (1994). Insect cell-expressed p180erbB3 possesses an impaired tyrosine kinase activity. *Proceedings of the National Academy of Sciences of the United States of America*, *91*(17), 8132–8136.
- Hahn, C.-G., Wang, H.-Y., Cho, D.-S., Talbot, K., Gur, R. E., Berrettini, W. H., ... Arnold, S. E. (2006). Altered neuregulin 1-erbB4 signaling contributes to NMDA receptor hypofunction in schizophrenia. *Nature Medicine*, *12*(7), 824–828. doi:10.1038/nm1418
- Hall, A., Paterson, H. F., Adamson, P., & Ridley, A. J. (1993). Cellular responses regulated by rho-related small GTP-binding proteins. *Philosophical Transactions of the Royal Society of London. Series B, Biological Sciences*, *340*(1293), 267–271. doi:10.1098/rstb.1993.0067
- Hamelers, I. H. L., Olivo, C., Mertens, A. E. E., Pegtel, D. M., van der Kammen, R. A., Sonnenberg, A., & Collard, J. G. (2005). The Rac activator Tiam1 is required for (alpha)3(beta)1-mediated laminin-5 deposition, cell spreading, and cell migration. *The Journal of Cell Biology*, *171*(5), 871–881. doi:10.1083/jcb.200509172
- Han, S., Yang, B.-Z., Kranzler, H. R., Oslin, D., Anton, R., Farrer, L. A., & Gelernter, J. (2012). Linkage analysis followed by association show NRG1 associated with cannabis dependence in African Americans. *Biological Psychiatry*, *72*(8), 637–644. doi:10.1016/j.biopsych.2012.02.038
- Hang, H. C., & Bertozzi, C. R. (2005). The chemistry and biology of mucin-type O-linked glycosylation. *Bioorganic & Medicinal Chemistry*, *13*(17), 5021–5034. doi:10.1016/j.bmc.2005.04.085
- Hanisch, F. G. (2001). O-glycosylation of the mucin type. *Biological Chemistry*, *382*(2), 143–149. doi:10.1515/BC.2001.022
- Hansen, A. H., Duellberg, C., Mieck, C., Loose, M., & Hippenmeyer, S. (2017). Cell Polarity in Cerebral Cortex Development-Cellular Architecture Shaped by Biochemical Networks. *Frontiers in Cellular Neuroscience*, *11*, 176. doi:10.3389/fncel.2017.00176
- Hapak, S. M., Ghosh, S., & Rothlin, C. V. (2018). Axon regeneration: antagonistic signaling pairs in neuronal polarization. *Trends in Molecular Medicine*, *24*(7), 615–629. doi:10.1016/j.molmed.2018.05.007
- Hapak, S. M., Rothlin, C. V., & Ghosh, S. (2018). PAR3-PAR6-atypical PKC polarity complex proteins in neuronal polarization. *Cellular and Molecular Life Sciences*, *75*(15), 2735–2761. doi:10.1007/s00018-018-2828-6
- Harari, D., Tzahar, E., Romano, J., Shelly, M., Pierce, J. H., Andrews, G. C., & Yarden, Y. (1999). Neuregulin-4: a novel growth factor that acts through the ErbB-4 receptor tyrosine kinase. *Oncogene*, *18*(17), 2681–2689. doi:10.1038/sj.onc.1202631

- Harsing, L. G., & Zigmond, M. J. (1997). Influence of dopamine on GABA release in striatum: evidence for D1-D2 interactions and non-synaptic influences. *Neuroscience*, *77*(2), 419–429. doi:10.1016/S0306-4522(96)00475-7
- Hashimoto, R., Straub, R. E., Weickert, C. S., Hyde, T. M., Kleinman, J. E., & Weinberger, D. R. (2004). Expression analysis of neuregulin-1 in the dorsolateral prefrontal cortex in schizophrenia. *Molecular Psychiatry*, *9*(3), 299–307. doi:10.1038/sj.mp.4001434
- Hause, R. J., Leung, K. K., Barkinge, J. L., Ciaccio, M. F., Chuu, C.-P., & Jones, R. B. (2012). Comprehensive binary interaction mapping of SH2 domains via fluorescence polarization reveals novel functional diversification of ErbB receptors. *Plos One*, *7*(9), e44471. doi:10.1371/journal.pone.0044471
- Hayashi, K., Kawai-Hirai, R., Harada, A., & Takata, K. (2003). Inhibitory neurons from fetal rat cerebral cortex exert delayed axon formation and active migration in vitro. *Journal of Cell Science*, *116*(Pt 21), 4419–4428. doi:10.1242/jcs.00762
- Hayes, L. N., Shevelkin, A., Zeledon, M., Steel, G., Chen, P.-L., Obie, C., ... Pletnikov, M. V. (2016). Neuregulin 3 Knockout Mice Exhibit Behaviors Consistent with Psychotic Disorders. *Molecular Neuropsychiatry*, *2*(2), 79–87. doi:10.1159/000445836
- He, B.-S., Zhang, L.-Y., Pan, Y.-Q., Lin, K., Zhang, L.-L., Sun, H.-L., ... Zhu, C.-B. (2016). Association of the DISC1 and NRG1 genetic polymorphisms with schizophrenia in a Chinese population. *Gene*, *590*(2), 293–297. doi:10.1016/j.gene.2016.05.035
- Hengst, U., Deglincerti, A., Kim, H. J., Jeon, N. L., & Jaffrey, S. R. (2009). Axonal elongation triggered by stimulus-induced local translation of a polarity complex protein. *Nature Cell Biology*, *11*(8), 1024–1030. doi:10.1038/ncb1916
- Henrique, D., & Schweisguth, F. (2003). Cell polarity: the ups and downs of the Par6/aPKC complex. *Current Opinion in Genetics & Development*, *13*(4), 341–350. doi:10.1016/S0959-437X(03)00077-7
- Hens, J. R., & Wysolmerski, J. J. (2005). Key stages of mammary gland development: molecular mechanisms involved in the formation of the embryonic mammary gland. *Breast Cancer Research*, *7*(5), 220–224. doi:10.1186/bcr1306
- Hering, H., & Sheng, M. (2001). Dendritic spines: structure, dynamics and regulation. *Nature Reviews. Neuroscience*, *2*(12), 880–888. doi:10.1038/35104061
- Hernandez, A. I., Blace, N., Crary, J. F., Serrano, P. A., Leitges, M., Libien, J. M., ... Sacktor, T. C. (2003). Protein kinase M zeta synthesis from a brain mRNA encoding an independent protein kinase C zeta catalytic domain. Implications for the molecular mechanism of memory. *The Journal of Biological Chemistry*, *278*(41), 40305–40316. doi:10.1074/jbc.M307065200

- Higashiyama, S., Horikawa, M., Yamada, K., Ichino, N., Nakano, N., Nakagawa, T., ... Ishiguro, H. (1997). A novel brain-derived member of the epidermal growth factor family that interacts with ErbB3 and ErbB4. *Journal of Biochemistry*, 122(3), 675–680.
- Higginbotham, H., Tanaka, T., Brinkman, B. C., & Gleeson, J. G. (2006). GSK3beta and PKCzeta function in centrosome localization and process stabilization during Slit-mediated neuronal repolarization. *Molecular and Cellular Neurosciences*, 32(1-2), 118–132. doi:10.1016/j.mcn.2006.03.003
- Hirai, T., & Chida, K. (2003). Protein kinase Czeta (PKCzeta): activation mechanisms and cellular functions. *Journal of Biochemistry*, 133(1), 1–7. doi:10.1093/jb/mvg017
- Hirano, Y., Yoshinaga, S., Takeya, R., Suzuki, N. N., Horiuchi, M., Kohjima, M., ... Inagaki, F. (2005). Structure of a cell polarity regulator, a complex between atypical PKC and Par6 PB1 domains. *The Journal of Biological Chemistry*, 280(10), 9653–9661. doi:10.1074/jbc.M409823200
- Hoffmann, I., Bueter, W., Zscheppang, K., Brinkhaus, M.-J., Liese, A., Riemke, S., ... Dammann, C. E. L. (2010). Neuregulin-1, the fetal endothelium, and brain damage in preterm newborns. *Brain, Behavior, and Immunity*, 24(5), 784–791. doi:10.1016/j.bbi.2009.08.012
- Hollmén, M., & Elenius, K. (2010). Potential of ErbB4 antibodies for cancer therapy. *Future Oncology*, 6(1), 37–53. doi:10.2217/fon.09.144
- Holmes, W. E., Sliwkowski, M. X., Akita, R. W., Henzel, W. J., Lee, J., Park, J. W., ... Lewis, G. D. (1992). Identification of heregulin, a specific activator of p185erbB2. *Science*, 256(5060), 1205–1210. doi:10.1126/science.256.5060.1205
- Howard, B. A., & Gusterson, B. A. (2000). The characterization of a mouse mutant that displays abnormal mammary gland development. *Mammalian Genome*, 11(3), 234–237.
- Howard, B., Panchal, H., McCarthy, A., & Ashworth, A. (2005). Identification of the scaramanga gene implicates Neuregulin3 in mammary gland specification. *Genes & Development*, 19(17), 2078–2090. doi:10.1101/gad.338505
- Hu, R., Cao, Q., Sun, Z., Chen, J., Zheng, Q., & Xiao, F. (2018). A novel method of neural differentiation of PC12 cells by using Opti-MEM as a basic induction medium. *International Journal of Molecular Medicine*, 41(1), 195–201. doi:10.3892/ijmm.2017.3195
- Hu, X., Hicks, C. W., He, W., Wong, P., Macklin, W. B., Trapp, B. D., & Yan, R. (2006). Bace1 modulates myelination in the central and peripheral nervous system. *Nature Neuroscience*, 9(12), 1520–1525. doi:10.1038/nn1797
- Huang, E. J., & Reichardt, L. F. (2003). Trk receptors: roles in neuronal signal transduction. *Annual Review of Biochemistry*, 72, 609–642. doi:10.1146/annurev.biochem.72.121801.161629

- Huang, Y. Z., Won, S., Ali, D. W., Wang, Q., Tanowitz, M., Du, Q. S., ... Mei, L. (2000). Regulation of neuregulin signaling by PSD-95 interacting with ErbB4 at CNS synapses. *Neuron*, 26(2), 443–455. doi:10.1016/S0896-6273(00)81176-9
- Hung, A. Y., & Sheng, M. (2002). PDZ domains: structural modules for protein complex assembly. *The Journal of Biological Chemistry*, 277(8), 5699–5702. doi:10.1074/jbc.R100065200
- Hung, T. J., & Kemphues, K. J. (1999). PAR-6 is a conserved PDZ domain-containing protein that colocalizes with PAR-3 in *Caenorhabditis elegans* embryos. *Development*, 126(1), 127–135.
- Huttenlocher, P. R., & Dabholkar, A. S. (1997). Regional differences in synaptogenesis in human cerebral cortex. *The Journal of Comparative Neurology*, 387(2), 167–178. doi:10.1002/(SICI)1096-9861(19971020)387:2<167::AID-CNE1>3.0.CO;2-Z
- Insolera, R., Chen, S., & Shi, S.-H. (2011). Par proteins and neuronal polarity. *Developmental Neurobiology*, 71(6), 483–494. doi:10.1002/dneu.20867
- Iwakura, Y., & Nawa, H. (2013). ErbB1-4-dependent EGF/neuregulin signals and their cross talk in the central nervous system: pathological implications in schizophrenia and Parkinson's disease. *Frontiers in Cellular Neuroscience*, 7, 4. doi:10.3389/fncel.2013.00004
- Izumi, Y., Hirose, T., Tamai, Y., Hirai, S., Nagashima, Y., Fujimoto, T., ... Ohno, S. (1998). An Atypical PKC Directly Associates and Colocalizes at the Epithelial Tight Junction with ASIP, a Mammalian Homologue of *Caenorhabditis elegans* Polarity Protein PAR-3. *The Journal of Cell Biology*, 143(1), 95–106. doi:10.1083/jcb.143.1.95
- Jackson-Fisher, A. J., Bellinger, G., Ramabhadran, R., Morris, J. K., Lee, K.-F., & Stern, D. F. (2004). ErbB2 is required for ductal morphogenesis of the mammary gland. *Proceedings of the National Academy of Sciences of the United States of America*, 101(49), 17138–17143. doi:10.1073/pnas.0407057101
- Janssen, M. J., Leiva-Salcedo, E., & Buonanno, A. (2012). Neuregulin directly decreases voltage-gated sodium current in hippocampal ErbB4-expressing interneurons. *The Journal of Neuroscience*, 32(40), 13889–13895. doi:10.1523/JNEUROSCI.1420-12.2012
- Jessell, T. M., Siegel, R. E., & Fischbach, G. D. (1979). Induction of acetylcholine receptors on cultured skeletal muscle by a factor extracted from brain and spinal cord. *Proceedings of the National Academy of Sciences of the United States of America*, 76(10), 5397–5401. doi:10.1073/pnas.76.10.5397
- Jiang, M., & Chen, G. (2006). High Ca²⁺-phosphate transfection efficiency in low-density neuronal cultures. *Nature Protocols*, 1(2), 695–700. doi:10.1038/nprot.2006.86
- Jiang, Q., Chen, S., Hu, C., Huang, P., Shen, H., & Zhao, W. (2016). Neuregulin-1 (Nrg1) signaling has a preventive role and is altered in the frontal cortex under the pathological

- conditions of Alzheimer's disease. *Molecular Medicine Reports*, 14(3), 2614–2624. doi:10.3892/mmr.2016.5542
- Jin, X., Hu, H., Mathers, P. H., & Agmon, A. (2003). Brain-derived neurotrophic factor mediates activity-dependent dendritic growth in nonpyramidal neocortical interneurons in developing organotypic cultures. *The Journal of Neuroscience*, 23(13), 5662–5673.
- Joberty, G., Petersen, C., Gao, L., & Macara, I. G. (2000). The cell-polarity protein Par6 links Par3 and atypical protein kinase C to Cdc42. *Nature Cell Biology*, 2(8), 531–539. doi:10.1038/35019573
- Johansson, A., Driessens, M., & Aspenström, P. (2000). The mammalian homologue of the *Caenorhabditis elegans* polarity protein PAR-6 is a binding partner for the Rho GTPases Cdc42 and Rac1. *Journal of Cell Science*, 113 (Pt 18), 3267–3275.
- Jones, F. E., Welte, T., Fu, X. Y., & Stern, D. F. (1999). ErbB4 signaling in the mammary gland is required for lobuloalveolar development and Stat5 activation during lactation. *The Journal of Cell Biology*, 147(1), 77–88. doi:10.1083/jcb.147.1.77
- Jones, J. T., Akita, R. W., & Sliwkowski, M. X. (1999). Binding specificities and affinities of egf domains for ErbB receptors. *FEBS Letters*, 447(2-3), 227–231.
- Joshi, D., Fullerton, J. M., & Weickert, C. S. (2014). Elevated ErbB4 mRNA is related to interneuron deficit in prefrontal cortex in schizophrenia. *Journal of Psychiatric Research*, 53, 125–132. doi:10.1016/j.jpsychires.2014.02.014
- Junttila, T. T., Sundvall, M., Määttä, J. A., & Elenius, K. (2000). Erbb4 and its isoforms: selective regulation of growth factor responses by naturally occurring receptor variants. *Trends in Cardiovascular Medicine*, 10(7), 304–310. doi:10.1016/S1050-1738(01)00065-2
- Kalus, P., Bondzio, J., Federspiel, A., Müller, T. J., & Zuschratter, W. (2002). Cell-type specific alterations of cortical interneurons in schizophrenic patients. *Neuroreport*, 13(5), 713–717. doi:10.1097/00001756-200204160-00035
- Kaneko, N., Sawada, M., & Sawamoto, K. (2017). Mechanisms of neuronal migration in the adult brain. *Journal of Neurochemistry*, 141(6), 835–847. doi:10.1111/jnc.14002
- Kao, W.-T., Wang, Y., Kleinman, J. E., Lipska, B. K., Hyde, T. M., Weinberger, D. R., & Law, A. J. (2010). Common genetic variation in Neuregulin 3 (NRG3) influences risk for schizophrenia and impacts NRG3 expression in human brain. *Proceedings of the National Academy of Sciences of the United States of America*, 107(35), 15619–15624. doi:10.1073/pnas.1005410107
- Karl, T., Duffy, L., Scimone, A., Harvey, R. P., & Schofield, P. R. (2007). Altered motor activity, exploration and anxiety in heterozygous neuregulin 1 mutant mice: implications for understanding schizophrenia. *Genes, Brain, and Behavior*, 6(7), 677–687. doi:10.1111/j.1601-183X.2006.00298.x

- Kasnauskiene, J., Ciuladaite, Z., Preiksaitiene, E., Utkus, A., Peciulyte, A., & Kučinskas, V. (2013). A new single gene deletion on 2q34: ERBB4 is associated with intellectual disability. *American Journal of Medical Genetics. Part A*, 161A(6), 1487–1490. doi:10.1002/ajmg.a.35911
- Kataria, H., Alizadeh, A., Shahriary, G. M., Saboktakin Rizi, S., Henrie, R., Santhosh, K. T., ... Karimi-Abdolrezaee, S. (2018). Neuregulin-1 promotes remyelination and fosters a pro-regenerative inflammatory response in focal demyelinating lesions of the spinal cord. *Glia*, 66(3), 538–561. doi:10.1002/glia.23264
- Kawaguchi, Y., & Kubota, Y. (1997). GABAergic cell subtypes and their synaptic connections in rat frontal cortex. *Cerebral Cortex*, 7(6), 476–486. doi:10.1093/cercor/7.6.476
- Keith, D., & El-Husseini, A. (2008). Excitation Control: Balancing PSD-95 Function at the Synapse. *Frontiers in Molecular Neuroscience*, 1, 4. doi:10.3389/neuro.02.004.2008
- Kelsom, C., & Lu, W. (2013). Development and specification of GABAergic cortical interneurons. *Cell & Bioscience*, 3(1), 19. doi:10.1186/2045-3701-3-19
- Kerber, G., Streif, R., Schwaiger, F.-W., Kreutzberg, G. W., & Hager, G. (2003). Neuregulin-1 isoforms are differentially expressed in the intact and regenerating adult rat nervous system. *Journal of Molecular Neuroscience*, 21(2), 149–165. doi:10.1385/JMN:21:2:149
- Khodosevich, K., & Monyer, H. (2010). Signaling involved in neurite outgrowth of postnatally born subventricular zone neurons in vitro. *BMC Neuroscience*, 11, 18. doi:10.1186/1471-2202-11-18
- Kim, A. S., Anderson, S. A., Rubenstein, J. L., Lowenstein, D. H., & Pleasure, S. J. (2001). Pax-6 regulates expression of SFRP-2 and Wnt-7b in the developing CNS. *The Journal of Neuroscience*, 21(5), RC132.
- Kim, H., Chan, R., Dankort, D. L., Zuo, D., Najoukas, M., Park, M., & Muller, W. J. (2005). The c-Src tyrosine kinase associates with the catalytic domain of ErbB-2: implications for ErbB-2 mediated signaling and transformation. *Oncogene*, 24(51), 7599–7607. doi:10.1038/sj.onc.1208898
- Kiryushko, D., Berezin, V., & Bock, E. (2004). Regulators of neurite outgrowth: role of cell adhesion molecules. *Annals of the New York Academy of Sciences*, 1014, 140–154. doi:10.1196/annals.1294.015
- Knoblich, J. A. (2001). Asymmetric cell division during animal development. *Nature Reviews. Molecular Cell Biology*, 2(1), 11–20. doi:10.1038/35048085
- Kogata, N., Zvelebil, M., & Howard, B. A. (2013). Neuregulin 3 and erbb signalling networks in embryonic mammary gland development. *Journal of Mammary Gland Biology and Neoplasia*, 18(2), 149–154. doi:10.1007/s10911-013-9286-4

- Kolibaba, K. S., & Druker, B. J. (1997). Protein tyrosine kinases and cancer. *Biochimica et Biophysica Acta*, 1333(3), F217–48.
- Kon, E., Cossard, A., & Jossin, Y. (2017). Neuronal polarity in the embryonic mammalian cerebral cortex. *Frontiers in Cellular Neuroscience*, 11, 163. doi:10.3389/fncel.2017.00163
- Krahn, M. P., Klopfenstein, D. R., Fischer, N., & Wodarz, A. (2010). Membrane targeting of Bazooka/PAR-3 is mediated by direct binding to phosphoinositide lipids. *Current Biology*, 20(7), 636–642. doi:10.1016/j.cub.2010.01.065
- Kramer, R., Bucay, N., Kane, D. J., Martin, L. E., Tarpley, J. E., & Theill, L. E. (1996). Neuregulins with an Ig-like domain are essential for mouse myocardial and neuronal development. *Proceedings of the National Academy of Sciences of the United States of America*, 93(10), 4833–4838.
- Kraus, M. H., Issing, W., Miki, T., Popescu, N. C., & Aaronson, S. A. (1989). Isolation and characterization of ERBB3, a third member of the ERBB/epidermal growth factor receptor family: evidence for overexpression in a subset of human mammary tumors. *Proceedings of the National Academy of Sciences of the United States of America*, 86(23), 9193–9197.
- Kriegstein, A., & Alvarez-Buylla, A. (2009). The glial nature of embryonic and adult neural stem cells. *Annual Review of Neuroscience*, 32, 149–184. doi:10.1146/annurev.neuro.051508.135600
- Krivoshaya, D., Tapia, L., Levinson, J. N., Huang, K., Kang, Y., Hines, R., ... El-Husseini, A. (2008). ErbB4-neuregulin signaling modulates synapse development and dendritic arborization through distinct mechanisms. *The Journal of Biological Chemistry*, 283(47), 32944–32956. doi:10.1074/jbc.M800073200
- Kudelka, M. R., Ju, T., Heimbürg-Molinaro, J., & Cummings, R. D. (2015). Simple sugars to complex disease--mucin-type O-glycans in cancer. *Advances in Cancer Research*, 126, 53–135. doi:10.1016/bs.acr.2014.11.002
- Kukshal, P., Bhatia, T., Bhagwat, A. M., Gur, R. E., Gur, R. C., Deshpande, S. N., ... Thelma, B. K. (2013). Association study of neuregulin-1 gene polymorphisms in a North Indian schizophrenia sample. *Schizophrenia Research*, 144(1-3), 24–30. doi:10.1016/j.schres.2012.12.017
- Kumar, V., Zhang, M.-X., Swank, M. W., Kunz, J., & Wu, G.-Y. (2005). Regulation of dendritic morphogenesis by Ras-PI3K-Akt-mTOR and Ras-MAPK signaling pathways. *The Journal of Neuroscience*, 25(49), 11288–11299. doi:10.1523/JNEUROSCI.2284-05.2005
- Kwon, O. B., Paredes, D., Gonzalez, C. M., Neddens, J., Hernandez, L., Vullhorst, D., & Buonanno, A. (2008). Neuregulin-1 regulates LTP at CA1 hippocampal synapses through activation of dopamine D4 receptors. *Proceedings of the National Academy of*

- Sciences of the United States of America*, 105(40), 15587–15592.
doi:10.1073/pnas.0805722105
- Kwon, O.-B., Longart, M., Vullhorst, D., Hoffman, D. A., & Buonanno, A. (2005). Neuregulin-1 reverses long-term potentiation at CA1 hippocampal synapses. *The Journal of Neuroscience*, 25(41), 9378–9383. doi:10.1523/JNEUROSCI.2100-05.2005
- Lai, C., & Lemke, G. (1991). An extended family of protein-tyrosine kinase genes differentially expressed in the vertebrate nervous system. *Neuron*, 6(5), 691–704.
- Lai, Chen, & Feng, L. (2004). Neuregulin induces proliferation of neural progenitor cells via PLC/PKC pathway. *Biochemical and Biophysical Research Communications*, 319(2), 603–611. doi:10.1016/j.bbrc.2004.05.027
- Lal, M., & Caplan, M. (2011). Regulated intramembrane proteolysis: signaling pathways and biological functions. *Physiology*, 26(1), 34–44. doi:10.1152/physiol.00028.2010
- Laumonnerie, C., & Solecki, D. J. (2018). Regulation of polarity protein levels in the developing central nervous system. *Journal of Molecular Biology*, 430(19), 3472–3480. doi:10.1016/j.jmb.2018.05.036
- Laviola, G., Macrì, S., Morley-Fletcher, S., & Adriani, W. (2003). Risk-taking behavior in adolescent mice: psychobiological determinants and early epigenetic influence. *Neuroscience and Biobehavioral Reviews*, 27(1-2), 19–31. doi:10.1016/S0149-7634(03)00006-X
- Law, A. J., Kleinman, J. E., Weinberger, D. R., & Weickert, C. S. (2007). Disease-associated intronic variants in the ErbB4 gene are related to altered ErbB4 splice-variant expression in the brain in schizophrenia. *Human Molecular Genetics*, 16(2), 129–141. doi:10.1093/hmg/ddl449
- Law, A. J., Lipska, B. K., Weickert, C. S., Hyde, T. M., Straub, R. E., Hashimoto, R., ... Weinberger, D. R. (2006). Neuregulin 1 transcripts are differentially expressed in schizophrenia and regulated by 5' SNPs associated with the disease. *Proceedings of the National Academy of Sciences of the United States of America*, 103(17), 6747–6752. doi:10.1073/pnas.0602002103
- Lee, H.-J., Jung, K.-M., Huang, Y. Z., Bennett, L. B., Lee, J. S., Mei, L., & Kim, T.-W. (2002). Presenilin-dependent gamma-secretase-like intramembrane cleavage of ErbB4. *The Journal of Biological Chemistry*, 277(8), 6318–6323. doi:10.1074/jbc.M110371200
- Lee, K. F., Simon, H., Chen, H., Bates, B., Hung, M. C., & Hauser, C. (1995). Requirement for neuregulin receptor erbB2 in neural and cardiac development. *Nature*, 378(6555), 394–398. doi:10.1038/378394a0
- Lee, K.-H., Lee, H., Yang, C. H., Ko, J.-S., Park, C.-H., Woo, R.-S., ... Lee, S.-H. (2015). Bidirectional Signaling of Neuregulin-2 Mediates Formation of GABAergic Synapses and Maturation of Glutamatergic Synapses in Newborn Granule Cells of Postnatal

- Hippocampus. *The Journal of Neuroscience*, 35(50), 16479–16493. doi:10.1523/JNEUROSCI.1585-15.2015
- Lee, S., Hjerling-Leffler, J., Zagha, E., Fishell, G., & Rudy, B. (2010). The largest group of superficial neocortical GABAergic interneurons expresses ionotropic serotonin receptors. *The Journal of Neuroscience*, 30(50), 16796–16808. doi:10.1523/JNEUROSCI.1869-10.2010
- Lelièvre, S. A. (2010). Tissue polarity-dependent control of mammary epithelial homeostasis and cancer development: an epigenetic perspective. *Journal of Mammary Gland Biology and Neoplasia*, 15(1), 49–63. doi:10.1007/s10911-010-9168-y
- Lemke, G. (1996). Neuregulins in development. *Molecular and Cellular Neurosciences*, 7(4), 247–262. doi:10.1006/mcne.1996.0019
- Lemke, G. E., & Brockes, J. P. (1984). Identification and purification of glial growth factor. *The Journal of Neuroscience*, 4(1), 75–83.
- Lewis, C. M., Levinson, D. F., Wise, L. H., DeLisi, L. E., Straub, R. E., Hovatta, I., ... Faraone, S. V. (2003). Genome scan meta-analysis of schizophrenia and bipolar disorder, part II: Schizophrenia. *American Journal of Human Genetics*, 73(1), 34–48. doi:10.1086/376549
- Lewis, D. A., Curley, A. A., Glausier, J. R., & Volk, D. W. (2012). Cortical parvalbumin interneurons and cognitive dysfunction in schizophrenia. *Trends in Neurosciences*, 35(1), 57–67. doi:10.1016/j.tins.2011.10.004
- Li, B., Woo, R.-S., Mei, L., & Malinow, R. (2007). The neuregulin-1 receptor erbB4 controls glutamatergic synapse maturation and plasticity. *Neuron*, 54(4), 583–597. doi:10.1016/j.neuron.2007.03.028
- Li, H., Chou, S.-J., Hamasaki, T., Perez-Garcia, C. G., & O’Leary, D. D. M. (2012). Neuregulin repellent signaling via ErbB4 restricts GABAergic interneurons to migratory paths from ganglionic eminence to cortical destinations. *Neural Development*, 7, 10. doi:10.1186/1749-8104-7-10
- Li, J., Kim, H., Aceto, D. G., Hung, J., Aono, S., & Kempfues, K. J. (2010). Binding to PKC-3, but not to PAR-3 or to a conventional PDZ domain ligand, is required for PAR-6 function in *C. elegans*. *Developmental Biology*, 340(1), 88–98. doi:10.1016/j.ydbio.2010.01.023
- Li, K.-X., Lu, Y.-M., Xu, Z.-H., Zhang, J., Zhu, J.-M., Zhang, J.-M., ... Li, X.-M. (2012). Neuregulin 1 regulates excitability of fast-spiking neurons through Kv1.1 and acts in epilepsy. *Nature Neuroscience*, 15(2), 267–273. doi:10.1038/nn.3006
- Lim, L., Mi, D., Llorca, A., & Marín, O. (2018). Development and functional diversification of cortical interneurons. *Neuron*, 100(2), 294–313. doi:10.1016/j.neuron.2018.10.009

- Lin, D., Edwards, A. S., Fawcett, J. P., Mbamalu, G., Scott, J. D., & Pawson, T. (2000). A mammalian PAR-3-PAR-6 complex implicated in Cdc42/Rac1 and aPKC signalling and cell polarity. *Nature Cell Biology*, 2(8), 540–547. doi:10.1038/35019582
- Liu, X., Hwang, H., Cao, L., Buckland, M., Cunningham, A., Chen, J., ... Zhou, M. (1998). Domain-specific gene disruption reveals critical regulation of neuregulin signaling by its cytoplasmic tail. *Proceedings of the National Academy of Sciences of the United States of America*, 95(22), 13024–13029.
- Liu, Xihui, Bates, R., Yin, D.-M., Shen, C., Wang, F., Su, N., ... Mei, L. (2011). Specific regulation of NRG1 isoform expression by neuronal activity. *The Journal of Neuroscience*, 31(23), 8491–8501. doi:10.1523/JNEUROSCI.5317-10.2011
- Liu, Y., Ford, B. D., Mann, M. A., & Fischbach, G. D. (2005). Neuregulin-1 increases the proliferation of neuronal progenitors from embryonic neural stem cells. *Developmental Biology*, 283(2), 437–445. doi:10.1016/j.ydbio.2005.04.038
- Loeb, J. A., Susanto, E. T., & Fischbach, G. D. (1998). The neuregulin precursor proARIA is processed to ARIA after expression on the cell surface by a protein kinase C-enhanced mechanism. *Molecular and Cellular Neurosciences*, 11(1-2), 77–91. doi:10.1006/mcne.1998.0676
- Long, W., Wagner, K.-U., Lloyd, K. C. K., Binart, N., Shillingford, J. M., Hennighausen, L., & Jones, F. E. (2003). Impaired differentiation and lactational failure of Erbb4-deficient mammary glands identify ERBB4 as an obligate mediator of STAT5. *Development*, 130(21), 5257–5268. doi:10.1242/dev.00715
- Longart, M., Chatani-Hinze, M., Gonzalez, C. M., Vullhorst, D., & Buonanno, A. (2007). Regulation of ErbB-4 endocytosis by neuregulin in GABAergic hippocampal interneurons. *Brain Research Bulletin*, 73(4-6), 210–219. doi:10.1016/j.brainresbull.2007.02.014
- Longart, Marines, Liu, Y., Karavanova, I., & Buonanno, A. (2004). Neuregulin-2 is developmentally regulated and targeted to dendrites of central neurons. *The Journal of Comparative Neurology*, 472(2), 156–172. doi:10.1002/cne.20016
- Loos, M., Mueller, T., Gouwenberg, Y., Wijnands, R., van der Loo, R. J., Neuro-BSIK Mouse Phenomics Consortium, ... Spijker, S. (2014). Neuregulin-3 in the mouse medial prefrontal cortex regulates impulsive action. *Biological Psychiatry*, 76(8), 648–655. doi:10.1016/j.biopsych.2014.02.011
- López-Bendito, G., Cautinat, A., Sánchez, J. A., Bielle, F., Flames, N., Garratt, A. N., ... Garel, S. (2006). Tangential neuronal migration controls axon guidance: a role for neuregulin-1 in thalamocortical axon navigation. *Cell*, 125(1), 127–142. doi:10.1016/j.cell.2006.01.042

- Louhivuori, L. M., Turunen, P. M., Louhivuori, V., Yellapragada, V., Nordström, T., Uhlén, P., & Åkerman, K. E. (2018). Regulation of radial glial process growth by glutamate via mGluR5/TRPC3 and neuregulin/ErbB4. *Glia*, 66(1), 94–107. doi:10.1002/glia.23230
- Loukola, A., Wedenoja, J., Keskitalo-Vuokko, K., Broms, U., Korhonen, T., Ripatti, S., ... Kaprio, J. (2014). Genome-wide association study on detailed profiles of smoking behavior and nicotine dependence in a twin sample. *Molecular Psychiatry*, 19(5), 615–624. doi:10.1038/mp.2013.72
- Lowery, L. A., & Van Vactor, D. (2009). The trip of the tip: understanding the growth cone machinery. *Nature Reviews. Molecular Cell Biology*, 10(5), 332–343. doi:10.1038/nrm2679
- Lu, H. S., Chang, D., Philo, J. S., Zhang, K., Narhi, L. O., Liu, N., ... Yanagihara, D. (1995). Studies on the structure and function of glycosylated and nonglycosylated neu differentiation factors. Similarities and differences of the alpha and beta isoforms. *The Journal of Biological Chemistry*, 270(9), 4784–4791.
- Luhmann, H. J., Fukuda, A., & Kilb, W. (2015). Control of cortical neuronal migration by glutamate and GABA. *Frontiers in Cellular Neuroscience*, 9, 4. doi:10.3389/fncel.2015.00004
- Ma, L., Huang, Y. Z., Pitcher, G. M., Valtschanoff, J. G., Ma, Y. H., Feng, L. Y., ... Mei, L. (2003). Ligand-dependent recruitment of the ErbB4 signaling complex into neuronal lipid rafts. *The Journal of Neuroscience*, 23(8), 3164–3175.
- Määttä, J. A., Sundvall, M., Junttila, T. T., Peri, L., Laine, V. J. O., Isola, J., ... Elenius, K. (2006). Proteolytic cleavage and phosphorylation of a tumor-associated ErbB4 isoform promote ligand-independent survival and cancer cell growth. *Molecular Biology of the Cell*, 17(1), 67–79. doi:10.1091/mbc.E05-05-0402
- Marchionni, M. A., Goodearl, A. D., Chen, M. S., Bermingham-McDonogh, O., Kirk, C., Hendricks, M., ... Kobayashi, K. (1993). Glial growth factors are alternatively spliced erbB2 ligands expressed in the nervous system. *Nature*, 362(6418), 312–318. doi:10.1038/362312a0
- Marín, O., & Rubenstein, J. L. R. (2003). Cell migration in the forebrain. *Annual Review of Neuroscience*, 26, 441–483. doi:10.1146/annurev.neuro.26.041002.131058
- Markram, H., Toledo-Rodriguez, M., Wang, Y., Gupta, A., Silberberg, G., & Wu, C. (2004). Interneurons of the neocortical inhibitory system. *Nature Reviews. Neuroscience*, 5(10), 793–807. doi:10.1038/nrn1519
- Martino, A., Ettore, M., Musilli, M., Lorenzetto, E., Buffelli, M., & Diana, G. (2013). Rho GTPase-dependent plasticity of dendritic spines in the adult brain. *Frontiers in Cellular Neuroscience*, 7, 62. doi:10.3389/fncel.2013.00062

- Matricon, J., Bellon, A., Frieling, H., Kebir, O., Le Pen, G., Beuvon, F., ... Krebs, M.-O. (2010). Neuropathological and Reelin deficiencies in the hippocampal formation of rats exposed to MAM; differences and similarities with schizophrenia. *Plos One*, 5(4), e10291. doi:10.1371/journal.pone.0010291
- Matsui, T., Watanabe, T., Matsuzawa, K., Kakeno, M., Okumura, N., Sugiyama, I., ... Kaibuchi, K. (2015). PAR3 and aPKC regulate Golgi organization through CLASP2 phosphorylation to generate cell polarity. *Molecular Biology of the Cell*, 26(4), 751–761. doi:10.1091/mbc.E14-09-1382
- Mechawar, N., Lacoste, B., Yu, W. F., Srivastava, L. K., & Quirion, R. (2007). Developmental profile of neuregulin receptor ErbB4 in postnatal rat cerebral cortex and hippocampus. *Neuroscience*, 148(1), 126–139. doi:10.1016/j.neuroscience.2007.04.066
- Mei, L., & Nave, K.-A. (2014). Neuregulin-ERBB signaling in the nervous system and neuropsychiatric diseases. *Neuron*, 83(1), 27–49. doi:10.1016/j.neuron.2014.06.007
- Mei, L., & Xiong, W.-C. (2008). Neuregulin 1 in neural development, synaptic plasticity and schizophrenia. *Nature Reviews. Neuroscience*, 9(6), 437–452. doi:10.1038/nrn2392
- Meier, S., Strohmaier, J., Breuer, R., Mattheisen, M., Degenhardt, F., Mühleisen, T. W., ... Wüst, S. (2013). Neuregulin 3 is associated with attention deficits in schizophrenia and bipolar disorder. *The International Journal of Neuropsychopharmacology*, 16(3), 549–556. doi:10.1017/S1461145712000697
- Métin, C., Baudoin, J.-P., Rakić, S., & Parnavelas, J. G. (2006). Cell and molecular mechanisms involved in the migration of cortical interneurons. *The European Journal of Neuroscience*, 23(4), 894–900. doi:10.1111/j.1460-9568.2006.04630.x
- Meyer, D., & Birchmeier, C. (1995). Multiple essential functions of neuregulin in development. *Nature*, 378(6555), 386–390. doi:10.1038/378386a0
- Meyer, D., Yamaai, T., Garratt, A., Riethmacher-Sonnenberg, E., Kane, D., Theill, L. E., & Birchmeier, C. (1997). Isoform-specific expression and function of neuregulin. *Development*, 124(18), 3575–3586.
- Mi, Z., Si, T., Kapadia, K., Li, Q., & Muma, N. A. (2017). Receptor-stimulated transamidation induces activation of Rac1 and Cdc42 and the regulation of dendritic spines. *Neuropharmacology*, 117, 93–105. doi:10.1016/j.neuropharm.2017.01.034
- Michailov, G. V., Sereda, M. W., Brinkmann, B. G., Fischer, T. M., Haug, B., Birchmeier, C., ... Nave, K.-A. (2004). Axonal neuregulin-1 regulates myelin sheath thickness. *Science*, 304(5671), 700–703. doi:10.1126/science.1095862
- Mishra, R., Hanker, A. B., & Garrett, J. T. (2017). Genomic alterations of ERBB receptors in cancer: clinical implications. *Oncotarget*, 8(69), 114371–114392. doi:10.18632/oncotarget.22825

- Mitchell, R. M., Janssen, M. J., Karavanova, I., Vullhorst, D., Furth, K., Makusky, A., ... Buonanno, A. (2013). ErbB4 reduces synaptic GABAA currents independent of its receptor tyrosine kinase activity. *Proceedings of the National Academy of Sciences of the United States of America*, *110*(48), 19603–19608. doi:10.1073/pnas.1312791110
- Mòdol-Caballero, G., Santos, D., Navarro, X., & Herrando-Grabulosa, M. (2017). Neuregulin 1 Reduces Motoneuron Cell Death and Promotes Neurite Growth in an in Vitro Model of Motoneuron Degeneration. *Frontiers in Cellular Neuroscience*, *11*, 431. doi:10.3389/fncel.2017.00431
- Montero, J. C., Rodríguez-Barrueco, R., Yuste, L., Juanes, P. P., Borges, J., Esparís-Ogando, A., & Pandiella, A. (2007). The extracellular linker of pro-neuregulin-alpha2c is required for efficient sorting and juxtacrine function. *Molecular Biology of the Cell*, *18*(2), 380–393. doi:10.1091/mbc.E06-06-0511
- Morais-de-Sá, E., Mirouse, V., & St Johnston, D. (2010). aPKC phosphorylation of Bazooka defines the apical/lateral border in Drosophila epithelial cells. *Cell*, *141*(3), 509–523. doi:10.1016/j.cell.2010.02.040
- Morar, B., Dragović, M., Waters, F. A. V., Chandler, D., Kalaydjieva, L., & Jablensky, A. (2011). Neuregulin 3 (NRG3) as a susceptibility gene in a schizophrenia subtype with florid delusions and relatively spared cognition. *Molecular Psychiatry*, *16*(8), 860–866. doi:10.1038/mp.2010.70
- Morris, J. K., Lin, W., Hauser, C., Marchuk, Y., Getman, D., & Lee, K. F. (1999). Rescue of the cardiac defect in ErbB2 mutant mice reveals essential roles of ErbB2 in peripheral nervous system development. *Neuron*, *23*(2), 273–283. doi:10.1016/S0896-6273(00)80779-5
- Moyer, C. E., Shelton, M. A., & Sweet, R. A. (2015). Dendritic spine alterations in schizophrenia. *Neuroscience Letters*, *601*, 46–53. doi:10.1016/j.neulet.2014.11.042
- Müller, T., Braud, S., Jüttner, R., Voigt, B. C., Paulick, K., Sheean, M. E., ... Birchmeier, C. (2018). Neuregulin 3 promotes excitatory synapse formation on hippocampal interneurons. *The EMBO Journal*, *37*(17). doi:10.15252/embj.201798858
- Munemitsu, S., Innis, M. A., Clark, R., McCormick, F., Ullrich, A., & Polakis, P. (1990). Molecular cloning and expression of a G25K cDNA, the human homolog of the yeast cell cycle gene CDC42. *Molecular and Cellular Biology*, *10*(11), 5977–5982.
- Muraki, K., & Tanigaki, K. (2015). Neuronal migration abnormalities and its possible implications for schizophrenia. *Frontiers in Neuroscience*, *9*, 74. doi:10.3389/fnins.2015.00074
- Muraoka-Cook, R. S., Feng, S.-M., Strunk, K. E., & Earp, H. S. (2008). ErbB4/HER4: role in mammary gland development, differentiation and growth inhibition. *Journal of Mammary Gland Biology and Neoplasia*, *13*(2), 235–246. doi:10.1007/s10911-008-9080-x

- Muraoka-Cook, R. S., Sandahl, M. A., Strunk, K. E., Miraglia, L. C., Husted, C., Hunter, D. M., ... Earp, H. S. (2009). ErbB4 splice variants Cyt1 and Cyt2 differ by 16 amino acids and exert opposing effects on the mammary epithelium in vivo. *Molecular and Cellular Biology*, 29(18), 4935–4948. doi:10.1128/MCB.01705-08
- Nadarajah, B., & Parnavelas, J. G. (2002). Modes of neuronal migration in the developing cerebral cortex. *Nature Reviews. Neuroscience*, 3(6), 423–432. doi:10.1038/nrn845
- Nagai-Tamai, Y., Mizuno, K., Hirose, T., Suzuki, A., & Ohno, S. (2002). Regulated protein-protein interaction between aPKC and PAR-3 plays an essential role in the polarization of epithelial cells. *Genes To Cells*, 7(11), 1161–1171. doi:10.1046/j.1365-2443.2002.00590.x
- Nakamura, N., Rabouille, C., Watson, R., Nilsson, T., Hui, N., Slusarewicz, P., ... Warren, G. (1995). Characterization of a cis-Golgi matrix protein, GM130. *The Journal of Cell Biology*, 131(6 Pt 2), 1715–1726. doi:10.1083/jcb.131.6.1715
- Nakano, N., Kanekiyo, K., Nakagawa, T., Asahi, M., & Ide, C. (2016). NTAK/neuregulin-2 secreted by astrocytes promotes survival and neurite outgrowth of neurons via ErbB3. *Neuroscience Letters*, 622, 88–94. doi:10.1016/j.neulet.2016.04.050
- Namba, T., Funahashi, Y., Nakamuta, S., Xu, C., Takano, T., & Kaibuchi, K. (2015). Extracellular and intracellular signaling for neuronal polarity. *Physiological Reviews*, 95(3), 995–1024. doi:10.1152/physrev.00025.2014
- Naoki, H., Nakamuta, S., Kaibuchi, K., & Ishii, S. (2011). Flexible search for single-axon morphology during neuronal spontaneous polarization. *Plos One*, 6(4), e19034. doi:10.1371/journal.pone.0019034
- Naqvi, H. A., Huma, S., Waseem, H., Zaidi, K. A., & Abidi, S. H. (2018). Association between a single nucleotide polymorphism in neuregulin-1 and schizophrenia in Pakistani patients. *The Journal of the Pakistan Medical Association*, 68(5), 747–752.
- Neddens, J., & Buonanno, A. (2010). Selective populations of hippocampal interneurons express ErbB4 and their number and distribution is altered in ErbB4 knockout mice. *Hippocampus*, 20(6), 724–744. doi:10.1002/hipo.20675
- Neddens, J., Fish, K. N., Tricoire, L., Vullhorst, D., Shamir, A., Chung, W., ... Buonanno, A. (2011). Conserved interneuron-specific ErbB4 expression in frontal cortex of rodents, monkeys, and humans: implications for schizophrenia. *Biological Psychiatry*, 70(7), 636–645. doi:10.1016/j.biopsych.2011.04.016
- Ni, C. Y., Murphy, M. P., Golde, T. E., & Carpenter, G. (2001). gamma -Secretase cleavage and nuclear localization of ErbB-4 receptor tyrosine kinase. *Science*, 294(5549), 2179–2181. doi:10.1126/science.1065412
- Nicolas, M., & Hassan, B. A. (2014). Amyloid precursor protein and neural development. *Development*, 141(13), 2543–2548. doi:10.1242/dev.108712

- Nishimura, Takashi, Kato, K., Yamaguchi, T., Fukata, Y., Ohno, S., & Kaibuchi, K. (2004). Role of the PAR-3-KIF3 complex in the establishment of neuronal polarity. *Nature Cell Biology*, 6(4), 328–334. doi:10.1038/ncb1118
- Nishimura, Takashi, Yamaguchi, T., Kato, K., Yoshizawa, M., Nabeshima, Y., Ohno, S., ... Kaibuchi, K. (2005). PAR-6-PAR-3 mediates Cdc42-induced Rac activation through the Rac GEFs STEF/Tiam1. *Nature Cell Biology*, 7(3), 270–277. doi:10.1038/ncb1227
- Nishimura, Tomoko, Ishima, T., Iyo, M., & Hashimoto, K. (2008). Potentiation of nerve growth factor-induced neurite outgrowth by fluvoxamine: role of sigma-1 receptors, IP3 receptors and cellular signaling pathways. *Plos One*, 3(7), e2558. doi:10.1371/journal.pone.0002558
- Norton, N., Moskvina, V., Morris, D. W., Bray, N. J., Zammit, S., Williams, N. M., ... O'Donovan, M. C. (2006). Evidence that interaction between neuregulin 1 and its receptor erbB4 increases susceptibility to schizophrenia. *American Journal of Medical Genetics. Part B, Neuropsychiatric Genetics*, 141B(1), 96–101. doi:10.1002/ajmg.b.30236
- O'Leary, N. A., Wright, M. W., Brister, J. R., Ciufu, S., Haddad, D., McVeigh, R., ... Ako-Adjei, D. (2016). Reference sequence (RefSeq) database at NCBI: current status, taxonomic expansion, and functional annotation. *Nucleic Acids Research*, 44(D1), D733–45. doi:10.1093/nar/gkv1189
- O'Tuathaigh, C M P, Babovic, D., O'Sullivan, G. J., Clifford, J. J., Tighe, O., Croke, D. T., ... Waddington, J. L. (2007). Phenotypic characterization of spatial cognition and social behavior in mice with “knockout” of the schizophrenia risk gene neuregulin 1. *Neuroscience*, 147(1), 18–27. doi:10.1016/j.neuroscience.2007.03.051
- O'Tuathaigh, Colm M P, O'Connor, A.-M., O'Sullivan, G. J., Lai, D., Harvey, R., Croke, D. T., & Waddington, J. L. (2008). Disruption to social dyadic interactions but not emotional/anxiety-related behaviour in mice with heterozygous “knockout” of the schizophrenia risk gene neuregulin-1. *Progress in Neuro-Psychopharmacology & Biological Psychiatry*, 32(2), 462–466. doi:10.1016/j.pnpbp.2007.09.018
- Olaya, J. C., Heusner, C. L., Matsumoto, M., Shannon Weickert, C., & Karl, T. (2018). Schizophrenia-relevant behaviours of female mice overexpressing neuregulin 1 type III. *Behavioural Brain Research*, 353, 227–235. doi:10.1016/j.bbr.2018.03.026
- Olaya, J. C., Heusner, C. L., Matsumoto, M., Sinclair, D., Kondo, M. A., Karl, T., & Shannon Weickert, C. (2018). Overexpression of Neuregulin 1 Type III Confers Hippocampal mRNA Alterations and Schizophrenia-Like Behaviors in Mice. *Schizophrenia Bulletin*, 44(4), 865–875. doi:10.1093/schbul/sbx122
- Olayioye, M. A., Beuvink, I., Horsch, K., Daly, J. M., & Hynes, N. E. (1999). ErbB receptor-induced activation of stat transcription factors is mediated by Src tyrosine kinases. *The Journal of Biological Chemistry*, 274(24), 17209–17218. doi:10.1074/jbc.274.24.17209

- Olayioye, M. A., Graus-Porta, D., Beerli, R. R., Rohrer, J., Gay, B., & Hynes, N. E. (1998). ErbB-1 and ErbB-2 acquire distinct signaling properties dependent upon their dimerization partner. *Molecular and Cellular Biology*, *18*(9), 5042–5051.
- Ozaki, M., Itoh, K., Miyakawa, Y., Kishida, H., & Hashikawa, T. (2004). Protein processing and releases of neuregulin-1 are regulated in an activity-dependent manner. *Journal of Neurochemistry*, *91*(1), 176–188. doi:10.1111/j.1471-4159.2004.02719.x
- Pakkenberg, B., & Gundersen, H. J. (1997). Neocortical neuron number in humans: effect of sex and age. *The Journal of Comparative Neurology*, *384*(2), 312–320. doi:10.1002/(SICI)1096-9861(19970728)384:2<312::AID-CNE10>3.0.CO;2-K
- Panchal, H., Wansbury, O., Parry, S., Ashworth, A., & Howard, B. (2007). Neuregulin3 alters cell fate in the epidermis and mammary gland. *BMC Developmental Biology*, *7*, 105. doi:10.1186/1471-213X-7-105
- Pandya, C. D., & Pillai, A. (2014). TrkB interacts with ErbB4 and regulates NRG1-induced NR2B phosphorylation in cortical neurons before synaptogenesis. *Cell Communication and Signaling*, *12*, 47. doi:10.1186/s12964-014-0047-9
- Papaleo, F., Yang, F., Paterson, C., Palumbo, S., Carr, G. V., Wang, Y., ... Law, A. J. (2016). Behavioral, Neurophysiological, and Synaptic Impairment in a Transgenic Neuregulin1 (NRG1-IV) Murine Schizophrenia Model. *The Journal of Neuroscience*, *36*(17), 4859–4875. doi:10.1523/JNEUROSCI.4632-15.2016
- Park, S. K., Solomon, D., & Vartanian, T. (2001). Growth factor control of CNS myelination. *Developmental Neuroscience*, *23*(4-5), 327–337. doi:10.1159/000048716
- Parker, S. S., Mandell, E. K., Hapak, S. M., Maskaykina, I. Y., Kusne, Y., Kim, J.-Y., ... Ghosh, S. (2013). Competing molecular interactions of aPKC isoforms regulate neuronal polarity. *Proceedings of the National Academy of Sciences of the United States of America*, *110*(35), 14450–14455. doi:10.1073/pnas.1301588110
- Parlapani, E., Schmitt, A., Wirths, O., Bauer, M., Sommer, C., Rueb, U., ... Falkai, P. (2010). Gene expression of neuregulin-1 isoforms in different brain regions of elderly schizophrenia patients. *The World Journal of Biological Psychiatry*, *11*(2 Pt 2), 243–250. doi:10.3109/15622970802022376
- Pasaje, C. F., Bae, J. S., Park, B. L., Cheong, H. S., Kim, J. H., Park, T. J., ... Woo, S. I. (2011). Neuregulin 3 does not confer risk for schizophrenia and smooth pursuit eye movement abnormality in a Korean population. *Genes, Brain, and Behavior*, *10*(8), 828–833. doi:10.1111/j.1601-183X.2011.00722.x
- Paterson, C., & Law, A. J. (2014). Transient overexposure of neuregulin 3 during early postnatal development impacts selective behaviors in adulthood. *Plos One*, *9*(8), e104172. doi:10.1371/journal.pone.0104172

- Paterson, C., Wang, Y., Hyde, T. M., Weinberger, D. R., Kleinman, J. E., & Law, A. J. (2017). Temporal, Diagnostic, and Tissue-Specific Regulation of NRG3 Isoform Expression in Human Brain Development and Affective Disorders. *The American Journal of Psychiatry*, *174*(3), 256–265. doi:10.1176/appi.ajp.2016.16060721
- Paul, M. D., & Hristova, K. (2018). The RTK interactome: overview and perspective on RTK heterointeractions. *Chemical Reviews*. doi:10.1021/acs.chemrev.8b00467
- Peles, E., Bacus, S. S., Koski, R. A., Lu, H. S., Wen, D., Ogden, S. G., ... Yarden, Y. (1992). Isolation of the neu/HER-2 stimulatory ligand: a 44 kd glycoprotein that induces differentiation of mammary tumor cells. *Cell*, *69*(1), 205–216.
- Perez-Garcia, C. G. (2015). Erbb4 in laminated brain structures: A neurodevelopmental approach to schizophrenia. *Frontiers in Cellular Neuroscience*, *9*, 472. doi:10.3389/fncel.2015.00472
- Petanjek, Z., Judaš, M., Šimic, G., Rasin, M. R., Uylings, H. B. M., Rakic, P., & Kostovic, I. (2011). Extraordinary neoteny of synaptic spines in the human prefrontal cortex. *Proceedings of the National Academy of Sciences of the United States of America*, *108*(32), 13281–13286. doi:10.1073/pnas.1105108108
- Peters, A., & Kara, D. A. (1985). The neuronal composition of area 17 of rat visual cortex. II. The nonpyramidal cells. *The Journal of Comparative Neurology*, *234*(2), 242–263. doi:10.1002/cne.902340209
- Peterson, F. C., Penkert, R. R., Volkman, B. F., & Prehoda, K. E. (2004). Cdc42 regulates the Par-6 PDZ domain through an allosteric CRIB-PDZ transition. *Molecular Cell*, *13*(5), 665–676. doi:10.1016/S1097-2765(04)00086-3
- Petilla Interneuron Nomenclature Group, Ascoli, G. A., Alonso-Nanclares, L., Anderson, S. A., Barrionuevo, G., Benavides-Piccione, R., ... Yuste, R. (2008). Petilla terminology: nomenclature of features of GABAergic interneurons of the cerebral cortex. *Nature Reviews. Neuroscience*, *9*(7), 557–568. doi:10.1038/nrn2402
- Pinkas-Kramarski, R., Eilam, R., Alroy, I., Levkowitz, G., Lonai, P., & Yarden, Y. (1997). Differential expression of NDF/neuregulin receptors ErbB-3 and ErbB-4 and involvement in inhibition of neuronal differentiation. *Oncogene*, *15*(23), 2803–2815. doi:10.1038/sj.onc.1201466
- Pinkas-Kramarski, R., Eilam, R., Spiegler, O., Lavi, S., Liu, N., Chang, D., ... Yarden, Y. (1994). Brain neurons and glial cells express Neu differentiation factor/herregulin: a survival factor for astrocytes. *Proceedings of the National Academy of Sciences of the United States of America*, *91*(20), 9387–9391.
- Pitcher, G. M., Beggs, S., Woo, R.-S., Mei, L., & Salter, M. W. (2008). ErbB4 is a suppressor of long-term potentiation in the adult hippocampus. *Neuroreport*, *19*(2), 139–143. doi:10.1097/WNR.0b013e3282f3da10

- Pitcher, G. M., Kalia, L. V., Ng, D., Goodfellow, N. M., Yee, K. T., Lambe, E. K., & Salter, M. W. (2011). Schizophrenia susceptibility pathway neuregulin 1-ErbB4 suppresses Src upregulation of NMDA receptors. *Nature Medicine*, *17*(4), 470–478. doi:10.1038/nm.2315
- Plowman, G. D., Culouscou, J. M., Whitney, G. S., Green, J. M., Carlton, G. W., Foy, L., ... Shoyab, M. (1993). Ligand-specific activation of HER4/p180erbB4, a fourth member of the epidermal growth factor receptor family. *Proceedings of the National Academy of Sciences of the United States of America*, *90*(5), 1746–1750.
- Polleux, F., & Snider, W. (2010). Initiating and growing an axon. *Cold Spring Harbor Perspectives in Biology*, *2*(4), a001925. doi:10.1101/cshperspect.a001925
- Pozas, E., & Ibáñez, C. F. (2005). GDNF and GFRalpha1 promote differentiation and tangential migration of cortical GABAergic neurons. *Neuron*, *45*(5), 701–713. doi:10.1016/j.neuron.2005.01.043
- Prata, D. P., Breen, G., Osborne, S., Munro, J., St Clair, D., & Collier, D. A. (2009). An association study of the neuregulin 1 gene, bipolar affective disorder and psychosis. *Psychiatric Genetics*, *19*(3), 113–116. doi:10.1097/YPG.0b013e32832a4f69
- Prieto, A L, O'Dell, S., Varnum, B., & Lai, C. (2007). Localization and signaling of the receptor protein tyrosine kinase Tyro3 in cortical and hippocampal neurons. *Neuroscience*, *150*(2), 319–334. doi:10.1016/j.neuroscience.2007.09.047
- Prieto, A L, Weber, J. L., & Lai, C. (2000). Expression of the receptor protein-tyrosine kinases Tyro-3, Axl, and mer in the developing rat central nervous system. *The Journal of Comparative Neurology*, *425*(2), 295–314. doi:10.1002/1096-9861(20000918)425:2<295::AID-CNE11>3.0.CO;2-G
- Prieto, Anne L., Weber, J. L., Tracy, S., Heeb, M. J., & Lai, C. (1999). Gas6, a ligand for the receptor protein-tyrosine kinase Tyro-3, is widely expressed in the central nervous system1Published on the World Wide Web on 2 December 1998.1. *Brain Research*, *816*(2), 646–661. doi:10.1016/S0006-8993(98)01159-7
- Qiu, R.-G., Abo, A., & Martin, G. S. (2000). A human homolog of the C. elegans polarity determinant Par-6 links Rac and Cdc42 to PKC ζ signaling and cell transformation. *Current Biology*, *10*(12), 697–707. doi:10.1016/S0960-9822(00)00535-2
- Rahman, A., Weber, J., Labin, E., Lai, C., & Prieto, A. L. (2018). Developmental Expression of Neuregulin-3 in the Rat Central Nervous System. *The Journal of Comparative Neurology*, *527*(4), 797–817. doi:10.1002/cne.24559
- Read, D. E., & Gorman, A. M. (2009). Involvement of Akt in neurite outgrowth. *Cellular and Molecular Life Sciences*, *66*(18), 2975–2984. doi:10.1007/s00018-009-0057-8

- Reichardt, L. F. (2006). Neurotrophin-regulated signalling pathways. *Philosophical Transactions of the Royal Society of London. Series B, Biological Sciences*, 361(1473), 1545–1564. doi:10.1098/rstb.2006.1894
- Rejon, C., Al-Masri, M., & McCaffrey, L. (2016). Cell polarity proteins in breast cancer progression. *Journal of Cellular Biochemistry*, 117(10), 2215–2223. doi:10.1002/jcb.25553
- Renschler, F. A., Bruekner, S. R., Salomon, P. L., Mukherjee, A., Kullmann, L., Schütz-Stoffregen, M. C., ... Wiesner, S. (2018). Structural basis for the interaction between the cell polarity proteins Par3 and Par6. *Science Signaling*, 11(517). doi:10.1126/scisignal.aam9899
- Rico, B., & Marín, O. (2011). Neuregulin signaling, cortical circuitry development and schizophrenia. *Current Opinion in Genetics & Development*, 21(3), 262–270. doi:10.1016/j.gde.2010.12.010
- Rieff, H. I., & Corfas, G. (2006). ErbB receptor signalling regulates dendrite formation in mouse cerebellar granule cells in vivo. *The European Journal of Neuroscience*, 23(8), 2225–2229. doi:10.1111/j.1460-9568.2006.04727.x
- Rieff, H. I., Raetzman, L. T., Sapp, D. W., Yeh, H. H., Siegel, R. E., & Corfas, G. (1999). Neuregulin induces gaba_a receptor subunit expression and neurite outgrowth in cerebellar granule cells. *The Journal of Neuroscience : The Official Journal of the Society for Neuroscience*, 19(24), 10757–10766. doi:10.1523/JNEUROSCI.19-24-10757.1999
- Riethmacher, D., Sonnenberg-Riethmacher, E., Brinkmann, V., Yamaai, T., Lewin, G. R., & Birchmeier, C. (1997). Severe neuropathies in mice with targeted mutations in the ErbB3 receptor. *Nature*, 389(6652), 725–730. doi:10.1038/39593
- Rimer, M., Barrett, D. W., Maldonado, M. A., Vock, V. M., & Gonzalez-Lima, F. (2005). Neuregulin-1 immunoglobulin-like domain mutant mice: clozapine sensitivity and impaired latent inhibition. *Neuroreport*, 16(3), 271–275.
- Rio, C., Buxbaum, J. D., Peschon, J. J., & Corfas, G. (2000). Tumor necrosis factor-alpha-converting enzyme is required for cleavage of erbB4/HER4. *The Journal of Biological Chemistry*, 275(14), 10379–10387. doi:10.1074/jbc.275.14.10379
- Rio, C., Rieff, H. I., Qi, P., Khurana, T. S., & Corfas, G. (1997). Neuregulin and erbB receptors play a critical role in neuronal migration. *Neuron*, 19(1), 39–50. doi:10.1016/S0896-6273(00)80346-3
- Rodgers, E. E., & Theibert, A. B. (2002). Functions of PI 3-kinase in development of the nervous system. *International Journal of Developmental Neuroscience*, 20(3-5), 187–197. doi:10.1016/S0736-5748(02)00047-3

- Roskoski, R. (2004). The ErbB/HER receptor protein-tyrosine kinases and cancer. *Biochemical and Biophysical Research Communications*, 319(1), 1–11. doi:10.1016/j.bbrc.2004.04.150
- Roy, K., Murtie, J. C., El-Khodor, B. F., Edgar, N., Sardi, S. P., Hooks, B. M., ... Corfas, G. (2007). Loss of erbB signaling in oligodendrocytes alters myelin and dopaminergic function, a potential mechanism for neuropsychiatric disorders. *Proceedings of the National Academy of Sciences of the United States of America*, 104(19), 8131–8136. doi:10.1073/pnas.0702157104
- Rubenstein, J. L. R. (2011). Annual Research Review: Development of the cerebral cortex: implications for neurodevelopmental disorders. *Journal of Child Psychology and Psychiatry, and Allied Disciplines*, 52(4), 339–355. doi:10.1111/j.1469-7610.2010.02307.x
- Rudy, B., Fishell, G., Lee, S., & Hjerling-Leffler, J. (2011). Three groups of interneurons account for nearly 100% of neocortical GABAergic neurons. *Developmental Neurobiology*, 71(1), 45–61. doi:10.1002/dneu.20853
- Sakakibara, A., & Hatanaka, Y. (2015). Neuronal polarization in the developing cerebral cortex. *Frontiers in Neuroscience*, 9, 116. doi:10.3389/fnins.2015.00116
- Sakamoto, I., Ueyama, T., Hayashibe, M., Nakamura, T., Mohri, H., Kiyonari, H., ... Saito, N. (2018). Roles of Cdc42 and Rac in Bergmann glia during cerebellar corticogenesis. *Experimental Neurology*, 302, 57–67. doi:10.1016/j.expneurol.2017.12.003
- Samuels, D. C., Hentschel, H. G., & Fine, A. (1996). The origin of neuronal polarization: a model of axon formation. *Philosophical Transactions of the Royal Society of London. Series B, Biological Sciences*, 351(1344), 1147–1156. doi:10.1098/rstb.1996.0099
- Sardi, S. P., Murtie, J., Koirala, S., Patten, B. A., & Corfas, G. (2006). Presenilin-dependent ErbB4 nuclear signaling regulates the timing of astrogenesis in the developing brain. *Cell*, 127(1), 185–197. doi:10.1016/j.cell.2006.07.037
- Schmid, R. S., McGrath, B., Berechid, B. E., Boyles, B., Marchionni, M., Sestan, N., & Anton, E. S. (2003). Neuregulin 1-erbB2 signaling is required for the establishment of radial glia and their transformation into astrocytes in cerebral cortex. *Proceedings of the National Academy of Sciences of the United States of America*, 100(7), 4251–4256. doi:10.1073/pnas.0630496100
- Schramm, A., Schulte, J. H., Astrahantseff, K., Apostolov, O., Limpt, V. van, Sievert, H., ... Eggert, A. (2005). Biological effects of TrkA and TrkB receptor signaling in neuroblastoma. *Cancer Letters*, 228(1-2), 143–153. doi:10.1016/j.canlet.2005.02.051
- Schroeder, J. A., & Lee, D. C. (1998). Dynamic expression and activation of ERBB receptors in the developing mouse mammary gland. *Cell Growth & Differentiation*, 9(6), 451–464.

- Schroering, A., & Carey, D. J. (1998). Sensory and motor neuron-derived factor is a transmembrane heregulin that is expressed on the plasma membrane with the active domain exposed to the extracellular environment. *The Journal of Biological Chemistry*, 273(46), 30643–30650.
- Schulze, W. X., Deng, L., & Mann, M. (2005). Phosphotyrosine interactome of the ErbB-receptor kinase family. *Molecular Systems Biology*, 1, 2005.0008. doi:10.1038/msb4100012
- Schwab, S. G., Eckstein, G. N., Hallmayer, J., Lerer, B., Albus, M., Borrmann, M., ... Wildenauer, D. B. (1997). Evidence suggestive of a locus on chromosome 5q31 contributing to susceptibility for schizophrenia in German and Israeli families by multipoint affected sib-pair linkage analysis. *Molecular Psychiatry*, 2(2), 156–160.
- Schwamborn, J. C., & Püschel, A. W. (2004). The sequential activity of the GTPases Rap1B and Cdc42 determines neuronal polarity. *Nature Neuroscience*, 7(9), 923–929. doi:10.1038/nn1295
- Selemon, L. D., & Zecevic, N. (2015). Schizophrenia: a tale of two critical periods for prefrontal cortical development. *Translational Psychiatry*, 5, e623. doi:10.1038/tp.2015.115
- Semple, B. D., Blomgren, K., Gimlin, K., Ferriero, D. M., & Noble-Haeusslein, L. J. (2013). Brain development in rodents and humans: Identifying benchmarks of maturation and vulnerability to injury across species. *Progress in Neurobiology*, 106-107, 1–16. doi:10.1016/j.pneurobio.2013.04.001
- Shamir, A., & Buonanno, A. (2010). Molecular and cellular characterization of Neuregulin-1 type IV isoforms. *Journal of Neurochemistry*, 113(5), 1163–1176. doi:10.1111/j.1471-4159.2010.06677.x
- Shamir, A., Kwon, O.-B., Karavanova, I., Vullhorst, D., Leiva-Salcedo, E., Janssen, M. J., & Buonanno, A. (2012). The importance of the NRG-1/ErbB4 pathway for synaptic plasticity and behaviors associated with psychiatric disorders. *The Journal of Neuroscience*, 32(9), 2988–2997. doi:10.1523/JNEUROSCI.1899-11.2012
- Sheng, M., & Hoogenraad, C. C. (2007). The postsynaptic architecture of excitatory synapses: a more quantitative view. *Annual Review of Biochemistry*, 76, 823–847. doi:10.1146/annurev.biochem.76.060805.160029
- Shi, F., Telesco, S. E., Liu, Y., Radhakrishnan, R., & Lemmon, M. A. (2010). ErbB3/HER3 intracellular domain is competent to bind ATP and catalyze autophosphorylation. *Proceedings of the National Academy of Sciences of the United States of America*, 107(17), 7692–7697. doi:10.1073/pnas.1002753107
- Shi, S.-H., Cheng, T., Jan, L. Y., & Jan, Y.-N. (2004). APC and GSK-3beta are involved in mPar3 targeting to the nascent axon and establishment of neuronal polarity. *Current Biology*, 14(22), 2025–2032. doi:10.1016/j.cub.2004.11.009

- Shi, S.-H., Jan, L. Y., & Jan, Y.-N. (2003). Hippocampal neuronal polarity specified by spatially localized mPar3/mPar6 and PI 3-kinase activity. *Cell*, *112*(1), 63–75. doi:10.1016/S0092-8674(02)01249-7
- Shibuya, M., Komi, E., Wang, R., Kato, T., Watanabe, Y., Sakai, M., ... Nawa, H. (2010). Measurement and comparison of serum neuregulin 1 immunoreactivity in control subjects and patients with schizophrenia: an influence of its genetic polymorphism. *Journal of Neural Transmission*, *117*(7), 887–895. doi:10.1007/s00702-010-0418-3
- Shimojima, K., Isidor, B., Le Caignec, C., Kondo, A., Sakata, S., Ohno, K., & Yamamoto, T. (2011). A new microdeletion syndrome of 5q31.3 characterized by severe developmental delays, distinctive facial features, and delayed myelination. *American Journal of Medical Genetics. Part A*, *155A*(4), 732–736. doi:10.1002/ajmg.a.33891
- Silberberg, G., Darvasi, A., Pinkas-Kramarski, R., & Navon, R. (2006). The involvement of ErbB4 with schizophrenia: association and expression studies. *American Journal of Medical Genetics. Part B, Neuropsychiatric Genetics*, *141B*(2), 142–148. doi:10.1002/ajmg.b.30275
- Simmons, D. M., Arriza, J. L., & Swanson, L. W. (1989). A Complete Protocol for *In Situ* Hybridization of Messenger RNAs in Brain and Other Tissues With Radio-labeled Single-Stranded RNA Probes. *Journal of Histotechnology*, *12*(3), 169–181. doi:10.1179/his.1989.12.3.169
- Singh, S., & Solecki, D. J. (2015). Polarity transitions during neurogenesis and germinal zone exit in the developing central nervous system. *Frontiers in Cellular Neuroscience*, *9*, 62. doi:10.3389/fncel.2015.00062
- Sklar, P., Pato, M. T., Kirby, A., Petryshen, T. L., Medeiros, H., Carvalho, C., ... Pato, C. N. (2004). Genome-wide scan in Portuguese Island families identifies 5q31-5q35 as a susceptibility locus for schizophrenia and psychosis. *Molecular Psychiatry*, *9*(2), 213–218. doi:10.1038/sj.mp.4001418
- Slamon, D. J., Clark, G. M., Wong, S. G., Levin, W. J., Ullrich, A., & McGuire, W. L. (1987). Human breast cancer: correlation of relapse and survival with amplification of the HER-2/neu oncogene. *Science*, *235*(4785), 177–182. doi:10.1126/science.3798106
- Solecki, D. J., Govek, E.-E., & Hatten, M. E. (2006). mPar6 alpha controls neuronal migration. *The Journal of Neuroscience*, *26*(42), 10624–10625. doi:10.1523/JNEUROSCI.4060-06.2006
- Songyang, Z., Shoelson, S. E., Chaudhuri, M., Gish, G., Pawson, T., Haser, W. G., ... Cantley, L. C. (1993). SH2 domains recognize specific phosphopeptide sequences. *Cell*, *72*(5), 767–778.
- Soriano, E. V., Ivanova, M. E., Fletcher, G., Riou, P., Knowles, P. P., Barnouin, K., ... McDonald, N. Q. (2016). aPKC Inhibition by Par3 CR3 Flanking Regions Controls

- Substrate Access and Underpins Apical-Junctional Polarization. *Developmental Cell*, 38(4), 384–398. doi:10.1016/j.devcel.2016.07.018
- Spike, B. T., Engle, D. D., Lin, J. C., Cheung, S. K., La, J., & Wahl, G. M. (2012). A mammary stem cell population identified and characterized in late embryogenesis reveals similarities to human breast cancer. *Cell Stem Cell*, 10(2), 183–197. doi:10.1016/j.stem.2011.12.018
- Stefansson, H., Sarginson, J., Kong, A., Yates, P., Steinthorsdottir, V., Gudfinnsson, E., ... St Clair, D. (2003). Association of neuregulin 1 with schizophrenia confirmed in a Scottish population. *American Journal of Human Genetics*, 72(1), 83–87.
- Stefansson, H., Sigurdsson, E., Steinthorsdottir, V., Bjornsdottir, S., Sigmundsson, T., Ghosh, S., ... Stefansson, K. (2002). Neuregulin 1 and susceptibility to schizophrenia. *American Journal of Human Genetics*, 71(4), 877–892. doi:10.1086/342734
- Steiner, H., Blum, M., Kitai, S. T., & Fedi, P. (1999). Differential expression of ErbB3 and ErbB4 neuregulin receptors in dopamine neurons and forebrain areas of the adult rat. *Experimental Neurology*, 159(2), 494–503. doi:10.1006/exnr.1999.7163
- Steinkamp, M. P., Low-Nam, S. T., Yang, S., Lidke, K. A., Lidke, D. S., & Wilson, B. S. (2014). erbB3 is an active tyrosine kinase capable of homo- and heterointeractions. *Molecular and Cellular Biology*, 34(6), 965–977. doi:10.1128/MCB.01605-13
- Steinthorsdottir, V., Stefansson, H., Ghosh, S., Birgisdottir, B., Bjornsdottir, S., Fasquel, A. C., ... Gulcher, J. R. (2004). Multiple novel transcription initiation sites for NRG1. *Gene*, 342(1), 97–105. doi:10.1016/j.gene.2004.07.029
- Stenman, J., Yu, R. T., Evans, R. M., & Campbell, K. (2003). Tlx and Pax6 co-operate genetically to establish the pallio-subpallial boundary in the embryonic mouse telencephalon. *Development*, 130(6), 1113–1122. doi:10.1242/dev.00328
- Stern, D. F. (2008). ERBB3/HER3 and ERBB2/HER2 duet in mammary development and breast cancer. *Journal of Mammary Gland Biology and Neoplasia*, 13(2), 215–223. doi:10.1007/s10911-008-9083-7
- Stiles, J., & Jernigan, T. L. (2010). The basics of brain development. *Neuropsychology Review*, 20(4), 327–348. doi:10.1007/s11065-010-9148-4
- Straub, R. E., MacLean, C. J., O'Neill, F. A., Walsh, D., & Kendler, K. S. (1997). Support for a possible schizophrenia vulnerability locus in region 5q22-31 in Irish families. *Molecular Psychiatry*, 2(2), 148–155.
- Subramanian, L., Remedios, R., Shetty, A., & Tole, S. (2009). Signals from the edges: the cortical hem and antihem in telencephalic development. *Seminars in Cell & Developmental Biology*, 20(6), 712–718. doi:10.1016/j.semcdb.2009.04.001

- Sun, M., Asghar, S. Z., & Zhang, H. (2016). The polarity protein Par3 regulates APP trafficking and processing through the endocytic adaptor protein Numb. *Neurobiology of Disease*, 93, 1–11. doi:10.1016/j.nbd.2016.03.022
- Sundvall, M., Korhonen, A., Paatero, I., Gaudio, E., Melino, G., Croce, C. M., ... Elenius, K. (2008). Isoform-specific monoubiquitination, endocytosis, and degradation of alternatively spliced ErbB4 isoforms. *Proceedings of the National Academy of Sciences of the United States of America*, 105(11), 4162–4167. doi:10.1073/pnas.0708333105
- Suzuki, A., Yamanaka, T., Hirose, T., Manabe, N., Mizuno, K., Shimizu, M., ... Ohno, S. (2001). Atypical protein kinase C is involved in the evolutionarily conserved par protein complex and plays a critical role in establishing epithelia-specific junctional structures. *The Journal of Cell Biology*, 152(6), 1183–1196. doi:10.1083/jcb.152.6.1183
- Suzuki, Atsushi, & Ohno, S. (2006). The PAR-aPKC system: lessons in polarity. *Journal of Cell Science*, 119(Pt 6), 979–987. doi:10.1242/jcs.02898
- Tabata, H., Yoshinaga, S., & Nakajima, K. (2012). Cytoarchitecture of mouse and human subventricular zone in developing cerebral neocortex. *Experimental Brain Research*, 216(2), 161–168. doi:10.1007/s00221-011-2933-3
- Takano, T., Xu, C., Funahashi, Y., Namba, T., & Kaibuchi, K. (2015). Neuronal polarization. *Development*, 142(12), 2088–2093. doi:10.1242/dev.114454
- Tal-Or, P., Erlich, S., Porat-Shliom, N., Goldshmit, Y., Ben-Baruch, G., Shaharabani, E., ... Pinkas-Kramarski, R. (2006). Ligand-independent regulation of ErbB4 receptor phosphorylation by activated Ras. *Journal of Cellular Biochemistry*, 98(6), 1482–1494. doi:10.1002/jcb.20815
- Tan, G.-H., Liu, Y.-Y., Hu, X.-L., Yin, D.-M., Mei, L., & Xiong, Z.-Q. (2011). Neuregulin 1 represses limbic epileptogenesis through ErbB4 in parvalbumin-expressing interneurons. *Nature Neuroscience*, 15(2), 258–266. doi:10.1038/nn.3005
- Tan, M., & Yu, D. (2013). Molecular Mechanisms of ErbB2-Mediated Breast Cancer Chemoresistance - Madame Curie Bioscience Database - NCBI Bookshelf.
- Tang, B. L. (2001). Protein trafficking mechanisms associated with neurite outgrowth and polarized sorting in neurons. *Journal of Neurochemistry*, 79(5), 923–930.
- Tang, J. X., Chen, W. Y., He, G., Zhou, J., Gu, N. F., Feng, G. Y., & He, L. (2004). Polymorphisms within 5' end of the Neuregulin 1 gene are genetically associated with schizophrenia in the Chinese population. *Molecular Psychiatry*, 9(1), 11–12. doi:10.1038/sj.mp.4001436
- Tasic, B., Menon, V., Nguyen, T. N., Kim, T. K., Jarsky, T., Yao, Z., ... Zeng, H. (2016). Adult mouse cortical cell taxonomy revealed by single cell transcriptomics. *Nature Neuroscience*, 19(2), 335–346. doi:10.1038/nn.4216

- Taveggia, C., Thaker, P., Petrylak, A., Caporaso, G. L., Toews, A., Falls, D. L., ... Salzer, J. L. (2008). Type III neuregulin-1 promotes oligodendrocyte myelination. *Glia*, *56*(3), 284–293. doi:10.1002/glia.20612
- Taveggia, C., Zanazzi, G., Petrylak, A., Yano, H., Rosenbluth, J., Einheber, S., ... Salzer, J. L. (2005). Neuregulin-1 type III determines the ensheathment fate of axons. *Neuron*, *47*(5), 681–694. doi:10.1016/j.neuron.2005.08.017
- Thompson, M., Lauderdale, S., Webster, M. J., Chong, V. Z., McClintock, B., Saunders, R., & Weickert, C. S. (2007). Widespread expression of ErbB2, ErbB3 and ErbB4 in non-human primate brain. *Brain Research*, *1139*, 95–109. doi:10.1016/j.brainres.2006.11.047
- Tidcombe, H., Jackson-Fisher, A., Mathers, K., Stern, D. F., Gassmann, M., & Golding, J. P. (2003). Neural and mammary gland defects in ErbB4 knockout mice genetically rescued from embryonic lethality. *Proceedings of the National Academy of Sciences of the United States of America*, *100*(14), 8281–8286. doi:10.1073/pnas.1436402100
- Ting, A. K., Chen, Y., Wen, L., Yin, D.-M., Shen, C., Tao, Y., ... Mei, L. (2011). Neuregulin 1 promotes excitatory synapse development and function in GABAergic interneurons. *The Journal of Neuroscience*, *31*(1), 15–25. doi:10.1523/JNEUROSCI.2538-10.2011
- Tokita, Y., Keino, H., Matsui, F., Aono, S., Ishiguro, H., Higashiyama, S., & Oohira, A. (2001). Regulation of neuregulin expression in the injured rat brain and cultured astrocytes. *The Journal of Neuroscience*, *21*(4), 1257–1264.
- Toriyama, M., Sakumura, Y., Shimada, T., Ishii, S., & Inagaki, N. (2010). A diffusion-based neurite length-sensing mechanism involved in neuronal symmetry breaking. *Molecular Systems Biology*, *6*, 394. doi:10.1038/msb.2010.51
- Troyer, K. L., & Lee, D. C. (2001). Regulation of mouse mammary gland development and tumorigenesis by the ERBB signaling network. *Journal of Mammary Gland Biology and Neoplasia*, *6*(1), 7–21.
- Turner, J. R., Ray, R., Lee, B., Everett, L., Xiang, J., Jepson, C., ... Blendy, J. A. (2014). Evidence from mouse and man for a role of neuregulin 3 in nicotine dependence. *Molecular Psychiatry*, *19*(7), 801–810. doi:10.1038/mp.2013.104
- Tzahar, E., Waterman, H., Chen, X., Levkowitz, G., Karunakaran, D., Lavi, S., ... Yarden, Y. (1996). A hierarchical network of interreceptor interactions determines signal transduction by Neu differentiation factor/neuregulin and epidermal growth factor. *Molecular and Cellular Biology*, *16*(10), 5276–5287.
- Uematsu, M., Hirai, Y., Karube, F., Ebihara, S., Kato, M., Abe, K., ... Kawaguchi, Y. (2008). Quantitative chemical composition of cortical GABAergic neurons revealed in transgenic venus-expressing rats. *Cerebral Cortex*, *18*(2), 315–330. doi:10.1093/cercor/bhm056

- Ullrich, A., Coussens, L., Hayflick, J. S., Dull, T. J., Gray, A., Tam, A. W., ... Schlessinger, J. (1984). Human epidermal growth factor receptor cDNA sequence and aberrant expression of the amplified gene in A431 epidermoid carcinoma cells. *Nature*, *309*(5967), 418–425. doi:10.1038/309418a0
- Vaht, M., Laas, K., Kiive, E., Parik, J., Veidebaum, T., & Harro, J. (2017). A functional neuregulin-1 gene variant and stressful life events: Effect on drug use in a longitudinal population-representative cohort study. *Journal of Psychopharmacology*, *31*(1), 54–61. doi:10.1177/0269881116655979
- Vartanian, T., Fischbach, G., & Miller, R. (1999). Failure of spinal cord oligodendrocyte development in mice lacking neuregulin. *Proceedings of the National Academy of Sciences of the United States of America*, *96*(2), 731–735.
- Vartanian, T., Goodearl, A., Viehöver, A., & Fischbach, G. (1997). Axonal neuregulin signals cells of the oligodendrocyte lineage through activation of HER4 and Schwann cells through HER2 and HER3. *The Journal of Cell Biology*, *137*(1), 211–220. doi:10.1083/jcb.137.1.211
- Vaskovsky, A., Lupowitz, Z., Erlich, S., & Pinkas-Kramarski, R. (2000). ErbB-4 activation promotes neurite outgrowth in PC12 cells. *Journal of Neurochemistry*, *74*(3), 979–987. doi:10.1046/j.1471-4159.2000.0740979.x
- Veikkolainen, V., Vaparanta, K., Halkilahti, K., Iljin, K., Sundvall, M., & Elenius, K. (2011). Function of ERBB4 is determined by alternative splicing. *Cell Cycle*, *10*(16), 2647–2657. doi:10.4161/cc.10.16.17194
- Vernay, A., & Cosson, P. (2013). Immunofluorescence labeling of cell surface antigens in Dictyostelium. *BMC Research Notes*, *6*, 317. doi:10.1186/1756-0500-6-317
- Villar-Cerviño, V., Kappeler, C., Nóbrega-Pereira, S., Henkemeyer, M., Rago, L., Nieto, M. A., & Marín, O. (2015). Molecular mechanisms controlling the migration of striatal interneurons. *The Journal of Neuroscience*, *35*(23), 8718–8729. doi:10.1523/JNEUROSCI.4317-14.2015
- Villegas, R., Villegas, G. M., Longart, M., Hernández, M., Maqueira, B., Buonanno, A., ... Castillo, C. (2000). Neuregulin found in cultured-sciatic nerve conditioned medium causes neuronal differentiation of PC12 cells. *Brain Research*, *852*(2), 305–318. doi:10.1016/S0006-8993(99)02109-5
- Vohra, B. P. S., Fu, M., & Heuckeroth, R. O. (2007). Protein kinase C ζ and glycogen synthase kinase-3 β control neuronal polarity in developing rodent enteric neurons, whereas SMAD specific E3 ubiquitin protein ligase 1 promotes neurite growth but does not influence polarity. *The Journal of Neuroscience*, *27*(35), 9458–9468. doi:10.1523/JNEUROSCI.0870-07.2007

- Vullhorst, D., Ahmad, T., Karavanova, I., Keating, C., & Buonanno, A. (2017). Structural Similarities between Neuregulin 1-3 Isoforms Determine Their Subcellular Distribution and Signaling Mode in Central Neurons. *The Journal of Neuroscience*, *37*(21), 5232–5249. doi:10.1523/JNEUROSCI.2630-16.2017
- Vullhorst, D., Mitchell, R. M., Keating, C., Roychowdhury, S., Karavanova, I., Tao-Cheng, J.-H., & Buonanno, A. (2015). A negative feedback loop controls NMDA receptor function in cortical interneurons via neuregulin 2/ErbB4 signalling. *Nature Communications*, *6*, 7222. doi:10.1038/ncomms8222
- Vullhorst, D., Neddens, J., Karavanova, I., Tricoire, L., Petralia, R. S., McBain, C. J., & Buonanno, A. (2009). Selective expression of ErbB4 in interneurons, but not pyramidal cells, of the rodent hippocampus. *The Journal of Neuroscience*, *29*(39), 12255–12264. doi:10.1523/JNEUROSCI.2454-09.2009
- Walker, R. M., Christoforou, A., Thomson, P. A., McGhee, K. A., Maclean, A., Mühleisen, T. W., ... Evans, K. L. (2010). Association analysis of Neuregulin 1 candidate regions in schizophrenia and bipolar disorder. *Neuroscience Letters*, *478*(1), 9–13. doi:10.1016/j.neulet.2010.04.056
- Wang, J. Y., Miller, S. J., & Falls, D. L. (2001). The N-terminal region of neuregulin isoforms determines the accumulation of cell surface and released neuregulin ectodomain. *The Journal of Biological Chemistry*, *276*(4), 2841–2851. doi:10.1074/jbc.M005700200
- Wang, K.-S., Xu, N., Wang, L., Aragon, L., Ciubuc, R., Arana, T. B., ... Xu, C. (2014). NRG3 gene is associated with the risk and age at onset of Alzheimer disease. *Journal of Neural Transmission*, *121*(2), 183–192. doi:10.1007/s00702-013-1091-0
- Wang, Y.-C., Chen, J.-Y., Chen, M.-L., Chen, C.-H., Lai, I.-C., Chen, T.-T., ... Liou, Y.-J. (2008). Neuregulin 3 genetic variations and susceptibility to schizophrenia in a Chinese population. *Biological Psychiatry*, *64*(12), 1093–1096. doi:10.1016/j.biopsych.2008.07.012
- Wang, Y.-N., Figueiredo, D., Sun, X.-D., Dong, Z.-Q., Chen, W.-B., Cui, W.-P., ... Mei, L. (2018). Controlling of glutamate release by neuregulin3 via inhibiting the assembly of the SNARE complex. *Proceedings of the National Academy of Sciences of the United States of America*, *115*(10), 2508–2513. doi:10.1073/pnas.1716322115
- Wang, Yiguo, Du, D., Fang, L., Yang, G., Zhang, C., Zeng, R., ... Chen, Z. (2006). Tyrosine phosphorylated Par3 regulates epithelial tight junction assembly promoted by EGFR signaling. *The EMBO Journal*, *25*(21), 5058–5070. doi:10.1038/sj.emboj.7601384
- Wang, Yun, Gupta, A., Toledo-Rodriguez, M., Wu, C. Z., & Markram, H. (2002). Anatomical, physiological, molecular and circuit properties of nest basket cells in the developing somatosensory cortex. *Cerebral Cortex*, *12*(4), 395–410. doi:10.1093/cercor/12.4.395

- Wang, Yun, Toledo-Rodriguez, M., Gupta, A., Wu, C., Silberberg, G., Luo, J., & Markram, H. (2004). Anatomical, physiological and molecular properties of Martinotti cells in the somatosensory cortex of the juvenile rat. *The Journal of Physiology*, *561*(Pt 1), 65–90. doi:10.1113/jphysiol.2004.073353
- Wang, Z. (2017). ErbB receptors and cancer. *Methods in Molecular Biology*, *1652*, 3–35. doi:10.1007/978-1-4939-7219-7_1
- Wansbury, O., Panchal, H., James, M., Parry, S., Ashworth, A., & Howard, B. (2008). Dynamic expression of ErbB pathway members during early mammary gland morphogenesis. *The Journal of Investigative Dermatology*, *128*(4), 1009–1021. doi:10.1038/sj.jid.5701118
- Weickert, C. S., Tiwari, Y., Schofield, P. R., Mowry, B. J., & Fullerton, J. M. (2012). Schizophrenia-associated HapICE haplotype is associated with increased NRG1 type III expression and high nucleotide diversity. *Translational Psychiatry*, *2*, e104. doi:10.1038/tp.2012.25
- Wen, D., Peles, E., Cupples, R., Suggs, S. V., Bacus, S. S., Luo, Y., ... Levy, R. B. (1992). Neu differentiation factor: a transmembrane glycoprotein containing an EGF domain and an immunoglobulin homology unit. *Cell*, *69*(3), 559–572. doi:10.1016/0092-8674(92)90456-M
- Wen, D., Suggs, S. V., Karunakaran, D., Liu, N., Cupples, R. L., Luo, Y., ... Jacobsen, V. L. (1994). Structural and functional aspects of the multiplicity of Neu differentiation factors. *Molecular and Cellular Biology*, *14*(3), 1909–1919.
- Wen, L., Lu, Y.-S., Zhu, X.-H., Li, X.-M., Woo, R.-S., Chen, Y.-J., ... Mei, L. (2010). Neuregulin 1 regulates pyramidal neuron activity via ErbB4 in parvalbumin-positive interneurons. *Proceedings of the National Academy of Sciences of the United States of America*, *107*(3), 1211–1216. doi:10.1073/pnas.0910302107
- Wen, Z., Chen, J., Khan, R. A. W., Song, Z., Wang, M., Li, Z., ... Shi, Y. (2016). Genetic association between NRG1 and schizophrenia, major depressive disorder, bipolar disorder in Han Chinese population. *American Journal of Medical Genetics. Part B, Neuropsychiatric Genetics*, *171B*(3), 468–478. doi:10.1002/ajmg.b.32428
- Wetsel, W. C., Khan, W. A., Merchenthaler, I., Rivera, H., Halpern, A. E., Phung, H. M., ... Hannun, Y. A. (1992). Tissue and cellular distribution of the extended family of protein kinase C isoenzymes. *The Journal of Cell Biology*, *117*(1), 121–133. doi:10.1083/jcb.117.1.121
- Wieduwilt, M. J., & Moasser, M. M. (2008). The epidermal growth factor receptor family: biology driving targeted therapeutics. *Cellular and Molecular Life Sciences*, *65*(10), 1566–1584. doi:10.1007/s00018-008-7440-8

- Wiesen, J. F., Young, P., Werb, Z., & Cunha, G. R. (1999). Signaling through the stromal epidermal growth factor receptor is necessary for mammary ductal development. *Development*, *126*(2), 335–344.
- Wiggin, G. R., Fawcett, J. P., & Pawson, T. (2005). Polarity proteins in axon specification and synaptogenesis. *Developmental Cell*, *8*(6), 803–816. doi:10.1016/j.devcel.2005.05.007
- Willem, M. (2016). Proteolytic processing of Neuregulin-1. *Brain Research Bulletin*, *126*(Pt 2), 178–182. doi:10.1016/j.brainresbull.2016.07.003
- Williams, N. M., Preece, A., Spurlock, G., Norton, N., Williams, H. J., Zammit, S., ... Owen, M. J. (2003). Support for genetic variation in neuregulin 1 and susceptibility to schizophrenia. *Molecular Psychiatry*, *8*(5), 485–487. doi:10.1038/sj.mp.4001348
- Wilson, K. J., Gilmore, J. L., Foley, J., Lemmon, M. A., & Riese, D. J. (2009). Functional selectivity of EGF family peptide growth factors: implications for cancer. *Pharmacology & Therapeutics*, *122*(1), 1–8. doi:10.1016/j.pharmthera.2008.11.008
- Wirth, M. J., Brun, A., Grabert, J., Patz, S., & Wahle, P. (2003). Accelerated dendritic development of rat cortical pyramidal cells and interneurons after biolistic transfection with BDNF and NT4/5. *Development*, *130*(23), 5827–5838. doi:10.1242/dev.00826
- Witte, H., & Bradke, F. (2008). The role of the cytoskeleton during neuronal polarization. *Current Opinion in Neurobiology*, *18*(5), 479–487. doi:10.1016/j.conb.2008.09.019
- Woldeyesus, M. T., Britsch, S., Riethmacher, D., Xu, L., Sonnenberg-Riethmacher, E., Abou-Rebyeh, F., ... Birchmeier, C. (1999). Peripheral nervous system defects in erbB2 mutants following genetic rescue of heart development. *Genes & Development*, *13*(19), 2538–2548.
- Wolpowitz, D., Mason, T. B., Dietrich, P., Mendelsohn, M., Talmage, D. A., & Role, L. W. (2000). Cysteine-rich domain isoforms of the neuregulin-1 gene are required for maintenance of peripheral synapses. *Neuron*, *25*(1), 79–91. doi:10.1016/S0896-6273(00)80873-9
- Woo, R.-S., Lee, J.-H., Yu, H.-N., Song, D.-Y., & Baik, T.-K. (2010). Expression of ErbB4 in the apoptotic neurons of Alzheimer's disease brain. *Anatomy & Cell Biology*, *43*(4), 332–339. doi:10.5115/acb.2010.43.4.332
- Woo, R.-S., Li, X.-M., Tao, Y., Carpenter-Hyland, E., Huang, Y. Z., Weber, J., ... Mei, L. (2007). Neuregulin-1 enhances depolarization-induced GABA release. *Neuron*, *54*(4), 599–610. doi:10.1016/j.neuron.2007.04.009
- Xie, F., Padival, M., & Siegel, R. E. (2007). Association of PSD-95 with ErbB4 facilitates neuregulin signaling in cerebellar granule neurons in culture. *Journal of Neurochemistry*, *100*(1), 62–72. doi:10.1111/j.1471-4159.2006.04182.x

- Xu, Q., Cobos, I., De La Cruz, E., Rubenstein, J. L., & Anderson, S. A. (2004). Origins of cortical interneuron subtypes. *The Journal of Neuroscience*, *24*(11), 2612–2622. doi:10.1523/JNEUROSCI.5667-03.2004
- Xu, R., Pankratova, S., Christiansen, S. H., Woldbye, D., Højland, A., Bock, E., & Berezin, V. (2013). A peptide antagonist of ErbB receptors, Inherbin3, induces neurite outgrowth from rat cerebellar granule neurons through ErbB1 inhibition. *Neurochemical Research*, *38*(12), 2550–2558. doi:10.1007/s11064-013-1166-1
- Xu, X., Roby, K. D., & Callaway, E. M. (2010). Immunochemical characterization of inhibitory mouse cortical neurons: three chemically distinct classes of inhibitory cells. *The Journal of Comparative Neurology*, *518*(3), 389–404. doi:10.1002/cne.22229
- Yamamoto, T., Ikawa, S., Akiyama, T., Semba, K., Nomura, N., Miyajima, N., ... Toyoshima, K. (1986). Similarity of protein encoded by the human c-erb-B-2 gene to epidermal growth factor receptor. *Nature*, *319*(6050), 230–234. doi:10.1038/319230a0
- Yan, L., Shamir, A., Skirzewski, M., Leiva-Salcedo, E., Kwon, O. B., Karavanova, I., ... Buonanno, A. (2018). Neuregulin-2 ablation results in dopamine dysregulation and severe behavioral phenotypes relevant to psychiatric disorders. *Molecular Psychiatry*, *23*(5), 1233–1243. doi:10.1038/mp.2017.22
- Yan, Y., Eipper, B. A., & Mains, R. E. (2016). Kalirin is required for BDNF-TrkB stimulated neurite outgrowth and branching. *Neuropharmacology*, *107*, 227–238. doi:10.1016/j.neuropharm.2016.03.050
- Yang, J.-M., Shen, C.-J., Chen, X.-J., Kong, Y., Liu, Y.-S., Li, X.-W., ... Li, X.-M. (2018). *erbb4* Deficits in Chandelier Cells of the Medial Prefrontal Cortex Confer Cognitive Dysfunctions: Implications for Schizophrenia. *Cerebral Cortex*. doi:10.1093/cercor/bhy316
- Yang, J.-M., Zhang, J., Chen, X.-J., Geng, H.-Y., Ye, M., Spitzer, N. C., ... Li, X.-M. (2013). Development of GABA circuitry of fast-spiking basket interneurons in the medial prefrontal cortex of *erbb4*-mutant mice. *The Journal of Neuroscience*, *33*(50), 19724–19733. doi:10.1523/JNEUROSCI.1584-13.2013
- Yang, S.-A. (2012). Association between a Missense Polymorphism (rs3924999, Arg253Gln) of Neuregulin 1 and Schizophrenia in Korean Population. *Experimental Neurobiology*, *21*(4), 158–163. doi:10.5607/en.2012.21.4.158
- Yang, Z., Xue, B., Umitsu, M., Ikura, M., Muthuswamy, S. K., & Neel, B. G. (2012). The signaling adaptor GAB1 regulates cell polarity by acting as a PAR protein scaffold. *Molecular Cell*, *47*(3), 469–483. doi:10.1016/j.molcel.2012.06.037
- Yao, J.-J., Sun, J., Zhao, Q.-R., Wang, C.-Y., & Mei, Y.-A. (2013). Neuregulin-1/ErbB4 signaling regulates Kv4.2-mediated transient outward K⁺ current through the Akt/mTOR pathway.

American Journal of Physiology. Cell Physiology, 305(2), C197–206.
doi:10.1152/ajpcell.00041.2013

- Yau, H.-J., Wang, H.-F., Lai, C., & Liu, F.-C. (2003). Neural development of the neuregulin receptor ErbB4 in the cerebral cortex and the hippocampus: preferential expression by interneurons tangentially migrating from the ganglionic eminences. *Cerebral Cortex*, 13(3), 252–264. doi:10.1093/cercor/13.3.252
- Yi, J. J., Barnes, A. P., Hand, R., Polleux, F., & Ehlers, M. D. (2010). TGF-beta signaling specifies axons during brain development. *Cell*, 142(1), 144–157. doi:10.1016/j.cell.2010.06.010
- Yin, D.-M., Chen, Y.-J., Lu, Y.-S., Bean, J. C., Sathyamurthy, A., Shen, C., ... Mei, L. (2013). Reversal of behavioral deficits and synaptic dysfunction in mice overexpressing neuregulin 1. *Neuron*, 78(4), 644–657. doi:10.1016/j.neuron.2013.03.028
- Yin, D.-M., Huang, Y.-H., Zhu, Y.-B., & Wang, Y. (2008). Both the establishment and maintenance of neuronal polarity require the activity of protein kinase D in the Golgi apparatus. *The Journal of Neuroscience*, 28(35), 8832–8843. doi:10.1523/JNEUROSCI.1291-08.2008
- Yin, D.-M., Sun, X.-D., Bean, J. C., Lin, T. W., Sathyamurthy, A., Xiong, W.-C., ... Mei, L. (2013). Regulation of spine formation by ErbB4 in PV-positive interneurons. *The Journal of Neuroscience*, 33(49), 19295–19303. doi:10.1523/JNEUROSCI.2090-13.2013
- Yogev, S., & Shen, K. (2017). Establishing Neuronal Polarity with Environmental and Intrinsic Mechanisms. *Neuron*, 96(3), 638–650. doi:10.1016/j.neuron.2017.10.021
- Yokota, Y., Eom, T.-Y., Stanco, A., Kim, W.-Y., Rao, S., Snider, W. D., & Anton, E. S. (2010). Cdc42 and Gsk3 modulate the dynamics of radial glial growth, inter-radial glial interactions and polarity in the developing cerebral cortex. *Development*, 137(23), 4101–4110. doi:10.1242/dev.048637
- Yokozeki, T., Wakatsuki, S., Hatsuzawa, K., Black, R. A., Wada, I., & Sehara-Fujisawa, A. (2007). Meltrin beta (ADAM19) mediates ectodomain shedding of Neuregulin beta1 in the Golgi apparatus: fluorescence correlation spectroscopic observation of the dynamics of ectodomain shedding in living cells. *Genes To Cells*, 12(3), 329–343. doi:10.1111/j.1365-2443.2007.01060.x
- Yoo, H. J., Woo, R.-S., Cho, S.-C., Kim, B.-N., Kim, J.-W., Shin, M.-S., ... Kim, S. A. (2015). Genetic association analyses of neuregulin 1 gene polymorphism with endophenotype for sociality of Korean autism spectrum disorders family. *Psychiatry Research*, 227(2-3), 366–368. doi:10.1016/j.psychres.2015.03.015
- Yoosefee, S., Shahsavand Ananloo, E., Joghataei, M.-T., Karimipour, M., Hadjighassem, M., Mohaghegh, H., ... Hatami, M. (2016). Association Between Neuregulin-1 Gene

- Variant (rs2439272) and Schizophrenia and Its Negative Symptoms in an Iranian Population. *Iranian Journal of Psychiatry*, 11(3), 147–153.
- Yoshimura, T., Arimura, N., & Kaibuchi, K. (2006). Signaling networks in neuronal polarization. *The Journal of Neuroscience*, 26(42), 10626–10630. doi:10.1523/JNEUROSCI.3824-06.2006
- Yun, K., Potter, S., & Rubenstein, J. L. (2001). Gsh2 and Pax6 play complementary roles in dorsoventral patterning of the mammalian telencephalon. *Development*, 128(2), 193–205.
- Zeledón, M., Eckart, N., Taub, M., Vernon, H., Szymanski, M., Wang, R., ... Valle, D. (2015). Identification and functional studies of regulatory variants responsible for the association of NRG3 with a delusion phenotype in schizophrenia. *Molecular Neuropsychiatry*, 1(1), 36–46. doi:10.1159/000371518
- Zhang, D., Sliwkowski, M. X., Mark, M., Frantz, G., Akita, R., Sun, Y., ... Godowski, P. J. (1997). Neuregulin-3 (NRG3): a novel neural tissue-enriched protein that binds and activates ErbB4. *Proceedings of the National Academy of Sciences of the United States of America*, 94(18), 9562–9567.
- Zhang, H., & Macara, I. G. (2006). The polarity protein PAR-3 and TIAM1 cooperate in dendritic spine morphogenesis. *Nature Cell Biology*, 8(3), 227–237. doi:10.1038/ncb1368
- Zhang, H., & Macara, I. G. (2008). The PAR-6 polarity protein regulates dendritic spine morphogenesis through p190 RhoGAP and the Rho GTPase. *Developmental Cell*, 14(2), 216–226. doi:10.1016/j.devcel.2007.11.020
- Zhang, L., Fletcher-Turner, A., Marchionni, M. A., Apparsundaram, S., Lundgren, K. H., Yurek, D. M., & Seroogy, K. B. (2004). Neurotrophic and neuroprotective effects of the neuregulin glial growth factor-2 on dopaminergic neurons in rat primary midbrain cultures. *Journal of Neurochemistry*, 91(6), 1358–1368. doi:10.1111/j.1471-4159.2004.02817.x
- Zhang, Q., Esrafilzadeh, D., Crook, J. M., Kapsa, R., Stewart, E. M., Tomaskovic-Crook, E., ... Huang, X.-F. (2017). Electrical Stimulation Using Conductive Polymer Polypyrrole Counters Reduced Neurite Outgrowth of Primary Prefrontal Cortical Neurons from NRG1-KO and DISC1-LI Mice. *Scientific Reports*, 7, 42525. doi:10.1038/srep42525
- Zhang, Q., Yu, Y., & Huang, X.-F. (2016). Olanzapine Prevents the PCP-induced Reduction in the Neurite Outgrowth of Prefrontal Cortical Neurons via NRG1. *Scientific Reports*, 6, 19581. doi:10.1038/srep19581
- Zhang, R., Du, X.-Y., Yu, J., Xu, N., Zheng, Y.-W., Zhao, Y.-L., ... Ma, J. (2013). No genetic evidence for Neuregulin 3 conferring risk of schizophrenia in the Chinese population. *Psychiatry Research*, 205(3), 279–281. doi:10.1016/j.psychres.2012.08.017

- Zhang, X., Zhu, J., Yang, G.-Y., Wang, Q.-J., Qian, L., Chen, Y.-M., ... Luo, Z.-G. (2007). Dishevelled promotes axon differentiation by regulating atypical protein kinase C. *Nature Cell Biology*, 9(7), 743–754. doi:10.1038/ncb1603
- Zhang, Z., Cui, J., Gao, F., Li, Y., Zhang, G., Liu, M., ... Li, R. (2019). Elevated cleavage of neuregulin-1 by beta-secretase 1 in plasma of schizophrenia patients. *Progress in Neuro-Psychopharmacology & Biological Psychiatry*, 90, 161–168. doi:10.1016/j.pnpbp.2018.11.018
- Zheng, C.-H., & Feng, L. (2006). Neuregulin regulates the formation of radial glial scaffold in hippocampal dentate gyrus of postnatal rats. *Journal of Cellular Physiology*, 207(2), 530–539. doi:10.1002/jcp.20591
- Zhou, L., Fisher, M. L., Cole, R. D., Gould, T. J., Parikh, V., Ortinski, P. I., & Turner, J. R. (2018). Neuregulin 3 Signaling Mediates Nicotine-Dependent Synaptic Plasticity in the Orbitofrontal Cortex and Cognition. *Neuropsychopharmacology*, 43(6), 1343–1354. doi:10.1038/npp.2017.278
- Zhu, X., Lai, C., Thomas, S., & Burden, S. J. (1995). Neuregulin receptors, erbB3 and erbB4, are localized at neuromuscular synapses. *The EMBO Journal*, 14(23), 5842–5848.
- Zmuda, J. F., & Rivas, R. J. (1998). The Golgi apparatus and the centrosome are localized to the sites of newly emerging axons in cerebellar granule neurons in vitro. *Cell Motility and the Cytoskeleton*, 41(1), 18–38. doi:10.1002/(SICI)1097-0169(1998)41:1<18::AID-CM2>3.0.CO;2-B
- Zoratto, F., Altabella, L., Tistarelli, N., Laviola, G., Adriani, W., & Canese, R. (2018). Inside the Developing Brain to Understand Teen Behavior From Rat Models: Metabolic, Structural, and Functional-Connectivity Alterations Among Limbic Structures Across Three Pre-adolescent Stages. *Frontiers in Behavioral Neuroscience*, 12, 208. doi:10.3389/fnbeh.2018.00208

AFRIDA RAHMAN

rahmanaf@indiana.edu www.linkedin.com/in/afrida-rahman-4aa93758

EXPERTISE AND TECHNIQUES:

• Immunofluorescence (i.e., immunocytochemistry and immunohistochemistry) • Microscopy / Confocal microscopy • Cryosectioning • Immunoprecipitation • Western blotting (i.e., gel electrophoresis and polyvinylidene fluoride membrane transfer) • Preparation of whole lysate from rat brain tissue • Preparation of primary neuronal cultures from rat embryos • Cell/tissue culture • DNA cloning • PCR • Bacterial transformations • Restriction digests • DNA ligations • DNA gel extraction • DNA mini/midipreps • Southern blotting • Preparation of GST fusion proteins • Data analyses (i.e., measurements of neurite outgrowth, Golgi positioning) • Densitometry / Western Blot Quantification • Data analyses in ImageJ / FIJI • Statistical analyses using SPSS and Excel

EDUCATION:

Indiana University, Bloomington IN

August 2012 – June 2019

Department of Psychological and Brain Sciences / Program in Neuroscience

Majors: Ph.D., (Dual Ph.D.) Psychology and Neural S

Major GPA: 3.93/4.00

Dissertation Title: The Neuregulin Growth Factors and Their Receptor ErbB4 in the Developing Brain: Delineation of Neuregulin-3 Expression and Neuritogenesis

Adviser: Anne L. Prieto, Ph.D.

Purdue University, West Lafayette IN

August 2008 – May 2012

Department of Psychological Sciences

Major: B.S., Psychology – Research Focused Honors / Behavioral Neuroscience

Minor: Biological Sciences

Major GPA: 3.90/4.00

Cumulative GPA: 3.70/4.00

Honors Thesis Adviser: Dr. Jeff Karpicke, Ph.D.

RESEARCH EXPERIENCE:

Ph.D. Candidate and Graduate/Research Assistant to Dr. Anne Prieto (August 2012 – present)

- Conducting research pertaining to cortical interneuronal differentiation, neuronal polarity, and neuregulin-ErbB4 complexes on the development of the central nervous system

Current Projects:

Rahman, A., Lai, C., & Prieto, A.L. (*in progress*). Neuregulin Activation of the Receptor Tyrosine Kinase ErbB4 Induces Receptor Association with the Par Polarity Complex.

Undergraduate Research Assistant to and Honors Thesis in conjunction with Dr. Jeff Karpicke (Spring 2010 – Spring 2012)

- Conducted research pertaining to studying strategies and their effects on learning/memory retention; designed and ran participants through experimental programs; scored data; organized data entry; implemented statistical analyses using SPSS; and submitted write-up of senior thesis to the college. Senior thesis research focused on collaborative study vs. individual study and its effects on later retention/memory.

Undergraduate Research Assistant to Dr. David Rollock (Fall 2011 – Spring 2012)

- Conducted research pertaining to Asian and Latino/a American acculturation on Purdue University's (West Lafayette) campus; focused on bibliographic work pertaining to struggles of acculturation in the South / East Asian and Latino/a American populations; coded and documented interviews; ran statistical analyses in SPSS; coded in SPSS; recruited participants; coded articles for meta-analysis regarding intergenerational conflict and acculturation.

PUBLICATIONS AND MANUSCRIPTS:

Rahman, A., Weber, J., Labin, E., Lai, C., & Prieto, A. L. (2019). *Developmental Expression of Neuregulin-3 in the Rat Central Nervous System. Journal of Comparative Neurology*, 527(4), 797-817.

Rahman, A., Lai, C., & Prieto, A.L. (in advanced stages). *The Neuregulins and Their Receptor ErbB4 Developmentally Regulate Neurite Outgrowth of Cortical GABAergic Interneurons*. Submitting to: *Molecular Neurobiology*.

POSTER PRESENTATIONS:

Rahman, A., Lai C., & Prieto, A.L. (2019 March) *The Neuregulins and ErbB4 Developmentally Regulate Neurite Outgrowth of Cortical GABAergic Interneurons*. Poster presented at 2019 Greater Indiana Society for Neuroscience Annual Meeting, Indianapolis, IN.

Rahman, A., Lai C., & Prieto, A.L. (2018 September) *The Neuregulins and ErbB4 in the Differentiation of Cortical Neurons: Neurite Outgrowth and Polarity*. Poster presented at 2018 Gill Symposium, Bloomington, IN.

Rahman, A., Lai, C., & Prieto, A.L. (2018 April) *ErbB4 and The Neuregulins in Neuronal Development: Neuritogenesis and Polarity*. Poster presented at 5th Annual Achievements of

Women in STIM (Science, Technology, Informatics, Mathematics) Poster Session, Bloomington IN.

Rahman, A., Lai, C., & Prieto, A.L. (2018 March) *The Role of the Neuregulins in Neuronal Differentiation: Neurite Outgrowth and Polarity*. Poster presented at 2018 Greater Indiana Society for Neuroscience Annual Meeting, West Lafayette, IN.

Rahman, A., Weber, J., Lai, C., & Prieto, A.L. (2017 September) *Characterization of the Spatiotemporal Localization of the Growth Factor Neuregulin-3 in the Embryonic and Postnatal Rat Central Nervous System*. Poster presented at 2017 Gill Symposium, Bloomington, IN.

Rahman, A., Lai, C., & Prieto, A.L. (2017 August) *Neuregulin activation of the receptor tyrosine kinase ErbB4 induces neurite outgrowth and receptor association with the Par polarity complex*. Poster presented at 2017 Genome, Cell, and Developmental Biology (GCDB) poster session, Bloomington, IN.

Rahman, A., Weber, J., Lai, C., & Prieto A.L. (2016 December) *Characterization of the Spatiotemporal Localization of the Growth Factor Neuregulin-3 in the Central Nervous System*. Poster presented at 2016 American Society for Cell Biology, San Francisco, CA.

Rahman, A., Lai, C., & Prieto, A.L. (2016 September) *Association of the Receptor Tyrosine Kinase ErbB4 with the Par polarity Complex and the Effects of Receptor Activation on Neurite Outgrowth*. Poster presented at 2016 Gill Symposium, Bloomington, IN.

Yu, J., Rahman, A., & Prieto, A.L. (2016 April) *Effects of NRG3 on the Proliferation and Differentiation of Neural Stem/Progenitor Cells*. Poster presented at 2016 J.R. Kantor Undergraduate Honors and Awards Banquet, Bloomington, IN.

Rahman, A., Labin, E., Weber, J., Wallace, N.S., Lai, C., & Prieto, A.L. (2015 September) *Expression of the Schizophrenia Susceptibility Gene Neuregulin-3 in the Central Nervous System*. Poster presented at 2015 Gill Symposium, Bloomington, IN.

Rahman, A., Labin, E., Weber, J., Wallace, N.S., Lai, C., & Prieto, A.L. (2015 September) *Expression of the Schizophrenia Susceptibility Gene Neuregulin-3 in the Central Nervous System*. Poster presented at 50th Anniversary of the Indiana University Program in Neuroscience Poster Session, Bloomington, IN.

Rahman, A., Labin, E., Weber, J., Wallace, N.S., Lai, C., & Prieto, A.L. (2014, April) *Expression of the Schizophrenia Susceptibility Gene Neuregulin-3 in the Central Nervous System*. Poster presented at 1st Annual Achievements of Women in STIM (Science, Technology, Informatics, Mathematics) Poster Session, Bloomington IN.

Rahman, A., Labin, E., Weber, J., Wallace, N.S., Lai, C., & Prieto, A.L. (2013, December) *Expression of the Schizophrenia Susceptibility Gene Neuregulin-3 in the Central*

Nervous System. Poster presented at 2013 Department Annual Research Symposium, Bloomington, IN.

Rahman, A., & Karpicke, J. (2012, April) *Collaborative vs. Individual Study and the Effects on Retention*. Poster presented at the 10th Annual Undergraduate Research Conference, West Lafayette, IN.

Rahman, A., & Karpicke, J. (2012, April) *Collaborative vs. Individual Study and the Effects on Retention*. Poster presented at the 2nd Annual College of Health and Human Sciences Honors & Research Poster Session, West Lafayette, IN.

ACADEMIC HONORS AND AWARDS:

Gill Outstanding Image Award (September 2018)

- Annual award open to faculty and students from IUB, IUPUI, and Purdue and recognizes an outstanding neuroscience image.

Neuroscience Travel Award (November 2016, November 2017, April 2018)

- Departmental award funding travel to Society for Neuroscience conferences in November 2016 and 2017, American Society for Cell Biology conference in December 2016, and Greater Indiana Society for Neuroscience conference in March 2018.

Provost's Travel Award for Women in Science (October 2017)

- College travel award given to women in scientific and mathematical fields for professional development. Award funded travel to Society for Neuroscience conference in November 2017.

College of Arts and Sciences Travel Award (November 2016)

- College award given to fund travel to American Society for Cell Biology conference in December 2016

Achievements of Women in STIM Poster Competition (April 2014)

- Winner of Achievements of "Women in STIM (Science, Technology, Informatics, Mathematics) Poster Competition" in Health and Social Sciences subdivision

Joseph Steinmetz Summer Research Award (April 2013)

- Award given to a graduate student who showed outstanding performance in psychological research and had a strong grant proposal

Dean's List (Spring 2010 – Spring 2012)

Semester Honors (Fall 2009 – Spring 2012)

John M. Hadley Award (April 2012)

- Award given to one senior Psychology student who presented excellent research at the Psychology Undergraduate Research Conference

Outstanding Senior in Psychological Sciences (April 2012)

- Award given to a senior in Psychology who shows excellence in academics, extracurricular service activities, and leadership

TEACHING EXPERIENCE:

Teaching assistant under Dr. Preston Garraghty for P426 – Lab in Behavioral Neurosciences (Spring 2019)

- Duties included working with students on oral presentations, including literature review and organization of PowerPoints; grading presentations.

Associate Instructor of P325-Psychology of Learning (Fall 2018)

- Duties included creating a course related to learning and memory; designing a syllabus, lectures, and exams; grading student presentations and exams; lecturing on material related to the psychology of learning; holding office hours; teaching undergraduates how we and animals learn and how learning can be manipulated

Lab Instructor of P211-Research Methods in Psychology (Fall 2014 / Fall 2015)

- Duties included creating a syllabus, homework assignments, rubrics and lectures; grading student manuscripts; having lab sections designed to teach students how to plan experiments, collect data, and write up manuscripts.

Mentorship of undergraduate researchers in the Cellular/Molecular Neuroscience Lab (Prieto Lab) (Fall 2012 – current)

- Duties include teaching undergraduate students cellular/molecular techniques; overseeing individual projects; mentoring in experimental design

Teaching assistant under Dr. Anne Prieto for P467-Diseases of the Nervous System (Spring 2015 / Spring 2017 / Spring 2018)

- Duties included grading exams and student presentations; meeting with students on a one-on-one basis

Teaching assistant under Dr. Preston Garraghty for P346-Neuroscience (Summer 2017)

- Duties included proctoring and grading exams; meeting with students for one-on-one help

Teaching assistant under Dr. Ben Motz for P101 online Introductory Psychology (Summer 2016)

- Duties included grading homework assignments and discussion posts

Teaching assistant under Dr. Lisa Thomassen for P101 and P155 Introductory Psychology (Summer 2014/ Summer 2015)

- Duties included grading homework assignments, holding office hours, writing exam questions, and holding review sessions prior to exams

Teaching assistant under Dr. Anne Prieto for P466-Molecular/Cellular Neurobiology (Spring 2013/ Fall 2013/Fall 2015/Fall 2016/Fall 2017)

- Duties included grading exams and student presentations

Teaching assistant under Dr. Anne Prieto for P346-Neuroscience (Fall 2012/ Fall 2013)

- Duties included grading exams and student presentations

PUBLIC OUTREACH AND SERVICES:

Getting You Into IU (GUI2IU) Student Ambassador (October 2017)

- Duties include giving guidance about graduate school, answering questions regarding the IU neuroscience program, and giving campus and lab tours

GUI2IU Graduate Student Panel (October 2016, November 2018)

- Volunteered to be on panel of graduate students and answer questions regarding graduate school from underrepresented undergraduates or master students

Poster Judge for Center of Excellence for Women in Technology (CEWiT) Women's Research Poster Competition (April 2016 / April 2017)

Grandview Elementary School's PTO Science Night (April 2016)

- Volunteered to help and educate local elementary school students about psychology and neuroscience with various demonstrations.

Managed Booth for Indiana University Neuroscience at Society for Neuroscience

Graduate School Fair (November 2014; October 2015; November 2016; November 2017)

- Led Indiana University's graduate school fair booth at the Society for Neuroscience conference. Duties included promoting IU neuroscience / psychology and gear undergraduates, postdocs, and postbacks to specific faculty they may want to work with in conjunction

DOCTORAL COMMITTEE:

Dr. Anne Prieto, Associate Professor

Department of Psychological and Brain Sciences / Neuroscience, Indiana University
Bloomington, Indiana 47404

Phone: (812) 855-4642

E-mail: aprieto@indiana.edu

Dr. Cary Lai, Professor

Department of Psychological and Brain Sciences / Neuroscience, Indiana University
Bloomington, Indiana 47404

Phone: (812) 856-4998

E-mail: carylai@indiana.edu

Dr. Andrea Hohmann, Professor, Jack and Linda Gill Chair

Department of Psychological and Brain Sciences / Neuroscience, Indiana University
Bloomington, Indiana 47404

Phone: (812) 856-0672

E-mail: hohmanna@indiana.edu

Dr. Kenneth Mackie, Distinguished Professor, Jack and Linda Gill Chair

Department of Psychological and Brain Sciences / Neuroscience, Indiana University
Bloomington, Indiana 47404

Phone: (812) 855-2042

E-mail: kmackie@indiana.edu